UNIVERSITA' DEGLI STUDI DI BARI ALDO MORO

Dipartimento di Scienze del suolo, della Pianta e degli Alimenti

DOTTORATO DI RICERCA IN SCIENZE DEL SUOLO E DEGLI ALIMENTI
CICLO XXXVIII

Settore Scientifico Disciplinare AGR/13 – Chimica Agraria

INNOVATIVE AND SUSTAINABLE SOLUTIONS FOR SOIL MANAGEMENT IN MARGINAL AREAS

Dottorando: Dott. Nicola Colatorti

NICOLA COLATORTI 20.04.2026 15:39:18 GMT+02:00

Supervisore: Ch.ma Prof.ssa Elisabetta Loffredo

ELISABETTA LOFFREDO 20.04.2026 20:04:39 GMT+02:00

Co-tutor: Ch.mo Prof. Claudio Cocozza

Coordinatore: Ch.ma Prof.ssa Erica Pontonio

ERICA PONTONIO 21.04.2026 09:52:27 GMT+02:00

Co- tutor: Dott. Carlo Porfido

ESAME FINALE 2026

Abstract

The intensification of agricultural and agro-industrial activities has led to an increasing accumulation of organic contaminants in soil and water bodies, creating an urgent need for sustainable strategies to mitigate their presence particularly in marginal areas. Against this backdrop, this PhD thesis explores the efficacy of various biosorbents originating from residual biomasses, such as digestate from olive pomace (DIG), gasification biochar (BC) and untreated agro-industrial by-products and waste like orange peels (OP), olive stones (OS), pistachio shells (PS), spent fungal growth substrate of *Pleurotus eryngii* (SFGS) and growth wheat straw (GWS) in removing contaminants of emerging concern (CECs) from aqueous solutions and soil. These materials, when applied to the soil, can counteract the ongoing decline of organic matter and improve its physical, chemical and biological fertility. Due to their properties such as the high carbon content, the porosity and presence of active surface functional group these materials can also modulate the bioavailability of both nutrients and xenobiotic chemical compounds in the soil.

DIG obtained exclusively from olive pomace exhibited a remarkable capacity to adsorb the pesticides boscalid and oxyfluorfen, significantly enhancing soil retention and modulating the growth of phytopathogenic fungi such as *Armillaria Mellea, Fusarium culmorum* and *Verticilium dahliae*, with species-dependent effects.

OP, OS and PS were highly efficienct at remove herbicides, insecticides, and bisphenol A, with adsorption kinetics best described by pseudo-second order model that indicate a chemisorption and isotherms best represented by the Freundlich model that indicate an adsorption on a heterogeneous surface.

High-temperature gasification BC, demonstrated excellent performance in adsorbing boscalid, reducing its leaching in soil columns and stimulating early root growth in horticultural species.

SFGS outperformed GWS in the removal of metalaxyl-M and cycloxydim, owing to fungal-induced modifications of the lignocellulosic matrix.

Finally, BC applied to different wastewater matrices (municipal, agro-industrial, and dairy) enabled the removal of over 90% of CECs, produced dose-dependent reductions in per- and polyfluoroalkyl substances (PFAS), and markedly decreased phytotoxicity, significantly improving seed germination and seedling development.

Overall, the findings demonstrate that biosorbents derived from agricultural residues are effective, versatile, and low-cost tools for the mitigation of organic contaminants, while simultaneously

promoting circular economy approaches. Their application can substantially contribute to water protection, soil health, and the transition toward more sustainable agro-environmental systems.

Riassunto

L'intensificazione delle attività agricole e agroindustriali ha determinato un crescente accumulo di contaminanti organici nel suolo e nei corpi idrici, creando un'urgente necessità di strategie sostenibili per mitigarne la presenza, in particolare nelle aree marginali. In questo contesto, la presente tesi di dottorato esplora l'efficacia di diversi biosorbenti derivanti da biomasse residuali, quali digestato da sansa di oliva (DIG), biochar da gassificazione (BC) e sottoprodotti e scarti agroindustriali non trattati come bucce di arancia (OP), noccioli di oliva (OS), gusci di pistacchio (PS), substrato esausto di coltivazione di *Pleurotus eryngii* (SFGS) e paglia di grano (GWS), nella rimozione di contaminanti emergenti (CEC) da soluzioni acquose e dal suolo.

Questi materiali, quando applicati al suolo, possono contrastare il progressivo declino della sostanza organica e migliorarne la fertilità fisica, chimica e biologica. Grazie alle loro proprietà, quali l'elevato contenuto di carbonio, la porosità e la presenza di gruppi funzionali superficiali attivi, tali materiali possono inoltre modulare la biodisponibilità sia dei nutrienti sia dei composti chimici xenobiotici nel suolo.

Il DIG ottenuto esclusivamente da sansa di oliva ha mostrato una notevole capacità di adsorbire i pesticidi boscalid e oxyfluorfen, migliorando significativamente la ritenzione nel suolo e modulando la crescita di funghi fitopatogeni quali *Armillaria mellea*, *Fusarium culmorum* e *Verticillium dahliae*, con effetti dipendenti dalla specie.

OP, OS e PS si sono dimostrati altamente efficienti nella rimozione di erbicidi, insetticidi e bisfenolo A, con cinetiche di adsorbimento meglio descritte dal modello di pseudo-secondo ordine, indicativo di un meccanismo di chemiadsorbimento, e isoterme meglio rappresentate dal modello di Freundlich, indicativo di adsorbimento su superficie eterogenea.

Il biochar ottenuto per gassificazione ad alta temperatura ha mostrato eccellenti prestazioni nell'adsorbimento del boscalid, riducendone la lisciviazione in colonne di suolo e stimolando la crescita precoce delle radici in specie orticole.

Il SFGS ha superato la paglia di grano nella rimozione di metalaxyl-M e cycloxydim, grazie alle modificazioni indotte dal fungo nella matrice lignocellulosica.

Infine, l'applicazione del BC a diverse matrici di reflui (urbani, agroindustriali e caseari) ha consentito la rimozione di oltre il 90% dei CEC, determinato riduzioni dose-dipendenti delle

sostanze alchiliche perfluorurate e polifluorurate (PFAS) e ridotto significativamente la fitotossicità, migliorando la germinazione dei semi e lo sviluppo delle plantule.

Nel complesso, i risultati dimostrano che i biosorbenti derivati da residui agricoli rappresentano strumenti efficaci, versatili ed economici per la mitigazione dei contaminanti organici, promuovendo al contempo approcci di economia circolare. La loro applicazione può contribuire in modo significativo alla tutela delle acque, alla salute del suolo e alla transizione verso sistemi agro-ambientali più sostenibili.

CHAPTER - 1
INTRODUCTION

1.1 Biosorbents from biomass recycling

In recent decades, the intensification of agricultural and industrial activities has led to a progressive accumulation of organic and inorganic contaminants in both aquatic systems and soils, with negative effects on environmental quality, soil fertility, and the safety of agri-food production (Kusuma et al. 2025, Lopes et al. 2024). In this context, the development of sustainable solutions for pollution mitigation and the restoration of ecosystem functions has stimulated growing interest in the use of biosorbents of natural origin (Tang 2024), in particular for the soil management in marginal areas.

Marginal areas are territories characterized by natural, economic, or structural constraints that reduce their productivity and competitiveness compared to more favourable areas. In the agricultural context, these areas are often characterized by soils of reduced fertility, slopes, limited water availability, unfavourable climatic conditions, and restricted access to infrastructure.
Biosorbents derived from agricultural biomass are promising adsorbent materials due to their abundance, renewability, and availability as agri-food by-products (Fertu et al., 2024). Residues such as straw, pruning waste, shells, husks, and pomace can be valorized for contaminant removal, supporting both waste reduction and circular economy strategies (Imran-Shaukat et al., 2022).

Although less efficient than conventional adsorbents, such as commercial activated carbon, agricultural biosorbents have lower cost and a reduced environmental impact, making them particularly suitable for large-scale applications.

From a chemical and structural perspective, these materials are mainly composed of a lignocellulosic matrix having numerous surface functional groups: (hydroxyl, both alcoholic and phenolic, carboxylic, aminic, etc.). These groups enable interactions with a wide range of contaminants through covalent bonding, complexation, ion exchange, and hydrophobic interactions (Sadeek et al. 2015), but it is also worth noting the large contribution of hydrogen bonds and similar weak interactions, especially in aqueous (polar) environment. These properties make biosorbents effective in wastewater and soil treatment. When used in soil remediation, they can reduce the bioavailability and mobility of pesticides, hydrocarbons, heavy metals, and industrial pollutants,

including endocrine-disrupting compounds, thereby limiting their transfer to crops and groundwater (Cho et al. 2023, Carnimeo et al. 2023, Ganesan & Thiyagarajan 2024, Phaty et al. 2025).

Within the category of biosorbents, a clear conceptual distinction can be made between processed (treated) and unprocessed (untreated) materials based on the degree of transformation of the original biomass. Treated biosorbents undergo thermochemical or biological treatments, such as pyrolysis or anaerobic digestion, that significantly alter their physicochemical properties, enhancing features like surface area, porosity, and functional groups. In contrast, untreated biosorbents consist of raw agro-industrial residues that are used directly, with only a grinding treatment and whose sorption capacity is mainly governed by their natural composition.

Both categories of carbon-rich materials offer valuable opportunities in agricultural and environmental applications, particularly as soil amendments and low-cost sorbents for contaminant removal. Processed materials include digestate (DIG) and biochar (BC), whereas unprocessed materials comprise residues such as orange peels, olive stones, pistachio shells, spent mushroom substrate, and wheat straw. Their widespread availability and low cost make them suitable candidates for sustainable strategies in soil remediation, wastewater treatment, and carbon sequestration.

.

1.1.1 Processed biosorbents

Digestate - Anaerobic digestion is a complex biological process through which organic matter is degraded by specialized microbial consortia in the absence of oxygen, resulting in the production of biogas and DIG. Biogas is mainly composed of methane (CH_4) and carbon dioxide (CO_2) and represents a renewable energy source (Qayyum et al. 2024). The methane content of biogas varies depending on the type of digested organic matter and the operating conditions of the process, typically ranging from approximately 50% to 80%. DIG is the solid and liquid by-product of the process, characterized by a significant content of nutrients and partially stabilized organic carbon (Guan et al. 2024).

From a biochemical perspective, anaerobic digestion proceeds through a sequence of interdependent microbial transformations that occur in four main stages. During the initial hydrolysis phase, organic macromolecules, such as polysaccharides, proteins, and lipids are broken down into low-molecular-weight soluble compounds, making them available to fermentative microorganisms. The products of hydrolysis are subsequently converted during acidogenesis into a mixture of volatile fatty acids, alcohols, molecular hydrogen (H_2), and CO_2. In the following acetogenesis stage, these

intermediates are further transformed predominantly into acetic acid (CH_3COOH), H_2, and CO_2, which constitute the main precursors for the final phase, i.e. methanogenesis, during which methanogenic microorganisms convert CH_3COOH and H_2 into CH_4, thereby determining the overall energy yield of anaerobic digestion.

The efficiency and stability of the process strongly depend on the balance among the different microbial communities involved and are influenced by operational parameters such as temperature, pH, hydraulic retention time, and the carbon-to-nitrogen ratio of the substrate (Basinas et al. 2025). The amount of biogas produced depends on the chemical composition of the feedstock, the presence of lignocellulosic residue, and the particle size of the starting biomass.

In addition to biogas production, anaerobic digestion plays a strategic role in the sustainable management of agricultural and agro-industrial wastes (Dinca et al. 2025). The resulting DIG can be valorised in agriculture as a soil amendment, contributing to nutrient recycling and the improvement of soil chemical and physical properties (Holatko et al.2023). Moreover, anaerobic digestion promotes the biodegradation of labile organic fractions, resulting in the partial stabilization of carbon through the enrichment of more recalcitrant organic compounds, with potential benefits in terms of increasing soil organic carbon content and mitigating greenhouse gas emissions (Sinatra et al. 2024). In environmental remediation strategies, this by-product can be exploited as biosorbent of various types of pollutants (Loffredo et al. 2021). In this context, anaerobic digestion can be regarded as a key technology within the framework of the circular economy and the transition toward more sustainable energy and agricultural systems.

Biochar - BC is a solid carbonaceous material obtained from the thermochemical conversion of biomass under conditions of limited or absent oxygen, through the process of gasification or pyrolysis, respectively. (Lehmann & Joseph 2009). Although this material has been produced and investigated for nearly two decades, a harmonized regulatory framework at the European level was introduced only with Regulation (EU) 2019/1009, which established specific requirements for its production, commercialization, and use as a soil improver. Scientific and practical interest in BC has increased considerably in recent years due to its physicochemical properties, environmental stability, and multifunctionality in agricultural, environmental, and energy-related applications (Ojeda et al., 2024; Xia et al., 2023).

BC is mainly produced through pyrolysis, a process typically carried out within a temperature range of 300–700 °C, depending on the characteristics of the feedstock and the intended application of the final material (Dayoub et al., 2024). Relatively low pyrolysis temperatures generally promote higher BC yields and a greater abundance of surface functional groups, whereas higher temperatures lead

to increased aromaticity, porosity, and carbon stability (Abdullah et al., 2023). Under more severe conditions, such as temperatures above 700 °C (800–1000 °C) and limited oxygen availability, typical of gasification processes, BC yield is lower and its structural properties are significantly altered., Tong et al. (2019) showed that as the pyrolysis temperature increases, the surface structure of biomass-derived char is progressively degraded, while pore structure parameters, including specific surface area, total pore volume, and average pore diameter, increase.

At higher pyrolysis temperature, the biomass char has more micro- and mesoporous. Yue et al. (2023) demonstrated that, as the gasification temperature increases, the intensities of the characteristic peaks of the functional groups on the surface of the biochar gradually decrease. Specifically, the aliphatic C–H groups (–CH_3 and –CH_2–) show a reduction in intensity. A similar trend is evident for carbonyl groups (C=O). Ether linkages (C–O–C) and in-plane C–H vibrations also decrease. Furthermore, hydroxyl groups (–OH) exhibit a marked decline. Finally, a reduction is also observed in the signals related to out-of-plane C–H bending vibrations.

In addition to the byproduct BC, pyrolysis and gasification generate valuable products, such as bio-oil and syngas. Bio-oil is a complex mixture of organic compounds that can be used as a fuel or as a source of value-added chemicals, while syngas, mainly composed of H_2, CO, CH_4, and CO_2, can be exploited for energy production or as an intermediate in industrial processes. The relative distribution of these products strongly depends on the operating conditions, particularly temperature, residence time, and heating rate (Lesiak 2024).

From a structural perspective, biochar is characterized by a high specific surface area, well-developed porosity, and remarkable chemical stability, properties that make it particularly suitable for interactions with a wide range of contaminants (Carnimeo et al. 2023). The presence of surface functional groups containing oxygen, nitrogen, and sulfur promotes both physical and chemical adsorption, rendering biochar effective for the removal and immobilization of organic and inorganic pollutants in contaminated soils and water systems.

In the agricultural context, the application of BC to soil can improve its physical, chemical, and biological properties by enhancing water-holding capacity, nutrient availability, and microbial activity (Xu et al. 2023, He et al. 2023). Moreover, due to the high stability of its aromatic structure, BC contributes to the increase of stable soil organic matter, representing a promising strategy for long-term carbon sequestration and climate change mitigation (Guo et al. 2025).

Overall, BC fits well within the frameworks of the circular economy and the bioeconomy, as it enables the valorisation of agricultural and agro-industrial waste into a value-added material that can

be used as biosorbent. However, the heterogeneity of BC, arising from both the feedstock and the production conditions, requires its in-depth characterization and a critical evaluation of its performance based on specific environmental and agronomic applications.

1.1.2 Unprocessed biosorbents

Orange peels - Citrus cultivation plays a central role in global fruit production, with worldwide yields surpassing 170 million tons annually, more than half of which are oranges (approximately 58%). In the Mediterranean region, Italy stands out as one of the principal citrus producers, following Spain, and the combined output of these two countries accounts for nearly four-fifths of total citrus production in Europe (FAOSTAT 2023). At the national level, citrus orchards occupy roughly 170,000 hectares, with average production levels reaching around 3 million tons per year over the last five years (FAOSTAT 2023). Orange peels (OP) are an abundant by-product of the citrus processing sector (60-65%) and constitute a biomass of considerable interest for agricultural and environmental applications (Consoli et al. 2023). Their valorisation is in line with the principles of the circular economy, allowing the reduction of organic waste and converting a low-value residue into a functional resource (Islam et al. 2023).

As regards the chemical composition, OP are mainly composed of cellulose, hemicellulose, pectin, lignin, phenolic compounds, flavonoids, and essential oils. The abundance of oxygen-containing functional groups (–OH, –COOH) confers a strong affinity for compounds and metals, making them particularly suitable for the retention of organic and inorganic pollutants (Duwiejuah et al. 2024). In fact, the adsorption capacity depends on the surface chemistry and the distribution of polar and nonpolar domains, as well as the functional groups present. Polar domains, characterised by the presence of oxygen- and nitrogen-containing functional groups, enable interactions in which charge separation predominates. These domains are therefore effective in interacting with similarly polar moieties of other molecules (including potential contaminants) or with ions in solution. These ions range from heavy metals and potentially toxic elements to ions whose excessive concentration may cause stress to various environmental compartments, particularly following interactions with the biosphere.In contrast, nonpolar domains consist of carbon chains or aromatic rings only, promoting interactions with similarly nonpolar components.

Several studies have demonstrated the effectiveness of OP in the removal of heavy metals, dyes, pesticides, and emerging contaminants (Michael-Igolina et al. 2023, Honorine et al. 2023, Khalfaoui et al. 2024). Overall, OP represent a typical agricultural residue with high valorisation potential.

Their recycling can combine sustainable waste management with useful applications in environmental remediation and soil quality improvement.

Olive stones -The olive tree (*Olea europaea* L.) is one of the most widely cultivated and economically relevant crops in the Mediterranean region and represents a key component of agricultural production at the global scale. Mediterranean countries such as Spain, Italy, and Greece are consistently among the leading producers, collectively contributing the majority of European and global production (Mairech et al. 2021). The olive oil industry represents a strategic agro-industrial sector within the European Union, with annual production reaching several million tons and supporting a complex supply chain that includes cultivation, harvesting, processing, and commercialization (Sun et al. 2025). The large-scale processing of olives for oil extraction inevitably generates significant amounts of solid and liquid residues. Among these by-products, olive stones (OS) represent 20.2%-38.2% of the total weight of olive (El Fessikh et al. 2025). OS are the hard, lignocellulosic inner part of the olive fruit. They are commonly referred to as the endocarp and are obtained through a mechanical separation process that occurs during or immediately after olive oil extraction.

OS are mainly composed of a lignocellulosic matrix rich in lignin, cellulose and hemicellulose, which confers good structural resistance and a high carbon content (Oncel & Ozbek 2025). Owing to their abundance and local availability in olive-growing regions, OS can be directly applied, without significant pretreatment, in specific agricultural and environmental contexts. From an agronomic perspective, the direct application of OS to soil can contribute to the improvement of soil physical properties, particularly by increasing porosity and enhancing aeration and drainage (El Fessikh et al. 2025). Their lignocellulosic structure, characterized by a high resistance to biological degradation, results in slow decomposition rates in soil, allowing for a fairly stable supply of organic carbon and favouring carbon accumulation over the medium to long term.

In environmental applications, untreated OS have also been used as raw biosorbent material, owing to the presence of surface functional groups capable of interacting with various chemical species (Ezzahi et al. 2025). Their direct use may still be advantageous in low-cost applications or preliminary mitigation strategies where operational simplicity and overall sustainability are key requirements.

Pistachio shells - Pistachio shells (PS) are an abundant lignocellulosic by-product generated by the nut-processing industry during pistachio production, a very important agricultural commodity worldwide. The shells account for a significant fraction of the total fruit mass and, due to the

continuous increase in global pistachio consumption, their management has become an issue of growing environmental and economic relevance (Fereidooni et al. 2024).

PS composition consists mainly of cellulose (approximately 40–45%), hemicellulose (20–30%), and lignin (25–30%), which are typical components of lignocellulosic biomass (Ozbek et al. 2020). This composition provides the material with high mechanical resistance, structural rigidity, considerable carbon content, as well as a naturally porous structure that promote its interaction with a great variety of chemical compounds.

The overall characteristics of PS make it a promising material for several applications. In agriculture, PS can be used as an organic soil amendment or as a component of plant growing substrates, contributing to soil structure, aeration, and water retention (Suarez-Caceres et al. 2025). However, due to their high lignin content, PS exhibit slow biodegradation rates, enabling a gradual release of organic carbon and promoting medium- to long-term carbon accumulation in soils.

In environmental applications, PS have been used as a low-cost biosorbents for contaminant removal from aqueous media, including dyes, heavy metals, and organic pollutants (Kayranli 2021, Zulkefli et al. 2025, Kaur et al. 2023). Their porous structure and surface functional groups enable interactions such as physical adsorption, hydrophobic interactions, and ion exchange. Although untreated PS generally exhibit lower adsorption efficiency than activated materials or biochar, their direct use may be advantageous in low-cost or preliminary remediation contexts. Overall, PS represent a clear example of agricultural residue with high valorisation potential, offering multiple application choices ranging from soil amendment to environmental remediation to energy production, in line with the principles of sustainable resource management and the circular economy (Maklavani et al. 2025).

Spent fungal growth substrate of *Pleurotus eryngii* - The spent fungal growth substrate (SFGS) of *P. eryngii* substrate is a residual biomass of growing scientific and practical interest, particularly in the context of the valorisation of agro-industrial by-products and circular economy strategies (Kim et al. 2025). This material originates from the production cycle of the king oyster mushroom. This mushroom is one of the most cultivated and commercially prized species, especially in southern Italy, due to its ease of production and inexpensiveness (Melanuouri et al. 2019).

Despite its potential, at the end of cultivation, SFGS is often regarded as waste, although it possesses significant environmental and technological value. The cultivation substrate of *P. eryngii* consists of wheat straw, residual fungal mycelium, and small amounts of exhausted sugar beet pulp. During fungal growth, the mycelium exhibits intense enzymatic activity typical of white-rot fungi,

leading to partial degradation of lignin, hemicellulose and cellulose. This biological process induces substantial modifications in the chemical and physical structure of the substrate, resulting in enrichment with fungal biomass, organic nitrogen, and reactive functional groups (Bisht & Negi 2025, Makkar et al. 2025).

Noteworthy, the production of non-specific extracellular oxidative enzymes (including laccases, manganese peroxidases and lignin peroxidases) by P. eryngii is responsible not only for the breakdown of lignocellulosic polymers but also for the degradation of numerous phenolic and non-phenolic contaminants, especially in the presence of redox-active mediators (Loffredo et al. 2016; Anton-Herrero et al. 2022). Even after the production cycle has ended, the spent substrate retains a porous structure, a high organic matter content and residual biological activity, making it a functionally active material. (Wang et al. 2025, Eliescu et al. 2020). Owing to these properties, the SFGS has attracted growing attention for various environmental applications. Traditionally used as a soil amendment or as a component in composting and vermicomposting processes (Abdeldaym et al. 2018, Frutos et al. 2016), it also shows considerable potential as low-cost adsorbent for the removal of contaminants from aqueous matrices (Schallemberger et al. 2022, Gupta et al. 2024).

In the context of growing environmental pressure and the urgent need for sustainable solutions for wastewater treatment and soil remediation, the SFGS emerges as a promising resource capable of integrating waste management with environmentally relevant technological applications. Its valorisation not only contributes to reducing the environmental impact of mushroom cultivation but also supports the development of innovative and sustainable materials for soil remediation and water treatment processes.

Growth Wheat straw – Growth wheat straw (GWS) is one of the inexpensive and abundant by-products of wheat cultivation. Every year, hundreds of millions of tons are produced worldwide, and most of it is either burned or left on agricultural land to naturally decompose (Sodkouieh et al. 2022). WS consists primarily of cellulose (around 30-40%), hemicellulose (20-30%) and lignin (15-20%). These proportions can vary depending on the wheat variety, pedoclimatic condition and the agricultural practices employed (Zhang et al. 2022). Therefore, GWS structure is a fibrous and relatively recalcitrant matrix, largely due to its lignin content and the complex linkages among structural polymers. This recalcitrance limits its natural biodegradability but simultaneously provides structural stability (Li et al. 2016). GWS is an important component of the cultivation substrates used for *Pleurotus spp*. and due to its abundance, low cost, and favourable chemical composition, it has also been investigated for environmental applications as a biosorbent (Dutta et al. 2015, Laidani et al.2019).

1.2 Humic Acid

Humic acid (HA) is a major fraction of humic substances, which also include fulvic acids and humin, and represent one of the most important components of soil organic matter (Senesi and Loffredo 2018). They originate from the long-term decomposition and transformation of plant and microbial residues through biological and chemical processes known as humification. As a result, humic acids are not single compounds but rather complex, heterogeneous macromolecular systems with variable composition and structure.

From a chemical perspective, humic acids are characterized by a high content of aromatic and aliphatic carbon structures and a wide range of oxygen-containing functional groups, such as carboxyl (-COOH), phenolic and alcoholic hydroxyl (-OH), carbonyl, and quinone groups. These functional groups give humic acids a high cation exchange capacity and strong reactivity, enabling them to interact with metal ions, organic compounds, and biological membranes through mechanisms such as complexation, ion exchange, hydrogen bonding, and hydrophobic interactions (Senesi and Loffredo 2018).

Humic acids play a crucial role in soil fertility and structure. They contribute to the formation and stabilization of soil aggregates, improve water retention and aeration, and enhance nutrient availability by chelating essential micronutrients while reducing their leaching losses.

1.3 Soil phytopathogenic fungi

Soil phytopathogenic fungi can infect plants through the root system or other underground tissues, causing a wide range of plant diseases that impair crop growth, yield, and overall health (Raaikimakers et al. 2008). These pathogens belong to various groups of filamentous fungi and fungus-like microorganisms and can survive in soil as mycelium, spores, or other resistant structures for long periods, even in the absence of an active host organism (Kay et al. 2024). Among soil phytopathogenic fungi, some species are particularly notable for their impact on agricultural and horticultural crops and for their ability to persist in the soil for long periods; three of these are *Armillaria Mellea, Fusarium Culmorum and Verticillium Dhaliae*.

A. mellea is a basidiomycete fungus responsible for so-called fibrous root rot. It is a polyphagous pathogen that affects numerous tree species and perennial crops, causing progressive plant decline (Devokta & Hammerschmidt 2020). *F. culmorum* is a filamentous fungus belonging to the genus *Fusarium*, known for causing root and crown rot as well as vascular diseases in various herbaceous crops (Scherm et al. 2019). *V. dahliae* is another important soil-borne pathogen responsible for

verticillium wilt, a vascular disease that causes yellowing, wilting, and reduced plant growth (Zhang et al. 2022). These soil phytopatogenic fungi pose a significant threat to crop health and yield, emphasizing the need for effective management strategies.

1.4 Wastewater

Wastewater refers to water whose original quality has been altered as a result of civil, industrial, or agricultural activities. Its management is a global issue of primary importance, as it is closely linked to the protection of water resources, public health, and environmental sustainability (Etsuyankpa et al. 2024). Wastewater contains a variable mixture of organic and inorganic substances, suspended solids, nutrients and microorganisms with a composition that strongly depends on its source (Silva 2023). The unregulated release of wastewater into the environment can degrade the quality of both surface and groundwater resources, stimulate eutrophication processes and lead to harmful effect to aquatic ecosystems (Preisner et al. 2020).

Wastewater treatment aims to reduce the pollutant load and restore conditions compatible with its discharge into the environment or with its reuse. To safeguard human health and the environment, when used for agricultural irrigation, it is essential that minimum water quality standards are met (Hernandez-Zanoletty et al. 2025). This condition is clearly stated by the Regulation (EU) 2020/741. Traditionally, treatment systems rely on a combination of physical, chemical, and biological processes designed to progressively improve water quality. At present, the most commonly employed treatment methods include ozonation, advanced oxidation processes, membrane filtration, reverse osmosis, and adsorption techniques.

The ozonation process is an advanced wastewater treatment technology based on the use of ozone (O_3). O_3 is a powerful oxidant capable to degrade a wide variety of recalcitrant organic contaminants and inactivating pathogens in wastewater (Mainardis et al. 2020). Thanks to its high oxidation potential, it can transform persistent substances such as solvents, agrochemicals, pharmaceuticals. Beyond its oxidative action, ozone is also effective against a broad range of pathogenic microorganisms including viruses, bacteria and protozoa (Leonteff et al. 2025). However, the industrial applications of ozonation are limited by its high costs and low ozone utilization caused by the mass transfer rate of ozone (Wu et al. 2012).

The advanced oxidation processes included electrochemical oxidation, fenton oxidation, photolysis and photocatalysis, radiation and sonolysis. The oxidation process is based on the generation of reactive oxygen species, such as hydroxyl radicals, in amounts sufficient to effectively treat

effluents. These reactive species are free radicals characterized by a very high redox potential, which enables them to readily oxidize other molecules while undergoing reduction themselves. Such radicals play a fundamental role in triggering advanced oxidation processes, as they are capable of breaking down complex and toxic pollutants into simpler, less harmful compounds (Saravanan et al.2022). These oxidation processes present different limitations. Some of these exhibit optimal efficiency under highly acidic conditions, thus requiring the use of acidifying agents, which not only increase operational complexity but also elevate the overall treatment costs. The high energy demands of certain processes further compound this issue. Furthermore, some of these inadvertently produce secondary pollutants, including toxic intermediate byproducts, during the degradation of complex organic compounds (Satyam & Patra 2025).

Membrane filtration is a process that uses membranes acting as molecular sieves, integrated into a film structure with or without fine pores or a mesh, to enable the separation of small particles and molecules. Membranes are typically classified based on their pore size, driving force, morphology, and material composition, which can be either organic or inorganic. The pore size is a critical determinant in membrane selection, influencing its suitability for separating different components in a mixture (Ezugbe & Rathilal 2020). Reverse osmosis is an advanced membrane filtration. It is based on the application of a pressure higher than the natural osmotic pressure, which forces water to pass through a semi-permeable membrane while retaining most dissolved solutes (Malaeb & Ayoub 2010). Like those presented previously, this method of treating wastewater also has several limitations such as the production of concentrated waste streams, membrane fouling and high costs (Azmi et al. 2025).

The process of adsorption relies on specific physicochemical interactions between adsorbent surfaces and target pollutants, usually resulting in the selective adsorption and, thereby, the effective removal of target pollutants from complex water matrices or at trace concentrations (Hu & Hao 2025). The possibility of using coproducts and by-products of bioenergy to decontamine wastewater makes this method more sustainable than those previously discussed (Loffredo 2022).

The increasing anthropogenic pressures and the growing complexity of human activities have, in fact, led to the need for increasingly effective and sustainable approaches. Therefore, wastewater is no longer considered solely as a waste product but rather as a potential resource to be managed in an integrated manner. The recovery of water is now a strategic objective, in line with the principles of circular economy and sustainable development (Zouboulis & Peleka 2025). Consequently, efficient wastewater management represents a key element in ensuring environmental protection and the responsible use of water resources

1.5 Contaminants of emerging concern (CECs)

Contaminants of emerging concern (CECs) are a broad and heterogeneous class of chemical compounds, either natural or synthetic, whose presence in the environment has only relatively recently been recognized and whose potential impacts on human health and ecosystems are not yet fully understood (Sauvè & Desrosiers 2014) .

This category encompasses a wide range of organic pollutants , including pharmaceuticals and their metabolites, personal care products, endocrine-disrupting compounds, industrial additives, per- and polyfluoroalkyl substances (PFAS), agrochemicals, and inorganic pollutants such as metal nanoparticles, that can as well considered together with heavy metals and analogous potential toxic elements (Cr, Pb, Hg, Cd, As). These contaminants are frequently detected in environmental matrices such as surface waters, groundwater, soils, and wastewater, typically at trace concentrations (ng/L–µg/L), yet they can, or could, still exert significant biological effects (Tran et al. 2018).

The growing concern surrounding CECs arises from several key factors: their continuous input into the environment due to human activities, their persistence and, in some cases, resistance to degradation, as well as their potential for bioaccumulation and biomagnification along the food chain. Even at low concentrations, many of these compounds can interfere with biological systems, leading to effects such as endocrine disruption, ecotoxicity in aquatic organisms, and the proliferation of antimicrobial resistance. Additionally, the combined presence of multiple CECs may result in mixture effects, which are often difficult to predict and assess using traditional risk evaluation frameworks (Kidd et al. 2024).

1.5.1 Organic pollutants

Among the CEC great interest exist for organic pollutants, that are the main target of this thesis. They are one of the two main classes of CEC and they originate from multiple anthropogenic sources. In particular, so called anthropogenic organic pollutants (AOPs) are hazardous chemical substances that have attracted significant international attention in recent years in academic research and policy boards. These compounds exhibit distinct physicochemical properties that allow them to bioaccumulate, persist in the environment by resisting degradation, and be transported over long distances (Mandal et al. 2024), thus determining negative effects on ecosystems and human health (Lu et al. 2024).

From a structural point of view, many AOPs contain aromatic rings, heterocyclic structures, or long aliphatic chains, often substituted with halogens, nitro, hydroxyl, carboxyl, or amino groups (El-

Shahavi et al.2010). Key physicochemical parameters governing the behaviour of organic pollutants include molecular weight, water solubility, and octanol–water partition coefficient (Kow) (Linkov et al. 2005). Compounds with high Kow values are hydrophobic and are preferentially adsorbed by organic matter, C-rich sediments, and biological tissues; in this last case, they bioaccumulate in animal and plant organs.

Conversely, more polar or ionizable compounds exhibit higher mobility in aqueous environments and are more difficult to remove.

AOPs include agrochemicals, industrial byproducts, endocrine-disrupting chemicals, pharmaceuticals, perfluorinated alkylated substances (PFAS) and others. Reducing the bioavailability of these compounds in soil and minimizing wastewater contamination are crucial for achieving the sustainable development goals.

1.5.2 Agrochemicals

Agrochemicals are used in agriculture to protect plants from diseases, pests, and weeds. This category mainly includes insecticides, fungicides, herbicides, acaricides, nematicides and plant growth regulators. Agrochemicals have been used for decades in conventional agriculture to ensure crop yields and reduce losses due to biotic attacks. However, their use is not without challenges. These substances can persist in the environment, migrate to surface and groundwater, accumulate in soils and living organisms, and sometimes exert toxic effects on non-target flora and fauna (Ortiz-Martinez et al. 2024).

The mobility and persistence of agrochemicals depend on their chemical and physical properties, such as water solubility, hydrophobicity, volatility, and resistance to biodegradation (Arp & Hale 2022). Therefore, sustainable management of agrochemicals requires integrated strategies, including the rational use of controlled doses, targeted application techniques, and the promotion of low-impact agricultural practices.

1.5.3 Endocrine-disrupting chemicals

Endocrine-disrupting chemicals (EDCs) are exogenous compounds of industrial origin that may interfere with synthesis, secretion, transport, metabolism of natural hormones, thus altering the endocrine and homeostatic systems (Loffredo 2022). These compounds are ubiquitously detected in consumer products, food and beverages containers, personal care products, and household cleaning products (European Commision, 2025).

EDCs comprise xenoestrogen compounds, namely synthetic biologically active compounds capable of mimicking the action of the steroid hormone 17β-estradiol. Owing to their extensive occurrence

in the environment, these substances are commonly referred to as environmental estrogens (EEs). According to their chemical structure, EEs can be classified into phenolic environmental estrogens (PhEEs), such as bisphenol A, nonylphenol, octylphenol and steroidal environmental estrogens (StEEs), such as estrone, 17β-estradiol, estriol (Loffredo 2022).

These pollutants can reach soil and wastewater through multiple pathways, mainly associated with anthropogenic activities and the life cycle of the products that contain them (Rodriguez-Hernandez et al. 2022). It is essential to develop and implement sustainable strategies aimed at preventing their entry into the food chain.

1.5.4 Pharmaceuticals

Pharmaceuticals are widely consumed and disposed of by industries, manufacturing plants, hospitals, farms, and institutions, making them a significant source of water and soil pollution (Hama Aziz et al., 2025). These compounds include antibiotics, analgesics, anti-inflammatories, hormones, beta-blockers, and lifestyle drugs, which have been detected in soils and aqueous systems at concentrations ranging from ng to mg L^{-1} (Sanusi et al., 2023).

These molecules can reach environmental systems through multiple routes, such as effluent release from wastewater treatment facilities, agro-zootechnical runoff, and inappropriate disposal of expired or unused pharmaceuticals. Their persistence and widespread occurrence raise significant concerns about possible adverse effects on ecosystems and human health (Szarka et al., 2024). Moreover, once pharmaceuticals enter aquatic environments, they can undergo various transformation and degradation processes until they are fully metabolized. However, both the parent compounds and their transformation products (metabolites) may persist, accumulate in water bodies and sediments, and bioaccumulate within ecosystems, where they can exert adverse effects on a wide range of non-target organisms (Bavumiragira et al., 2022).

Antibiotics are considered one of the most critical classes of pharmaceuticals due to the potential threats they pose to aquatic ecosystems and human health. Their presence in wastewater discharge can promote the development and spread of antimicrobial-resistant bacteria, thereby disrupting ecological balance and increasing environmental and public health risks (Sanusi et al., 2023). Hence, the urgent need to monitor pharmaceutical residues in urban wastewater and intervene with suitable advanced treatment strategies to mitigate the environmental and health risks associated with these compounds.

1.5.5 Per- and polyfluoroalkyl substances (PFAS)

Per- and polyfluoroalkyl substances (PFAS) are synthetic fluorinated chemicals distinguished by their remarkable chemical and thermal stability, as well as by unique surfactant, water-repellent, and oil-repellent properties (Addicks et al. 2025). Owing to these characteristics, PFAS have been extensively used in a wide range of industrial and consumer applications, including textiles, food packaging, leather products, aqueous film-forming foams, floor coatings, and electroplating processes (Dai et al. 2025).

According to the nature of their functional groups, PFAS include two families: perfluoroalkyl carboxylic acids (PFCAs) and perfluoroalkyl sulfonates (PFSAs). Additionally, PFAS are often classified as long- or short-chain compounds based on the length of the perfluorinated carbon chain. Long-chain PFAS comprise PFCAs containing at least seven perfluorinated carbon atoms and PFSAs containing at least six perfluorinated carbon atoms, as well as substances that can degrade into long-chain perfluoroalkyl acids (PFAAs) (Li et al. 2023). In contrast, short-chain PFAS are more frequently detected in groundwater, a behaviour commonly attributed to their lower Kow and higher water solubility. Due to their strong resistance to environmental degradation, PFAS are often referred to as “forever chemicals,” leading to their persistence and accumulation in water, soil, and living organisms (Brunn et al. 2024). This widespread occurrence raises significant concerns, as exposure to PFAS has been associated with a range of adverse health effects, including immunotoxicity, reproductive and renal disorders, and reduced birth weight (Sharma et al. 2024).

In summary, these characteristics identify PFAS as a class of emerging contaminants of major environmental and public health concern, highlighting the urgent need for effective monitoring, risk assessment, and the development of sustainable remediation strategies.

Objectives

A first objective of this PhD thesis was to investigate the capacity of selected biosorbents to adsorb various organic pollutants. The materials examined include both bioenergy byproducts, namely DIG and BC, and several unprocessed waste biomasses, such as OP, OS, PS, SPS, and WS. To achieve this objective, adsorption and desorption experiments were carried using different classes of agrochemicals, including the fungicides boscalid and metalaxyl-M, the herbicides metribuzin, oxyfluorfen and cycloxydim, the insecticide imidacloprid, and the EDC bisphenol A (BPA). In particular, the ability of BC to reduce the leaching of boscalid in soil was evaluated.

Preliminarily, various characterization techniques were applied to the biosorbents in order to gain qualitative insights into the adsorption process, with particular emphasis on the interaction mechanisms between the target molecules and the different materials. Successively, adsorption kinetics, as well as adsorption and desorption isotherms, were studied and the corresponding sorption parameters were calculated by modelling experimental data with appropriate theoretical equations.

Another objective of this PhD thesis was to investigate the effects of DIG, alone and in combination with a soil HA, on the in vitro growth of three soil phytopathogenic fungi: *A. mellea*, *F. culmorum*, and *V. dahliae*. In addition, germination tests were carried out on cucumber and sunflower plants to evaluate the phytotoxicity and biostimulatory properties of BC.

Finally, this thesis aimed to assess the capacity of BC to remove organic pollutants from industrial and municipal wastewaters. Before and after treatment with BC, the treated wastewater was evaluated for its phytotoxic effects on the germination of different horticultural species, namely cucumber, lettuce and tomato. Part of this latter investigation was carried out during a four-month research internship at the "Centro de Investigaciones de la Energía Solar" (CIESOL), University of Almería, Spain.

References

Abdeldaym, E. A., Traversa, A., Cocozza, C., & Brunetti, G. (2018). Effects of a 2-Year Application of Different Residual Biomasses on Soil Properties and Potato Yield. Clean - Soil, Air, Water, 46(12). https://doi.org/10.1002/clen.201800261

Abdullah, N., Mohd Taib, R., Mohamad Aziz, N. S., Omar, M. R., & Md Disa, N. (2023). Banana pseudo-stem biochar derived from slow and fast pyrolysis process. Heliyon, 9(1). https://doi.org/10.1016/j.heliyon.2023.e12940

Addicks, G. C., Rowan-Carroll, A., Leingartner, K., Williams, A., Meier, M. J., Lorusso, L., Yauk, C. L., & Atlas, E. (2025). Identification of four mechanisms of toxicity for per- and polyfluoroalkyl substances through transcriptomic profiling in human liver spheroids exposed to 24 PFAS. Toxicological Sciences, 207(1), 161–180. https://doi.org/10.1093/toxsci/kfaf075

Antón-Herrero, R., García-Delgado, C., Baena, N., Mayans, B., Delgado-Moreno, L., & Eymar, E. (2022). Assessment of Different Spent Mushroom Substrates to Bioremediate Soils Contaminated

with Petroleum Hydrocarbons. Applied Sciences (Switzerland), 12(15). https://doi.org/10.3390/app12157720

Arp, H. P. H., & Hale, S. E. (2022). Assessing the Persistence and Mobility of Organic Substances to Protect Freshwater Resources. In ACS Environmental Au (Vol. 2, Number 6, pp. 482–509). American Chemical Society. https://doi.org/10.1021/acsenvironau.2c00024

Azmi, L. S., Jabit, N. 'Ain, Ismail, S., Ku Ishak, K. E. H., & Abdullah, T. K. (2025). Membrane filtration technologies for sustainable industrial wastewater treatment: a review of heavy metal removal. In Desalination and Water Treatment (Vol. 323). Elsevier B.V. https://doi.org/10.1016/j.dwt.2025.101321

Basinas, P., Chamrádová, K., Rybková, Z., Rusín, J., & Malachová, K. (2025). Biological pretreatment of anaerobic digestion solid by-product with white rot fungi: Assessment of digestate delignification and investigation of process parameters improving the biodegradation performance of sludge. Chemical Engineering Journal, 512. https://doi.org/10.1016/j.cej.2025.162292

Bavumiragira, J. P., Ge, J., & Yin, H. (2022). Fate and transport of pharmaceuticals in water systems: A processes review. In Science of the Total Environment (Vol. 823). Elsevier B.V. https://doi.org/10.1016/j.scitotenv.2022.153635

Bisht, T., & Negi, P. S. (2026). Mushroom by-products as ingredients for food applications: A review of health and sustainability benefits. Food and Humanity, 6. https://doi.org/10.1016/j.foohum.2025.100966

Brunn, H., Arnold, G., Körner, W., Rippen, G., Steinhäuser, K. G., & Valentin, I. (2023). PFAS: forever chemicals—persistent, bioaccumulative and mobile. Reviewing the status and the need for their phase out and remediation of contaminated sites. In Environmental Sciences Europe (Vol. 35, Number 1). Springer. https://doi.org/10.1186/s12302-023-00721-8

Carnimeo, C., Colatorti, N., D'Orazio, V., Trotti, P., & Loffredo, E. (2023). Potential of Biochar from Wood Gasification to Retain Endocrine Disrupting Chemicals. Materials, 16(2). https://doi.org/10.3390/ma16020569

Cho, B. G., Lee, J. H., Kim, H. I., Mun, S. B., Jin, S. R., Kim, D. G., Cho, C. W., & Yun, Y. S. (2023). Modeling for the estimating the adsorption property of fruit waste-based biosorbents for the removal of organic micropollutants. Environmental Research, 225. https://doi.org/10.1016/j.envres.2023.115593

Consoli, S., Caggia, C., Russo, N., Randazzo, C. L., Continella, A., Modica, G., Cacciola, S. O., Faino, L., Reverberi, M., Baglieri, A., Puglisi, I., Milani, M., Longo Minnolo, G., & Barbagallo, S. (2023). Sustainable Use of Citrus Waste as Organic Amendment in Orange Orchards. Sustainability (Switzerland), 15(3). https://doi.org/10.3390/su15032482

Cristóvão, M. B., Sério, J., Marques, A. P., Bento-Silva, A., Gossard, M., Vergara-Diaz, O., Silva, A. F., Nunes, M., Bronze, M. R., de Oliveira, P. B., Crespo, M. T. B., Crespo, J. G., & Pereira, V. J. (2026). Treatment of wastewater effluents using nanofiltration and low pressure UV photolysis to produce high quality water for food production. Water Research, 289. https://doi.org/10.1016/j.watres.2025.124782

Dai, Y., Ding, D., Cui, M., Duan, P., Liu, Y., Liu, X., Yue, T., Zhao, J., Wang, Z., & Xing, B. (2025). Biotransformation of per- and polyfluoroalkyl substances (PFAS) in organisms. In Chemical Engineering Journal (Vol. 524). Elsevier B.V. https://doi.org/10.1016/j.cej.2025.168618

Dayoub, E. B., Tóth, Z., Soós, G., & Anda, A. (2024). Chemical and Physical Properties of Selected Biochar Types and a Few Application Methods in Agriculture. In Agronomy (Vol. 14, Number 11). Multidisciplinary Digital Publishing Institute (MDPI). https://doi.org/10.3390/agronomy14112540

Devkota, P., & Hammerschmidt, R. (2020). The infection process of Armillaria mellea and Armillaria solidipes. In Physiological and Molecular Plant Pathology (Vol. 112). Academic Press. https://doi.org/10.1016/j.pmpp.2020.101543

Dincă, M. N., Ferdeș, M., Zăbavă, B. Ștefania, Ionescu, M., Moiceanu, G., & Paraschiv, G. (2025). Effective Valorization of Anaerobic Digestate—A Sustainable Approach to Circular Economy. In Applied Sciences (Switzerland) (Vol. 15, Number 16). Multidisciplinary Digital Publishing Institute (MDPI). https://doi.org/10.3390/app15168939

Dutta, A., Diao, Y., Jain, R., Rene, E. R., & Dutta, S. (2016). Adsorption of Cadmium from Aqueous Solutions onto Coffee Grounds and Wheat Straw: Equilibrium and Kinetic Study. Journal of Environmental Engineering, 142(9). https://doi.org/10.1061/(asce)ee.1943-7870.0001015

Duwiejuah, A. B., Payne, J., & Yahaya, D. (2024). Adsorption of toxic metals from landfill leachate using orange and banana peel powders as adsorbents. Sustainable Environment, 10(1). https://doi.org/10.1080/27658511.2024.2405295

El Fessikh, M., Elhrech, H., El Yahyaoui El Idrissi, A., Lee, L. H., Abdulmonem, W. Al, El Omari, N., & Bouyahya, A. (2025). Sustainable valorization of olive stone by-products: Opportunities and

challenges. In Journal of Food Composition and Analysis (Vol. 142). Academic Press Inc. https://doi.org/10.1016/j.jfca.2025.107495

Eliescu, A., Georgescu, A. A., Nicolescu, C. M., Bumbac, M., Cioateră, N., Mureșeanu, M., & Buruleanu, L. C. (2020). Biosorption of Pb(II) from Aqueous Solution Using Mushroom (Pleurotus ostreatus) Biomass and Spent Mushroom Substrate. Analytical Letters, 53(14), 2292–2319. https://doi.org/10.1080/00032719.2020.1740722

El-Shahawi, M. S., Hamza, A., Bashammakh, A. S., & Al-Saggaf, W. T. (2010). An overview on the accumulation, distribution, transformations, toxicity and analytical methods for the monitoring of persistent organic pollutants. In Talanta (Vol. 80, Number 5, pp. 1587–1597). Elsevier B.V. https://doi.org/10.1016/j.talanta.2009.09.055

Etsuyankpa, M. B., Augustine, A. U., Musa, S. T., Mathew, J. T., Ismail, H., Salihu, A. M., & Mamman, A. (2024). An Overview of Wastewater Characteristics, Treatment and Disposal: A Review. Journal of Applied Sciences and Environmental Management, 28(5), 1553–1572. https://doi.org/10.4314/jasem.v28i5.28

European Commission, Directorate-General for Health and Food Safety. (2025). Assessment of the experience gained from the application of the scientific criteria for the determination of endocrine-disrupting properties set under Regulation (EC) No 1107/2009 and Regulation (EU) No 528/2012 (pp. 1–34). European Commission https://health.ec.europa.eu/document/download/841bf3d9-33ab-4d4d-9fd2-22d99a9b492c_en?filename=endocrine_application-criteria_assessment_en.pdf

Ezugbe, E. O., & Rathilal, S. (2020). Membrane technologies in wastewater treatment: A review. In Membranes (Vol. 10, Number 5). MDPI AG. https://doi.org/10.3390/membranes10050089

Ezzahi, K., Rabichi, I., Rochdi, N., Idouhli, R., Hafidi, M., Baçaoui, A., Yaacoubi, A., Rochdi, R., & EL Fels, L. (2025). Innovative Dynamic Filtration of Olive Mill Wastewater: Comparing the Efficiency of Biochar and Olive Stone. Water, Air, and Soil Pollution, 236(9). https://doi.org/10.1007/s11270-025-08231-4

FAOSTAT. (n.d.). Retrieved January 27, 2026, from https://www.fao.org/faostat/en/#data/QCL

Fereidooni, L., Morais, A. R. C., & Shiflett, M. B. (2025). Environmental applications of pistachio waste: A review. In Journal of Environmental Management (Vol. 380). Academic Press. https://doi.org/10.1016/j.jenvman.2025.124927

Ferţu, D. I., Ciobanu, A. A., Cara, I. G., Motrescu, I., Ahmad, I., Nacu, G., & Bulgariu, L. (2024). Circular Approach of Using Soybean Biomass for the Removal of Toxic Metal Ions from Wastewater. Water (Switzerland), 16(24). https://doi.org/10.3390/w16243663

Frutos, I., García-Delgado, C., Cala, V., Gárate, A., & Eymar, E. (2017). The use of spent mushroom compost to enhance the ability of Atriplex halimus to phytoremediate contaminated mine soils. Environmental Technology (United Kingdom), 38(9), 1075–1084. https://doi.org/10.1080/09593330.2016.1217938

Ganesan, M., & Thiyagarajan, C. (2024). Adsorption and desorption kinetics of lead from aqueous solutions by biosorbents. Chemical Papers, 78(2), 993–1008. https://doi.org/10.1007/s11696-023-03136-0

Guan, D., Zhao, J., Wang, Y., Fu, Z., Zhang, D., Zhang, H., Xie, J., Sun, Y., Zhu, J., & Wang, D. (2024). A critical review on sustainable management and resource utilization of digestate. In Process Safety and Environmental Protection (Vol. 183, pp. 339–354). Institution of Chemical Engineers. https://doi.org/10.1016/j.psep.2024.01.029

Guo, Y., Sang, Z., Zhang, R., & Tan, L. (2025). Research Progress on the Coupling of Carbon Sequestration by Soil Biochar and the Treatment of Organically Polluted Soil. In Water, Air, and Soil Pollution (Vol. 236, Number 15). Springer Nature. https://doi.org/10.1007/s11270-025-08499-6

Gupta, G., Maurya, S., Jha, P. N., & Chauhan, P. S. (2024). Valorization of Spent Mushroom Substrate (SMS) as a sustainable approach to remediation of xenobiotic compounds in groundwater - A comprehensive review. Groundwater for Sustainable Development, 26. https://doi.org/10.1016/j.gsd.2024.101290

Hama Aziz, K. H., Mustafa, F. S., Karim, M. A. H., & Hama, S. (2025). Pharmaceutical pollution in the aquatic environment: advanced oxidation processes as efficient treatment approaches: a review. In Materials Advances (Vol. 6, Number 11, pp. 3433–3454). Royal Society of Chemistry. https://doi.org/10.1039/d4ma01122h

He, K., Liu, Q., Zhang, J., Zhang, G., & Li, G. (2023). Biochar Enhances the Resistance of Legumes and Soil Microbes to Extreme Short-Term Drought. Plants, 12(24). https://doi.org/10.3390/plants12244155

Hernández-Zanoletty, A., Berruti, I., Jambrina-Hernández, E., Oller, I., Polo-López, M. I., Plaza-Bolaños, P., & Agüera, A. (2025). Up-scaling solar photochemistry quaternary treatment of urban

wastewaters to a demonstrative level. Journal of Environmental Chemical Engineering, 13(3). https://doi.org/10.1016/j.jece.2025.116766

Holatko, J., Hammerschmiedt, T., Kucerik, J., Kintl, A., Baltazar, T., Malicek, O., Latal, O., & Brtnicky, M. (2023). Fertilisation of permanent grasslands with digestate and its effect on soil properties and sustainable biomass production. European Journal of Agronomy, 149. https://doi.org/10.1016/j.eja.2023.126914

Honorine, A. T., Daouda, A., Domga, T., Richard, D., & Bertrand, N. G. (2023). Efficient adsorption of tartrazine from an aqueous solution using a low-cost orange peel powder. Journal of Water and Health, 21(8), 1017–1031. https://doi.org/10.2166/wh.2023.033

Hu, Q., & Hao, L. (2025). Adsorption Technologies in Wastewater Treatment Processes. In Water (Switzerland) (Vol. 17, Number 15). Multidisciplinary Digital Publishing Institute (MDPI). https://doi.org/10.3390/w17152335

Imran-Shaukat, M., Wahi, R., & Ngaini, Z. (2022). The application of agricultural wastes for heavy metals adsorption: A meta-analysis of recent studies. Bioresource Technology Reports, 17. https://doi.org/10.1016/j.biteb.2021.100902

Islam, M. R., Wang, Q., Guo, Y., Wang, W., Sharmin, S., & Ebere Enyoh, C. (2023). Physico-Chemical Characterization of Food Wastes for Potential Soil Application. Processes, 11(1). https://doi.org/10.3390/pr11010250

Kaur, P., Kumar, A., Babu, J. N., & Kumar, S. (2023). Tetracycline removal via three-way synergy between pistachio shell powder, zerovalent copper or iron, and peroxymonosulfate activation. Journal of Hazardous Materials Advances, 12. https://doi.org/10.1016/j.hazadv.2023.100385

Kay, W. T., O'Neill, P., Gurr, S. J., & Fones, H. N. (2024). Long-term survival of asexual Zymoseptoria tritici spores in the environment. BMC Biology, 22(1). https://doi.org/10.1186/s12915-024-02060-3

Kayranli, B. (2022). Cadmium removal mechanisms from aqueous solution by using recycled lignocelluloses. Alexandria Engineering Journal, 61(1), 443–457. https://doi.org/10.1016/j.aej.2021.06.036

Khalfaoui, A., Benalia, A., Selama, Z., Hammoud, A., Derbal, K., Panico, A., & Pizzi, A. (2024). Removal of Chromium (VI) from Water Using Orange peel as the Biosorbent: Experimental, Modeling, and Kinetic Studies on Adsorption Isotherms and Chemical Structure. Water (Switzerland), 16(5). https://doi.org/10.3390/w16050742

Kidd, K.A., Backhaus, T., Brodin, T., Inostroza, P.A. and McCallum, E.S. (2024), Environmental Risks of Pharmaceutical Mixtures in Aquatic Ecosystems: Reflections on a Decade of Research. Environ Toxicol Chem, 43, 549-558. https://doi.org/10.1002/etc.5726

Kim, J. W., Dognini, C., Shams, A., Pecchia, J., Zhu, Y., Yang, Y., Jing, Y., & Gürsoy, B. (2026). From edible mushrooms to sustainable materials: Sound absorption of mycelium-based composites cultivated on spent mushroom substrates. Applied Acoustics, 241. https://doi.org/10.1016/j.apacoust.2025.111000

Kusuma, H. S., Amenaghawon, A. N., Darmokoesoemo, H., & Putra, N. R. (2025). Advancements in adsorption-based water purification: Multifunctional adsorbents, sustainability, and integration in wastewater matrices. In Journal of Molecular Structure (Vol. 1348). Elsevier B.V. https://doi.org/10.1016/j.molstruc.2025.143529

Laidani, Y., Henini, G., Hanini, S., & Fekaouni, A. (2019). STUDIES OF THE BIOSORPTION OF TEXTILE DYE ONTO WHEAT STRAW (Vol. 20, Number 4).

Lehmann J, Joseph S (2009) Biochar for environmental management: science and technology. Earthscan, London

Leontieff, D. A., Ikehata, K., Inanaga, Y., & Furukawa, S. (2025). Ozone for Industrial Wastewater Treatment: Recent Advances and Sector Applications. In Processes (Vol. 13, Number 8). Multidisciplinary Digital Publishing Institute (MDPI). https://doi.org/10.3390/pr13082331

Lesiak, P. (2024). Review of Methods for Converting Biomass into Biofuels. Rocznik Ochrona Srodowiska, 26, 84–93. https://doi.org/10.54740/ros.2024.009

Li, H., Dong, Q., Zhang, M., Gong, T., Zan, R., & Wang, W. (2023). Transport behavior difference and transport model of long- and short-chain per- and polyfluoroalkyl substances in underground environmental media: A review. In Environmental Pollution (Vol. 327). Elsevier Ltd. https://doi.org/10.1016/j.envpol.2023.121579

Li, M., Pu, Y., & Ragauskas, A. J. (2016). Current understanding of the correlation of lignin structure with biomass recalcitrance. In Frontiers in Chemistry (Vol. 4, Number NOV). Frontiers Media S. A. https://doi.org/10.3389/fchem.2016.00045

Linkov, I., Ames, M. R., Crouch, E. A. C., & Satterstrom, F. K. (2005). Uncertainty in octanol-water partition coefficient: Implications for risk assessment and remedial costs. Environmental Science and Technology, 39(18), 6917–6922. https://doi.org/10.1021/es0485659

Loffredo, E. (2022). Recent Advances on Innovative Materials from Biowaste Recycling for the Removal of Environmental Estrogens from Water and Soil. In Materials (Vol. 15, Number 5). MDPI. https://doi.org/10.3390/ma15051894

Loffredo, E., Carnimeo, C., Silletti, R., & Summo, C. (2021). Use of the solid by-product of anaerobic digestion of biomass to remove anthropogenic organic pollutants with endocrine disruptive activity. Processes, 9(11). https://doi.org/10.3390/pr9112018

Loffredo, E., Castellana, G., & Taskin, E. (2016). A Two-Step Approach to Eliminate Pesticides and Estrogens from a Wastewater and Reduce Its Phytotoxicity: Adsorption onto Plant-Derived Materials and Fungal Degradation. Water, Air, and Soil Pollution, 227(6). https://doi.org/10.1007/s11270-016-2883-2

Lopes, J. R. A., Mendonça, Z. L. L., da Silva, J. P. S., Amaral, A., & Netto, A. M. (2024). Enhancing herbicide adsorption in low-fertility soil using sugarcane biochar: Insights from Imazapic dynamics. Journal of Contaminant Hydrology, 266. https://doi.org/10.1016/j.jconhyd.2024.104412

Lü, H., Tang, G. X., Huang, Y. H., Mo, C. H., Zhao, H. M., Xiang, L., Li, Y. W., Li, H., Cai, Q. Y., & Li, Q. X. (2024). Response and adaptation of rhizosphere microbiome to organic pollutants with enriching pollutant-degraders and genes for bioremediation: A critical review. In Science of the Total Environment (Vol. 912). Elsevier B.V. https://doi.org/10.1016/j.scitotenv.2023.169425

Lu, Y., Gu, K., Shen, Z., Tang, C. S., Shi, B., & Zhou, Q. (2023). Biochar implications for the engineering properties of soils: A review. In Science of the Total Environment (Vol. 888). Elsevier B.V. https://doi.org/10.1016/j.scitotenv.2023.164185

Mainardis, M., Buttazzoni, M., De Bortoli, N., Mion, M., & Goi, D. (2020). Evaluation of ozonation applicability to pulp and paper streams for a sustainable wastewater treatment. Journal of Cleaner Production, 258. https://doi.org/10.1016/j.jclepro.2020.120781

Mairech, H., Lopez-Bernal, A., Moriondo, M., Dibari, C., Regni, L., Proietti, P., Villalobos, F.J., Testi, L. (2021). Sustainability of olive growing in the Mediterranean area under future climate scenarios: Exploring the effects of intensification and deficit irrigation. European Journal of Agronomy, 129, 126319. https://doi.org/10.1016/j.eja.2021.126319

Makkar, S., Singh, A., Annepu, S. K., & Nehra, K. (2025). Assessment of heavy metal contamination and pesticide residues in fruitbodies, cultivation substrate, and spent mushroom substrate of Lentinula edodes (Berk.) Pegler for sustainable applications. Journal of Material Cycles and Waste Management. https://doi.org/10.1007/s10163-025-02415-0

Maklavani, N. M. P., Maskani, M., & karimi, S. (2025). Systematic review of pistachio shell waste: Environmental applications, sustainable approaches, and nanotechnology insights. In Cleaner Waste Systems (Vol. 10). Elsevier B.V. https://doi.org/10.1016/j.clwas.2025.100219

Malaeb, L., & Ayoub, G. M. (2011). Reverse osmosis technology for water treatment: State of the art review. In Desalination (Vol. 267, Number 1, pp. 1–8). https://doi.org/10.1016/j.desal.2010.09.001

Mandal, A., Senthil Kumar, P., Poorva, C. S., Raju, L. S., Balasubramani, S. R., & Rangasamy, G. (2024). Research progress of persistent organic pollutants in water: classification, sources, potential risks, and treatment approaches. Water Practice and Technology, 19(3), 937–959. https://doi.org/10.2166/wpt.2024.031

Melanouri, E. M., Dedousi, M., & Diamantopoulou, P. (2022). Cultivating Pleurotus ostreatus and Pleurotus eryngii mushroom strains on agro-industrial residues in solid-state fermentation. Part I: Screening for growth, endoglucanase, laccase and biomass production in the colonization phase. Carbon Resources Conversion, 5(1), 61–70. https://doi.org/10.1016/j.crcon.2021.12.004

Michael-Igolima, U., Abbey, S. J., Ifelebuegu, A. O., & Eyo, E. U. (2023). Modified Orange Peel Waste as a Sustainable Material for Adsorption of Contaminants. Materials, 16(3). https://doi.org/10.3390/ma16031092

Ojeda, G., Gil, J. M., Mattana, S., Bachmann, J., Quenea, K., & Sobral, A. J. F. N. (2024). Biochar ageing effects on soil respiration, biochar wettability and gaseous CO2 adsorption. Mitigation and Adaptation Strategies for Global Change, 29(2). https://doi.org/10.1007/s11027-024-10107-7

Oncel, B., & Ozbek, C. (2025). Optimization of olive stone powder tea production: infusion conditions, bioactive compounds, and sensory evaluation using response surface method. Journal of Food Measurement and Characterization, 19(6), 4278–4291. https://doi.org/10.1007/s11694-025-03252-3

Ortiz-Martínez, M., Restori-Corona, B., Hernández-García, L., & Alonso-Segura, D. (2024). Polysaccharides and Composite Adsorbents in the Spotlight for Effective Agrochemical Residue Removal from Water. In Macromol (Vol. 4, Number 4, pp. 785–804). Multidisciplinary Digital Publishing Institute (MDPI). https://doi.org/10.3390/macromol4040047

Özbek, H. N., Koçak Yanık, D., Fadıloğlu, S., & Fahrettin, G. (2021). Effect of microwave-assisted alkali pre-treatment on fractionation of pistachio shell and enzymatic hydrolysis of cellulose-rich residues. Journal of Chemical Technology and Biotechnology, 96(2), 521–531. https://doi.org/10.1002/jctb.6569

Pathy, A., Naeth, M.A., Chang, S.X. (2025). Crop straw biochar enhances hydrocarbon adsorption in ground water. Chemosphere, 393, 144775. https://doi.org/10.1016/j.chemosphere.2025.144775

Preisner, M., Neverova-Dziopak, E., & Kowalewski, Z. (2020). Analysis of eutrophication potential of municipal wastewater. Water Science and Technology, 81(9), 1994–2003. https://doi.org/10.2166/wst.2020.254

Qayyum, S., Tahir, A., Mian, A. H., Zeb, S., Siddiqui, M. F., & Rehman, B. (2025). Optimizing biogas production through anaerobic digestion: transforming food waste and agricultural residues into renewable energy within a circular economy paradigm. Biomass Conversion and Biorefinery, 15(19), 26027–26043. https://doi.org/10.1007/s13399-024-05651-w

Raaijmakers, J. M., Paulitz, T. C., Steinberg, C., Alabouvette, C., & Moënne-Loccoz, Y. (2009). The rhizosphere: A playground and battlefield for soilborne pathogens and beneficial microorganisms. Plant and Soil, 321(1–2), 341–361. https://doi.org/10.1007/s11104-008-9568-6

Regulation - 2020/741 - EN - EUR-Lex. (n.d.). Retrieved January 27, 2026, from https://eur-lex.europa.eu/eli/reg/2020/741/oj/eng

Rodríguez-Hernández, J. A., Araújo, R. G., López-Pacheco, I. Y., Rodas-Zuluaga, L. I., González-González, R. B., Parra-Arroyo, L., Sosa-Hernández, J. E., Melchor-Martínez, E. M., Martínez-Ruiz, M., Barceló, D., Pastrana, L. M., Iqbal, H. M. N., & Parra-Saldívar, R. (2022). Environmental persistence, detection, and mitigation of endocrine disrupting contaminants in wastewater treatment plants – a review with a focus on tertiary treatment technologies. In Environmental Science: Advances (Vol. 1, Number 5, pp. 680–704). Royal Society of Chemistry. https://doi.org/10.1039/d2va00179a

Sadeek, S.A, Negm, N.A., Hefni, H.H.H., Abdel Wahab, M.M. (2015). Metal adsorption by agricultural biosorbents: Adsorption isotherm, kinetic and biosorbents chemical structures, International Journal of Biological Macromolecules, 81, 400-409 http://dx.doi.org/10.1016/j.ijbiomac.2015.08.031

Saravanan, A., Deivayanai, V. C., Kumar, P. S., Rangasamy, G., Hemavathy, R. V., Harshana, T., Gayathri, N., & Alagumalai, K. (2022). A detailed review on advanced oxidation process in treatment of wastewater: Mechanism, challenges and future outlook. Chemosphere, 308. https://doi.org/10.1016/j.chemosphere.2022.136524

Satyam, S., & Patra, S. (2025). The Evolving Landscape of Advanced Oxidation Processes in Wastewater Treatment: Challenges and Recent Innovations. In Processes (Vol. 13, Number 4). Multidisciplinary Digital Publishing Institute (MDPI). https://doi.org/10.3390/pr13040987

Sauvè S., & Desrosiers M. (2014). A review of what is an emerging contaminant. Chemistry central journal 8,15 https://doi.org/10.1186/1752-153X-8-15

Schallemberger, J. B., Matias, W. G., Libardi, N., Nagel-Hassemer, M. E., & Puerari, R. C. (2023). Effect of Spent Mushroom Substrate on Azo Dye Removal and Effluent Treatment. Brazilian Archives of Biology and Technology, 66. https://doi.org/10.1590/1678-4324-2023210843

Scherm, B., Balmas, V., Spanu, F., Pani, G., Delogu, G., Pasquali, M., & Migheli, Q. (2013). Fusarium culmorum: Causal agent of foot and root rot and head blight on wheat. Molecular Plant Pathology, 14(4), 323–341. https://doi.org/10.1111/mpp.12011

Senesi, N., Loffredo, E. (2018). The Chemistry of soil organic matter. In: Sparks DL (ed) Soil Physical Chemistry, 2nd ed. CRC Press, Boca Raton FL, pp 239–370. https://doi:10.1201/9780203739280

Sharma, N., Kumar, V., Sugumar, V., Umesh, M., Sondhi, S., Chakraborty, P., Kaur, K., Thomas, J., Kamaraj, C., & Maitra, S. S. (2024). A comprehensive review on the need for integrated strategies and process modifications for per- and polyfluoroalkyl substances (PFAS) removal: Current insights and future prospects. Case Studies in Chemical and Environmental Engineering, 9. https://doi.org/10.1016/j.cscee.2024.100623

Silva, J. A. (2023). Wastewater Treatment and Reuse for Sustainable Water Resources Management: A Systematic Literature Review. In Sustainability (Switzerland) (Vol. 15, Number 14). Multidisciplinary Digital Publishing Institute (MDPI). https://doi.org/10.3390/su151410940

Sinatra, M., Giannettta, B., Plaza, C., Galluzzi, G., Squartini, A., Zaccone, C. (2024). Anaerobic digestate influences the carbon distribution in soil organic matter pools after six months from its application. Soil & Tillage Research, 239, 106049 https://doi.org/10.1016/j.still.2024.106049

Sodkouieh, S. M., Kalantari, M., & Shamspur, T. (2023). Methylene blue adsorption by wheat straw-based adsorbents: Study of adsorption kinetics and isotherms. Korean Journal of Chemical Engineering, 40(4), 873–881. https://doi.org/10.1007/s11814-022-1230-0

Suárez-Cáceres, G. P., Lokuhitige, S., Kaufman, N. T., Alghaithy, A., Hishaw, M. B., Donis-Gonzalez, I. R., Fernández-Cabanás, V. M., & Gross, J. A. (2025). Suitability of walnut and pistachio shells as soilless substrates for producing Genovese basil in aquaponic systems. Frontiers in Horticulture, 4. https://doi.org/10.3389/fhort.2025.1486312

Sun, Q., Huang, M., Zeng, J., Ma, M., Li, J., & Le, T. (2025). Beyond waste to bioactive potential: advances in olive by-product valorization and resource recovery. In Food Chemistry (Vol. 496). Elsevier Ltd. https://doi.org/10.1016/j.foodchem.2025.146727

Szarka, A., Vnuková, L., Keršňáková, Z., Viktoryová, N., & Hrouzková, S. (2024). Contamination with Pharmaceuticals in Aquatic Environment: Focus on Analytical Methodologies. In Applied Sciences (Switzerland) (Vol. 14, Number 19). Multidisciplinary Digital Publishing Institute (MDPI). https://doi.org/10.3390/app14198645

Tang, K. H. D. (2024). Valorization of organic waste as biosorbents for wastewater treatment. In Water Emerging Contaminants and Nanoplastics (Vol. 3, Number 4). OAE Publishing Inc. https://doi.org/10.20517/wecn.2024.53

Tong, W., Liu, Q., Yang, C., Cai, Z., Wu, H., Ren, S. (2019). Effect of pore structure on CO2 gasification reactivity of biomass chars under high-temperature pyrolysis. Journal of the Energy Institute, 93, 962-976 https://doi.org/10.1016/j.joei.2019.08.007

Tran N.H., Reinhard M., Gin K.Y. (2018). Occurrence and fate of emerging contaminants in municipal wastewater treatment plants from different geographical regions-a review. Water Research, 133, 182-207 https://doi.org/10.1016/j.watres.2017.12.029

Wang, Yuan, Mao, Z., Lu, D., Sun, F., Li, Y., Wang, Yuqian, Zhang, Z., & Sun, S. (2025). Effect of a Spent Mushroom Substrate-Based Fungal-Bacterial Consortium on the Degradation of Phenanthrene and Pyrene and Microbial Communities in Soils. Journal of Soil Science and Plant Nutrition. https://doi.org/10.1007/s42729-025-02749-6

Wu, D., Yang, Z., Wang, W., Tian, G., Xu, S., & Sims, A. (2012). Ozonation as an advanced oxidant in treatment of bamboo industry wastewater. Chemosphere, 88(9), 1108–1113. https://doi.org/10.1016/j.chemosphere.2012.05.011

Xu, W., Xu, H., Delgado-Baquerizo, M., Gundale, M. J., Zou, X., & Ruan, H. (2023). Global meta-analysis reveals positive effects of biochar on soil microbial diversity. Geoderma, 436. https://doi.org/10.1016/j.geoderma.2023.116528

Yue, Y., Jin, X., Deng, L. (2023). Experimental Study on Properties of Syngas, Tar, and Biochar Derived from Different Gasification Methods. Applied sciences, 13, 11490. https://doi.org/10.3390/app132011490

Zhang, D. D., Dai, X. F., Klosterman, S. J., Subbarao, K. V., & Chen, J. Y. (2022). The secretome of Verticillium dahliae in collusion with plant defence responses modulates Verticillium wilt symptoms. Biological Reviews, 97(5), 1810–1822. https://doi.org/10.1111/brv.12863

Zhang, L., Larsson, A., Moldin, A., & Edlund, U. (2022). Comparison of lignin distribution, structure, and morphology in wheat straw and wood. In Industrial Crops and Products (Vol. 187). Elsevier B.V. https://doi.org/10.1016/j.indcrop.2022.115432

Zouboulis, A., & Peleka, E. (2025). Building a Circular Economy Option Through Wastewater Treatment and a Resource Recovery Approach. 10. https://doi.org/10.3390/proceedings2025121010

Zulkefli, M. Z., Mokhtar, H., Mahadi, C., & Jamil, Z. (2025). Sunflower seed shells (SS) and pistachio seed shells (PS) as natural adsorbents for methylene blue removal from aqueous environment. AIP Conference Proceedings, 3322(1). https://doi.org/10.1063/5.0290160

CHAPTER – 2
DIGESTATE FROM OLIVE MILL WASTE MODULATES ABIOTIC AND BIOTIC PROCESSES IN SOIL: RETENTION OF AGROCHEMICALS AND INHIBITION OF FUNGAL PATHOGENS

The work reported in this chapter has been published in Scientia Horticulturae, 337, 2024

https://doi.org/10.1016/j.scienta.2024.113545

Abstract

A new type of solid digestate (DG) obtained exclusively from two-phase olive pomace was characterised and evaluated for physicochemical and biological properties. In slurry-type experiments, the adsorption of the fungicide boscalid and the herbicide oxyfluorfen on non-amended loam soil (SOIL) and on soil amended with DG at doses of 1 % (SOIL-DG 1), 3 % (SOIL-DG 3) and 6 % (SOIL-DG 6) (w/w) was quantified and modelled. The DG showed a remarkable and stable capacity to adsorb the compounds over a temperature range of 5–40 °C. Based on the data of the adsorption isotherms conducted at 20 °C, the distribution coefficients of SOIL, SOIL-DG 1, SOIL-DG 3 and SOIL-DG 6 were, respectively, 1.3, 2.2, 2.2 and 3.4 mg kg^{-1} for boscalid and 2.0, 2.1, 2.2 and 5.9 mg kg^{-1} for oxyfluorfen, which suggested a significant increase in soil retention capacity after the addition of DG, especially at the highest dose. The desorption of both compounds from all treatments, especially from SOIL-DG 6, was slower than adsorption and incomplete (hysteresis coefficient < 1), thus indicating a prolonged permanence of the molecules on the soil. In lab-scale experiments, the phytopathogenic fungi *Armillaria mellea, Fusarium culmorum* and *Verticillium dahliae* were exposed to 0.02, 0.1, 0.5 and 1 % (w/w) DG alone, and 0.02 and 0.1 % DG preliminary interacted with 100 mg L^{-1} of soil humic acid (HA-DG). Fungal response was clearly influenced by the species, the treatment and the dosage adopted. In general, all treatments did not significantly modify the growth rate of *A. mellea* and *V. dahliae*, whereas all DG treatments, especially HA-DG, caused evident suppressive effects on *F. culmorum*. Based on the results of this study, it can be concluded that the addition of DG to the soil can regulate the bioavailability of agrochemicals in pore water and exert an inhibitory or irrelevant action depending on the phytopathogenic fungus.

2.1 Introduction

Olive pomace (OP), composed of parts of pulp, peel and stone, is the main by-product of olive pressing to obtain virgin olive oil. This material is particularly copious in olive-growing areas where olive oil represents one of the main agro-industrial products on which the local economy is based. In Italy, approximately 3 million tons of OP are produced annually, and the Apulia region contributes one third of the entire Italian production of oil olives (Valenti et al., 2017). Due to the abundance of OP and its composition, its management, especially storage, can represent a problem for the olive oil industry. Raw OP has various applications in many production sectors such as the extraction of olive pomace oil, addition to the soil as fertilizer, combustion for thermal purposes, fermentation, preparation of biostimulants, use as food, beverage and feed additive, and as an ingredient in pharmaceuticals and cosmetics (Dantas Palmeira et al., 2023; Tolisano et al., 2023). The recycling of OP is a real necessity to safeguard the environment and implement circularity in the olive oil sector.

The growing global demand for renewable energy in recent years has encouraged the use of waste biomass, such as OP, for bioenergy production (WBA, 2022). For this purpose, OP is usually mixed with agro-zootechnical wastes, such as crop residues and manure, or, less commonly, is used alone. Given its physicochemical properties and very high moisture, OP is well suited for microbiological processes. Anaerobic digestion (AD) technology consists of a conversion of organic residues into more stable material and is carried out by anaerobic bacteria and archea (Singh and Kalia, 2017; Braguglia et al., 2018). This technology represents a sustainable solution to the need for new energy sources and the urgency of sequestering the carbon present in organic waste. In addition to producing biogas, i.e. a mixture of CH_4, CO_2, and small quantities of other gases, this process releases a large quantity of very humid (about 90–95 % moisture) and heterogeneous by-product which contains approximately 60–80 % (on dry matter) of undecomposed organic material. After a separation process, the raw anaerobic material originates a solid digestate (DG) and a clarified liquid digestate (Wang and Lee, 2021).

Although the AD technology emerged as a subject of interest in the last years of the seventeenth century (Pullen, 2015), recently, it has had a rapid development for energy needs, so that the global amount of biogas produced has tripled in the last decade (Karimi et al., 2022). In olive mill farms, the possibility of directing OP to the biogas plant represents a sustainable approach which ensures stable extra income.

During the AD process, biomass is biodegraded, homogenised and partially sanitized. The more labile organic components (sugars, lipid substances, proteins) are rapidly converted into biogas,

while the more recalcitrant ones (lignocellulosic fraction) accumulate in the DG along with mineral elements that are essential for plant nutrition (Nkoa, 2014). The physicochemical properties of DG are strictly dependent on the type of ingestate and on the process parameters adopted, such as moisture, retention time and temperature in the digestor (Singh and Kalia, 2017). DG contains a mixture of undecomposed or partially decomposed substances, anaerobic microorganisms, enzymes, volatile fatty acids, microbic metabolites and inorganic particulate. After exposure to the open air and the activity of aerobic microorganisms, the formation of a humic-like fraction takes place in the DG (Provenzano et al., 2014).

In general, the DG is characterized by low content of dry matter, high levels of P, N (mainly as NH_4^+-N) and K, and pH value in the range 6.7 – 9.2 (Teglia et al., 2011). The direct application of DG to agricultural land is a common practice even if it raises concern for the very high N content which can cause ammonia or nitrogen oxides emission in the atmosphere and/or nitrate leaching into natural water. Other concerns of DG spreading on the soil is related to its content of agrochemicals and antibiotics (Wang and Lee, 2021; Brueck et al., 2023), potentially toxic elements (heavy metals) and occasional plant and animal pathogens (Peng and Pivato, 2019) that pose a serious threat to human health and ecosystem security. However, the abundance of phytonutrients is the reason of the wide use of DG as organic amendment (Möller and Müller, 2012; Caruso et al., 2018). DG spreading on the soil has been authorised by the European Commission (2019), while national or regional legislations have set limits to its application based primarily on the total N content.

The wide variability of DG characteristics is due to the considerable diversity of biomass used to feed the AD process. In the last years, this material has been mainly studied for its composition and stability (Provenzano et al., 2016). Undoubtedly, when a single type of biomass is used, such as OP only, DG properties are more stable, and this facilitates the choice of its destination and the most suitable dosage. In any case, a comprehensive DG characterization is essential to assure its sustainable and reliable use.

The addition of DG to the soil increases the content of soil organic matter, provides nutritional and edaphic benefits to plants, and reduces the demand for chemical fertilizers, which provides economic and environmental benefits (Cristina et al., 2020). Moreover, DG can regulate all the processes to which organic xenobiotics undergo in soil, such as adsorption, movement, leaching, dissipation, which in turn control their bioavailability (Loffredo et al., 2021; Dollinger et al., 2022). This is particularly important in sandy soils, where soil organic matter is scarce, and/or where plant protection products are abundantly applied. Low retention capacity of these chemicals by the soil leads to soil and water pollution.

Among widely adopted agrochemicals, there are oxyfluorfen and boscalid. Oxyfluorfen [2-chloro-1-(3-ethoxy-4-nitrophenoxy)−4-(trifluoromethyl)benzene] is a diphenyl ether herbicide used in pre- and post-emergence to control broad-leaf weeds in several crops. The spread of oxyfluorfen in the environment is very dangerous due to its carcinogenic potential and long persistence in water and soil (EPA, 1992). The carboxamide boscalid [2-chloro-N-[2-(4-chlorophenyl)phenyl]pyridine-3-carboxamide] is a widely adopted broad-spectrum fungicide having a very long persistence in the environment (Chen and Zhang, 2010). The hydrophobic nature of these molecules (high Kow values) suggests their strong interaction with both natural and anthropogenic soil organic matter (Senesi et al., 2015).

Although DG is increasingly added to cultivated soil, and despite the well-known risks associated with this practice, its effects on soil microbiota is rather neglected (Tang et al., 2021; Karimi et al., 2022). Fungi are a very important component of soil microbiota since they ensure the maintenance of the soil carbon cycle, with consequent turnover of organic matter and continuous release of nutrients (Sanchez 2009). Furthermore, fungi can contribute to eliminate organic contaminants by means of mycodegradation (Castellana and Loffredo, 2014). However, several soilborne fungi can be very dangerous for susceptible crops and cause drastic reductions in the quantity and quality of products, resulting in huge economic loss. Fungal control is very difficult, and chemical treatments are generally considered the most effective remedy. However, the need to limit the use of chemicals has prompted researchers to investigate new eco-compatible methods for the control of phytopathogenic fungi. Studies conducted in the last two decades have shown surprising suppressiveness of pathogenic fungi by native soil organic matter, including humic acids (HA) (Loffredo et al., 2007, 2008) and fulvic acids (Moliszewska and Pisarek, 1996), and by the HA-like fraction of compost (El-Masry et al., 2002; Loffredo and Senesi, 2009), vermicompost (Szczech and Smolinska, 2001), biochar (Taskin et al., 2019) and hydrochar (Parlavecchia et al., 2021). Therefore, the appropriate use of such amendments might partially replace synthetic fungicides, with considerable benefits for the environment.

The basidiomycete *Armillaria mellea* and the ascomycetes *Fusarium culmorum* and *Verticillium dahlia*e are among the most dangerous fungi for several crops. The species *A. mellea* belongs to the Physalacriaceae family and is a root pathogen mainly of woody plants (about 500 species) but also of herbaceous plants in temperate regions. This fungus is a facultative necrotrophic pathogen, being able to attack both living and dead root tissues and causing typically non-specific symptoms to the aerial part, up to the gradual or sudden plant decay (Devkota and Hammerschmidt, 2020). The mycelium of *A. mellea* can persist for a long time, even decades, in the infected dead roots left in the soil, which represent a source of primary inoculum. *F.*

culmorum belongs to the Nectriaceae family and is one of the main agents of foot and root rot of cereals. It can cause significant economic loss due to yield reduction, worse grain quality, as well as kernels contamination with mycotoxins (Scherm et al., 2013). This pathogen is also very resistant, being able to survive in adverse conditions for a long time. *V. dahliae* is a cosmopolitan fungus with a notable longevity in soil where its resting propagules, called microsclerotia, persist up to 14 years in the absence of host plants (Schnathorst, 1981). *V. dahliae* infects over 400 different dicotyledonous plants, including tomato, potato, aubergine, strawberry, flax, olive trees and grapevine (Bhat and Subbarao, 1999).

Measurements of *in vitro* growth of the fungal colony can be interpreted with various models (Dantigny et al., 2005; Tao et al., 2014). Very few investigations have been conducted on the impact of DG on soil-resident fungi (Tao et al., 2014; Santi et al., 2015; Brezáni et al., 2019). In a study by Walsh et al. (2012), DG addition to soil appeared irrelevant on fungal community, while Tao et al. (2014) demonstrated a suppressive activity of both raw and liquid DG on some phytopathogenic fungi. The limited knowledge on this topic and the conflicting results reported in the literature suggest further investigation before drawing definitive conclusions on this matter. Furthermore, most of the information available in the literature concerns DG samples obtained exclusively from livestock manure or waste of mixed plant-animal origin. As far as we know, this is the first study on the impact of DG from OP only on soil fungi.

In soil, DG interacts chemically with native organic matter, especially HA. It is reasonable that the simultaneous presence of DG and HA in soil may influence the biotic community differently than DG alone or HA alone (Kulikova et al., 2005). This hypothesis has already been verified on *Sclerotinia sclerotiorum* treated both with allelopathic compounds or HA individually and with their combination (Loffredo and Traversa, 2014). In that study, the authors observed that the allelochemical-HA combination modified or even reversed the effects of the individual applications.

Based on the above considerations, the present study investigated: (i) the contribution of DG supply to the soil adsorption capacity of two common agrochemicals; and (ii) the effects of various doses of DG alone and in combination with a soil HA on the *in vitro* growth of three phytopathogenic fungi.

2.2 Materials and methods

2.2.1. Digestate, soil, chemicals, humic acid and fungi

The DG sample used was collected in an Apulian oil mill with adjoining biogas plant (AGROLIO S.r.l., Andria, Italy). The crude DG was released after approximately 45-day AD of two-phase olive pomace only. It had a dry matter content < 10 % (w/v); after centrifugation for solid/liquid separation, the solid DG was collected and stored in glass containers at a temperature of 4 °C.

A loam soil was sampled at 0–10 cm depth in the olive grove of the experimental station of University of Bari located at Valenzano, Southern Italy (41° 02′ N; 16° 90′ E). The soil was air-dried, sieved at particle size < 2 mm to remove the coarser fraction and thoroughly homogenized.

Boscalid (Cas number188425-85-6) and oxyfluorfen (CAS number 42874-03-3) at purity ≥ 99 % and 98 %, respectively, were purchased from Sigma Aldrich s.r.l., Milano, Italy. Molecular mass, water solubility and log Kow of boscalid are 343.2 g mol^{-1}, 4.6 mg L^{-1} at 25 °C and 2.96, while the same parameters of oxyfluorfen are, in the order, 361.7 g mol^{-1}, approximately 1 mg L^{-1} and 4.73 (PubChem Open Chemistry Database at the National Institutes of Health (NIH), 2023). Methanol (HPLC grade) solutions of boscalid and oxyfluorfen were prepared individually at a concentration of 2000 mg L^{-1}. Successively, aqueous mixtures of the two compounds were prepared by combining appropriate aliquots of each methanol solution and diluting with a mixture of double-distilled water/methanol (95:5, v/v). All other chemicals used in the experiments were of extra pure grade.

The HA sample was the standard HA isolated from a prairie soil located near Joliet, Ill, USA, belonging to the standard and reference collection of humic and fulvic acids of the International Society of Humic Substances (IHSS 2022). HA properties are: 10.2 meq g^{-1} total acidity, 8.3 and 1.9 meq g^{-1} COOH and phenolic OH contents, respectively, 581and 41 g kg^{-1} C and N contents (on dry- and ash-free basis), respectively (IHSS, 2023).

Isolates of *A. mellea* (Vahl) P. Kumm., 1871, *F. culmorum* (Wm. G. Sm.) Sacc., 1892, and *V. dahliae* Kleb., 1913 were kindly provided by the collection of prof. Antonio Ippolito of the Department of Soil, Plant and Food Sciences of the University of Bari, Bari, Italy. Fungal mycelium was cultivated on potato dextrose agar (PDA, Oxoid, 4 % w/v) in Petri dishes in the dark at 20 ± 1 °C. To maintain the characteristics of the fungal culture stable until the end of the experiments, every 20 days, a 2-mm diameter disk of the colony was transferred on fresh PDA. Fungal inoculation was performed in an AsalAir vertical 700 laminar flow hood (Cernusco sul Naviglio, Italy) using 2-mm PDA disk covered with mycelium collected from the growing margin of young colonies and placed in the center of new plates.

2.2.2 Soil and digestate characterization

Soil properties were determined according to the official methods of soil analysis (Gazzetta Ufficiale della Repubblica Italiana (GU), 1999). Briefly, soil moisture was measured after heating the soil at 105 °C overnight; the pH was potentiometrically measured in a soil/water suspension (1:2.5, w/v); electrical conductivity (EC) was measured at 25 °C in the water extract obtained from a soil/water suspension (1:2, w/v); organic C, total N, and available P were determined by the Walkley-Black, the Kjeldahl, and the Olsen method, respectively; cation exchange capacity (CEC) was determined by using 0.1 M $BaCl_2$ buffered to pH 8.2 with triethanolamine (2.25 %, v/v). Soil characteristics are shown in Table 1.

Table 1. Main soil characteristics.

Parameter	Value
Sand (%)	36
Silt (%)	43
Clay (%)	21
pH[a]	7.45 ± 0.03
EC[b] (dS m^{-1})	0.20 ± 0.003
Moisture (%)	4.4 ± 0.5
Organic C (g kg^{-1}.)	37.94 ± 2.34
Total N (g kg^{-1}.)	2.98 ± 0.08
Available P (mg kg^{-1}.)	2.38
C/N	12.7
K (mg kg^{-1})	101.0
CEC (cmol+ kg^{-1})	39.0 ± 3.8

[a] soil/H_2O: 1:2.5 (w/v); [b] soil/H_2O: 1:2 (w/v).

Proximate analysis of the DG sample, including pH, electrical conductivity (EC), moisture and ash content, was performed according to the official methods of analysis of fertilizers. The pH and EC were measured in a DG/water suspension (1:10, w/v); the ash content was measured after burning the sample in a muffle furnace at a temperature of 550 °C for 4 h Organic C was determined by the Springer-Klee method (Gazzetta Ufficiale della Repubblica Italiana (GU), 2000); total N and ammonia N were determined according to the procedures reported in European Commission (2003). Some characteristics of the air-dried digestate are referred in Table 2.

Table 2. Main digestate properties.

Parameter	Value
pH[a]	9.21 ± 0.03 [b]
Moisture (%)	34.20 ± 0.48
Electrical conductivity[a] (dS/m)	0.42 ± 0.02
Total volatile solids (% d.m.)	96.96 ± 0.61
Fixed total solids (% d.m.)	2.00 ± 0.23
Organic C (% d.m.)	51.03 ± 0.39
Total N (% d.m.)	1.23 ± 0.06
NH_4-N (% d.m.)	0.062
C/N ratio	41.5
Total P (% d.m.)	0.075

[a] digestate/H_2O, 1:10 w/v. [b] SD (n = 3); d.m.: dry matter

Scanning electron microscopy coupled with energy-dispersive X-ray spectroscopy (SEM-EDX) analysis was performed to study DG micromorphology. For the purpose, the sample was fixed with an adhesive carbon tape, metalized with Au/Pd and analyzed using a Hitachi TM3000 scanning electron microscope (Hitachi, Tokyo, Japan) equipped with an Oxford Swift ED3000 microanalysis system. Backscattered electrons were detected, and SEM micrographs of DG were captured at both 500 × and 1800 × magnifications.

2.2.3 Sorption and desorption experiments

The capacity of DG to adsorb boscalid and oxyfluorfen was evaluated in batch equilibrium experiments at temperatures of 5, 10, 20, 30 and 40 °C. For the purpose, aliquots of 20 mg of DG were interacted with 20 mL of aqueous mixtures of the compounds at the individual concentration of 2 mg L^{-1}, thus obtaining a solution/DG ratio equal to 1000. All samples were mechanically shaken at 350 *g* for 16 h to reach the steady state. Previous experiments demonstrated a rapid adsorption of the two compounds on DG (Loffredo et al. 2024), and the achievement of the equilibrium condition in about 2 h. Subsequently, the suspensions were centrifuged at 10,000 *g* for 10 min and a volume of 15 mL of supernatant solution was collected from each sample to determine the equilibrium concentration of the compounds using ultra-high performance liquid chromatography (UHPLC) analysis as reported in the next section.

Adsorption isotherms of the compounds onto unamended soil (SOIL) and soil amended with DG at 1 % (SOIL-DG 1), 3 % (SOIL-DG 3) and 6 % (w/w) (SOIL-DG 6) were performed in batch equilibrium mode. Approximately, the dose of 1 % DG is equivalent to a soil application of 7 t ha^{-1} which corresponds to 30 kg ha^{-1} total N, considering a soil depth of 5 cm and a soil bulk density of 1.4 g cm^{-3}. Therefore, the DG doses adopted were consistent with those recommended for field applications (30–60 t ha^{-1}) (Velechovský et al., 2021). Volumes of 10 mL of aqueous mixtures of boscalid and oxyfluorfen at individual concentrations of 0.1, 0.2, 0.5, 1 and 2 mg L^{-1} were added to 2 g of each substrate in glass flasks. To reach equilibrium, samples were stirred for 24 h at 20 °C in the dark. After that, samples were centrifuged at 10,000 *g* for 10 min and the equilibrium concentration of the compounds in the supernatant solution was measured by UHPLC according to the protocol described in the next section.

Desorption of the compounds from all treatments was started immediately after adsorption using the samples added with the maximum concentration (2 mg L^{-1}) of the compounds. At each desorption step, 7 mL of supernatant solution (of 10 mL initially added) was replaced with double distilled water and the sample was stirred again for 24 h at 20 °C to reach new equilibrium. Subsequently, the sample was centrifuged, and the concentration of the compounds was determined as described previously for the adsorption experiments. All adsorption and desorption experiments were triplicated.

The concentration of the compounds on each adsorbent, q_e (mg kg^{-1}), was calculated from the equation: $qe = (C_0 - Ce)\ V/m$, where C_0 and Ce (mg L^{-1}) are the initial and the equilibrium concentration in solution, respectively, V (mL) is the solution volume and m (g) the adsorbent mass. Data obtained were statistically treated by one-way analysis of variance (ANOVA) to evaluate possible significant differences between the means of different treatments.

2.2.4 Chromatographic analysis and data modelling

The concentration of residual compounds in the supernatant solution was determined by UHPLC. All samples were previously filtered using 0.45 μm Millipore™ cellulose acetate filters and subsequently loaded into a WPS-3000 autosampler. A Dionex Ultimate UPLC 3000 RSLC (Waltham, MA, USA) instrument equipped with an HPG-3200 RS pump, and a TCC-3000 column compartment connected to a Supelco™ LC-18 column (150 mm ×3 mm ×3 μm) was used for analyses. Isocratic elution was adopted with water/methanol (30/70, v/v) flowing at 0.8 mL min^{-1}. A DAD-3000 RS diode array detector (Dionex, Waltham, MA, USA) set at wavelengths of 207 and 210 nm was used for boscalid and oxyfluorfen detection, respectively. The external standard method was used to quantify the compounds.

Sorption and desorption isotherm data were described using the linear Henry model and the non-linear empirical Freundlich and Langmuir models. The equations applied and the meaning of the various parameters are reported in Table 3. The Freundlich equation fits well when solute molecules form a multilayer on the adsorbent and this has surface heterogeneity, while the Langmuir equation is proper for solutes forming a monolayer on the adsorbent without interacting with each other and when the surface of the adsorbent is homogeneous. The Freundlich (K_F and 1/n) and Langmuir (b and K_L) parameters were calculated by the non-linear regression method using the solver add-in component of Microsoft® Excel® and a trial-and-error procedure to minimize the sum of squared residuals (SSR) between experimental and theoretical data. The accordance of the theoretical model to the experimental data was evaluated on the basis of the correlation coefficient, $r = \sqrt{\frac{\sum(q_e m - \overline{q_e})^2}{\sum(q_e m - \overline{q_e})^2 + \sum(q_e m - q_e)^2}}$, where $q_e m$ is the theoretical adsorbed concentration of the compound (mg kg^{-1}) at equilibrium, q_e is the experimental concentration (mg kg^{-1}), and $\overline{q_e}$ is the average q_e. Furthermore, the linear Henry equation was also employed to calculate the distribution coefficient, Kd, from the slope, and the organic-carbon-partition coefficient, K_{OC}, by: $K_{OC} = (Kd \times 100)/(\%\ OC)$), which is a measure of the quantity of solute adsorbed per unit of organic carbon of the adsorbent.

Table 3. Theoretical models used to describe sorption data.

SORPTION MODELS		
Henry	Freundlich	Langmuir
$q_e = Kd\ C_e$	$q_e = K_F C_e^{1/n}$	$q_e = \frac{(K_L C_e b)}{(1 + K_L C_e)}$
q_e (mg g^{-1}): equilibrium concentration of the adsorbed compound C_e (mg L^{-1}): equilibrium concentration of the compound in solution		
Kd (mg kg^{-1}): distribution coefficient	K_F (mg kg^{-1}): Freundlich adsorption constant (sorption capacity)	b (mg kg^{-1}): maximum adsorption capacity of the adsorbent
	1/n: degree of nonlinearity between C_e and q_e n: sorption intensity	K_L (L mg^{-1}): Langmuir constant (energy of adsorption/affinity of the solute for the adsorbent

Desorption isotherm data were also theoretically evaluated using the Henry and the Freundlich equations. This allowed to calculate the desorption parameters Kd_{des}, K_{OCdes}, K_{Fdes}, and $1/n_{des}$ as

described for the corresponding sorption parameters. Finally, the hysteresis coefficient, H, was calculated according to: $H = (1/n_{des})/(1/n_{ads})$. A hysteresis occurs for H value < 1, which indicates slow and incomplete desorption of the compound.

2.2.5 Experiments on fungi

Appropriate amounts of DG were suspended in double distilled water to obtain dosages of 0.02 (DG 0.02), 0.1 (DG 0.1), 0.5 (DG 0.5) and 1% (DG 1) (w/v). In another set of experiments, DG 0.02 and DG 0.1 were preliminary interacted with 100 mg L^{-1} HA (HA-DG 0.02 and HA-DG 0.1) under magnetic stirring for 16 h at room temperature (~ 20 ± 1 °C), in the dark.

Each suspension and double distilled water (control) was added with PDA (4%, w/v) and autoclaved at a temperature of 121 °C for 15 min. Subsequently, a volume of 20 mL of each medium was collected under stirring and poured into a 9 cm-diameter Petri dish. After cooling and solidification at room temperature (~ 20 ± 1 °C), under axenic conditions, the fungus was inoculated as described in section 2.1. The samples were then kept in a 60043/THTL thermostated chamber (F.lli Della Marca S.r.l., Roma, Italy) at a constant temperature of 20 °C, in the dark. During fungal growth in the plates, the colony radius (in mm) was measured until its extension was possible for all samples (colony diameter ≤ 4.4 mm), i.e., 14, 5 and 18 d for *A. mellea*, *F. culmorum* and *V. dahliae*, respectively. Each experiment was replicated five times.

The radial growth rate of the fungus, μ (mm h^{-1}) was calculated applying the linear model with breakpoint: $r\ (mm) = \mu\ (t - \lambda)$, where r is the radius, t is the sampling time (h) and λ is the lag time (h), i.e., the time required for the completion of the germination process (Dantigny et al. 2005). This model describes very well the growth of the colony, which is confirmed by the high values generally observed for the regression coefficient ($r \geq 0.99$). The appropriateness of this model allows to calculate the parameters μ and λ even before the complete coverage of the plate by the mycelium. In general, when fungus inoculation is carefully conducted, there is not a significant relationship between μ and λ (Dantigny et al. 2005). Using the colony diameter values (D) measured during the experiments, the absolute growth rate (AGR, mm h^{-1}) of the mycelium was calculated according to the expression: $AGR = \frac{D-2}{t}$, where the constant 2 is the inoculum diameter (mm), and t is the incubation time (h) (Tao et al. 2014). The μ values obtained for the various treatments were statistically analysed by ANOVA, and the means compared to the control by the least significant difference (LSD) test at $P \leq 0.05$, $P \leq 0.01$ and $P \leq 0.001$.

2.3 Results and discussion

2.3.1. Physicochemical properties of the digestate

As is well known, DG properties are largely dependent on the type of organic waste used to feed the digester and on the duration of the AD process. The unique nature of the DG considered in this study, i.e., obtained exclusively from olive pomace, is the reason for its rather different composition compared to that of other DGs generally obtained from animal manure only or mixed plant and animal biomass (Möller and Müller, 2012). In facts, results of proximate analysis indicated that pH, ash, moisture and EC were somehow different from those averagely found for other DGs originated from mixed feedstock. In particular, the pH value (9.2) of our DG was similar to that measured for a DG obtained from 60 % maize silage and animal residues (Mukherjee et al., 2016) but higher than that found for a sewage sludge DG (Cristina et al., 2020). The high pH value measured for this DG was possibly due to a high content of alkaline and alkaline earth metals. The amount of fixed total solids (2 % on dry matter) was in the average for DG (Table 2). The EC value of 0.42 dS m^{-1} was lower than that found for a mixed feedstock DG (Loffredo et al., 2021) and a sewage sludge DG (Cristina et al., 2020). Results of ultimate analysis showed an organic C content (51 % on dry matter) higher than that usually recorded for this type of material (25–41 %) (Cesaro, 2021) and for a swine manure DG (Hung et al., 2017), but very similar to that of a mixed biomass DG (Loffredo et al., 2021). Differently, as expected, the total N content was lower than that of other DGs, reasonably attributable to its exclusive vegetal nature. Higher total N contents are reported for a swine manure DG (Hung et al., 2017) and a sewage sludge DG (Cristina et al., 2020).

2.3.2. SEM analysis

Fig. 1 shows SEM images of the DG at 600 × and 1800 × magnifications. This technique allows to evaluate the surface micromorphology of a material and inquire on the allocation and distribution of pores. The lower magnification gave a general overview of the material and denoted an apparent scarce homogeneity (Fig. 1A). In facts, roughness, small cavities, furrows, and a sort of thin network, probably formed by vessels of the olive tissues, were evident. At higher magnification, surface heterogeneity was more evident. The morphological texture of the DG exhibited irregularly shaped cavities, mostly less than 10 µm, and coiled filamentary structures composed of lignocellulosic and mineral constituents (Fig. 1B). The pores generated by the cell walls and vascular tissues were not so evident perhaps due to the intense pressure exerted during the pressing of the olives. SEM micrographs of a swine manure DG showed a smooth and compact surface typical of DG obtained from animal waste (Hung et al., 2017). Diffuse porosity and

large surface area are of primary importance to ensure physical and chemical interaction with organic and mineral constituents and high adsorption capacity of the material.

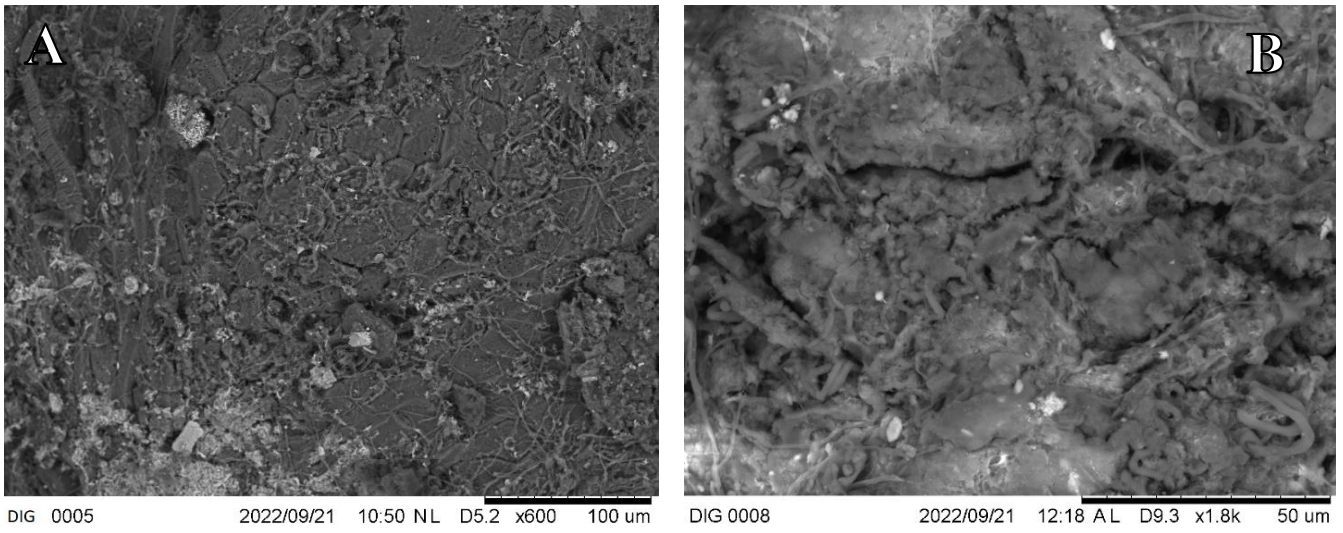

Figure 1. Scanning electron micrographs at magnifications of 600× (A) and 1800× (B). Images were taken with secondary electrons.

2.3.3. Sorption and desorption of the agrochemicals on digestate and soil

The quantities of each compound adsorbed at equilibrium on the mass unit of DG at various temperatures are reported in Table 4. The sorption study conducted at temperatures between 5 and 40 °C allowed the evaluation of the retention efficiency of the compounds by the DG in different application conditions, such as different seasons, different latitudes and different depths. Statistical treatment (ANOVA) of the data showed that the quantities of each compound adsorbed at equilibrium at the five temperatures considered were not significantly different ($P \leq 0.05$) (Table 4). As far as we know, there is no information in the literature on this matter, therefore a comparison between our results and those of other authors is not possible. The only work reporting the effects of temperature on the adsorption of boscalid only was conducted using zeolites as adsorbent; the authors concluded that the temperature had no significant influence on the sorption process (Silvestrini et al., 2015). At the various temperatures, the quantities of boscalid and those of oxyfluorfen adsorbed on the DG were almost identical, the absorbed oxyfluorfen being (on average) only 2 % higher than the adsorbed boscalid (Table 4). Considering the very low water solubility of both compounds (few mg per L at 25 °C), these results were expected. The DG used in this study showed a sorption capacity of boscalid that was approximately three times higher than that of a DG produced from mixed feedstock (Loffredo et al., 2021) and much higher than that of a soil/30 % DG biomixture (Mukherjee et al., 2016). Although, as expected, the quantity of boscalid adsorbed on the

DG was lower than that adsorbed on other organic matrices richer in carbon, such as biochar (Mukherjee et al., 2016), it is relevant for the purpose of preventing the transfer of the compound into natural waters with consequent contamination. Due to their good capacity to adsorb oxyfluorfen and other pesticides, local organic wastes from olive oil production were employed in the preparation of biobed systems (Delgado-Moreno et al., 2017).

Table 4. Concentration (mg kg^{-1}) of the adsorbed compounds onto DG at various temperatures.

Compound	Temperature (°C)				
	5	**10**	**20**	**30**	**40**
boscalid	1557.44 ± 25.61	1577.56 ± 16.47	1595.88 ± 11.59	1591.36 ± 22.61	1578.09 ± 18.65
oxyfluorfen	1608.11 ± 9.33	1618.52 ± 16.71	1622.91 ± 10.58	1630.15 ± 32.66	1616.45 ± 21.36

Note: data were analysed by ANOVA (n = 3) and no statistically significant differences were found between the means of the various treatments.

Adsorption isotherms were performed to describe quantitatively the interaction between the soil and the two compounds at a fixed temperature. The experiments were carried out on both untreated soil and soil treated with 1, 3 and 6 % DG (w/w). By interpreting adsorption data with different models, we calculated the sorption parameters, such as the adsorption constant and the maximum adsorption, and obtained information on the mechanism of interaction between the DG and the molecules, including the type of DG surface and the allocation of the compounds on it. The adsorption data were described with the Freundlich, Langmuir and Henry equations. The Freundlich model is the most appropriate one for reversible adsorption on substrates that have heterogeneous surfaces and when the solute molecules form a multilayer on the surface of the substrate. The Langmuir equation describes very well the adsorption on homogeneous surfaces and when the solute forms a monolayer on the adsorbent, being irrelevant the interactions among the adsorbed molecules. The Henry equation was used to calculate the distribution coefficient, Kd_{ads}, which expresses the sorption efficiency of a substrate. The adsorption parameters (Kd_{ads}, KF_{ads} and $1/n_{ads}$) and the coefficient K_{OCads} are reported in Table 5. To estimate the congruence between the experimental data and the theoretical model, both the correlation coefficient (r) and the sum of squared residuals (SSR) were considered.

Table 5. Sorption parameters of the compounds on different soil treatments.

Compound	Theoretical models											
	HENRY				FREUNDLICH				LANGMUIR			
	SSR	r	Kd_{ads} mg kg $^{-1}$	K_{OCads} mg kg $^{-1}$	SSR	R	K_{Fads} [a] mg kg $^{-1}$	1/n	SSR	r	b [a] mg kg $^{-1}$	K_L [b] L mg^{-1}
						SOIL						
Boscalid	0.06	0.995	1.29	34.04	0.01	0.999	1.21	1.25	0.06	0.988	458.42	0.003
Oxyfluorfen	0.07	0.997	2.03	53.69	0.07	0.993	2.04	0.99	0.07	0.993	34.38	0.064
						SOIL-DG 1						
Boscalid	0.19	0.992	2.17	50.77	0.03	0.996	2.23	0.78	0.02	0.998	7.53	0.439
Oxyfluorfen	0.18	0.992	2.12	49.62	0.15	0.986	2.09	1.11	0.19	0.982	3115.11	0.001
						SOIL-DG 3						
Boscalid	0.04	0.998	2.24	42.99	0.03	0.998	2.22	1.07	0.04	0.996	1048.81	0.002
Oxyfluorfen	0.15	0.994	2.21	42.50	0.02	0.998	2.08	1.24	0.15	0.986	4273.03	0.001
						SOIL-DG 6						
Boscalid	0.04	0.999	3.45	52.11	0.03	0.999	3.45	0.95	0.04	0.998	67.73	0.054
Oxyfluorfen	0.34	0.996	5.93	89.39	0.32	0.991	6.00	1.04	0.34	0.990	240.19	0.025

Based on r and SSR values, the adsorption of both compounds on all soil treatments was well described by the Freundlich model, although high r values were also obtained applying the other equations, especially the Henry model (Table 5). Therefore, it was evident that both unamended soil and DG/soil mixtures had heterogeneous surfaces on which the adsorbed compounds formed multiple layers.

Native and exogenous soil organic matter exert a remarkable influence on the dynamic of organic xenobiotics in soil, interacting through various mechanisms and influencing the adsorption process both quantitatively and qualitatively (Senesi et al., 2015). Chemical and physical adsorption may occur simultaneously, although, based on the physicochemical properties of the interacting species, one mechanism generally prevails on the other. Chemical and physical bonding of different strength, such as hydrogen, ionic, covalent bonding, electron donor-acceptor interaction, ligand exchange, van der Waals forces and others, are responsible of the intensity and duration of adsorption (Senesi et al., 2015). The presence of a multitude of functional groups, including carboxylic and phenolic OH, alcoholic OH, ketonic C=O, amine groups and others, on DG surface controls the retention and release of organic compounds. Unprotonated, non-ionizable and non-polar or low-polar molecules,

such as boscalid and oxyfluorfen, may be linked to soil organic matter through non-specific hydrophobic interaction or partitioning processes between water and hydrophobic sites of DG (Senesi et al., 2015). Of course, experimental conditions, including pH and ionic strength, can affect both retention and release of the compounds.

Considering the values of the sorption parameters, Kd_{ads}, K_{Fads} and K_{OCads}, it was evident that the addition of the DG, especially at the highest dose, increased the overall retention of both compounds on the soil. The K_{Fads} value of boscalid on SOIL-DG 1, SOIL-DG 3 and SOIL-DG 6 were, respectively, 1.8, 1.8 and 2.8 times higher than that on SOIL, while that of oxyfluorfen on SOIL nearly tripled when 6 % DG was added (Table 5). Furthermore, the sorption parameters were higher for oxyfluorfen than for boscalid on SOIL and SOIL-DG 6 treatments and were similar in the other treatments (Table 5). The maximum K_{OCads} values of both compounds were observed in the treatment with the highest DG dose (SOIL-DG 6) (Table 5).

Little information is present in the literature on the extent and modeling of the adsorption of boscalid and oxyfluorfen on soil. Vallee et al. (2014) studied the adsorption of boscalid on two different soils and reported K_{Fads} values of 4.7 and 8.5 µg g^{-1}. Pérez-Lucas et al. (2021) added composted sheep manure in an agricultural soil and observed a noticeable increase in boscalid adsorption which was attributed to the increase in organic matter. In a very recent study, Bhatt et al. (2023) investigated the adsorption kinetics of boscalid on different soils and reported equilibrium adsorptions between 12.1 and 14.3 µg g^{-1}, the latter value for the soil with the highest organic matter content. The Kd values calculated by Hall et al. (2015) for oxyfluorfen adsorption on three Hawaiian soils ranged from 166 to 351 µg g^{-1}. In a study on oxyfluorfen adsorption on different soils, Wu et al. (2019), found K_{Fads} values ranging from 62 to 116 µg g^{-1}. Even though the DG used in this study had a greater adsorbent capacity of the compounds than other DGs, the overall adsorbent capacity of the treated soil was lower than that reported in the above-cited studies; this is reasonably due to the lower clay content and, above all, the lower organic matter content of the soil used here. A significant increase (2.6 times, from 28 to 72 µg g^{-1}) in oxyfluorfen adsorption on a sandy clay loam soil was observed after the addition of olive-oil mill waste (Calderón et al., 2015).

The desorption data and the plot of the Freundlich model of both compounds on all treatments are shown in Fig. 2, while the desorption parameters obtained by fitting the experimental data in the Henry and Freundlich models are referred in Table 6. The release of boscalid and oxyfluorfen from each treatment occurred differently than adsorption. After three desorption steps, approximately 73, 74, 64 and 37 % of the initially adsorbed boscalid, and 74, 72, 65 and 35 % of adsorbed oxyfluorfen were desorbed from SOIL, SOIL-DG 1, SOIL-DG 3 and SOIL-DG 6, respectively (Fig. 2). For both

molecules, all K_{Fdes} values were higher and all $1/n_{des}$ values were lower than the corresponding adsorption parameters (Table 5), which denoted a poor reversibility, i.e., a hysteretic behavior. The capacity of the soil to release the compounds in the diluted solution followed the order SOIL-DG 6 < SOIL-DG 3 < SOIL-DG 1 < SOIL. This last sequence is exactly the reversal of that seen for the adsorbent capacity of the treatments. The hysteresis phenomenon is dependent on the type of binding between the solute and the adsorbent and hinders the complete release of the compound (Senesi et al., 2015). Both the native organic matter of the soil, such as humic substances, and that introduced with amendments, such as DG, generally form both weak and strong bonds with organic xenobiotics; the weak bonds favor the rapid release of the compounds while the strong bonds cause sorption hysteresis. Recently, Bonnar et al. (2023) studied the adsorption of oxyfluorfen in rice soils and reported that the maximum release of the adsorbed compound was 27 %, which indicated a significant sorption hysteresis in all soils.

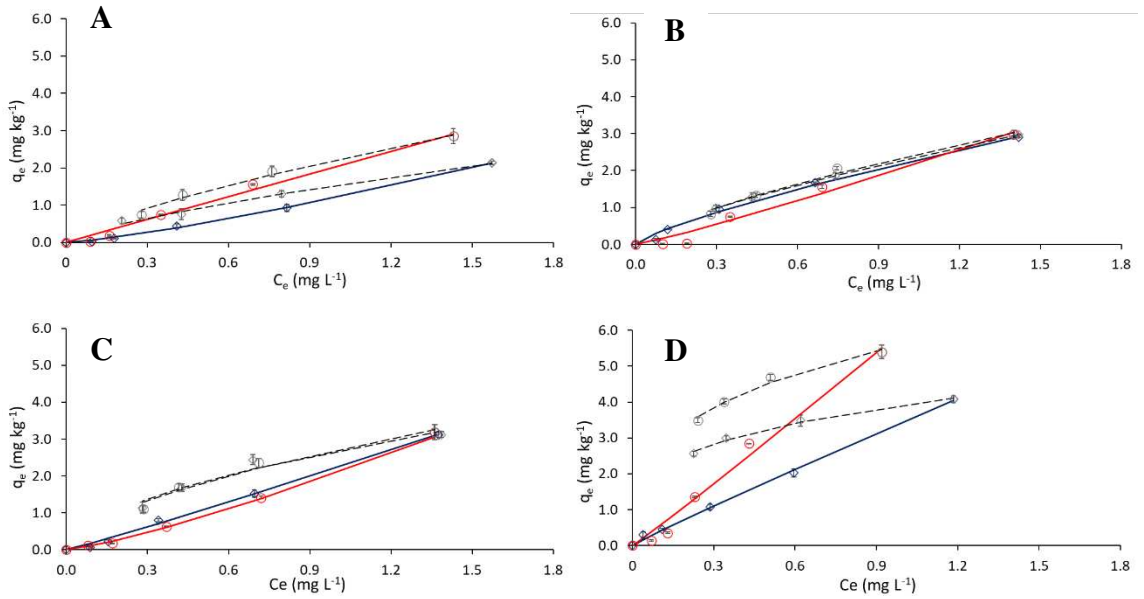

Figure 2. Adsorption and desorption isotherms of boscalid (blue colour) and oxyfluorfen (red colour) on unamended soil (A) and soil amended with DG at 1 (B), 3 (C) and 6% (D). The points indicate experimental data, while solid and dashed lines are plots of the Freundlich model for adsorption and desorption, respectively. The vertical bar on each point is the standard error (n = 3).

Table 6. Desorption parameters of the compounds from different soil treatments.

Compound	Theoretical models								
	HENRY				FREUNDLICH				H
	SSR	r	Kd_{des} mg kg^{-1}	K_{OCdes} mg kg^{-1}	SSR	R	K_{Fdes} mg kg^{-1}	$1/n_{ads}$	
				SOIL					
Boscalid	0.14	0.990	1.45	38.33	0.01	0.996	1.54	0.71	0.57
Oxyfluorfen	0.27	0.990	2.18	57.42	0.03	0.994	2.23	0.72	0.73
				SOIL-DG 1					
Boscalid	0.39	0.987	2.27	53.13	0.10	0.979	2.32	0.71	0.91
Oxyfluorfen	0.30	0.990	2.34	54.69	0.04	0.998	2.38	0.72	0.65
				SOIL-DG 3					
Boscalid	1.13	0.971	2.65	50.80	0.11	0.973	2.68	0.56	0.52
Oxyfluorfen	0.88	0.978	2.69	51.62	0.07	0.985	2.71	0.59	0.48
				SOIL-DG 6					
Boscalid	6.46	0.924	4.39	66.24	0.01	0.997	3.92	0.27	0.28
Oxyfluorfen	8.04	0.948	7.47	112.62	0.04	0.991	6.61	0.31	0.30

2.3.4 Fungal response to digestate treatment

In recent years, the agricultural practice of spreading DG directly into the soil has gained more and more relevance. Despite this, information on the impact of this material on soil-resident fungi is very scarce. It is very important to understand the possible benefits of DG on the biological fertility of the soil as well as the risks related to the promotion of microorganisms harmful to plants. Fig. 3 shows the appearance of fungal colonies on PDA substrate not treated (control) and treated with DG only and HA-DG interaction products. To evaluate the *in vitro* growth of fungi and estimate the mycelium growth rate, different models have been proposed (Dantigny et al., 2005; Tao et al., 2014). The linear model with breakpoint suggested by Dantigny et al. (2005) is generally very accurate to describe the growth data of filamentous fungi on PDA. In facts, fitting the growth in this model, frequently, the values of the regression coefficient are very close to the unit, which ensures accurate calculation of the growth parameters, such as radial growth rate, μ, and lag time, λ (Dantigny et al., 2005). The latter parameter represents the time between fungal inoculation and the beginning of hyphal elongation. Another valid parameter for estimating the mycelium extension over time is the absolute growth rate (AGR), which is considered the best parameter to ascertain stimulating or inhibitory effects of specific substances or external conditions on fungi (Tao et al., 2014).

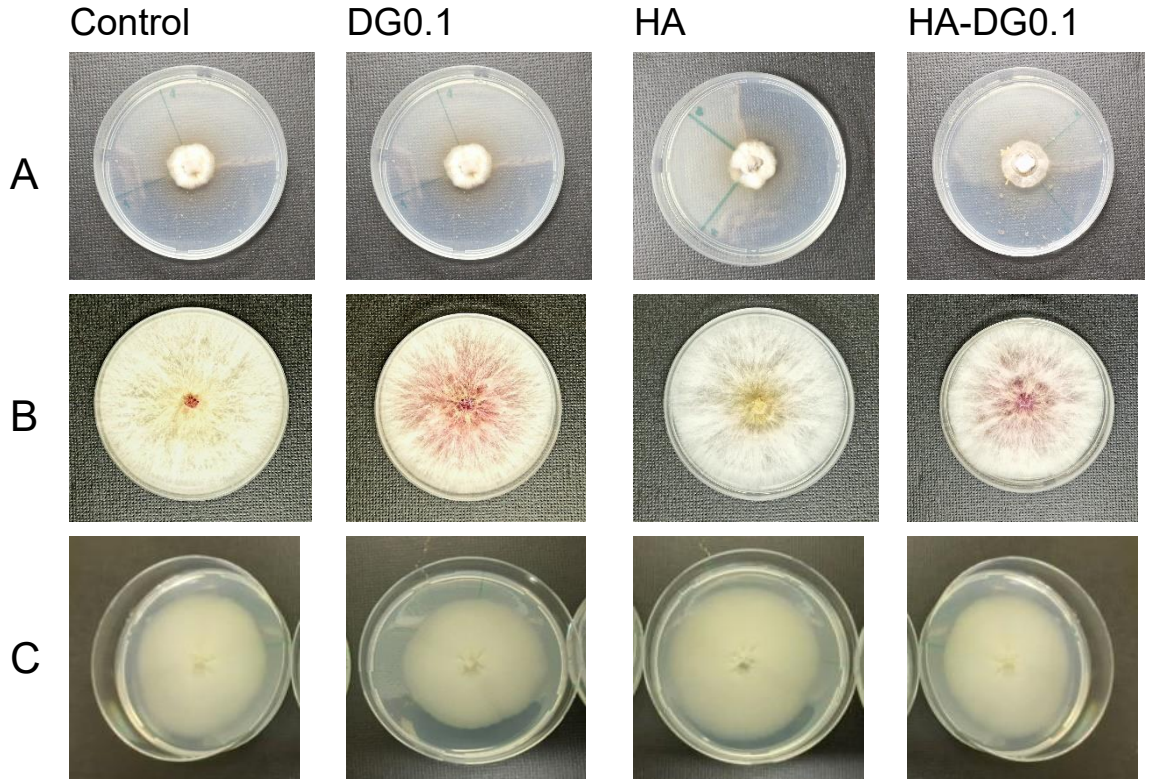

Figure 3. Fungal colony of *A. mellea* at 288 h from inoculation (A), *F. culmorum* at 120 h from inoculation (B) and *V. dahliae* at 350 h from inoculation (C).

2.3.4.1. Armillaria mellea

The radial extension of the mycelium was measured at regular intervals up to 14 d after inoculation. The experiments were ended before the fungus reached the edge of the plate because, after 14 d, the colonies of some samples started generating fungal rhizomorphs randomly. In the experimental conditions adopted, *A. mellea* showed the slowest growth among the fungi considered in this study. The data collected in the various samplings highlighted that none of the treatments substantially changed the growth trend of the fungus compared to the control. This occurred for both non-interacted DG and HA-interacted DG and is clearly illustrated in Fig. 4 where the linear fits to the experimental data appear nearly parallel to each other and to the control.

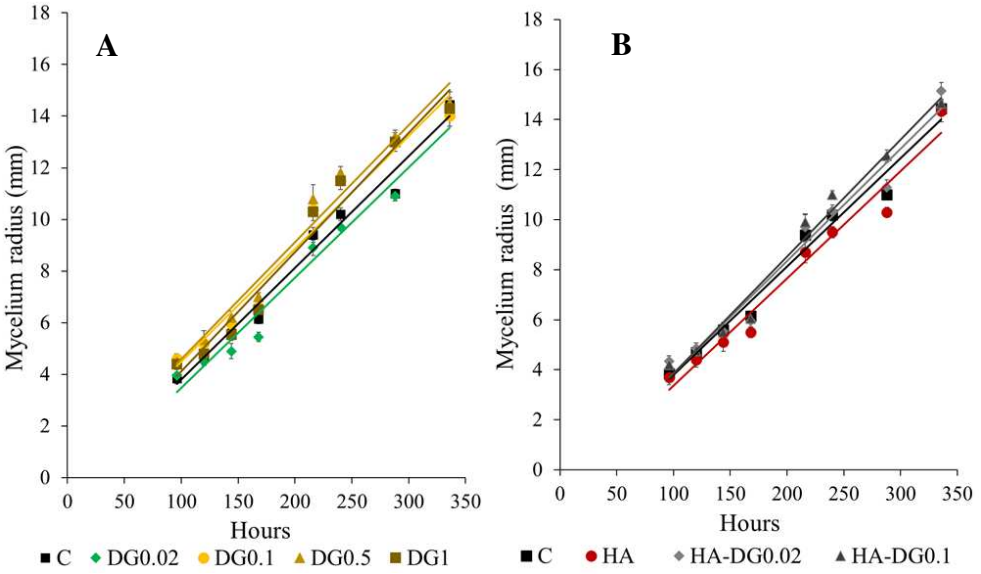

Figure 4. Effects of DG alone (A) and DG interacted with HA (B) at various doses on the radial extent of *A. mellea* as a function of time. The graph shows the experimental points with standard errors (n = 5) and linear plots.

Linear regressions of growth data showed r values ranging from 0.983 to 0.990, while statistical analysis of data (ANOVA) indicated that all treatments were not statistically different from the control (Table 7). On the other hand, a great variability of the lag time (λ) was observed. Compared to the control, HA caused the longest latency time (~ 20 h) which was almost twice that of the control, indicating a marked delay of the growth initiation induced by this substrate (Table 7). Since there were no changes in growth rate or other evident effects of DG alone or HA-interacted DG in the *in vitro* experiments, it can be hypothesized that the addition of DG to the soil may not significantly affect the pathogenic activity of this fungus. Compared to the control, only slight

differences in AGR were observed for all treatments (Fig. 5), which confirmed the irrelevant impact of any DG treatment on *A. mellea*.

Table 7. Growth parameters of the fungi calculated from the linear model.

TREATMENT	μ (mm h^{-1})	λ (h)	R
	Armillaria mellea		
Control	0.043 ± 0.001[a]	11.64 ± 2.53	0.990
DG0.02	0.043 ± 0.001	18.60 ± 2.41	0.987
DG0.1	0.043 ± 0.001	16.81 ± 2.33	0.983
DG0.5	0.046 ± 0.002	15.03 ± 4.22	0.986
DG1	0.046 ± 0.002	11.70 ± 2.14	0.985
HA	0.043 ± 0.002	20.03 ± 3.21	0.983
HA-DG0.02	0.045 ± 0.000	14.65 ± 5.89	0.983
HA-DG0.1	0.047 ± 0.000	17.24 ± 2.47	0.990
	Fusarium culmorum		
Control	0.379 ± 0.002	18.25 ± 0.90	0.997
DG0.02	0.370 ± 0.005	18.59 ± 0.62	0.991
DG0.1	0.354 ± 0.010*	18.36 ± 1.33	0.990
DG0.5	0.347 ± 0.004**	19.08 ± 0.41	0.992
DIG1	0.358 ± 0.003*	18.46 ± 0.43	0.992
HA	0.412 ± 0.002**	16.70 ± 0.60	0.996
HA-DG0.02	0.356 ± 0.011*	16.98 ± 0.99	0.995
HA-DG0.1	0.313 ± 0.012***	15.13 ± 0.84	0.993
	Verticillium dahliae		
Control	0.091 ± 0.001	54.27 ± 2.10	0.997
DG0.02	0.091 ± 0.001	11.48 ± 1.06	0.998
DG0.1	0.092 ± 0.002	42.17 ± 7.46	0.993
DG0.5	0.088 ± 0.002	52.63 ± 1.72	0.989
DG1	0.092 ± 0.002	64.94 ± 3.17	0.989
HA	0.080 ± 0.005	19.78 ± 6.52	0.995
HA-DG0.02	0.082 ± 0.009	40.03 ± 10.72	0.997
HA-DG0.1	0.080 ± 0.005	8.17 ± 1.55	0.997

μ: radial growth rate; λ: lag time; [a]Standard error (n = 5); *$P \leq 0.05$, **$P \leq 0.01$, ***$P \leq 0.001$ according to the least significant difference (LSD) test. No significant difference between each treatment and the control was found for *A. mellea* and *V. dahliae*.

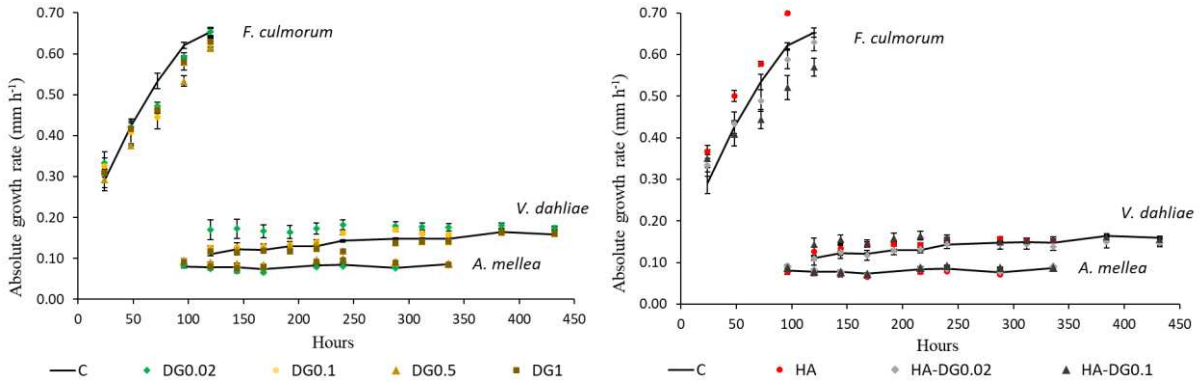

Figure 5. Absolute growth rate of the fungal colonies.

To date, this is the first report concerning the impact of anaerobic DG on the growth of *A. mellea* on solid substrate, therefore a comparison between our results and those of other studies is not possible. Musatti et al. (2017) found that *A. mellea* was not able to grow in submerged conditions using DG as the only carbon and energy source. Applying different soil amendments on *Armillaria* spp., Otieno et al. (2003) found that coffee pulp slightly reduced the vitality of the fungus *A. gallica*, while Malecka et al. (2015) found that Scots pine sawdust, composted bark, and woody debris caused no relevant effects on *A. ostoyae*.

2.3.4.2. Fusarium culmorum

In the experimental conditions adopted, the growth of *F. culmorum* was very rapid and the mycelium reached the edge of the plate in just 5 days (Fig. 3). Linear regression of the mycelium growth data of any treatment showed their excellent alignment, and the correlation coefficients ranged from 0.990 to 0.997 (n = 5) (Table 7). Unlike what observed for *A. mellea*, this fungus responded significantly differently to the various treatments. This is evident by observing the linear plot of the mycelium growth data (Fig. 6). The treatment lines, except for DG0.02, showed different slopes from that of the control (Fig. 6). In general, DG addition slowed down the mycelial extension, which graphically corresponded to lines with a lower slope than the control.

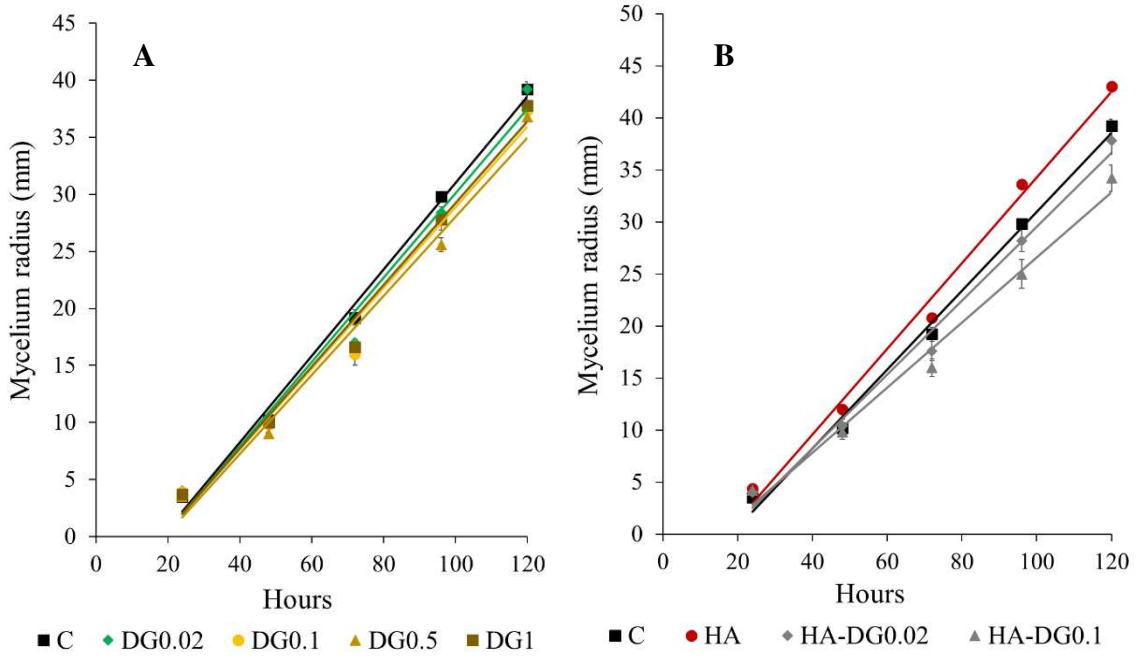

Figure 6. Effects of DG alone (A) and DG interacted with HA (B) at various doses on the radial extent of *F. culmorum* as a function of time. The graph shows the experimental points with standard errors (n = 5) and linear plots.

With the exclusion of DG 0.02 treatment, which was statistically equal to the control, and HA treatment, which showed the highest μ value, all other μ values were significantly or highly significantly lower than the control (Table 7). In this study, HA alone appeared to stimulate hyphal elongation, compared to the control (Table 7). However, when HA was present in combination with the DG, a clear inhibition was observed even at the lowest DG dose; the suppressive action reached its maximum expression in HA-DG0.1 combination (Table 6).

Previous studies demonstrated that the main fraction of stable soil organic matter, namely HA, could control plant diseases caused by fungal phytopathogens, especially when abundantly present in the rhizosphere (Pascual et al., 2002; Loffredo et al., 2007, 2008, 2009). However, the activity of HA depends not only on its physicochemical, structural and functional properties amd on the environmental conditions but also on the fungal species considered. Furthermore, there is previous evidence on changing, or even reversing, the activity of bioactive compounds on soil-resident fungi after interaction with HAs (Loffredo and Traversa, 2014). The high adsorption capacity of HA towards both hydrophilic and, especially, hydrophobic compounds (Senesi et al., 2015) might explain the change in HA activity observed for this fungus. Slowing down the growth of the fungus is very important in soils where the fungus lives and attacks the vegetation as the margin of time gained allows the plants to grow and strengthen, thus avoiding, at least in part, the fungal attack.

Only slight differences in the latency time of this fungus were observed between the various treatments and the control (Table 7). Although HA-DG 0.1 produced the strongest inhibition on *F. culmorum*, it also showed the shortest latency time (Table 7). This result agrees with the lack of correlation between growth rate and lag time reported by Dantigny et al. (2005). Finally, AGR data (Fig. 5) confirmed that all DG and HA-DG treatments reduced fungal growth, compared to the control.

Unfortunately, there are no previous laboratory or field studies on the influence of DG on the growth of *F. culmorum*, while some investigations concern other *Fusarium* spp. Previous studies demonstrated suppressive effects on the fungus *F. oxysporum* by various organic amendments, including DG (Loffredo and Senesi, 2009; Pane et al., 2014; Tao et al., 2014). An antifungal activity of a cow slurry DG on *F. solani* was found by Vitti et al. (2021). In a recent field study, a sewage sludge DG showed suppressive effectiveness on the Fusarium vascular wilt disease caused by *F. oxysporum* f. sp. *lycopersici* (De Corato et al., 2023).

2.3.4.3. Verticillium dahlia

Compared to the control, no morphological changes were observed for *V. dahliae* mycelium during the 18-day growth in the presence of any DG or HA-DG treatment at any concentration (Fig. 3).

Radial mycelial growth on PDA only (control) and PDA supplemented with DG and/or HA as well as linear plots of the experimental data are depicted in Fig. 7. Linear regression of the experimental data showed r values ranging from 0.989 to 0.998 (Table 7). Similarly to what was observed for *A. mellea*, also in the case of this fungus, none of the doses of DG applied significantly modified the mycelial growth, compared to the control. Graphically, the interpolation of the fungal growth data in the various treatments appeared as a series of lines almost parallel to each other and parallel to the control (Fig. 7).

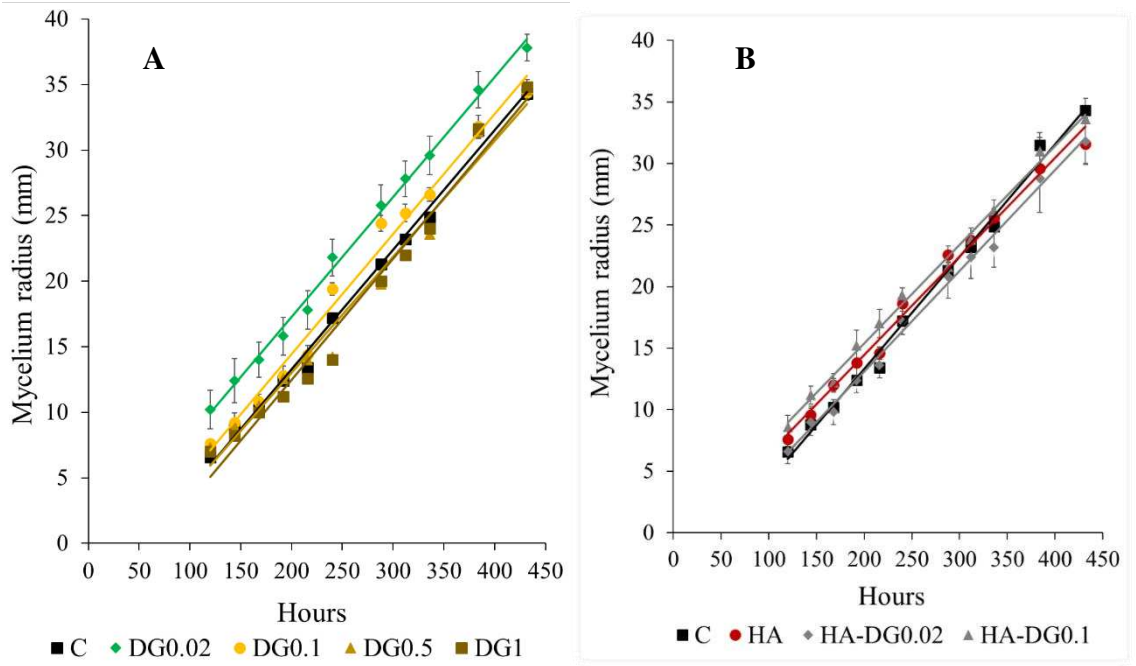

Figure 7. Effects of DG alone (A) and DG interacted with HA (B) at various doses on the radial extent of *V. dahliae* as a function of time. The graph shows the experimental points with standard errors (n = 5) and linear plots.

As previously reported for *A. mellea*, only the latency time was quite different in the various treatments, being minimum in HA-DG0.1 and maximum in DG1 (Table 7). However, under field conditions, the latency time does not appear to significantly influence the growth and pathogenicity of the fungus (Dantigny et al., 2005). These results are in agreement with the results of previous studies conducted both *in vivo* and *in vitro* by Pane et al. (2014) who found that a sterilized liquid extract from animal waste DG did not show significant inhibition of *V. dahliae*. Differently, in field trials, a liquid DG from mixed feedstock showed a noticeable reduction (50 %) in the *V. dahliae* density (Wei et al., 2016). To the best of our knowledge, no further information on this matter is available in the literature.

3.4 Conclusions

The anaerobic digestion of OP, a waste released in large quantities in geographical areas such as Apulia region, provides renewable energy (biogas or biomethane) and releases a byproduct, namely solid DG, which appears to improve the chemical and biological fertility of soil. This study demonstrated that a new DG produced exclusively from two-phase OP has a noticeable adsorbent capacity of the fungicide boscalid and the herbicide oxyfluorfen and, when incorporated into the soil, contributes significantly to the increase in the overall adsorbent capacity of the soil. This action

is of extreme importance as it limits the transfer of agrochemicals into natural surface and ground waters and reduces their absorption by cultivated plants with consequent lower risk of entry into the human and animal food chain. The results obtained also demonstrated that the sorption capacity of the DG remains unchanged over a wide range of temperatures, guaranteeing its effectiveness in various environmental and geographical conditions. The examination of the effects of DG on some important fungi that devastate agricultural crops highlighted suppressive effects on *F. culmorum*, effects that were even more intense after the interaction of DG with the humic fraction of the soil, which is what happens in real field conditions. Further studies could help to understand the biochemical mechanisms underlying this phenomenon and which possible DG modification could enhance its suppressiveness on phytopathogenic fungi. Inhibitory effects were not observed on *A. mellea* and *V. dahliae* whose growth appeared unaltered at normal field dosage of the DG. However, considering the benefits of DG on soil fertility and the need to dispose of this byproduct, even the irrelevant activity observed on the latter fungi can be considered favourably. Ultimately, the production and use of DG from OP appears to be a sustainable and recommendable strategy in both the energy and agricultural sectors.

References

Bhat, R.G., Subbarao, K.V. (1999). Host range specificity in Verticillium dahliae. Phytopathology 89, 1218–1225. https://doi.org/10.1094/PHYTO.1999.89.12.1218

Bhatt, D., Srivastava, A., Srivastava, P.C. (2023). An insight into the sorption kinetics of boscalid onto soils: Effect of general soil properties. Chemosphere 325 https://doi.org/10.1016/j.chemosphere.2023.138274

Braguglia, C.M., Gallipoli, A., Gianico, A., Pagliaccia, P. (2018). Anaerobic bioconversion of food waste into energy: A critical review. Bioresource Technology 248, 37-56. https://doi.org/10.1016/j.biortech.2017.06.145

Brezáni, A., Svobodová, K., Jablonský, I., Tlustoš, P. (2019). Cultivation of medicinal mushrooms on spruce sawdust fermented with a liquid digestate from biogas stations. International Journal of Medicinal Mushrooms 21, 215-223. https://doi.org/10.1615/IntJMedMushrooms.2019030022

Brueck, C.L., Nason, S.L., Multra, M.G., Prasse, C. (2023). Assessing the fate of antibiotics and agrochemicals during anaerobic digestion of animal manure. Science of the Total Environment 856, 159156. https://doi.org/10.1016/j.scitotenv.2022.159156

Calderón, M.J., Real, M., Cabrera, A., Koskinen, W.C., Cornejo, J., Hermosín, M.C. (2015). Influence of olive oil mill waste amendment on fate of oxyfluorfen in southern Spain soils. Clean - Soil, Air, Water, 43, 1107-1113. https://doi.org/10.1002/clen.201400560

Caruso, C., Maucieri, C., Barco, A., Barbera, A.C., Borin, M. (2018). Effects of mycorrhizal inoculation and digestate fertilisation on triticale biomass production using fungicide-coated seeds. Irish Journal of Agricultural and Food Research 57, 42-51. https://doi.org/10.1515/ijafr-2018-0005

Castellana, G., Loffredo, E. (2014). Simultaneous removal of endocrine disruptors from a wastewater using white rot fungi and various adsorbents. Water, Air, and Soil Pollution 225, 1872. https://doi.org/10.1007/s11270-014-1872-6

Cesaro, A. (2021). The valorization of the anaerobic digestate from the organic fractions of municipal solid waste: Challenges and perspectives. Journal of Environmental Management 280, 111742. https://doi.org/10.1016/j.jenvman.2020.111742

Chen, L., Zhang, S. (2010). Dissipation and residues of boscalid in strawberries and soils. Bulletin of Environmental Contamination and Toxicology 84, 301–304. https://doi.org/10.1007/s00128-010-9934-y.

Dantas Palmeira, J., Araújo, D., C. Mota, C., Alves, Rita C., P. P. Oliveira, M.B., Ferreira, H.M.N. (2023). Fermentation as a strategy to valorize olive pomace, a by-product of the olive oil industry. Fermantation 9, 442. https://doi.org/10.3390/fermentation9050442

Dantigny, P., Guilmart, A., Bensoussan, M. (2005). Basis of predictive mycology. International Journal of Food Microbiology 100, 187-196. https://doi.org/10.1016/j.ijfoodmicro.2004.10.013

Devkota, P., Hammerschmidt, R. (2020). The infection process of *Armillaria mellea* and *Armillaria solidipes*. Physiological and Molecular Plant Patology 112, 101543. https://doi.org/10.1016/j.pmpp.2020.101543

Dollinger, J., Bourdat-Deschamps, M., Pot, V., Serre, V., Bernet, N., Deslarue, G., et al. (2022). Leaching and degradation of S-metolachlor in undisturbed soil cores amended with organic wastes. Environmental Science and Pollution Research, 29, 20098-20111. https://doi.org/10.1007/s11356-021-17204-z

El-Masry, M.H., Khalil, A.I., Hassouna, M.S., Ibrahim, H.A.H. (2002). In situ and in vitro suppressive effect of agricultural composts and their water extracts on some phytopathogenic fungi. World Journal of Microbiology and Biotechnology 18, 551-558. https://doi.org/10.1023/A:1016302729218

EPA (1992). Pesticide Tolerance for Oxyfluorfen. USEPA, Washington, USA (Fed Regist 57-22202) (accessed on 24 May 2023).

European Commission (EC) 2003. Regolamento CE, N. 2003/2003, 13 October 2003 relativo ai concimi. https://eur-lex.europa.eu/legal-content/IT/TXT/PDF/?uri=CELEX:02003 R2003-20141215&from=BG

European Commission (EC) 2019. https://eur-lex.europa.eu/legalcontent/EN/TXT/PDF/?uri=CELEX:32019R1691 (accessed on 24 May 2023).

Gazzetta Ufficiale della Repubblica Italiana (GU). DM 13-09-1999. Metodi ufficiali di analisi chimica del suolo. https://www.gazzettaufficiale.it/eli/gu/1999/10/21/248/so/185/sg/pdf (accessed 12 May 2023).

Gazzetta Ufficiale della Repubblica Italiana (GU). DM 21-12-2000. Metodi ufficiali di analisi per i fertilizzanti. https://www.gazzettaufficiale.it/eli/id/2001/01/26/21/sg/pdf (accessed 12 May 2023).

Hall, K.E., Ray, C., Ki, S.J., Spokas, K.A., Koskinen, W.C. (2015). Pesticide sorption and leaching potential on three Hawaiian soils. Journal of Environmental Management 159, 227-234. https://doi.org/10.1016/j.jenvman.2015.04.046

Karimi, B., Sadet-Bourgeteau, S., Cannavacciuolo, M., Chauvin, C., Flamin, C., et al. (2022). Impact of biogas digestates on soil microbiota in agriculture: A review. Environmental Chemistry Letters 20, 3265-3288. https://doi.org/10.1007/s10311-022-01451-8

Kulikova, N.A., Stepanova, E.V., Koroleva, O.V. (2005). Mitigating activity of humic substances: direct Influence on Biota. In: Use of humic substances to remediate polluted environments: from theory to practice. Perminova I.V. et al. (eds.), Springer, The Netherlands, pp. 285–309. https://doi.org/10.1007/1-4020-3252-8_14

IHSS Natural organic matter research 2022. https://humic-substances.org/ (accessed on 10 June 2023).

Loffredo, E., Berloco, M., Casulli, F., Senesi, N. (2007). In vitro assessment of the inhibition of humic substances on the growth of two strains of *Fusarium oxysporum*. Biology and Fertility of Soils 43, 759-769. https://doi.org/10.1007/s00374-006-0160-z

Loffredo, E., Berloco, M., Senesi, N. (2008) The role of humic fractions from soil and compost in controlling the growth in vitro of phytopathogenic and antagonistic soil-borne fungi. Ecotoxicology and Environmental Safety 69, 350-357. https://doi.org/10.1016/j.ecoenv.2007.11.005

Loffredo, E., Carnimeo, C., Silletti, R., Summo, C. (2021). Use of the solid by-product of anaerobic digestion of biomass to remove anthropogenic organic pollutants with endocrine disruptive activity. Processes 9, 2018. https://doi.org/10.3390/pr9112018

Loffredo, E., Senesi, N. (2009). In vitro and in vivo assessment of the potential of compost and its humic acid fraction to protect ornamental plants from soil-borne pathogenic fungi. Scientia Horticulturae, 122, 432-439. https://doi.org/10.1016/j.scienta.2009.05.030

Loffredo, E., Traversa, A. (2014). Soil and compost humic fractions regulate the response of *Sclerotinia sclerotiorum* to exogenously added allelochemical compounds. Biology and Fertility of Soils 50, 1281-1290. https://doi.org/10.1007/s00374-014-0944-5

Loffredo, E., Carnimeo, C., D'Orazio, V. *et al.* (2024). Sorption and release of the pesticides oxyfluorfen and boscalid in digestate from olive pomace and in digestate-amended soil. Journal of Soils and Sediments, 24, 1489–1506. https://doi.org/10.1007/s11368-024-03748-3

Malecka M., Kwašna H., Szewczyk W. (2015). Fungal communities in barren forest soil after amendment with different wood substrates and their possible effects on trees, pathogens, insects and nematodes. Journal of Plant Protection Research 55, 301-311. https://doi.org/10.1515/jppr-2015-0042

Moliszewska, E., Pisarek, I. (1996). Influence of humic substances on the growth of two phytopathogenic soil fungi. Environment International 22, 579-584. https://doi.org/10.1016/0160-4120(96)00048-7

Möller, K., Müller, T. (2012). Effects of anaerobic digestion on digestate nutrient availability and crop growth: A review. Engineering in Life Sciences 12, 242–257. https://doi.org/10.1002/elsc.201100085

Mukherjee, S., Weihermüller, L., Tappe, W., Hofmann, D., Köppchen, S., Laabs, V., et al. (2016). Sorption-desorption behaviour of bentazone, boscalid and pyrimethanil in biochar and digestate based soil mixtures for biopurification systems. Science of the Total Environment, 559, 63-73. https://doi.org/10.1016/j.scitotenv.2016.03.145

Musatti, A., Ficara, E., Mapelli, C., Sambusiti, C., Rollini, M. (2017). Use of solid digestate for lignocellulolytic enzymes production through submerged fungal fermentation. Journal of Environmental Management 199, 1-6. https://doi.org/10.1016/j.jenvman.2017.05.022

Nkoa, R. (2014). Agricultural benefits and environmental risks of soil fertilization with anaerobic digestates: A review. Agronomy for Sustainable Development 34, 473-492. https://doi.org/10.1007/s13593-013-0196-z

Otieno W., Jeger M., Termorshuizen A. (2003). Effect of infesting soil with *Trichoderma harzianum* and amendment with coffee pulp on survival of *Armillaria*. Biological Control 26, 293-301. https://doi.org/10.1016/S1049-9644(02)00168-8

Pane C., Celano G., Zaccardelli M. (2014). Metabolic patterns of bacterial communities in aerobic compost teas associated with potential biocontrol of soilborne plant diseases. Phytopathologia Mediterranea 53, 277-286. https://doi.org/10.14601/Phytopathol_Mediterr-13363

Parlavecchia, M., Gattullo, R., Perri, G., Loffredo, E. (2021). Modulatory effects of biochar, hydrochar and vermicompost on the growth of horticultural plants and phytopathogenic fungi. Acta Horticulturae 1311, 541-548. https://doi.org/10.17660/ 2021.1311.69

Pascual, J.A., Garcia, C., Hernandez, T., Lerma, S., Lynch, J.M. (2002). Effectiveness of municipal waste compost and its humic fraction in suppressing *Pythium ultimum*. Microbial Ecology 44, 59–68. https://doi.org/10.1007/s00248-001-0040-x

Peng, W., Pivato, A. (2019). Sustainable management of digestate from the organic fraction of municipal solid waste and food waste under the concepts of back to earth alternatives and circular economy. Waste Biomass Valorization 10, 465–481. https://doi.org/10.1007/s12649-017-0071-2

Pérez-Lucas, G., El Aatik, A., Vela, N., Fenoll, J., Navarro, S. (2021). Exogenous organic matter as strategy to reduce pesticide leaching through the soil. Archives of Agronomy and Soil Science, 67, 934-945. https://doi.org/10.1080/03650340.2020.1768531

Provenzano, M.R., Cavallo, O., Malerba, A.D., Di Maria, F., Cucina, M., Massaccesi, L., Gigliotti, G. (2016). Co-treatment of fruit and vegetable waste in sludge digesters: Chemical and spectroscopic investigation by fluorescence and Fourier transform infrared spectroscopy. Waste Management 50, 283-289. https://doi.org/10.1016/j.wasman.2016.02.026

PubChem Open Chemistry Database at the National Institutes of Health (NIH), U.S. National Library of Medicine. Available online: https://pubchem.ncbi.nlm.nih.gov/compound/8814 (accessed on 20 June 2023).

Pullen, T. (2015). Anaerobic digestion-making biogas-making energy. Routledge, New York, NY. https://doi.org/10.4324/9781315770772

Sanchez, C. (2009). Lignocellulosic residues: Biodegradation and bioconversion by fungi. Biotechnology Advances 27, 185-194. https://doi.org/10.1016/j.biotechadv.2008.11.001

Salvestrini, S., Vanore, P., Iovino, P., Leone, V., Capasso, S. (2015). Adsorption of simazine and boscalid onto acid-activated natural clinoptilolite. Environmental Engineering and Management Journal 14, 1705-1712. https://doi.org/10.30638/eemj.2015.181

Santi, G., Muzzini, V.G., Galli, E., Proietti, S., Moscatello, S., Battistelli, A. (2015). Mycelial growth and enzymatic activities of white-rot fungi on anaerobic digestates from industrial biogas plants. Environmental Engineering and Management Journal 14, 1713-1719. https://doi.org/10.30638/eemj.2015.182

Scherm B., Balmas V., Spanu F., Pani G., Delogu G., Pasquali M., Migheli Q. (2013). *Fusarium culmorum*: causal agent of foot and root rot and head blight on wheat. Molecular Plant Pathology 14, 323-341. https://doi.org/10.1111/mpp.12011

Schnathorst W.C. (1981). Life cycle and epidemiology of *Verticillium*. In: Fungal wilt diseases of plants. Mace, M.E., Bell, A.A., Beckman, C.H. (eds). Academic Press, New York, pp. 81-111.

Senesi, N., Loffredo, E., D'Orazio, V., Brunetti, G. et al. (2015). Adsorption of pesticides by humic acids from organic amendments and soils. In: Humic Substances and Chemical Contaminants. C.E. Clapp et al. (eds.). Soil Sci. Soc. Am. Madison, WI, USA, pp. 129-153 https://doi.org/10.2136/2001.humicsubstances.c8

Singh, L., Kalia, V.C. (2017). Waste Biomass Management—A Holistic Approach; Springer International Publishing AG: Cham, Switzerland.

Szczech, M., Smolinska, U. (2001). Comparison of suppressiveness of vermicomposts produced from animal manures and sewage sludge against phytophthora *Nicotianae breda* de haan var. nicotianae. Journal of Phytopathology 149, 77-82. https://doi.org/10.1046/j.1439-0434.2001.00586.x

Tang, Y., Luo, L., Carswell, A., Misselbrook, T., Shen, J., Han, J. (2021). Changes in soil organic carbon status and microbial community structure following biogas slurry application in a wheat-rice rotation. Science of the Total Environment 757, 143786. https://doi.org/10.1016/j.scitotenv.2020.143786

Tao, X., Shang, B., Dong, H., Chen, Y., Xin, H. (2014). Effects of digestate from swine manure digester on in vitro growth of crop fungal pathogens: A laboratory study. Transactions of the ASABE 57, 1803-1810. https://doi.org/10.13031/trans.57.10622

Taskin, E., Perri, G., Loffredo, E. (2019). Impact of type and dose of biochar and hydrochar on growth response of phytopathogenic and antagonistic soil resident fungi. Fresenius Environmental Bulletin 28, 9070-9076.

Teglia, C., Tremier, A., Martel, J.-L. (2011). Characterization of solid digestates: Part 1, review of existing indicators to assess solid digestates agricultural use. Waste Biomass Valorization 2, 43–58. https://doi.org/ 10.1007/s12649-010-9051-5

Tolisano, C., Luzi, F., Regni, L., Proietti, P., Puglia, D., Gigliotti, G. et al. (2023). A way to valorize pomace from olive oil production: Lignin nanoparticles to biostimulate maize plants. Environmental Technology and Innovation, 31, 103216. https://doi.org/10.1016/j.eti.2023.103216

U.S. National Library of Medicine. PubChem Open Chemistry Database at the National Institutes of Health (NIH). Available online: https://pubchem.ncbi.nlm.nih.gov (accessed on 10 May 2023).

Valenti, F., Arcidiacono, C., Chinnici, G., Cascone, G., Porto, S.M.C. (2017). Quantification of olive pomace availability for biogas production by using a GIS-based model. Biofuels, Bioproducts and Biorefining 11, 784-797. https://doi.org/10.1002/bbb.1784

Velechovský, J., Malík, M., Kaplan, L., Tlustoš, P. (2021). Application of individual digestate forms for the improvement of hemp production. Agriculture 11. https://doi.org/10.3390/agriculture11111137

Vallée, R., Dousset, S., Billet, D., Benoit, M. (2014). Sorption of selected pesticides on soils, sediment and straw from a constructed agricultural drainage ditch or pond. Environmental Science and Pollution Research 21, 4895-4905. https://doi.org/10.1007/s11356-013-1840-5

Walsh, J.J., Rousk, J., Edwards-Jones, G., Jones, D.L., Williams, A.P. (2012). Fungal and bacterial growth following the application of slurry and anaerobic digestate of livestock manure to temperate pasture soils. Biology and Fertility of Soils 48, 889-897. https://doi.org/10.1007/s00374-012-0681-6

Wang, W., Lee, D-J. (2021). Valorization of anaerobic digestion digestate: A prospect review. Bioresource Technology 323, 124626. https://doi.org/10.1016/j.biortech.2020.124626

Wei F., Passey T., Xu X. (2016). Effects of individual and combined use of biofumigation-derived products on the viability of *Verticillium dahliae* microsclerotia in soil. Crop Protection 79, 170-176. https://doi.org/10.1016/j.cropro.2015.09.008

World Bioenergy Association (WBA). Annual report 2022. https://www.worldbioenergy.org/uploads/230510%20Annual%20Report%202022%20Public.pdf (accessed on 29 May 2023).

Wu, C., Liu, X., Wu, X., Dong, F., Xu, J., Zheng, Y. (2019). Sorption, degradation and bioavailability of oxyfluorfen in biochar-amended soils. Science of the Total Environment 658, 87-94. https://doi.org/10.1016/j.scitotenv.2018.12.059

CHAPTER – 3
UNTREATED PLANT WASTE OF THE MEDITERRANEAN REGION AS BIOADSORBENT OF PERSISTENT ORGANIC POLLUTANTS

The work reported in this chapter has been published in Heliyon, Volume 10, Issue 23, (2024) https://doi.org/10.1016/j.heliyon.2024.e40740

Abstract

The excessive and/or improper use of plant protection products (PPPs) can generate alarming levels of residues in the environment, compromising both soil fertility and food safety. Various organic wastes released in large amounts by agro-industrial activity are currently studied and applied as bioadsorbents for water and soil decontamination. This study explored the capacity of untreated orange peel (OP), olive stones (OS) and pistachio shells (PS) to adsorb the PPPs oxyfluorfen (OXY), metribuzin (MET) and imidacloprid (IMI), and the xenoestrogen bisphenol A (BPA) from water. The physicochemical, microstructural, and spectroscopic characteristics of the adsorbents were first evaluated using TXRF, SEM and FTIR-ATR techniques. Adsorption kinetics showed that each pollutant was rapidly (~ 24 h) retained by all adsorbents according to a pseudo-second order model, which suggested a prevalent chemisorption. Interpretation of the sorption isotherm data with various theoretical equations showed that all molecules on all adsorbents preferentially followed the Freundlich model. Among the materials, OS showed the highest adsorbent capacity with K_F values equal to 713, 317, 359 and 736 mg kg^{-1} for OXY, MET, IMI, and BPA, respectively. The desorption of each compound from all materials was hysteretic. Based on the overall results obtained, it appears that all three materials tested may have interesting applications for the retention of organic pollutants, especially very hydrophobic ones. This paves the way for further investigations into natural adsorbents as sustainable tools for environmental remediation.

3.1 Introduction

In recent decades, intensive agricultural practices have not always complied with the recommended guidelines (E.D. 2009/128/CE) for the use of plant protection products (PPPs), with harmful consequences of contaminating soil, ground- and surface water (Mottes et al. 2013, Gentil et al. 2020). Repeated applications of PPPs and the accumulation of their residues in soil over the years can compromise not only soil fertility and crop productivity but also food quality and safety (Regueiro et al.2013, Carnimeo et al. 2022). Among PPPs, herbicides and insecticides are largely

employed to protect tree and herbaceous crops. Oxyfluorfen [2-chloro-1-(3-ethoxy-4-nitrophenoxy)-4-(trifluoromethyl) benzene] (OXY) is a diphenyl ether herbicide used to eliminate broadleaf weeds and acts by interrupting the final phase of chlorophyll synthesis (Camadro et al. 1995). Metribuzin [(4-amino-6-tert-butyl-3-(methylsulfanil)-1,2,4-triazine-5(4H)-one] (MET) is a triazinone herbicide widely used in both pre- and post-emergence to control broadleaf weeds, especially annual ones, in various crops (Mehdizadeh et al. 2019). Being a quite soluble molecule, MET has a great potential for leaching to groundwater (USEPA 2023). Imidacloprid [1-((6-chlor-3-pyridinyl) methyl)-N-nitro-2-imidazolidinimine] (IMI) is one of the most used insecticides on a global scale and is currently suspected of exterminating pollinators and harming users (Crossthwaite et al. 2017). This systemic neonicotinoid insecticide is employed in soil applications, directly on vegetation and to control pet parasites (Ensley 2018).

In addition to PPPs, endocrine disrupting chemicals (EDCs) can be released in soil by amendment practices that use not completely depolluted sludge and wastewater (Endocrine Disruptor List 2023). Among EDCs, bisphenol A [2,2-(4,4 dihydroxyphenyl) propane] (BPA) is one of the most widely produced chemical compounds in the world, with an estimated annual production of about 8 million tons (Chen et al. 2020). BPA is a component of polycarbonate, epoxy resins, medical devices, paints, electrical and electronic components; it has a great relevance for its estrogenic and antiandrogenic effects (Calafat et al. 2008).

Both PPPs and EDCs often coexist in the soil and can be easily absorbed by plant roots and accumulated into edible plant parts, such as fruits, tubers, rhizomes, stems and flowers, thus entering the animal and human food chain (Carnimeo et al. 2022, den Braver-Sewradj et al. 2020).

The techniques currently used to remove organic pollutants from soil and wastewater include adsorption on organic and mineral matrices (Grassi et al. 2012, Loffredo et al. 2022), membrane filtration systems (Martí-Calatayud et al. 2020), reverse osmosis (Liu et al. 2021), oxidation (Dao et al. 2020), ozone treatment (Paucar et al. 2018) and photolysis (Grassi et al. 2012). Among these methods, the adsorption process is efficient, economical and environmentally friendly (Loffredo & Taskin 2017). In the last years, bioenergy byproducts and derivatives, such as biochar, hydrochar, digestate and compost, are successfully employed for soil and wastewater remediation (Loffredo 2022). With a view to environmental and economic sustainability, recent research has focused on widely available agricultural waste and by-products to be used as bioadsorbents of organic and inorganic contaminants (Hansen et al. 2010, Krstić et al. 2018, Kayranli et al. 2021). This nature-based and low-cost approach has a clear character of simplicity and effectiveness and is acclaimed by the population (Loffredo et al. 2020, El Refay et al. 2022).

Three agro-industrial by-products that are particularly abundant in the Mediterranean area that could be used for bioremediation practices are orange peel (OP), olive stones (OS) and pistachio shells (PS). Orange is one of the most consumed fruits in the Mediterranean countries, with a global production exceeding 5 million tons in 2022 (FAOSTAT 2022). About 70% of the citrus products are processed (Siles et al. 2016), and that generates large amounts of biowaste. The dominant components of OP are cellulose, hemicellulose, pectin, lignin, chlorophyll pigments and low molecular weight compounds (Dey et al. 2021). Olive cultivation occupies about 5 million hectares of the Mediterranean area (FAOSTAT 2022) and the disposal of waste from the olive oil industry (including olive stones) is a worrying environmental issue, especially in major producing countries such as Spain and Italy (Sciubba et al. 2021, Di Giacomo & Romano 2022). In recent years, the pistachio fruit has had growing appreciation by consumers and the agri-food industry, reaching a global production of 1 million tons in 2022 (FAOSTAT 2022), of which the shells accounts for 15% of the product (Hosseinzaei et al. 2022). OS and PS are similar in lignin, cellulose, and hemicellulose contents (Moubarik & Grimi 2014, Senturk & Alzein 2020).

These by-products have been used so far mostly as fuels, with consequent loss of C in the atmosphere and release of air-pollutants (carbon monoxide, nitrogen oxides, and particulates such as soot and ash from combustion) (Rodriguez et al. 2008, Mahato et al. 2019). Another current use of the three by-products is the thermochemical and biological treatment to produce bioenergy and C-rich solid residues, such as biochar, digestate and compost (Hosseinzaei et al. 2022, Read et al. 2021, Schmidt et al. 2023), which contributes to carbon sequestration strategies aimed at mitigating climate change (Reuland et al. 2023, Giannetta et al. 2023). Biochar, digestate and compost have shown excellent capacity in the retention of both organic and inorganic pollutants (Paradelo et al.2020 , Loffredo et al. 2024, Ambaye et al. 2020): as such, they are often applied for soil restoration. In this context, biochar and activated carbon are particularly interesting because of their high surface area, long term stability and high carbon content (Ahmad et al. 2014, Jeguirim et al. 2018). However, the thermochemical conversion of biomass, requires large energy inputs, posing questions from the point of view of economic and environmental sustainability (Safarian 2018). Furthermore, the efficiency of the biochemical conversion of waste, such as composting and anaerobic digestion, is strictly related to the feedstock; biowastes such as OS and PS are not the most suitable due to the high lignin content and the resulting high C/N ratio (Moubarik & Grimi 2014, Senturk & Alzein 2020). Differently, the direct use of untreated wastes does not require energy-intensive processing and specialized equipment and can represent an effective and economic alternative due to the low cost, wide availability and a chemical structure suitable for the retention

of contaminants (Eniola et al. 2023, Patel 2012). To the best of our knowledge, these materials have never been tested as adsorbents of organic contaminants (Frezzini et al. 2019).

In light of the above, the main objective of this study was to assess the effectiveness of three agro-industrial by-products, orange peel, olive stones and pistachio shells, to act as natural adsorbents of some chemicals, namely OXY, MET, IMI and BPA, from water. Quantitative data were obtained from adsorption kinetics and adsorption/desorption isotherms. Furthermore, to relate the sorption capacity of these materials to their properties and structure, a preliminary extensive characterization was carried out using total reflection X-ray fluorescence (TXRF) spectroscopy, scanning electron microscopy (SEM) analysis and Fourier transform infrared (FTIR) spectroscopy.

3.2 Materials and methods

3.2.1 Chemicals and adsorbents

The four molecules OXY, MET, IMI and BPA at purities of 99.0, 98.0, 99.0 and 99.0%, respectively, were purchased from Sigma-Aldrich S.r.l, Milano, Italy. Structural formula and some chemical properties of the compounds are reported in Table 1. All other chemicals of extra pure grade were obtained from commercial sources and used without further purification.

Table 1. Some properties of the compounds; molecular weight expressed in g·mol^{-1}, water solubility measured at 25 °C and expressed in mg·L^{-1}

Compound	Chemical structure	Molecular weight	Water solubility	log Kow
Oxyfluorfen	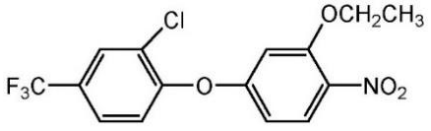	361.70	~ 2	4.73
Metribuzin	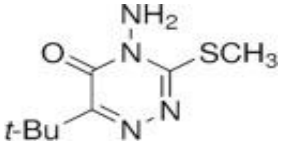	214.29	1200	1.70
Imidacloprid	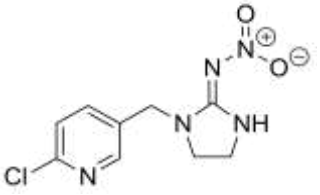	255.70	610	0.57
Bisphenol A	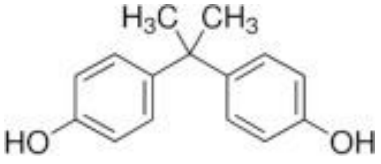	228.29	300	3.32

Data from PubChem open chemistry database at the National Institutes of Health (2024).

Adsorbents obtained from OP, OS and PS were used. OP was collected from 'Navelina' orange (*Citrus sinensis* L.), a variety for fresh consumption, purchased at the local market. OS were supplied by the cooperative 'Il Sannicandrese', Sannicandro di Bari, Italy, while PS were of domestic origin. Before experiments, the materials were repeatedly washed with tap water, soaked in deionized water for approximately 1 h to remove residual impurities, dried at a temperature of 40 °C for 36 h and finally ground to < 1-mm particles.

3.2.2 Adsorbent characterization

3.2.2.1 Basic characterization

Physicochemical characterization of the three adsorbents was carried out according to conventional methods. Moisture was measured after heating the adsorbents at 105 °C overnight. Bulk density (BD) was measured using a 500 mL graduated cylinder filled with a known sample mass and tapped manually for 60 s to ensure the absence of large void spaces, before measuring the final volume occupied by the sample mass. The ash content was determined after drying the samples in a muffle furnace at the temperature of 550 °C for 4 h. The pH and EC were measured using a pH meter and a conductivity meter (adsorbent/H_2O, 1:10, w/v), respectively. Total organic matter was determined by the loss on ignition method (Shamrikova et al. 2024).

3.2.2.2 Elemental analysis

Minor and trace elements present in the three adsorbents were analysed by TXRF spectroscopy using a S2 Picofox Spectrometer (Bruker Nano GmbH, Berlin, Germany). The instrument was equipped with a Mo microfocus tube (30 W, 50 kV, 600 μA), a multilayer monochromator, and an XFlash® silicon drift detector with a 30 mm^2 active area. The energy resolution, measured at the Kα of Mn, was < 150 eV (10 kcps). For such analysis, dried samples were finely powdered using a vibratory ball mill (model MM200, Retsch) for 5 min. Then, for each sample, 10 mg of powder were suspended in 3 mL of Triton X-100 (1:100, v/v in bidistilled water) using 10 mL plastic tubes and left for 10 minutes in an ultrasonic bath. After that, 10 mL of a 1000 mg L^{-1} Y standard (Sigma-Aldrich) were added to each suspension as internal standard. Finally, after vortexing for 30 s, 10 μL of suspension were pipetted onto siliconized quartz carriers and left until complete dryness on a heating plate (50 °C) under laminar flow hood. All samples were analysed in triplicate for 1000 s, and the results were obtained with the software Spectra 7 (Bruker Gmbh, Germany).

3.2.2.3 SEM analysis

SEM analysis was performed to investigate the surface micromorphology of the adsorbents. The sample was fixed with an adhesive carbon tape, metallized with Au, and analysed with a high-resolution field emission scanning electron microscope VP FE-SEM ΣIGMA 300 (ZEISS, Oberkochen, Germany). The SEM micrographs of the three adsorbents were captured at 1500 × magnifications using a 5 kV acceleration potential.

3.2.2.4 FTIR-ATR spectroscopy

FTIR spectroscopy coupled with attenuated total reflectance (ATR) was used to investigate functional groups belonging to the chemical bulks of the three materials. A Perkin Elmer Two Spectrophotometer equipped with A 2×2 mm diamond crystal was exploited. After fine pot milling 0.2 g of each dried sample, 2.5-mg sub-samples were spread over diamond surface and analysed (4000-400 cm^{-1} range, 4 cm^{-1} resolution, 32 scan, 2 cm sec^{-1} rate). Each recorded scan set was averaged, corrected against ambient air as background and treated with ATR correction correlative function. To highlight the emerging bands, the smoothing function of the workstation was not needed.

3.2.3 Adsorption kinetics

An adsorption kinetics study was conducted in batch mode to quantify the adsorption of OXY, MET, IMI and BPA on the three adsorbents and to estimate the time needed to reach the adsorption equilibrium. Aliquots of 10 mg of adsorbents were interacted with 20 mL of an aqueous solution (solution/adsorbent ratio equal to 2000) of the four molecules, each at a concentration of 2 mg L^{-1}, in glass centrifuge tubes. The suspensions were stirred for 0.017, 0.083, 0.17, 0.25, 0.5, 1, 4, 16 and 24 hours in the dark at 310 rpm and 20 ± 1 °C. After each time, the suspensions were centrifuged at 10,000 *g* for 10 min at 10 ºC. The equilibrium concentration of each compound in the supernatant solution was determined by ultra-high performance liquid chromatography (UHPLC) as described in section 2.5. All experiments were performed in triplicate.

The amount of each compound adsorbed on the adsorbent at each time t, qt (mg kg^{-1}), was calculated by the equation $q_t = (C_0 - C_t)\ V/m$, where C_0 (mg L^{-1}) is the initial concentration of the compound in solution, C_t (mg L^{-1}) is the concentration of the compound at time t, V (mL) is the volume of the solution and m (g) is the mass of the adsorbent. The equilibrium time was established when at two successive times the quantity of compound adsorbed was unchanged according to the Student's *t* test ($p \leq 0.05$).

3.2.4 Adsorption and desorption isotherms

Adsorption isotherms were studied to quantitatively evaluate the adsorption of the four molecules on the adsorbents and obtain the values of the adsorption parameters. Volumes of 20 mL of an aqueous solution of the molecules, each at concentrations of 0.1,0.2,0.5,1 and 2 mg L^{-1}, were added to aliquots of 10 mg of adsorbent in glass centrifuge tubes. The samples were stirred for 24 h in the dark at 20 ± 1 °C to achieve the steady state. Subsequently, the suspensions were centrifuged at 10,000 g for 10 min at 10 ºC. The equilibrium concentration of the compounds was determined using UHPLC as described in the next section. Desorption experiments were started immediately after adsorption, adopting the samples added with the molecules at 2 mg L^{-1}. At each of the three subsequent desorption steps, a volume of 16 mL of supernatant solution was replaced with the same volume of double distilled water. The samples were stirred again for 24 h at 20 ± 1°C and centrifuged in the conditions reported above. The solution concentration of the compounds at each desorption step was measured using UHPLC (see next section). All adsorption and desorption experiments were triplicated.

3.2.5 Chromatographic analysis

The four compounds were quantified by an UHPLC apparatus (Dionex Ultimate 3000 RSLC, Waltham, MA, USA) equipped with an HPG-3200 RS pump, a WPS-3000 automatic sampler, and a TCC-3000 column compartment connected to a Supelco™ LC-18 column (250 mm × 4.6 mm × 5 µm). The mobile phase was a mixture of water (A) and acetonitrile (B) flowing at 0.8 mL min^{-1}. The elution gradient was: 0-1 min, 60% A; 1-4 min from 60 to 40% A; 4-8 min, from 40% to 30% A; 8-12 min, from 30 to 10% A. The retention times of OXY, MET, IMI and BPA were 4.8, 3.5, 1.8, and 7.6 min, respectively. The compound OXY, MET and IMI were detected using a diode series detector DAD-3000 RS (Dionex Ultimate 3000 RSLC, Waltham MA, USA) at wavelengths of 210, 294 and 269 nm, respectively, while BPA was quantified using a FLD-3400 RS (Dionex Ultimate 3000 RSLC, Waltham,MA, USA) fluorescence detector operating at wavelengths of 230 and 310 nm for excitation and emission, respectively.

3.2.6 Theoretical equations

To investigate the adsorption mechanism, experimental kinetics data were interpreted with the pseudo-first order (PFO)(Kumar 2006) and pseudo-second order (PSO)(Ho & McKay 1999) models. The non-linear form of the pseudo-first order equation is expressed as:$q_t = q_e (1–exp^{–k1t})$, where q_e and qt are the amount of solute adsorbed per mass unit of adsorbent (mg kg^{-1}) at equilibrium and at time t, respectively, and $k_1(h^{-1})$ is the PFO adsorption constant. The non-linear regression was used to obtain q_e and k_1 values. The non-linear form of the PSO equation is:

$qt = \frac{q_e^2 k_2 t}{1 + k_2 q_e t}$,where q_e and q_t were already described and k_2 (kg mg^{-1} h^{-1}) is the PSO constant. Also for this equation, the non-linear regression was adopted to calculate the values of the parameters q_e and k_2. Adsorption and desorption isotherms data were interpreted with the Henry, Freundlich and Langmuir equations. The linear model of Henry is given by: $q_e = K_d C_e$, where q_e is the amount of compound adsorbed per unit of substrate (mg kg^{-1}) at equilibrium, C_e is the equilibrium concentration of the solute in solution (mg L^{-1}) and K_d is the distribution coefficient. The Freundlich equation is expressed as: $q_e = K_f C_e^{1/n}$, where 1/n indicates the degree of non-linearity between the solute concentration in solution and on the adsorbed, while q_e and C_e have the meaning already mentioned above. The Freundlich constants, K_F and n indicate, respectively, the capacity and the intensity of adsorption. The Langmuir equation is given by: $q_e = (K_L C_e b)/(1+K_L c_e)$, where q_e and C_e were defined previously, b represents the maximum adsorption capacity (mg kg^{-1}) and K expresses the adsorption energy (L mg^{-1}). The Freundlich (K_F and 1/n) and Langmuir (b and K_L) parameters were calculated using the non-linear regression method.

3.3 Results and discussion

3.3.1 Characterization of adsorbents

3.3.1.1 Basic characterization and elemental analysis

Basic properties of OP, OS and PSare reported in Table 2. All adsorbents showed an acidic pH, which is typical of these matrices (Turan & Mesci 2011, Khalfaoui et al. 2024). The latter property suggests the suitability of these adsorbents in alkaline soils which are quite common in the Mediterranean region. EC values followed the order OS< OP< PS. As expected, the organic matter content of each adsorbent was very high (Table 2).

Table 2. Some properties of the adsorbents

Parameter	Orange peel	Olive stones	Pistachio shells
pH[a]	4.94 ± 0.10[b]	5.27 ± 0.02	4.95 ± 0.11
EC[a] (dS m^{-1})	1.10 ± 0.01	0.19 ± 0.01	2.01 ± 0.04
Moisture (%)	9.50 ± 0.25	10.24 ± 0.38	6.46 ± 0.55
Ash (%)	2.97	0.54	3.20
BD (g cm^{-3})	0.49	0.53	0.53
Organic matter (% dw)	97.05 ± 0.06	99.35 ± 0.21	96.81 ± 0.24

[a]adsorbent/doble distilled H_2O 1:10 (w/v); [b] SD (n = 3).

Several studies in the scientific literature report the compositional profile of such materials in terms of cellulose, hemicellulose, and lignin contents, which generally range as a whole within values of 80-99% (dw) for OS (Garcia-Martin et al. 2020) and 70-87% (dw) for PS (Balasundar et al. 2019, Celik et al. 2021). Gaind (2020) reported a total content of 98.9% for OP. Furthermore, in these studies, the analysis of the chemical composition is generally limited to the major elements, such as C, H, N, O and S, since they influence the performance in their thermal conversion, such as combustion, which is currently their most common destination (Garci-Martin et al. 2020). In contrast, less attention has been paid to minor and trace elements of these matrices (including hazardous metals), with very little published data. Indeed, while it is considered of primary importance to measure the concentration of elements such as Cr, Sr, Ni, Cu and so on in the edible parts of nuts (Davarynejad et al. 2013), the metal load of shells and stones is generally neglected. However, for the purpose of this work, the inorganic content of these plant parts is of interest since, once incorporated into the soil, they could be a beneficial supply of plant nutrients but also a source of potentially toxic elements. For such a purpose, TXRF analysis was performed to evaluate qualitatively and quantitatively several major, minor and trace elements, namely P, S, K, Ca, Ti, Cr, Mn, Fe, Ni, Cu, Zn, Br, Rb, Sr and Pb, in each adsorbent (Table 3 and Figure 1).

Table 3. TXRF elemental analysis of the three adsorbents.

Element	**Orange peel** (**mg kg^{-1} dw**)	**Olive stones**	**Pistachio shells**
P	1211.9 ± 85.2[a]	1402.3 ± 56.4	1223.7 ± 28.4
S	162.3 ± 32.7	<LOQ	249.4 ± 8.5
K	5581.8 ± 228.1	1041.3 ± 36.1	2003.5 ± 117.6
Ca	5231.7 ± 336.6	1140.9 ± 104.4	905.3 ± 16.8
Ti	< LOQ	< LOQ	3.6 ± 0.3
Cr	< LOQ	< LOQ	10.3 ± 1.7
Mn	4.7 ± 0.7	4.8 ± 0.1	4.2 ± 0.2
Fe	22.8 ± 1.7	67.0 ± 8.3	99.9 ± 2.9
Ni	< LOQ	2.1 ± 0.3	5.6 ± 0.4
Cu	4.1 ± 0.3	6.0 ± 0.0	64.4 ± 8.4
Zn	4.0 ± 0.3	2.5 ± 0.2	8.6 ± 1.1
Br	3.7 ± 0.3	1.5 ± 0.2	4.0 ± 0.2
Rb	2.6 ± 0.3	1.5 ±0.5	2.5 ± 0.2
Sr	39.2 ± 1.0	< LOQ	2.8 ± 0.2
Pb	2.3 ± 0.4	1.9 ± 0.4	1.8 ± 0.1

[a] standard error (n = 3).

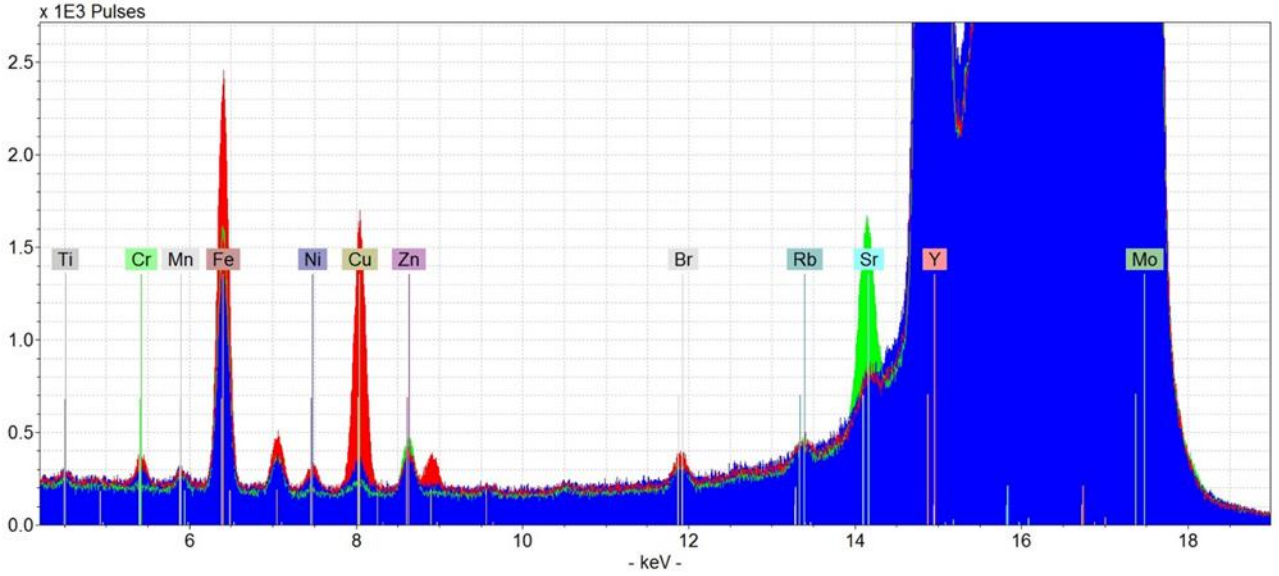

Figure 1. Selected region of TXRF spectra of orange peel (green spectrum), olive stones (blue spectrum) and pistachio shells (red spectrum) showing some trace elements peaks. The Y peak (14.958 keV) and the Mo signals are attributable to the internal standard, and the Mo Compton and Rayleigh scattering, respectively.

Among the major elements, P concentration was similar for all the three adsorbents, ranging from 0.12 to 0.14%, while K content was significantly higher in OP compared to the other adsorbents. The P and K concentrations detected in OP (1212 and 5582 mg Kg^{-1}, respectively) are in accordance with what was found by Gaind, who measured in orange peel 0.1 and 0.75 % of P and K, respectively. The S element was higher in PS than in OP and below the limit of detection in OS. The Ca content was similar in OS and PS (~ 0.1%) and much higher in OP. Both in OS and PS, Ca and K concentrations were similar to those reported in the literature for these materials (Celik et al. 2021, Garcia et al. 2014).

Regarding trace elements, PS showed the highest concentrations of Fe (100 mg kg^{-1}) and Cu (64 mg kg^{-1}); these values, although of the same order of magnitude, were quite different from those reported by Celik et al. for Fe (420 mg kg^{-1}) and Cu (5.3 mg kg^{-1}). However, both the plant variety and the characteristics of the local soil can markedly influence the uptake and accumulation of these elements in the fruits and therefore in the shells (Davarynejad et al. 2013, Nguyen et al. 2023) Besides, the higher Fe content of PS with respect to the other bioadsorbents under investigation could be related to shells' intrinsic physiological function: indeed, in pistachio, as for other nuts, the primary role of the stony pericarp (i.e., the shell) is to surround and protect the inner kernel. Indeed, in this regard, it has been observed that an increase of heavy metal content in shells is correlated to an improvement of their physico-mechanical characteristics, such as density and tensile strength

(Celik et al. 2019). Differently from PS, Ti was below the instrumental limit of quantification (LOQ) in the other two adsorbents. The lowest Fe and Cu contents were found in orange peel (23 and 4 mg kg^{-1}, respectively). All other elements detected never exceeded some units of mg kg^{-1}, with the only exception of Sr (39.2 mg kg^{-1}) in OP (Table 3). The content of the potentially toxic Pb was approximately 2 mg kg^{-1} in each sample, while Zn concentration followed the order: OS < OP < PS, accounting for 8.6, 4.0 and 2.5 mg kg^{-1}, respectively. Cr concentration was higher in PS than the other biosorbents.

In light of the overall results of TXRF analysis, we can conclude that the incorporation of these materials into the soil, in addition to be an organic supply useful for the immobilization of contaminants, can provide important elements for plant nutrition (P, K, S, Fe and so on) without the risk of adding potentially toxic elements, which might happen with organic amendments derived from technological processes (Hilber et al. 2017).

3.3.1.2 SEM analysis

The SEM analysis is a useful tool to morphologically characterize complex organic matrices such as plant parts. Images of the three adsorbents obtained at ×1500 magnifications are shown in Figure 2. A heterogeneous surface, irregular structures, niches along with pores of different sizes and shapes were observed in all adsorbents. These features can favour the adsorption of pollutants on both the outer and inner parts of the adsorbents.

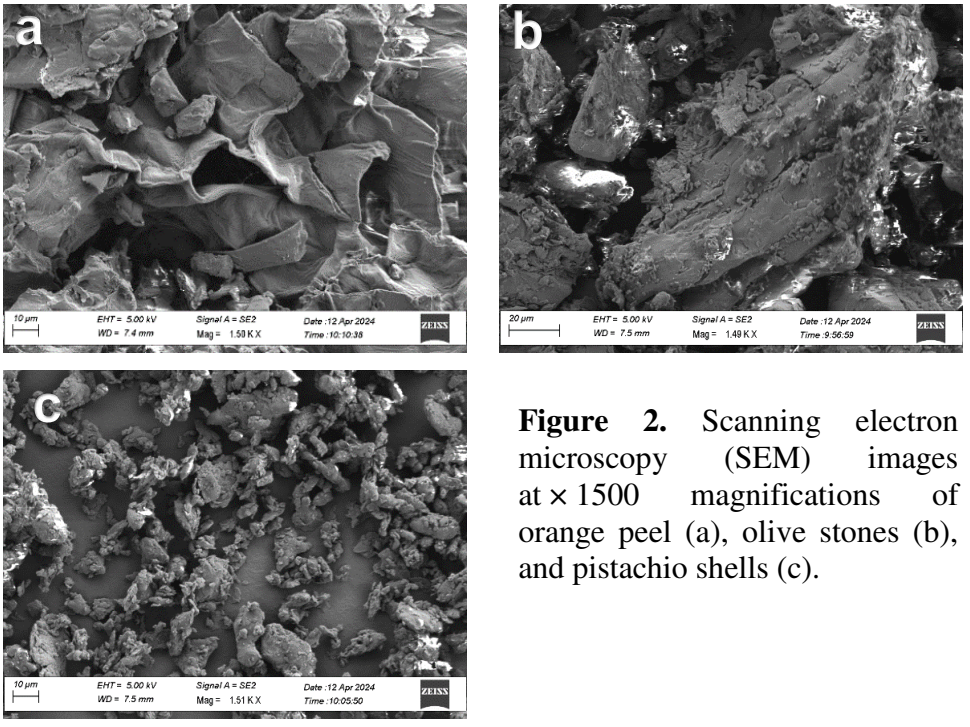

Figure 2. Scanning electron microscopy (SEM) images at × 1500 magnifications of orange peel (a), olive stones (b), and pistachio shells (c).

3.3.1.3 FTIR-ATR analysis

Infrared investigations often offer advantages in characterization of complex biomasses, such as avoiding differential and detrimental treatment of the sample, the lack of the use of secondary reactions for derivatization, and the use of simultaneous measurements to speed up the investigation and related comparison. The Fourier-transform infrared (FTIR) spectroscopy was used here to focus and light on the presence of biomacromolecular functional groups found in OP, OS and PS. By a direct FTIR-ATR characterization of the OP biomass (Fig. 3a), significative signals set at ν = 3297.2 (-OH from carbohydrates of cellulose, water), 2915.0, 2855.0 (-CH S signal, symmetric, asymmetric peaked aliphatic chains, terpenoids), 2344.2-1985.3 aromatic overtones (W signal), 1742.3 (-C=O stretching, carboxyl), 1656.2 (-C=C- stretching), 1490.1, 1421.7 (-CH bending vibr.), 1013.2 (C–O–H or C–O–R from ester moieties and saccharides), 979.0, 879.0, 587.63 (finger print) were found. Signals are so ascribable to fatty acid esters, terpenoids and cellulose-like matrix moieties typical of this composite, and in line with literature (McKendry 2022, Zapata et al. 2009). The FTIR-ATR spectra of OS and PS (Fig. 3b and 3c) appeared very different from OP, although they were both almost overlapping. After recording spectra, the 1737 cm^{-1} peak sets for C=O of carboxylic acids, while 1641-1580 peaked signals can be mostly attributed to C=O stretching and N-H bending of amide moieties and the fully enriched presence of peaks from 1590 to 1460 cm^{-1} are due to C=C moiety found in aromatic lignolic/lignin-like compounds (Blasi et al. 2022). The related spectra report signals at 1240-1250 cm^{-1} likely attributed to the stretching C–O moiety of the guaiacyl ring, while 900-894 cm^{-1} signals can be attributed to the syringyl residue (Rahim et al. 2018). As reported in the literature (El Hage et al. 2009), shells of dried fruits contain high level of hemicellulose (C–O–C of glycosidic link, around 1200-1050 cm^{-1}) (HSU et al. 2021).

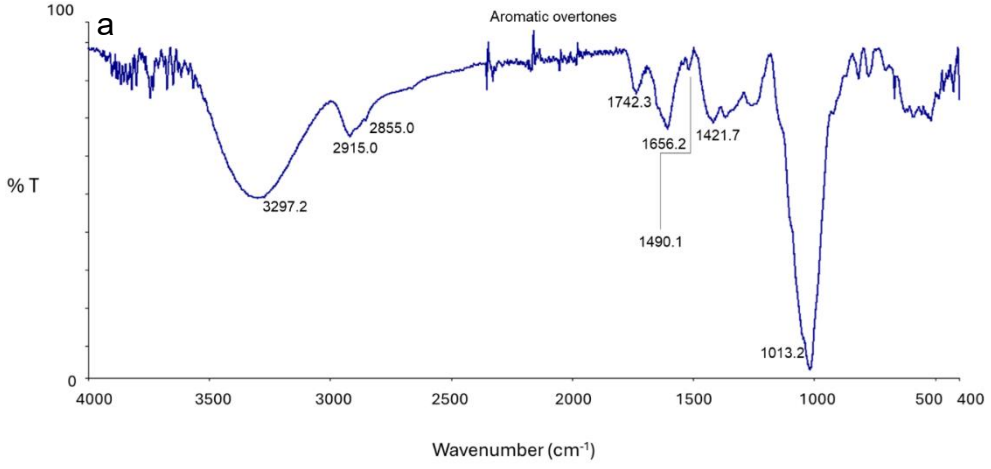

Figure 3. FTIR-ATR spectra of orange peel (a), ***continued***.

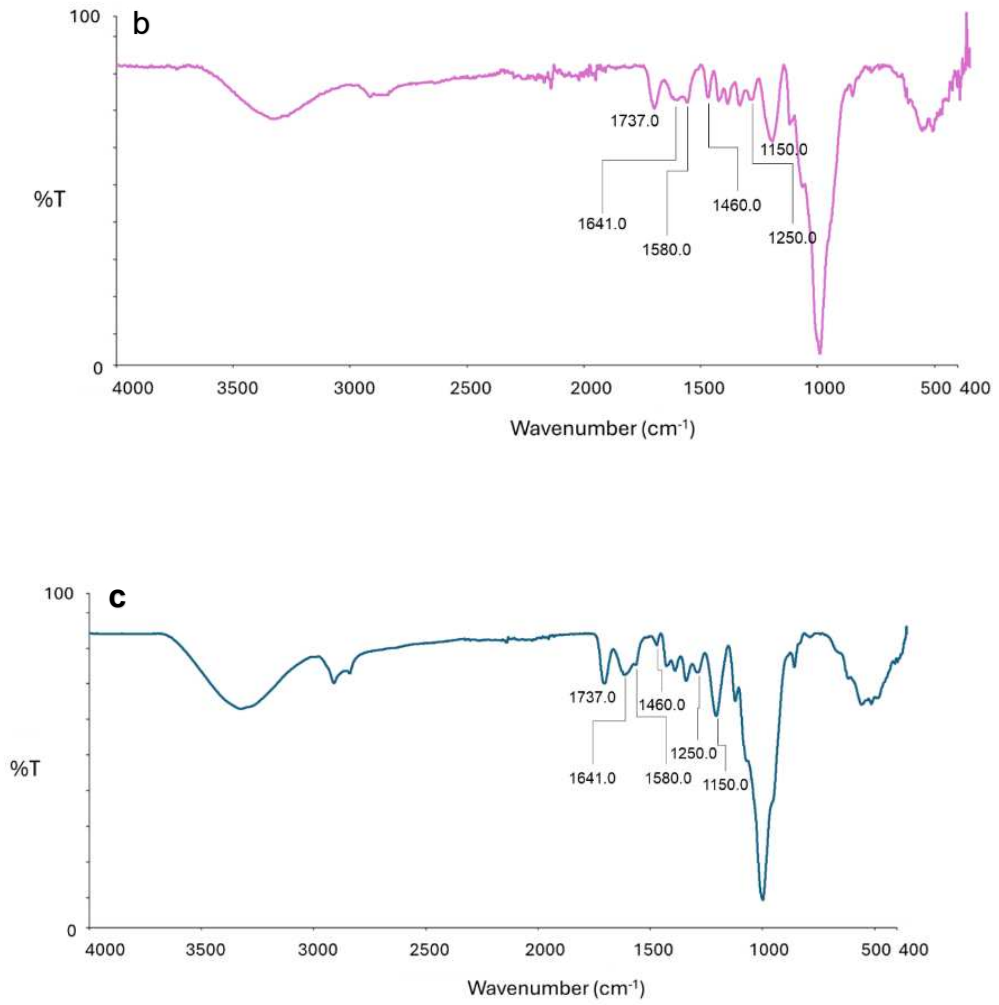

Figure 3. continued, olive stones (b), and pistachio shells (c).

Under a biosorption and remediation point of view, and with an attempted focus on the molecular bases, cellulose macrostructures could in principle give direct interaction exploiting the polar -C-O and O-H functional groups with metal and charged organic pollutants. This dipole:ion and dipole:dipole interactions, with cumulative nature, are often dependent on the rate of humidity and the chemical environment surrounding or standing remediation process, while less affected by pH variations. -COOH and -NH_2 moieties are more switchable functional groups, often belonging to glycoconjugate and complex organic carboxyl acids, and natural polyamines. Varying pH values the buffering solution effect becomes so important, facilitating dipole:ion and ion:ion interaction at the matrix bulk or surface. In all these adsorbents, the presence of OH-enriched cellulosic moieties and the abundance of π-π stacked aromatic structures with a certain degree of oxidation induced us to think this bulk chemistry as ideally exploitable to surface catch organic polar pollutants aiming to cheap bioremediation applications. In details, poly-hydroxy-indoles, oxidized catechols and lignin-

based macrostructures allow a certain hetero π-π stacking with the aromatic mono- and bi- or poly-nuclear aromatic pollutants (Buscemi et al. 2021), and these interactions strongly depend on the effective distance between pollutants and the matrix, the time of exposure, and the presence of different ligand-like interfering chemical species. All these functional groups, specifically all bio- and nature-based, are extraordinary because they can act combinatorically in the same matrix, and this property is rarely exhibited by artificial, industrial and pre-formed composites reported in literature, silica nanotubes, nanoparticles, nanorods, magnetic metal:organic frameworks, metal:zeolite composites (Del Praud-Audelo et al. 2021) .

3.3.2 Adsorption kinetics

The study of adsorption kinetics allows to quantitatively evaluate the retention of compounds present in solution on solid matrices and to establish the equilibrium time of the process. This study also provides information on the type of interaction between the adsorbent and the solute. Based on the adsorption kinetic curves, each molecule reached the adsorption equilibrium in a relatively short time (Fig. 4). The Student's t-test ($P \leq 0.05$) applied to the amounts of compound adsorbed at the different sampling times indicated an equilibrium time of about 24 hours for the three adsorbents (Fig. 4).

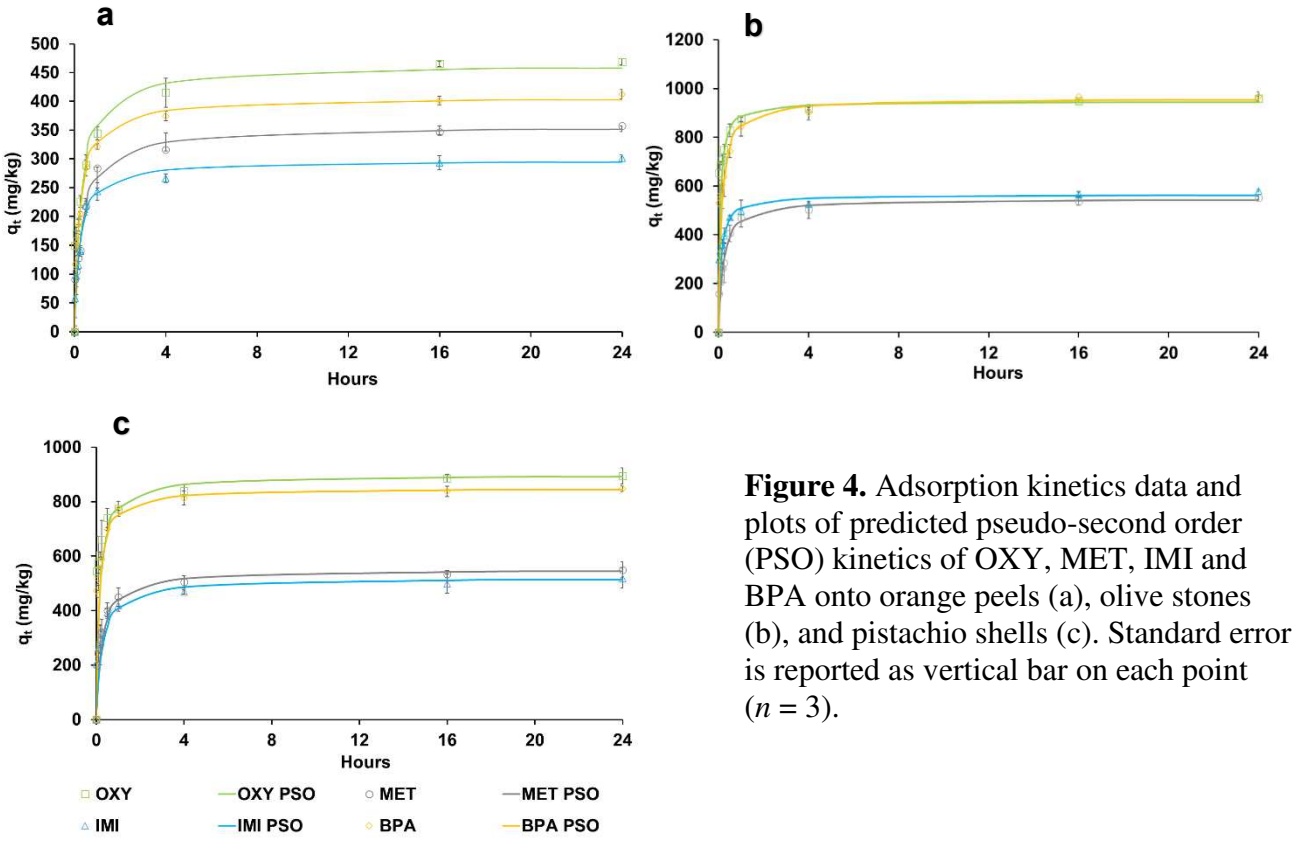

Figure 4. Adsorption kinetics data and plots of predicted pseudo-second order (PSO) kinetics of OXY, MET, IMI and BPA onto orange peels (a), olive stones (b), and pistachio shells (c). Standard error is reported as vertical bar on each point ($n = 3$).

The ability of OP to remove contaminants such as heavy metals (Akinhanmi et al. 2020) and dyes (Ahmed et al. 2020) from aqueous solutions was demonstrated in recent studies; the authors attributed this property to the large surface area per mass unit of the material. Citrus peel can be an excellent adsorbent since it contains high levels of biomolecules (e,g., lignin, cellulose and pectin) and essential oils, which can promote adsorbent-contaminant bonds (Micheal-Igolima et al. 2023). Similarly, the use of OS as a bioadsorbent for the removal of heavy metals (e.g., Cd (II), Cu (II), Pb (II) and Cr (VI)) from wastewater is well documented (Martin-Lara et al. 2014, Hodaifa et al. 2014, Amar et al. 2020, Agarwal et al. 2022). Furthermore, the relevant capacity of PS to adsorb heavy metals, dyes and antibiotics from aqueous media has been recently reported (Kayranli et al. 2022, Shaikhiev et al. 2023).

Using the non-linear regression method, experimental data of adsorption kinetics were described with the PFO and PSO equations. Results obtained are shown in Table 4. Values of the correlation coefficient, r, close to the unit and low values of the sum of squared residuals, SSR, indicate a good correspondence between the experimental data and the model. The results of the kinetic study showed in general a good capacity of the three adsorbents to retain the four molecules from the aqueous medium.

At equilibrium, on all materials, the amounts of adsorbed OXY and BPA were much higher than those of adsorbed MET and IMI. This was expected based on the log Kow values of the compounds. Comparing the overall adsorption efficiency of the three adsorbents for all molecules, a similar behaviour was shown by olive stones and pistachio shells, whereas orange peel was less effective (Fig. 4). At equilibrium, the quantities of adsorbed OXY, MET, IMI and BPA on OS (the most effective adsorbent) were, respectively, 959, 551, 580 and 968 mg kg^{-1} (Table 4). Based on r and SSR values, the PSO equation was the best fit for all molecules (Table 4). Previous studies showed that very often the best fit of experimental kinetic data of many organic compounds was the PSO model (Kumar 2006, Revellame et al. 2020). The latter model assumes that the limiting phase of adsorption is the formation of high-energy bonds, such as covalent and hydrogen bonds, between the solute and the adsorbent (chemisorption) or the number of unoccupied adsorption sites on the adsorbent surface, also according to the isotherms, and the slower desorption (Ho & McKay 1999).

Table 4. Kinetic PFO and PSO parameters for the adsorption of the compounds on the adsorbents

Adsorbent	Compound	PFO model					PSO model			
		$q_{e,exp}$	r	SSR	$q_{e,1}$ (mg g^{-1})	k_1 (h^{-1})	r	SSR	q_{e2} (mg g^{-1})	k_2 (kg mg^{-1} h^{-1})
Orange peels	OXY	468.8	0.951	5870	440.83	2.19	0.990	861	463.80	0.007
	MET	357.5	0.985	1079	338.59	2.02	0.991	602	356.68	0.008
	IMI	301.4	0.966	1234	283.22	2.70	0.979	699	297.38	0.014
	BPA	412.1	0.961	2760	387.82	2.63	0.981	418	407.12	0.010
Olive stones	OXY	959.0	0.847	7322	1327.34	1.09	0.999	600	960.96	0.009
	MET	551.3	0.845	2321	1305.92	1.02	0.999	1173	553.70	0.007
	IMI	579.9	0.839	4612	1316.66	1.09	0.999	1043	581.18	0.008
	BPA	967.8	0.874	14270	2040.19	1.13	0.999	1458	975.03	0.006
Pistachio shells	OXY	894.5	0.852	12113	1674.61	1.10	0,999	2102	898.32	0.007
	MET	549.2	0.840	4992	1542.13	1.09	0.999	410	550.92	0.007
	IMI	519.1	0.834	5301	1465.22	1.08	0.999	994	519.12	0.007
	BPA	847.8	0.847	4839	1380.27	1.09	0.999	260	849.93	0.009

3.3.3 Adsorption and desorption isotherms

The adsorption isotherm study describes quantitatively the interaction between an adsorbent and a solute at a given temperature and provide adsorption parameters, such as the adsorption constant and maximum adsorption, which allow to compare the efficiency of different adsorbents for the same solute or the affinity of different solutes for the same adsorbent. To interpret the experimental data, we used the theoretical Freundlich, Langmuir and Henry models. The Freundlich model is based on the hypotheses that (i) the adsorbent has a heterogeneous surface; (ii) the adsorption energy decreases exponentially as the active sites become saturated; and (iii) the solute forms a multilayer coating on the adsorbent; (iv) in diluted systems saturation is never achieved. The

Langmuir model is based on the following assumptions: (i) adsorption occurs at specific sites on a homogeneous surface of the adsorbent; (ii) only one molecule of solute binds to each site; (iii) the adsorption energy involved is equivalent for all sites; (iv) there is no chemical interaction between adjacent adsorbed molecules; (v) at equilibrium, the solute molecules form a monolayer on the surface of the adsorbent. The Henry model describes a linear distribution of the solute between the adsorbent and the solution. Based on the values of r and SSR obtained applying the theoretical models to the experimental data, the adsorption of all compounds onto the three adsorbents was best described by the Freundlich model, although the other models were often adequate (Table 5). Figure 5 shows the experimental isotherm data and the plots of the Freundlich model, while Table 5 refers the adsorption parameters calculated by interpreting the data at equilibrium with the Freundlich, Langmuir and Henry models. The Freundlich model interpreted very well the adsorption isotherm data of a number of contaminants on various untreated organic waste (Frezzini et al. 2019). Based on $K_{F\ ads}$ values, the sorption efficiency of the adsorbents for all compounds followed the order: OS > PS > OP (Table 5).

Table 5. Adsorption parameters obtained for OXY, MET, IMI, BPA onto the three adsorbents

Compound	Henry			Freundlich				Langmuir			
	r	SSR	$K_{d\ ads}$[a]	r	SSR	$K_{F\ ads}$	$1/n_{\ ads}$	r	SSR	b[a]	K_L[b]
Orange peels											
OXY	0.999	178	267.7	0.999	135	270.25	0.97	0.999	133	9407	0.03
MET	0.999	266	192.25	0.999	157	187.61	1.06	0.998	279	6995	0.002
IMI	0.999	96	165.37	0.999	23	168.91	0.95	0.999	18	3158	0.05
BPA	0.999	43	228.20	0.999	25	226.44	1.02	0.999	60	3347	0.006
Olive stones											
OXY	0.992	2129	668.19	0.999	485	699.04	0.76	0.998	1199	2428	0.42
MET	0.999	177	318.43	0.999	174	319.12	0.99	0.999	188	45682	0.007
IMI	0.997	2430	346.30	0.999	572	361.55	0.85	0.996	1225	2977	0.14
BPA	0.991	23950	678.81	0.999	977	711.35	0.74	0.998	1559	20309	0.46
Pistachio shells											
OXY	0.994	13476	605.14	0.999	105	632.97	0.78	0.999	1408	2548.4	0.11
MET	0.999	81	317.26	0.999	81	317.44	1	0.999	97.07	32479	0.1
IMI	0.999	114	297.15	0.999	105	295.98	1.01	0.999	138	27956	0.11
BPA	0.994	11818	568.66	0.999	511	595.79	0.79	0.999	213.6	2431	0.34

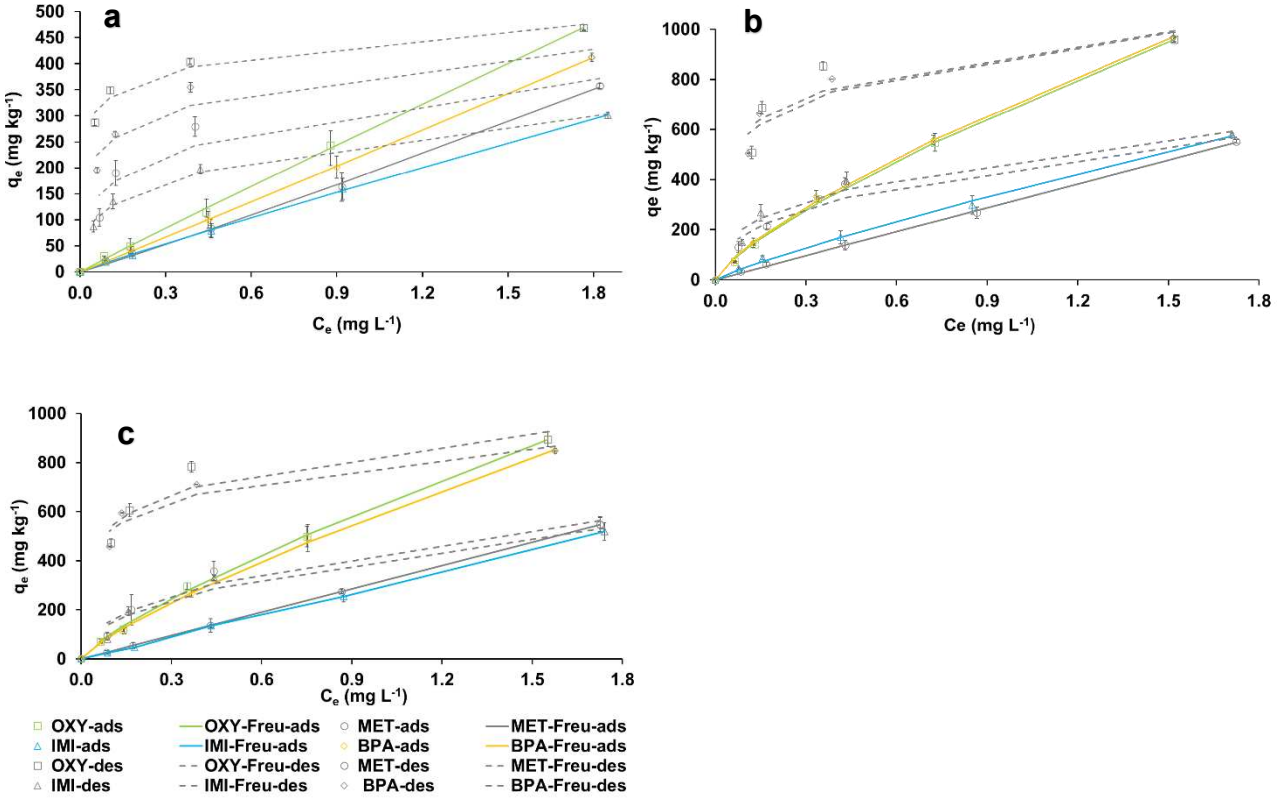

Figure 5. Experimental data and Freundlich model fit of adsorption/desorption isotherms of OXY, MET, IMI and BPA onto orange peels (a), olive stones (b), and pistachio shells (c). Standard error is reported as vertical bar on each point (n = 3).

The desorption study describes quantitatively the release of a compound from an adsorbent into the aqueous phase. Experimental desorption data and theoretical curves obtained by applying the Freundlich model are shown in Figure 5, while Freundlich ($K_{F\ des}$ and $1/n_{\ des}$), Langmuir ($K_{L\ des}$ and b) and Henry ($K_{d\ des}$) desorption parameters are shown in Table 6. Desorption of each molecule from any adsorbent was generally slower and incomplete, indicating the occurrence of a hysteresis process. Also in the case of desorption, the Freundlich model was the best fit for all compounds. The highest $K_{F\ des}$ values were recorded for olive stones, which indicates that in general the higher the adsorption capacity of an adsorbent the lower the release of the compound.

Table 6. Desorption parameters obtained for OXY, MET, IMI, BPA onto the three adsorbents.

Compound	Henry			Freundlich				Langmuir			
	r	SSR	$K_{d\ des}$[a]	R	SSR	$K_{F\ des}$	$1/n_{\ des}$	r	SSR	b[a]	K_L[b]
Orange peels											
OXY	0.745	261026	315.58	0.979	723	443.31	0.12	0.980	71	460.87	30.31
MET	0.844	72461	227.06	0.945	3569	313.91	0.28	0.993	442	388.05	6.55
IMI	0.880	34972	182.74	0.996	175	251.26	0.30	0.977	1316	311.96	6.12
BPA	0.787	153686	271.90	0.954	2338	382.80	0.18	0.999	53	425.57	13.80
Olive stones											
OXY	0.795	873362	778.95	0.885	24336	917.77	0.18	0.959	8847	1045.4	10.08
MET	0.907	90534	363.71	0.976	4680	457.54	0.39	0.997	286	658.23	3.06
IMI	0.896	115396	387.03	0,977	4356	487.74	0.36	0.933	1260	663.04	3.78
BPA	0.812	774711	777.53	0.948	11373	909.89	0.20	0.982	4119	1026.2	10.22
Pistachio shells											
OXY	0.800	720507	705.34	0.933	12937	849.81	0.20	0.996	822	963.11	10.35
MET	0.925	69006	357.76	0.974	5633	442.28	0.45	0.998	529	688.36	2.35
IMI	0.926	60156	333.85	0.972	5588	414.81	0.45	0.993	1275	649.03	2.33
BPA	0.795	659112	651.79	0.953	7339	797.96	0.18	0.985	2413	881.84	12.76

[a]($mg\ kg^{-1}$) [b]($L\ mg^{-1}$)

To the best of our knowledge, this is the first work that examined OP, OS and PS for the removal of the four compounds; therefore, a comparison between our results and those of previous studies is not possible. Wu et al. (2019) studied the adsorption of OXY on a peanut shells biochar and reported a $K_{F\ ads}$ value that was comparable to that found in this study for OS. Using a straw-derived adsorbent to retain MET, Cara et al. (2015) report a $K_{F\ ads}$ value lower than that found in our work for any adsorbent. The removal of IMI by biocomposites of polypyrol, polyaniline, sodium alginate and peanut shells reported by Ishtiaq et al. (2020) was lower than that observed here for the less efficient OP. In a recent study by Loffredo et al. (2021), the ability of a digestate from agricultural waste to remove MET and BPA from water appeared lower (K_F values 1.9 and 1.8 times lower, respectively) than that of OP. Moussavi and Khosravi (2011) studied the adsorption of methylene blue on PS and reported a K_F value of 112.3 $mg\ kg^{-1}$, which is much lower than those found in this study for any pollutant considered. Cobas et al. (2016) studied the adsorption of IMI on chestnut

shells and obtained a K_F value that was comparable to those found for the same compound on the three adsorbents examined here. Delgado-Moreno et al. (2017) studied the adsorption of OXY and IMI on different biomixtures, among which vermicompost, whose adsorption capacity is well recognized and reported sorption constants similar to those found in this study.

3.4 Conclusions

OP, OS and PS, due to their large surface area and porosity, the abundance of reactive functional groups and their elemental composition, can behave as bioadsorbents of organic pollutants, especially highly hydrophobic ones. This study quantified the ability of these wastes to remove the pesticides OXY, MET and IMI, and the xenoestrogen BPA from the aqueous medium. The study of adsorption kinetics and the application of kinetic models to experimental data demonstrated that adsorption occurred predominantly as chemisorption, and that the steady state was reached in a relatively short time on all adsorbents. The values of adsorption constants obtained from sorption isotherms and data modeling using the theoretical models of Henry, Freundlich and Langmuir indicated that the high efficiency of the three adsorbents, especially OS, in removing the compounds, especially the most hydrophobic OXY and BPA. Desorption of all molecules was slower than adsorption and incomplete (hysteresis) suggesting a persistent ability of the materials to retain the molecules, which is important in remediation applications. Although this study requires further investigation, the overall results obtained demonstrated that unprocessed, low-cost and widely available agro-industrial byproducts can be usefully recycled for the removal of organic contaminants, confirming once again that waste could become a resource. Finally, these materials incorporated into the soil, in addition to representing a useful enrichment of organic matter and plant nutrients, can immobilize contaminants, thus reducing the risks of contamination of food products and the transfer of contaminants into the human and animal food chain.

References

Ab Rahim, A.H., Man, Z., Sarwono, A., Wan Hamzah, W.S., Yunus, N.M., Wilfred, C.D. (2018) Extraction and comparative analysis of lignin extract from alkali and ionic liquid pretreatment. Journal of Physics: Conference Series 1123, 012052.

Agarwal, A., Upadhyay, U., Sreedhar, I., Anitha, K.L. (2022). Simulation studies of Cu(II) removal from aqueous solution using olive stone. Cleaner Materials 5, 100128. https://doi.org/10.1016/j.clema.2022.100128

Ahmad, M., Rajapaksha, A.U., Lim, J.E., Zhang, M., Bolan, N., Mohan, D., Vithanage, M., Lee, S.S., Ok, Y.S. (2014). Biochar as a sorbent for contaminant management in soil and water: a review. Chemosphere 99, 19–33. https://doi.org/10.1016/j.chemosphere.2013.10.071

Ahmed, M., Mashkoor, F., Nasar, A. (2020). Development, characterization, and utilization of magnetized orange peel waste as a novel adsorbent for the confiscation of crystal violet dye from aqueous solution. Groundwater for Sustainable Development 10, 100322. https://doi.org/10.1016/j.gsd.2019.100322

Akinhanmi, T.F., Ofudje, E.A.O., Adeogun, A.I., Aina, P., Mayowa, I.G. (2020). Orange peel as low-cost adsorbent in the elimination of Cd(II) ion: kinetics, isotherm, thermodynamic and optimization evaluations. Bioresources and Bioprocessing 7, 34. https://doi.org/10.1186/s40643-020-00320-y

Ambaye, T.G., Vaccari, M., van Hullebusch, E.D., Amrane, A., Rtimi, S. (2021). Mechanisms and adsorption capacities of biochar for the removal of organic and inorganic pollutants from industrial wastewater. International Journal of Environmental Science and Technology 18, 3273–3294. https://doi.org/10.1007/s13762-020-03060-w

Amar, M.B., Walha, K., Salvado, V. (2020). Evaluation of Olive Stones for Cd(II), Cu(II), Pb(II) and Cr(VI) Biosorption from Aqueous Solution: Equilibrium and Kinetics. International Journal of Environmental Research 14 193–204. https://doi.org/10.1007/s41742-020-00246-5

Balasundar, P., Narayanasamy, P., Senthil, S., Al-Dhabi, N.A., Prithivirajan, R., Shyam, R., Kumar, R., Ramkumar, T., Subrahmanya Bhat, K. (2019). Physico-chemical study of pistachio nutshell particles as a bio-filler for eco-friendly composites. Materials Research Express 6, 105339. https://doi.org/10.1088/2053-1591/ab3b9b

Blasi, D., Mesto, D., Cotugno, P., Calvano, C.D., Lo Presti, M., Farinola, G.M. (2022). Revealing the effects of the ball milling pretreatment on the ethanosolv fractionation of lignin from walnut and pistachio shells. Green Chemistry Letters and Reviews 15, 893–902. https://doi.org/10.1080/17518253.2022.2143244

Buscemi, G., Vona, D., Ragni, R., Comparelli, R., Trotta, M., Milano, F., Farindola, G.M. (2021). Polydopamine/Ethylenediamine Nanoparticles Embedding a Photosynthetic Bacterial Reaction Center for Efficient Photocurrent Generation. Advanced Sustainable Systems 5, 2000303. https://doi.org/10.1002/adsu.202000303

Calafat, A.M., Ye, X., Wong, L.Y., Reidy, J., Needham, L.L.(2008). Exposure of the U.S. Population to Bisphenol A and 4-tertiary-Octylphenol: 2003–2004. Environmental Health Perspectives 116, 39–44. https://doi.org/10.1289/ehp.10753

Camadro, J.M., Matringe, M., Thome, F., Brouillet, N., Mornet, R., Labbe, P. (1995). Photoaffinity Labeling of Protoporphyrinogen Oxidase, the Molecular Target of Diphenylether-Type Herbicides. European Journal of Biochemistry 229, 669–674. https://doi.org/10.1111/j.1432-1033.1995.0669j.x

Carnimeo, C., Gelsomino, A., Cirrottola, G., Panuccio, M.R., Loffredo, E. (2022). Compost and vermicompost in cucumber rhizosphere promote plant growth and prevent the entry of anthropogenic organic pollutants. Scientia Horticulturae 303, 111250. https://doi.org/10.1016/j.scienta.2022.111250

Cara, I.G., Trincă, L.C., Trofin, A.E., Cazacu, A., Ţopa, D., Peptu, C.A., Jităreanu, G. (2015). Assessment of some straw-derived materials for reducing the leaching potential of metribuzin residues in the soil. Applied Surface Science 358, 586–594. https://doi.org/10.1016/j.apsusc.2015.08.141

Celik, Y.H., Yalcin, R., Topkaya, T., et al. (2021). Characterization of Hazelnut, Pistachio, and Apricot Kernel Shell Particles and Analysis of Their Composite Properties. Journal of Natural Fibers 18, 1054–1068. https://doi.org/10.1080/15440478.2020.1739593

Chen, L., Li, D., Huang, Y., Zhu, W., Ding, Y., Guo, C. (2020). Preparation of sludge-based hydrochar at different temperatures and adsorption of BPA. Water Science & Technology 82, 255–265. https://doi.org/10.2166/wst.2020.096

Cobas, M., Meijide, J., Sanromán, M.A., Pazos, M. (2016). Chestnut shells to mitigate pesticide contamination. Journal of the Taiwan Institute of Chemical Engineers 61, 166–173.

Crossthwaite, A.J., Bigot, A., Camblin, P., Goodchild, J., Lind, R.J., Slater, R., Maienfisch, P. (2017). The invertebrate pharmacology of insecticides acting at nicotinic acetylcholine receptors. Journal of Pesticide Science 42, 67–83. https://doi.org/10.1584/jpestics.D17-019

Dao, K.C., Yang, C.C., Chen, K.F., Tsai, Y.P. Recent Trends in Removal Pharmaceuticals and Personal Care Products by Electrochemical Oxidation and Combined Systems. Water 12 (2020) 1043. https://doi.org/10.3390/w12041043

Davarynejad, G.H., Zarei Mohamadabad, M., Tamas, N.P. (2013). Identification and Quantification of Heavy Metals Concentrations in Pistacia. Notulae Scientia Biologicae 5, 438–444. https://doi.org/10.15835/nsb549115

Delgado-Moreno, L., Nogales, R., Romero, E. (2017). Wastes from the olive oil production in sustainable bioremediation systems to prevent pesticides water contamination. International Journal of Environmental Science and Technology 14, 2471–2484. https://doi.org/10.1007/s13762-017-1335-x

Den Braver-Sewradj, S.P., Spronsen, R. van, Hessel, E.V.S. (2020). Substitution of bisphenol A: a review of the carcinogenicity, reproductive toxicity, and endocrine disruption potential of alternative substances. Critical Reviews in Toxicology 50. https://doi.org/10.1080/10408444.2019.1701986

Dey, S., Basha, S.R., Babu, G.V., Nagendra, T. (2021). Characteristic and biosorption capacities of orange peels biosorbents for removal of ammonia and nitrate from contaminated water. Cleaner Materials 1, 100001. https://doi.org/10.1016/j.clema.2021.100001

Di Giacomo, G., Romano, P. (2022). Evolution of the Olive Oil Industry along the Entire Production Chain and Related Waste Management. Energies 15 https://doi.org/10.3390/en15020465

Ensley, S.M. Chapter 40 (2018) – Neonicotinoids. Veterinary Toxicology (Third Edition) 521–524. https://doi.org/10.1016/B978-0-12-811410-0.00040-4

Eniola, J.O., Sizirici, B., Fseha, Y., Shaheen, J.F., Aboulella, A.M. (2023). Application of conventional and emerging low-cost adsorbents as sustainable materials for removal of contaminants from water. Environmental Science and Pollution Research 30, 88245–88271. https://doi.org/10.1007/s11356-023-28399-8

European Directive 2009/128/CE. Official Journal of the European Union L 309/71 (2009).

El Hage, R., Brosse, N., Chrusciel, L., Sanchez, C., Sannigrahi, P., Ragauskas, A. (2009). Characterization of milled wood lignin and ethanol organosolv lignin from miscanthus. Polymer Degradation and Stability 94, 1632–1638. https://doi.org/10.1016/j.polymdegradstab.2009.07.007

El Refay, H.M., Raslan, A.M., Atia, A.M.E. (2022). Application of Low-Cost Adsorption Technique on Organic Pollutant Dye Removal by Bio-Waste Adsorbents. Egyptian Journal of Chemistry 65, 977–991. https://doi.org/10.21608/ejchem.2022.132441.5847

FAOSTAT 2022. Crops and livestock products: Orange https://www.fao.org/faostat/en/#data/QCL/visualize Accessed 19th Apr 2024

FAOSTAT 2022. Crops and livestock products: Olive https://www.fao.org/faostat/en/#data/QCL/visualize Accessed 19th Apr 2024

FAOSTAT 2022. Crops and livestock products: Pistachio https://www.fao.org/faostat/en/#data/QCL/visualize Accessed 19th Apr 2024

Frezzini, M.A., Massimi, L., Astolfi, M.L., Canepari, S., Giuliano, A. (2019). Food Waste Materials as Low-Cost Adsorbents for the Removal of Volatile Organic Compounds from Wastewater. Materials 12, 4242. https://doi.org/10.3390/ma12244242

Gaind, S. (2017). Exploitation of Orange Peel for Fungal Solubilization of Rock Phosphate by Solid State Fermentation. Waste and Biomass Valorization 8, 1351–1360. https://doi.org/10.1007/s12649-016-9682-2

García Martín, J.F., Cuevas, M., Feng, C.H., et al. (2020) Energetic Valorisation of Olive Biomass: Olive-Tree Pruning, Olive Stones, and Pomaces. Processes 8, 511. https://doi.org/10.3390/pr8050511

García, G.B., Calero de Hoces, M., Martínez García, C., Cotes Plomino, M.T., Ronda Galvez, A., Martin-Lara, M.A. (2014). Characterization and modeling of pyrolysis of the two-phase olive mill solid waste. Fuel Processing Technology 126, 104–111. https://doi.org/10.1016/j.fuproc.2014.04.020

Gentil, C., Fantke, P., Mottes, C., Basset-Mens, C. (2020). Challenges and ways forward in pesticide emission and toxicity characterization modeling for tropical conditions. International Journal of Life Cycle Assessment 25, 1290–1306. https://doi.org/10.1007/s11367-019-01685-9

Giannetta, B., Plaza, C., Cassetta, M., Mariotto, G., Benavente-Ferraces, I., Garcia-Gilas, J.C., Panettieri, M., Zaccone, C. (2023). The effects of biochar on soil organic matter pools are not influenced by climate change. Journal of Environmental Management 341, 118092. https://doi.org/10.1016/j.jenvman.2023.118092

Grassi, M., Kaykioglu, G., Belgiorno, V., Lofrano, G. (2012). Removal of Emerging Contaminants from Water and Wastewater by Adsorption Process. In: Emerging Compounds Removal from Wastewater 15–37. https://doi.org/10.1007/978-94-007-3916-1_2

Hansen, H.K., Arancibia, F., Gutiérrez, C. (2010). Adsorption of copper onto agriculture waste materials. Journal of Hazardous Materials 180, 442–448. https://doi.org/10.1016/j.jhazmat.2010.04.050

Hilber, I., Bastos, A.C., Loureiro, S., et al. (2017). The different faces of biochar: contamination risk versus remediation tool. Journal of Environmental Engineering and Landscape Management 25, 86–104. https://doi.org/10.3846/16486897.2016.1254089

Ho, Y.S., McKay, G. (1999). Pseudo-second order model for sorption processes. Process Biochemistry 34 , 451–465. https://doi.org/10.1016/S0032-9592(98)00112-5

Hodaifa, G., Alami, S.B.D., Ochando-Pulido, J.M., Víctor-Ortega, M.D. (2014). Iron removal from liquid effluents by olive stones on adsorption column: breakthrough curves. Ecological Engineering 73, 270–275. https://doi.org/10.1016/j.ecoleng.2014.09.049

Hosseinzaei, B., Hadianfard, M.J., Aghabarari, B., García-Rollán, M., Ruiz-Rosas, R., Rosas, J.M., Rodríguez-Mirasol, J., Cordero, T. (2022). Pyrolysis of pistachio shell, orange peel and saffron petals for bioenergy production. Bioresource Technology Reports 19, 101209. https://doi.org/10.1016/j.biteb.2022.101209

Hsu, S.L., Patel, J., Zhao, W. Chapter 10 – Vibrational spectroscopy of polymers. In: Molecular Characterization of Polymers (2021) 369–407. https://doi.org/10.1016/B978-0-12-819768-4.00010-5

Ishtiaq, F., Bhatti, H.N., Khan, A., Iqbal, M., Kausar, A. (2020). Polypyrole, polyaniline and sodium alginate biocomposites and adsorption-desorption efficiency for imidacloprid insecticide. International Journal of Biological Macromolecules 147, 217–232. https://doi.org/10.1016/j.ijbiomac.2020.01.022

Jeguirim, M., Belhachemi, M., Limousy, L., Bennici, S. (2018). Adsorption/reduction of nitrogen dioxide on activated carbons: Textural properties versus surface chemistry – A review. Chemical Engineering Journal 347, 493–504. https://doi.org/10.1016/j.cej.2018.04.063

Khalfaoui, A., Benalia, A., Selam, Z., Hammoud, A., Derbal, K., Panico, A., Pizzi, A. (2024). Removal of Chromium (VI) from Water Using Orange peel as the Biosorbent. Water 16, 742. https://doi.org/10.3390/w16050742

Krstić, V., Urošević, T., Pešovski, B. (2018). A review on adsorbents for treatment of water and wastewaters containing copper ions. Chemical Engineering Science 192, 273–287. https://doi.org/10.1016/j.ces.2018.07.022

Kumar, K.V. (2006). Linear and non-linear regression analysis for the sorption kinetics of methylene blue onto activated carbon. Journal of Hazardous Materials 137, 1538–1544. https://doi.org/10.1016/j.jhazmat.2006.04.036

Liu, S., Tong, X., Liu, S., An, D., Yan, J., Chen, Y., Crittenden, J. (2021). Multi-functional tannic acid (TA)-Ferric complex coating for forward osmosis membrane with enhanced micropollutant removal

and antifouling property. Journal of Membrane Science 626, 119171. https://doi.org/10.1016/j.memsci.2021.11917

Loffredo, E. (2022). Recent advances on innovative materials from biowaste recycling for the removal of environmental estrogens from water and soil. Materials 15, 1894. https://doi.org/10.3390/ma15051894

Loffredo, E., Taskin, E. (2017). Adsorptive removal of ascertained and suspected endocrine disruptors from aqueous solution using plant-derived materials. Environmental Science and Pollution Research 24, 19159–19166. https://doi.org/10.1007/s11356-017-9595-z

Loffredo, E., Carnimeo, C., Silletti, R., Summo, C. (2021). Use of the Solid By-Product of Anaerobic Digestion of Biomass to Remove Anthropogenic Organic Pollutants with Endocrine Disruptive Activity. Processes 9, 11. https://doi.org/10.3390/pr9112018

Loffredo, E., Scarcia, Y., Parlavecchia, M. (2020). Removal of ochratoxin A from liquid media using novel low-cost biosorbents. Environmental Science and Pollution Research 27, 34484–34494. https://doi.org/10.1007/s11356-020-09544-z

Loffredo, E., Carnimeo, C., D'Orazio, V., Colatorti, N. (2024). Sorption and release of the pesticides oxyfluorfen and boscalid in digestate from olive pomace and in digestate-amended soil. Journal of Soils and Sediments 24, 1489–1506. https://doi.org/10.1007/s11368-024-03748-3

Mahato, N., Sinha, M., Sharma, K., Koteswararao, R., Cho, M.H. (2019). Modern extraction and purification techniques for obtaining high purity food-grade bioactive compounds and value-added co-products from citrus wastes. Foods 8, 523. https://doi.org/10.3390/foods8110523

Martí-Calatayud, M.C., Heßler, R., Schneider, S., Bohner, C., Yüce, S., Wessling, M., Sena, R.F., Athayde Júnior, G.B. (2020). Transients of micropollutant removal from high-strength wastewaters in PAC-assisted MBR and MBR coupled with high-retention membranes. Separation and Purification Technology 246, 116863. https://doi.org/10.1016/j.seppur.2020.116863

Martin-Lara, M.A., Blázquez, G., Trujillo, M.C., Pérez, A., Calero, M. (2014). New treatment of real electroplating wastewater containing heavy metal ions by adsorption onto olive stone. Journal of Cleaner Production 81, 120–129. https://doi.org/10.1016/j.jclepro.2014.06.036

McKendry, P. (2022). Energy production from biomass (part 1): Overview of biomass. Bioresource Technology 83, 37–46. https://doi.org/10.1016/S0960-8524(01)00118-3

Mehdizadeh, M., Izadi-Darbandi, E., Yazdi, M.T.N.P., Rastgoo, M., Malaekeh-Nikouei, B., Nassirli, H. (2019). Impacts of different organic amendments on soil degradation and phytotoxicity of

metribuzin. International Journal of Recycling of Organic Waste in Agriculture 8, 113–121. https://doi.org/10.1007/s40093-019-0280-8

Michael-Igolima, U., Abbazia, S.J., Ifelebuegu, A.O., Eyo, E.U. (2023). Modified Orange Peel Waste as a Sustainable Material for Adsorption of Contaminants. Materials 16, 1092. https://doi.org/10.3390/ma16031092

Mottes, C., Lesueur-Jannoyer, M., Le Bail, M., Malezieux, E. (2014). Pesticide transfer models in crop and watershed systems: a review. Agronomy for Sustainable Development 34, 229–250. https://doi.org/10.1007/s13593-013-0176-3

Moubarik, A., Grimi, N. (2014). Valorization of olive stone and sugar cane bagasse by-products as biosorbents for the removal of cadmium from aqueous solution. Food Research International 73, 169–175. https://doi.org/10.1016/j.foodres.2014.07.050

Moussavi, G., Khosravi, R.(2011). The removal of cationic dyes from aqueous solutions by adsorption onto pistachio hull waste. Chemical Engineering Research and Design 89, 2182–2189. https://doi.org/10.1016/j.cherd.2010.11.024

Nguyen, C., Loison, J.P., Motard, C., Dauguet, S. (2024). Cadmium partitioning between hulls and kernels in three sunflower varieties: consequences for food/feed chain safety. Environmental Science and Pollution Research 31, 1674–1680. https://doi.org/10.1007/s11356-023-31631-0

Paradelo, R., Al-Zawahreh, K., Barral, M.T. (2020). Utilization of Composts for Adsorption of Methylene Blue from Aqueous Solutions: Kinetics and Equilibrium Studies. Materials 13, 2179. https://doi.org/10.3390/ma13092179

Patel, S. (2012). Potential of fruit and vegetable wastes as novel biosorbents: summarizing the recent studies. Reviews in Environmental Science and Biotechnology 11, 365–380. https://doi.org/10.1007/s11157-012-9297-4

Paucar, N.E., Kim, I., Tanaka, H., Sato, C. (2019). Ozone treatment process for the removal of pharmaceuticals and personal care products in wastewater. Ozone: Science & Engineering 41, 3–16. https://doi.org/10.1080/01919512.2018.1482456

Reda, R.M., El Gaafary, N.M., Rashwan, A.A., Mahsoub, F., El-Gazzar, N. (2022). Evaluation of olive stone biochar as valuable and inexpensive agro-waste adsorbent for the adsorption and removal of inorganic mercury from Nile tilapia aquaculture systems. Aquaculture Research 53, 1676–1692. https://doi.org/10.1111/are.15699

Regueiro, J., López-Fernández, O., Rial-Otero, R., Cancho-Grande, B., Simal-Gándara, J. (2015). A review on the fermentation of foods and the residues of pesticides—biotransformation of pesticides and effects on fermentation and food quality. Critical Reviews in Food Science and Nutrition 55, 839–863. https://doi.org/10.1080/10408398.2012.677872

Reuland, G., Sleutel, S., Li, H., Dekker, H., Sigurnjak, I., Meers, E. (2023). Quantifying CO2 Emissions and Carbon Sequestration from Digestate-Amended Soil Using Natural 13C Abundance as a Tracer. Agronomy 13, 2501. https://doi.org/10.3390/agronomy13102501

Revellame, E.D., Fortela, D.L., Sharp, W., Hernandez, R., Zappi, M.E. (2020). Adsorption kinetic modeling using pseudo-first order and pseudo-second order rate laws: A review. Cleaner Engineering and Technology 1, 100032. https://doi.org/10.1016/j.clet.2020.100032

Rodríguez, G., Lama, A., Rodríguez, R., Jiménez, A., Guillén, R., Fernández-Bolaños, J. (2008). Olive stone an attractive source of bioactive and valuable compounds. Bioresource Technology 99, 5261–5269. https://doi.org/10.1016/j.biortech.2007.11.027

Safarian, S. (2023). Climate Impact Comparison of Biomass Combustion and Pyrolysis with Different Applications for Biochar Based on LCA. Energies 16, 5541. https://doi.org/10.3390/en16145541

Schmidt, M.P., Ashworth, D.J., Celis, N., Ibekwe, A.M. (2023). Optimizing date palm leaf and pistachio shell biochar properties for antibiotic adsorption by varying pyrolysis temperature. Bioresource Technology Reports 21. https://doi.org/10.1016/j.biteb.2022.101325

Sentürk, I., Alzein, M. (2020). Adsorptive removal of basic blue 41 using pistachio shell adsorbent. Sustainable Chemistry and Pharmacy 16, 100254. https://doi.org/10.1016/j.scp.2020.100254

Shamrikova, E.V., Vanchikova, E.V., Kyzyurova, E.V., Zhangurov, E.V. (2024). Methods for Measuring Organic Carbon Content in Carbonate-Containing Soils: A Review. Eurasian Soil Science 57, 380–394. https://doi.org/10.1134/S1064229323603104

Shaikhiev, I.G., Kraysman, N.V., Sverguzova, S.V. (2023). Review of Pistachio Shell Use to Remove Pollutants from Aqua Media. Biointerface Research in Applied Chemistry 13 (2023). https://doi.org/10.33263/BRIAC134.389

Siles, J.A., Vargas, F., Gutiérrez, M.C., Chica, A.F., Martín, M.A. (2016). Integral valorisation of waste orange peel using combustion, biomethanisation and co-composting technologies. Bioresource Technology 211, 173–182. https://doi.org/10.1016/j.biortech.2016.03.056

Turan, N.G., Mesci, B. (2011). Use of pistachio shells as an adsorbent for the removal of zinc(II) ion. Clean - Soil, Air, Water 39, 475–481. https://doi.org/10.1002/clen.201000297

USEPA Office of Water. Candidate contaminant list regulatory determination support document for metribuzin (2023).

Wu, C., Liu, X., Wu, X., Dong, F., Xu, J., Zheng, Y. (2019). Sorption, degradation and bioavailability of oxyfluorfen in biochar-amended soils. Science of the Total Environment 658, 87–94. https://doi.org/10.1016/j.scitotenv.2018.12.059

Zapata, B., Balmaseda, J., Fregoso-Israel, E., Torres-García, E. (2009). Thermo-kinetics study of orange peel in air. Journal of Thermal Analysis and Calorimetry 98, 309–315. https://doi.org/10.1007/s10973-009-0146-9

CHAPTER – 4
MULTIFUNCTIONALITY OF BIOCHAR FROM WOOD GASIFICATION: CONTROL OF PESTICIDE DYNAMICS AND EARLY PLANT GROWTH

The work reported in this chapter has been published in Journal of Sustainable Agriculture and Environment, Volume 4, Iusse 4, (2025), https://doi.org/10.1002/sae2.70097

Abstract

Biochar can play a relevant role in the soil-plant system by affecting both the dynamics of agrochemicals and plant growth. This study investigated the potential of a poplar wood biochar produced at 850°C to control the retention and leaching of the long-persistent fungicide boscalid (BOS) in soil and the early growth of agricultural plants. Biochar characterization included advanced analyses such as inductively coupled plasma-atomic emission spectroscopy (ICP-AES), scanning electron microscopy (SEM), Fourier transform infrared (FTIR) spectroscopy and Brunauer-Emmet-Teller (BET) analysis. BOS adsorption/desorption was evaluated by performing sorption kinetics and isotherms, and by modeling the experimental data with various theoretical equations. Bioassays on horticultural plants were also conducted. Adsorption studies demonstrated a noticeable and rapid retention of BOS on biochar according to a pseudo-second order kinetic model, which denoted the contribution of chemisorption. The adsorption isotherms of BOS fitted well the Freundlich model and showed distribution coefficients (K_d) values of 5.5, 23.5 and 28.3 mg g^{-1} at interaction temperatures of 10, 20°C and 30°C, respectively. A minimal release of BOS was observed after four desorption cycles, indicating a long-term retention of the compound on biochar. Leaching experiments in soil columns showed that the addition of 1, 2% and 5% biochar was effective in countering the downward movement of BOS, and that such activity was directly proportional to the dose. Bioassays on cucumber and sunflower treated with 0.04% and 0.1% (w/v) biochar did not show inhibitory effects, but rather a stimulation of root elongation of cucumber at the higher dose. The overall results obtained confirmed the multifunctionality of this material, which, in a context of sustainable agriculture and soil health protection, can play a substantial role in controlling the dynamics of organic xenobiotics in soil without exerting inhibitory effects on the tested plants.

4.1 Introduction

The continuous decrease of soil organic matter (SOM) content in agroecosystems, mainly due to intensive and super-intensive agricultural practices, has prompted the application of organic amendments as carbon (C) source for microorganisms and for the recovery of soil health and fertility (Hou et al. 2022). These organic amendments are complex structures typically derived from the activity of living organisms or from the thermochemical conversion of organic waste.

Among them, biochar stands out for its potential benefits in numerous environmental, agricultural, and industrial contexts. Biochar is a carbonaceous product obtained by thermochemical decomposition (pyrolysis and gasification) of various types of biomass in absence or limited availability of oxygen and at temperatures between 300°C and 1000°C (Lehmann and Joseph 2024). Biochar application to soil represents a sustainable and long-lasting strategy for C sequestration due to its intrinsic biochemical recalcitrance (Wang et al. 2015). In recent years, this material has aroused great interest for its beneficial effects on the protection of plants and soil microbial communities from organic and inorganic contaminants (Llovet et al. 2021).

In-depth knowledge of the physicochemical characteristics of biochar is essential as they influence the abiotic and biotic processes that occur in the soil after its application and suggest its optimal use and dosage. Biochar properties are deeply affected by feedstock and process temperature. The presence of reactive surface functional groups and a porous structure make this material a good adsorbent for hydrophilic and, especially, hydrophobic contaminants such as agrochemicals and heavy metals (Parlavecchia et al. 2020; Nkoh et al. 2022; Kumar et al. 2022).

Agrochemicals such as herbicides, fungicides, insecticides, and nematicides are widely used in conventional agriculture for crop protection. Their repeated application to soil and plants over the years, especially at incorrect dosage, may result in residue levels that not only impair the biological fertility of soil and plant growth but also compromise food safety (Parlavecchia et al. 2020). In fact, most of pesticides, especially the less hydrophobic ones, can be absorbed by the roots of plants and transferred into the different tissues where they accumulate (Carnimeo et al. 2022). This is particularly dangerous for food crops, as toxic residues can reach the edible organs of plants and enter the animal and human food chain. Moreover, more polar pesticides can pose serious environmental risks due to their movement in soil and transport into surface and groundwater (Jongbloed et al. 2004; Dugan et al. 2023). Boscalid (BOS) is one of the most widely used fungicides as it controls fungal diseases of a large variety of crops, including grape, apple, strawberry, tomato and cucumber. Crop residues left or incorporated into the soil and the long persistence of this compound can cause soil contamination (Nandi et al. 2025). BOS can affect the

diversity and functioning of soil microbial communities, especially fungi, that play a crucial role in the formation of stable SOM and nutrient cycling. BOS leaching in soil, especially in very humid climates or where high irrigation volumes are applied, can be a serious environmental issue which can be counteracted by the addition of exogenous organic matter (Pérez-Lucas et al. 2020).

Adsorption is an efficient, economical and environmentally friendly method for removing pollutants from soil and water (Yang et al. 2019; Loffredo et al. 2021a, 2021b). This process involves the retention of a molecule (adsorbate) on the surface of a solid material (adsorbent) via physical or chemical interactions. In addition to pollutant retention, biochar can also improve the physicochemical properties of soil and positively influence the early stages of plant development (Gascó et al. 2016). However, the effects of biochar on seed germination and seedling growth are variable and depend on multiple factors, including the type of biomass used, the conditions of the production process, the application rates, and the specific characteristics of the crop species (Liu et al. 2021).

Despite the proven agronomic relevance of biochar and the environmental risks of BOS, there is still a significant gap in the scientific literature regarding their interaction in water and in the soil. Furthermore, there is a complete lack of studies on the effects of gasification biochar, i.e., biochar produced at very high temperatures, on plant germination and early growth.

Considering the above, this study aims to investigate (i) the structural and compositional properties of a poplar wood gasification biochar produced at high temperature (850°C); (ii) its capacity to adsorb and release BOS in water; (iii) its potential to reduce BOS leaching in soil; and (iv) its effects on the early growth of cucumber and sunflower crops.

4.2 Materials and Methods

4.2.1 Biochar, Chemicals, Soil and Plants

Biochar was provided by RESET S.p.a. company, Rome, Italy. It was produced from poplar wood through the gasification process at temperature of 850°C and the SyngaSmart® technology.

BOS (2-chloro-N-[2-(4-chlorophenyl) phenyl] pyridine-3-carboxamide) (Cas number 188425-85-6) with purity ≥ 99.0% was purchased from Sigma-Aldrich S.r.l., Milano, Italy. Chemical structure and some properties of BOS are shown in Table S1. All other chemicals used were purchased from commercial companies and were used without further purification.

A loam soil was sampled from the 0–10 cm soil layer of an olive grove located at an experimental station of the University of Bari in Valenzano, Southern Italy (41°02′ N; 16°90′ E). The soil sample

was air-dried, sieved to < 2 mm to remove the skeleton fraction, and thoroughly mixed before analyses. Some soil properties are summarized as follows: 36% sand, 43% silt, 21% clay, 4.4% moisture, pH 7.4, EC 0.20 dS m^{-1} at 25°C, 37.9 g kg^{-1} total organic C, 2.98 g kg^{-1} total N (Colatorti et al. 2024).

Cucumber (*Cucumis sativus* L.) and sunflower (*Heliantus annus* L.) seeds were purchased from L'ortolano S.r.l., Cesena, and Tesoro della terra S.r.l., Andria, Italy, respectively.

4.2.2 Biochar Characterization

Physicochemical properties of biochar were determined as follows: moisture content was measured using a Radwag MA 110.R moisture balance equipped with infrared lamps; pH and EC were measured in biochar-water extract 1:10 (w/v) using a pH meter (CRISON micropH 2001) and a conductivity meter (CRISON microCM 2201), respectively. Bulk density (BD) was measured using a 1 L graduated cylinder filled with a known sample mass and tapped manually for 60 s to ensure the absence of large void spaces. Total C and N contents were determined by dry combustion using a Thermo Flash 2000 NC Soil Analyser. Water holding capacity (WHC) was determined by saturating the dry sample with water for 8 h and weighting it after a 24 h leaching period.

Nutrients and trace elements of biochar were determined using a Inductively Coupled Plasma Atomic Emission Spectrophotometry (ICP-AES, Perkin Elmer Optima 4300 DV, PerkinElmer Inc., Waltham, MA, USA). Before analytical measurements, the sample was treated with the chelating agent DPTA (diethylenetriamine-pentaacetic-acid) at a concentration of 0.005 M at a ratio of 1:25 (v/v). The mixture was mechanically shaken at 180 U min^{-1} for 2 h, filtered and analysed with ICP-AES.

Scanning electron microscopy (SEM) was employed to study the surface structural features of biochar. A small sample of the material was coated with a thin layer of Au/Pd and examined using a Hitachi TM3000 scanning electron microscope (Hitachi, Tokyo, Japan). Backscattered electrons were utilized to capture SEM images of biochar at 0.5 and 2.5 k magnifications. Fourier transform infrared (FTIR) spectrum of biochar was obtained using a Thermo Nicolet iS50 FTIR spectrophotometer equipped with Nicolet Omnic 6.0 software. A dried biochar sample of 400 µg was mixed with 400 mg of dried KBr (FTIR grade) and pulverized using an agate mortar and pestle. The mixture was then pressed under vacuum at 6000 kg cm^{-1} for 10 min, thus obtaining a pellet that was analysed in 4000–400 cm^{-1} wavenumber range with a resolution of 2 cm^{-1} and 16 scans min^{-1} for the acquisition.

BET (Brunauer, Emmett and Teller) analysis was conducted to quantitatively evaluate the specific surface area of biochar. The technique is based on the physisorption of an inert gas (N_2, Ar or Kr) on the surface of a material by applying relative pressure (P/P_0) values ranging from 0.05 to 0.30 (multi-point). The adsorption-desorption isotherms of N_2 on biochar were determined at −196°C. The sample was first outgassed at 120°C for 16 h to remove moisture and other impurities and then analysed with Autosorb AS-1 Quantachrome instrument. Total pore volume of biochar was derived from the amount of gas adsorbed at a relative pressure close to unity (P/P_0 equal to 0.9) to ensure that the pores were filled with N_2. The micropore volume (pore diameter or width < 2.0 nm) and their specific surface area were obtained according to the t-plot method where amounts adsorbed on the porous sample are plotted against the corresponding multilayer thickness, on a P/P_0 range of 0.1-0.35. The mesopore volume was obtained by subtracting the micropore volume from the total pore volume. Finally, average pore size was estimated using the Barret-Joyner-Halenda (BJH) method (Brunauer et al. 1938). Measurements were performed in a Quantachrome Autosorb AS-1 instrument using As1-Win software.

4.2.3 Adsorption study

The effects of different solution:biochar ratios on BOS adsorption were evaluated in slurry-type experiments. Aliquots of 1, 2, 5, 10, and 20 mg biochar were added to 10 mL of an aqueous solution of BOS at a concentration of 2 mg L^{-1} (solution:biochar ratios of 10,000, 5000, 2000, 1000 and 500, respectively) and kept under magnetic stirring at a temperature of 26 ± 1°C for an equilibration time of 120 minutes. Then, the samples were centrifuged at 10,000 *g* for 10 minutes, and the supernatants were analysed using high-performance liquid chromatography (HPLC) (section 2.5). Each experiment was run in triplicate. The quantity of adsorbed BOS at equilibrium, q_t (mg g^{-1}), was calculated using the equation:

$$q_t = (C_0 - C_t)\, V/m \qquad [1]$$

where C_0 (mg L^{-1}) represents the initial concentration of the molecule in solution, C_t (mg L^{-1}) is the concentration at time t (120 minutes in these experiments), V (L) is the solution volume, and m (g) is the biochar mass.

To evaluate the adsorption rate of BOS onto biochar and determine the equilibrium time, sorption kinetics were conducted at a temperature of 26 ± 1 °C. A solution:biochar ratio of 10,000 was adopted. Volumes of 20 mL of 2 mg L^{-1} aqueous solution of BOS was interacted with 2 mg biochar in glass centrifuge tubes. The suspensions were stirred in the dark for times ranging from 0 to 120 min. Afterward, the samples were centrifuged at 10,000 g for 10 minutes, and the supernatants were analysed by HPLC. All experiments were performed in triplicate. The concentration of the adsorbed compound at time t, q_t (mg g^{-1}), was calculated using equation [1]. The equilibrium time was

identified as the time when the amount of compound adsorbed remained unchanged based on Student's t-test ($P \leq 0.05$).

Two theoretical models were applied to interpret the experimental data of sorption kinetics, the pseudo-first order (PFO) and the pseudo-second order (PSO) model. The PFO equation (Kumar, 2006) is expressed by:

$$q_t = q_e (1 - \exp^{-k_1 t}) \quad [2]$$

being q_e and q_t (mg kg^{-1}) the amount of compound adsorbed at equilibrium and at time t, respectively, and k_1 (h^{-1}) is the PFO rate constant. The PSO equation (Ho, 2006) is given by:

$$q_t = (q_e^2 k_2 t)/(1 + q_e k_2 t) \quad [3]$$

being qt and qe already described and k_2 (kg mg^{-1} h^{-1}) the PSO rate constant. The non-linear regression method was used to fit experimental data to both models using the solver add-in component of Microsoft Excel and a trial-and-error procedure which minimized the sum of squared residuals (SSR) between observed and theoretical data.

Adsorption isotherms of BOS on biochar were performed at temperatures of 10, 20 and 30 ± 1 °C, using the slurry-type equilibrium method. Volumes of 20 mL of aqueous solutions of BOS at concentrations of 0.1, 0.2, 0.5, 1, and 2 mg L^{-1} were added to 2 mg biochar in glass centrifuge tubes. The samples were kept under continuous magnetic stirring in a thermostated chamber (F.lli Della Marca S.r.l., Rome, Italy) in the dark for 120 min. Subsequently, the samples were processed and analysed as described for adsorption kinetics. All experiments were triplicated.

The desorption study was conducted at a temperature of 20°C immediately after adsorption using the sample added with the highest BOS concentration (2 mg L^{-1}) and continued for four desorption cycles. Residual concentrations of the compound in the supernatant solution were measured by HPLC as detailed in section 2.5.

To describe sorption and desorption isotherms data, three theoretical models were considered: the two-parameter Freundlich and Temkin models, and the linear Henry equation. The Freundlich model, which is well suitable for heterogeneous surfaces and multilayer adsorption, is expressed as:

$$q_e = K_F C_e^{1/n} \quad [4]$$

where q_e (mg g^{-1}) and C_e are, respectively, the concentration of the compound on the adsorbent and in solution at equilibrium, K_F (mg g^{-1}) is the Freundlich sorption constant, and 1/n describes the non-linearity and intensity of the sorption process. The Temkin model assumes a linear variation of the adsorption enthalpy during the adsorption process and a competition between adsorption sites with different binding energies. It is given by:

$$q_e = B \ln(A_T C_e) \quad [5]$$

where q_e and C_e have the same meaning as in eq. 4, A_T is the Temkin equilibrium constant (mg g^{-1}),

and B (J mol^{-1}) is the Temkin coefficient, i.e., a measure of the process enthalpy. The B value is calculated from $B = RT/b_T$, with b_T being a constant related to the heat of adsorption, T is the absolute temperature (K), and R is the universal gas constant (8.314 J mol^{-1} K^{-1}). All isotherm parameters were calculated through the non-linear regression by minimizing the sum of squared residuals (SSR) between observed and predicted values. In addition, the linear Henry model, expressed as:

$$q_e = K_d C_e \quad [6]$$

was used to calculate the distribution coefficient K_d (L kg^{-1}) and the organic C (OC) normalized partition coefficient K_{OC}, calculated as: $K_{OC} = (K_d \times 100)/\%$ OC which represents the amount of compound adsorbed per unit of OC. Desorption data were described using the Freundlich and Henry equations that allowed to calculate K_{Fdes}, $1/n_{des}$ and K_{ddes}.

4.2.4 Leaching Experiments

Leaching experiments were performed in triplicate using columns (7 cm diameter × 30 cm height) prepared by overlapping plexiglass cylinders. Each column was filled up to a height of 20 cm with 700 g of unamended soil (control) or soil amended, in the upper 10 cm, with biochar at doses of 1, 2% and 5% (w/w). Considering a soil density of 1.4 t ha^{-1} and 10 cm-depth, the lowest (1%) and the highest (5%) biochar doses correspond, respectively, to soil applications of approximately 14 and 70 t ha^{-1}. Therefore, the tested biochar rates were chosen based on the amendment doses, including biochar, commonly applied to soils in our region (Castellini et al. 2025) and on the amendment rates reported in similar studies (Loffredo et al. 2021b; Alessandrino 2024). To prevent loss of soil particles, a layer of glass wool was placed in the bottom of the column. All soil columns were moistened to reach 60% of the soil water holding field capacity. Experiments were performed at room temperature (approximately 20°C) and protected from direct light. After 2 h, a volume of 1.75 mL of 1 mg mL^{-1} methanol solution of BOS was added into the uppermost layer (about 2 cm) of the soil column to reach a concentration of 2.5 µg g^{-1} BOS in the whole column. A volume of 40 mL of distilled water was added to the column every day for four consecutive days. Due to the short experimental time and based on the half-life data of BOS reported in the literature (Karlsson et al. 2016), the biological dissipation of the compound was considered negligible. At the end of experiments, the soil columns were sectioned (0–2, 2–4, 4–6, 6–8, 8–10, 10–15, and 15–20 cm) and each layer was collected and homogenized. A 40 g subsample from each section was added with 100 mL methanol and mechanically shaken for 16 h. Then, the suspensions were filtered and 10 mL of each filtrate was centrifuged at 10,000 *g* for 10 min. Subsequently, supernatants were analysed by HPLC as described in the next section.

4.2.5 HPLC Protocol

All samples were filtered through 0.45 μm Millipore™ cellulose acetate filters. HPLC analyses were performed using a Shimadzu Nexera series system (Kyoto, Japan) which included a LC- 40D XR pump, a SIL-40C XR autosampler, and a CTO-40C column compartment equipped with a Shimadzu Shim-pack GIST-HP C-18 column (150 mm × 3 mm × 3 μm). The mobile phase was water/acetonitrile (40/60, v/v) and flowed at 0.6 mL min^{-1}. The retention time of BOS was 3.9 min. The molecule was quantified using an SPD-M40 photodiode array detector at a wavelength of 207 nm.

4.2.6 Plant Assays

Plant assays were conducted using 9-cm diameter Petri dishes where 6 cucumber seeds or 5 sunflower seeds were placed. Each species was treated with 5 mL distilled water alone (control) or added with 2 or 5 mg biochar; the seeds were germinated in a growth chamber (Phytotron model 60043/THTL, F. lli Della Marca s.r.l., Rome) in the dark, at a temperature of 22 ± 1°C for 6 days. All experiments were performed in triplicate. At the end of experiments, root length, shoot length, fresh weight and dry weight (70°C for 2 h) of each seedling were measured. Biometric data of the seedlings were statistically analysed using ANOVA and the means were compared with the control using the least significant difference (LSD) test at $p \leq 0.05$, $p \leq 0.01$, and $p \leq 0.001$.

4.3 Results and Discussion

4.3.1 Biochar Characterization

The physicochemical properties of biochar (Table 1) were within the range of those reported in the literature for wood biochars produced at high temperature (Mukome and Parikh 2016; Moreno et al. 2022). Proximate analysis showed alkaline pH and high ash content. Wang et al. (2022) reported that generally, the ash content is directly related to the production temperature and the duration of the thermal process. The alkaline nature of this material, along with the high EC value, can be attributed to the retention of alkali and alkaline earth metals during the production process. As expected, total organic C (~77%) was quite high, which is typical of the solid byproduct of biomass gasification. These characteristics of biochar are reasonably ascribable to chemical rearrangements, such as dehydration, decarboxylation and aromatization reactions, occurred during the thermochemical process (Taskin et al. 2019). Similar values of C and N contents are reported in the literature for other wood gasification biochars (Qian et al. 2015). In general, phosphorus (P) is quite abundant in wood biochars (Qian et al. 2013). The P content of this biochar was higher than that reported by Taskin et al. (2019) for a red spruce pellets biochar.

Table 1. Physicochemical properties and trace element content of biochar.

Parameter	BC
pH	9.67 ± 0.29
EC (dS m^{-1})	3.34 ± 0.25
Moisture (%)	8.32 ± 0.24
BD (g cm^{-3})	0.36 ± 0.20
WHC (%)	315 ± 10
Ash (%)	17.6 ± 0.13
Total C (g kg^{-1} d.w.)	767 ± 1.52
Total N (g kg^{-1} d.w.)	5.1 ± 0.06
Total P (mg kg^{-1} d.w.)	340 ± 11
Trace elements (mg kg^{-1} d.w.)	
Cd	< 1.0
Ni	5.3 ± 0.001
Al	5.0 ± 0.003
Cu	23.7 ± 0.005
Fe	76.5 ± 0.013
Mn	28.8 ± 0.005
Zn	16.0 ± 0.003

All values are the mean ± SD (n = 3). BD: bulk density; WHC: water holding capacity.

Trace element analysis of biochar (Table 1) showed concentrations ranging from few mg kg^{-1}, as in the case of Ni and Al, up to tens of mg kg^{-1} for Cu, Fe, Mn and Zn. In addition to the type of feedstock, operative temperature and residence time in the reactor may influence the elemental composition of this material. Leijenhorst et al. (2016) investigated the transfer of mineral elements from the feedstock to the pyrolysis products and found that metals such as Ca, Mg, Fe, Cu, Ni, Cd, Cr, Co, Mn, Zn, Al and Pb remained largely in the solid biochar at the end of the process. The elemental composition of the biochar sample used here was comparable, especially for Cu and Mn contents, to that of a biochar obtained from grapevine residues (Colantoni et al. 2016).

The SEM technique allowed to explore the micromorphology of biochar surface and the abundance and distribution of pores (Figure S1). SEM images clearly revealed the presence of plant cell walls and xylem vessels whose structure was not completely devastated during the intense thermal

process. A diffuse porosity, originated from the release of small volatile molecules (H_2O, CO, CO_2, CH_4 and H_2) during the thermochemical process, was also observed. Similar morphological characteristics were reported for wood pyrolysis/gasification biochars (El-Naggar et al. 2019; Taskin et al. 2019). Porosity is a very important property for all biochar applications, especially when the material is used as bioadsorbent for decontamination purposes (Mohan et al. 2014).

The FTIR spectrum of biochar (Figure S2) showed a limited number of absorption bands generally of low relative intensity, which suggests a predominantly aromatic nature of the material and a poor variety of surface functional groups (Figure S2). It is known that, during the gasification treatment, chemical rearrangements induced by high temperatures, such as dehydrogenation, decarboxylation and polymerization of aromatic moieties, originate the typical carbonaceous structure of this material. In detail, the wavenumbers and assignments of the main absorption bands of biochar spectrum were the following: 3440 cm^{-1}, O─H stretching of inter- and intramolecular hydrogen bonds, water and N─H stretching; asymmetric (2954–2918 cm^{-1}) and symmetric (2850 cm^{-1}) stretching vibrations of aliphatic C─H bond of methyl and methylene groups; 1621 cm^{-1}, C═C aromatic skeletal stretching vibration; 1568–1360 cm^{-1}, ascribable to ligno-cellulosic submolecular groups (syringyl units and furanosic-like structures) and catechol-related moieties (─C─O and ─C─N groups); 1258 cm^{-1}, C─O stretching of phenolic groups, indicative of guaiacyl units of lignin; 1123 cm^{-1}, asymmetric C─O─S stretching vibration; 1031 cm^{-1}, symmetric stretching of aliphatic C─O─C, and methoxy groups of lignin; 873 cm^{-1}, aromatic C─H bending (Taskin et al. 2019). Similar FTIR spectra were reported by Qian et al. (2013) for a red cedar biochar obtained through gasification at 800°C and by Taskin et al. (2019) for biochars produced from red spruce and grapevine pruning residues.

BET analysis is commonly used to measure the specific surface area ($m^2\ g^{-1}$) of an adsorbent material and provides an indication of the total porosity, both of which are of great significance when the material is used for contaminant removal. The BET equation, developed by Brunauer et al. (1938) is used to calculate the specific surface area. The results of BET analysis of biochar are outlined in Table 2. The high BET value obtained (~400 $m^2\ g^{-1}$) suggests a remarkable potential to retain organic molecules and metals. It is known that the specific surface area of biochar is generally much higher than that of other adsorbents originated from processed biomasses, i.e., hydrochar, digestate, compost and so on. However, this parameter is also affected by the production conditions adopted, especially the pyrolysis/gasification temperature.

Table 2. BET surface area and pore properties of biochar.

Pore properties	Value
BET surface area	400.95 $m^2 g^{-1}$
t-plot micropore volume	0.129 $cm^3 g^{-1}$
t-plot surface area (micropore)	248.77 $m^2 g^{-1}$
Total pore volume	0.317 $cm^3 g^{-1}$
Mesopore volume	0.188 $cm^3 g^{-1}$
Average pore width	3.8 nm

Comparing various biochar produced at different temperatures, Hung et al. (2017) and Tsai et al. (2018) observed a direct relationship between pyrolysis temperature and BET surface area. The N_2 adsorption/desorption isotherms and the pore size distribution curve are shown in Figure S3a and S3b, respectively. Based on IUPAC (International Union of Pure and Applied Chemistry) classification, the N_2 adsorption isotherm was of type IV (Lowell et al. 2006). This isotherm shape is typical of mesoporous materials that show strong adsorption at low pressures followed by a sharp increase with capillary condensation in the pores. In agreement with what reported by Lowell et al. (2006), the isotherm showed a hysteresis loop (irreversible process) during the adsorption/desorption cycle between approximately 0.45 and 0.55 P/P_0. Furthermore, at relative pressure below 0.45, the desorption curve did not coincide with the adsorption curve, indicating the presence of a occluded microporous structure, which is often exhibited by carbonaceous materials (Marsh and Rodriguez-Reinoso 2006; Rouquerol et al. 2013). The pore size distribution of biochar with a peak at approximately 3.8 nm was clearly observed (Figure S3b), which denoted the presence of mesoporosity. According to the literature survey by Mukome and Parikh (2016), high pyrolysis temperatures increase the aromaticity of biochar, which in turn enhances its surface area and porosity. The average pore size we found in this study is similar to that reported by Hung et al. (2017) for a biochar obtained by pyrolysis at a temperature of approximately 800°C.

4.3.2 Adsorption Study

The amount of BOS adsorbed on biochar at equilibrium adopting different solution:adsorbent ratios are depicted in Figure S4. As the ratio increased from 500 to 10,000, the amount of BOS adsorbed increased significantly with each subsequent ratio (Figure S4). A tenfold increase in the

ratio, i.e., from 500 to 5000, resulted in an approximately tenfold increase (from 0.83 to 8.79 mg g^{-1}) in BOS adsorption. The observed increase can be reasonably attributed to the greater availability of adsorption sites, including the more internal ones, which occurs at low adsorbent dose. Generally, organic solutes are more easily adsorbed onto a substrate when their interaction with the solvent is weak. Several studies highlighted a negative correlation between the adsorption efficiency of C-rich materials and the water solubility of organic pollutants (Loffredo and Taskin 2017). At the maximum solution:biochar ratio (10,000), ~89% of the initial amount of BOS was adsorbed by biochar within 2 h of contact.

Numerous studies demonstrated the excellent adsorptive property of biochar towards agrochemicals (Loffredo and Taskin 2017; Parlavecchia et al. 2019; Gautam et al. 2021), antibiotics (Stylianou et al. 2021) and heavy metals (Shakya et al. 2022). Comparing the adsorption capacity of different organic amendments (compost, vermicompost, hydrochar and biochar), it is evident that biochar is by far the most effective for BOS adsorption (Parlavecchia et al. 2020). Based on these results, the highest solution:biochar ratio was selected for subsequent experiments.

The adsorption kinetics study allows to know the rate at which a solute is retained on a substrate over time, and to obtain information on the type of interaction between the adsorbent and the solute. The adsorption kinetic curve of BOS revealed that the equilibrium was achieved in a very short time, with a very rapid initial retention on the readily accessible external sites of biochar, followed by a slower adsorption at the less accessible innermost reactive sites (Figure S5). The Student t-test applied to the quantities of BOS adsorbed at different times indicated that the compound reached the steady state in approximately 30 min (Figure S5). At the steady state, 17.6 mg g^{-1} of BOS was adsorbed from the aqueous medium (Figure S5 and Table 3). The rate at which a hydrophobic compound is adsorbed on biochar is much higher than that on substrates much poorer in organic matter, such as soil. Bhatt et al. (2023) found that the adsorption of BOS onto a clay soil reached the stationary state in about 48 h.

Table 3. Kinetic PFO and PSO parameters obtained through the nonlinear regression for the adsorption of boscalid on biochar.

Parameter		Pseudo-First Order				Pseudo-Second Order			
	$q_{e,exp}$ (mg g^{-1})	r	SSR	$q_{e,1}$ (mg g^{-1})	k_1 (h^{-1})	r	SSR	$q_{e,2}$ (mg g^{-1})	k_2 (g mg^{-1} h^{-1})
Value	17.6	0.999	4.26	16.5	2.60	0.999	3.47	16.7	0.53

To obtain information on the adsorption mechanism of BOS on biochar, the kinetic data were described using the PFO (Equation 2) and PSO (Equation 3) models. Table 3 shows the values of PFO and PSO kinetics parameters obtained through the nonlinear regression, along with the correlation coefficients, r, and the sum of the squared residuals, SSR, which expresses the accordance between experimental data and models. Compared to the use of linearized PFO and PSO equations, nonlinear modeling has been considered more accurate as it provides more realistic kinetic parameters (Revellame et al. 2020). Based on r and SSR values, both models seemed well suited to interpret the experimental data, with the PSO equation showing a slightly better correspondence. Previous research has frequently shown that the PSO kinetic model is more effective in describing the adsorption kinetics of many organic compounds (Kumar and Sivanesan 2006). This model assumes the formation of chemical bonds, such as covalent, ionic or hydrogen bonds, between the solute and the adsorbent that can limit the speed of the adsorption process (Ho and McKay 1999).

Adsorption isotherms were performed to quantitatively study the interaction between BOS and biochar at different temperatures and to obtain information on the mechanisms of the process. Experimental adsorption data obtained at temperatures of 10, 20, and 30°C were fitted into the two-parameter Freundlich and Temkin models that are commonly used to describe adsorption on heterogeneous adsorbents. The linear Henry equation was also considered to calculate the distribution coefficient, K_d, and the organic C partition coefficient, K_{OC}. The Freundlich model assumes that the adsorption sites exhibit varying energies and that the heat of adsorption decreases exponentially as coverage increases. The Temkin model assumes that the solute molecules interact each other thus influencing the heat of adsorption which decreases linearly as coverage increases.

The results of this study confirmed the high efficiency of biochar as adsorbent of hydrophobic compounds, such as BOS, with adsorption intensity increasing with temperature (Figure 1 and Table 4). The lower adsorption capacity observed at 10°C can be attributed to reduced molecular diffusion, limitations in intraparticle transport processes and the endothermic nature of adsorption, which enhances the interaction between BOS and biochar at higher temperatures. Based on r and SSR values, the Freundlich model fitted very well the experimental adsorption data at all three temperatures. A study by Taha et al. (2014) on the adsorption of BOS onto a biochar produced from rice straw and maize residues at 450°C reported a slightly lower K_d value compared to that observed in the present study, which could be attributed to the lower pyrolysis temperature used. Higher process temperature produces biochar with greater specific surface area, which enhances its ability to adsorb organic compounds (Tang et al. 2013). The strong retention of BOS on biochar was followed by a very poor and extremely slow desorption (Figure 1b). Given the physicochemical

properties of the biochar used here and the marked hydrophobicity of the BOS molecule, this behaviour was expected. The high production temperature of biochar plays a key role in its adsorption/desorption capacity, as it leads to a substantial reduction in polar surface functional groups, thereby increasing its hydrophobic nature (Wang et al. 2022)

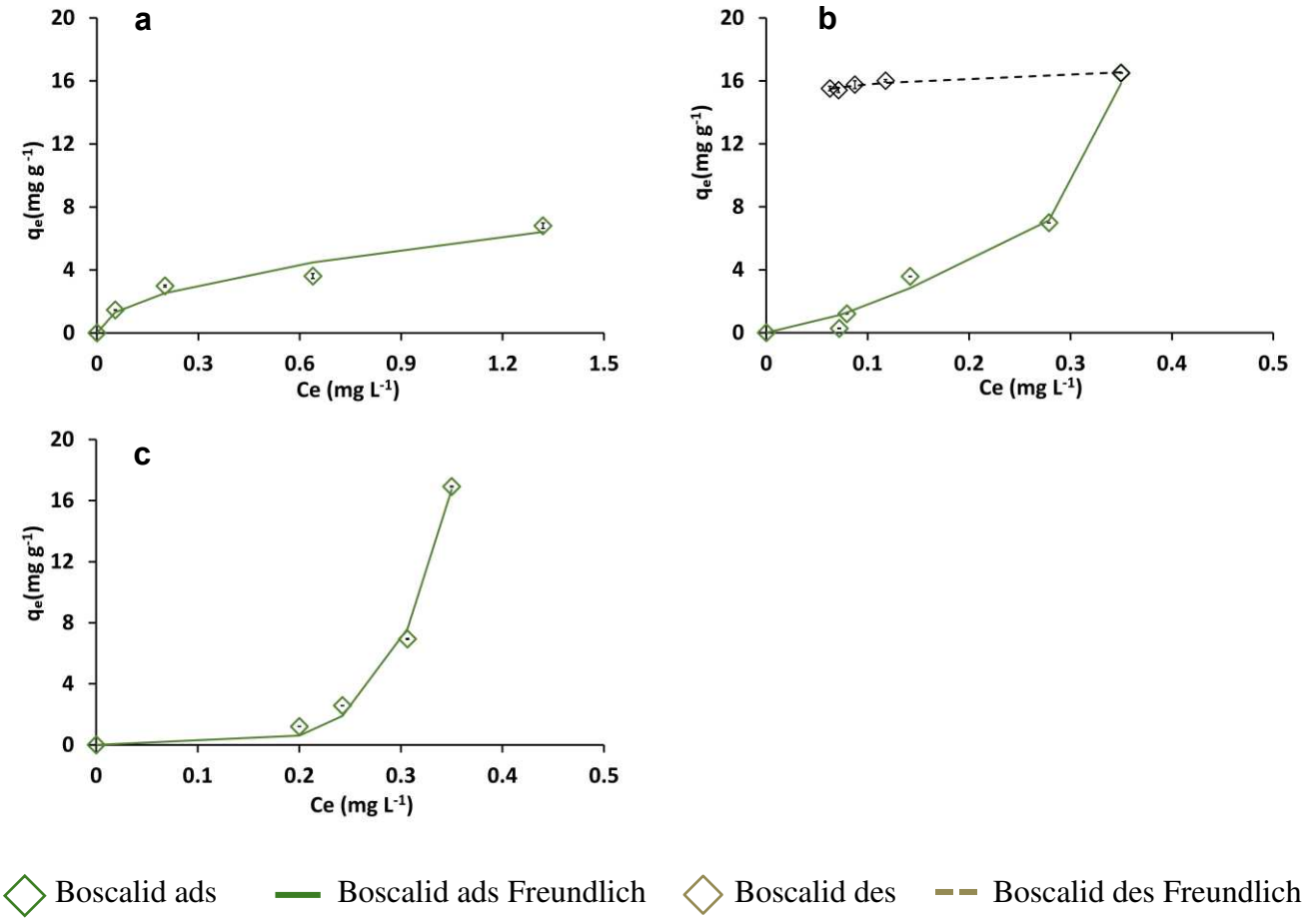

Figure 1. Adsorption isotherms of the fungicide boscalid on biochar performed at temperatures of 10 °C (a), 20 °C (b) and 30 °C (c). Desorption isotherm (b, dashed line) was performed at a temperature of 20°C. Experimental points are shown along with plot of the Freundlich model. Standard error is reported as vertical bar on each point (n = 3).

Table 4. Adsorption and desorption parameters for boscalid on biochar.

Adsorption													
10°C													
Parameter	Henry				Freundlich				Temkin				
	r	SSR	K_d (mg g^{-1})	K_{OC} (mg g^{-1})	r	SSR	K_F (mg g^{-1})	1/n	r	SSR	A_T (mg g^{1})	B (J mol^{-1})	b_T
Value	0.963	5.09	5.46	7.12	0.964	1.13	5.59	0.50	0.918	2.38	39.7	1.48	1589
20°C													
Parameter	Henry				Freundlich				Temkin				
	r	SSR	K_d (mg g^{-1})	K_{OC} (mg g^{-1})	r	SSR	K_F (mg g^{-1})	1/n	r	SSR	A_T (mg g^{1})	B (J mol^{-1})	b_T
Value	0.979	2.68	23.5	30.7	0.998	8.60	262	2.67	0.998	0.13	15.3	4.78	509
30 °C													
Parameter	Henry				Freundlich				Temkin				
	r	SSR	K_d (mg g^{-1})	K_{OC} (mg g^{-1})	r	SSR	K_F (mg g^{-1})	1/n	r	SSR	A_T (mg g^{1})	B (J mol^{-1})	b_T
Value	0.858	90.36	28.3	36.9	0.996	1.33	866	4.09	0.964	28.0	4.87	25.8	97.5

Desorption							
Parameter	Henry			Freundlich			
	r	SSR	K_d (mg g^{-1})	r	SSR	K_F (mg g^{-1})	1/n
Value	0.801	448668	72636	0.97	50049	17222	0.038

4.3.3 Leaching Experiment

The distribution of BOS at different soil depths was evaluated both in unamended soil and in soil amended with biochar at doses of 1, 2% and 5% (w/w). The leaching profile of BOS clearly showed that the presence of biochar significantly reduced the vertical mobility of the fungicide (Figure **2**). In the unamended soil, appreciable amounts of BOS were detected not only in the upper layers (0–2 cm and 2–4 cm) but also as deep as the 6–8 cm layer. In contrast, biochar-amended soil showed marked retention of BOS in the upper layer (0–2 cm), being more significant at higher application rates. Notably, the biochar-amended soil at 5% rate retained about 90% of BOS in the upper surface layer. The BOS leaching pattern showed a clear dose-dependent effect, with increasing biochar dose progressively enhancing BOS retention in the uppermost soil layer. The reduced presence of BOS in the deeper layers of the amended soil confirmed the strong sorptive capacity of biochar and its effectiveness in restricting the downward transport of the fungicide.

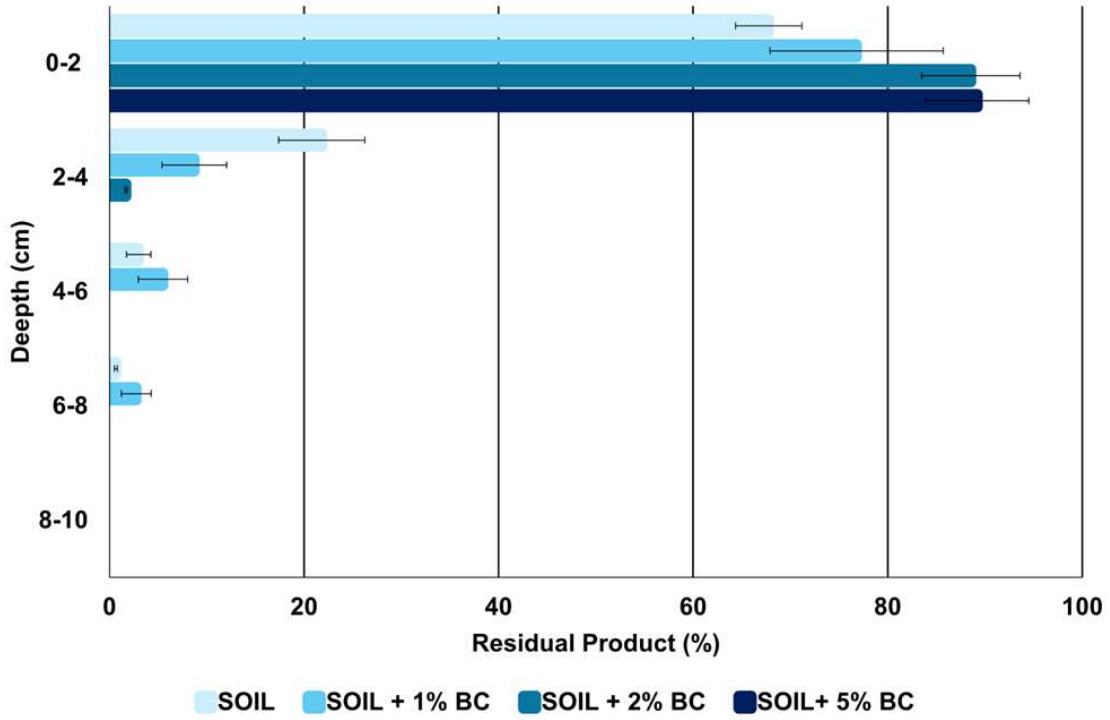

Figure 2. Residual boscalid at different depths of unamended soil and soil amended with biochar at rates of 1, 2 and 5% (w/w). The horizontal line on each bar indicates the standard error (n = 3).

In a previous study conducted in soil columns, Rodríguez-Liébana et al. (2014) compared the capacity of different amendments, including biochar, to retain the hydrophobic fungicide fenarol; the authors concluded that sewage sludge and composted sewage sludge showed a retention efficiency much lower than biochar. Pérez-Lucas et al. (2020) added a sheep manure compost in packed soil columns with the purpose to reduce BOS leaching, and found a much greater leaching of the compound than that reported in this study. In very recent works, Nandi et al. (2025) and Negi et al. (2024) explored the effectiveness of biochar in reducing BOS leaching and demonstrated its ability to immobilize the compound in the upper soil layers.

4.3.4 Plant Assays

In addition to interacting with soil organic xenobiotics, biochar can also influence the biotic component of soil, including germination and plant growth. An evaluation of this activity was carried out by measuring some biometric parameters indicative of plant response (Figure 3). To this end, two horticultural species of agronomic relevance, cucumber and sunflower, were chosen as test crops. Both plants are frequently used in germination assays, and their different seed size and physiology allowed us to explore potential variability in plant response.

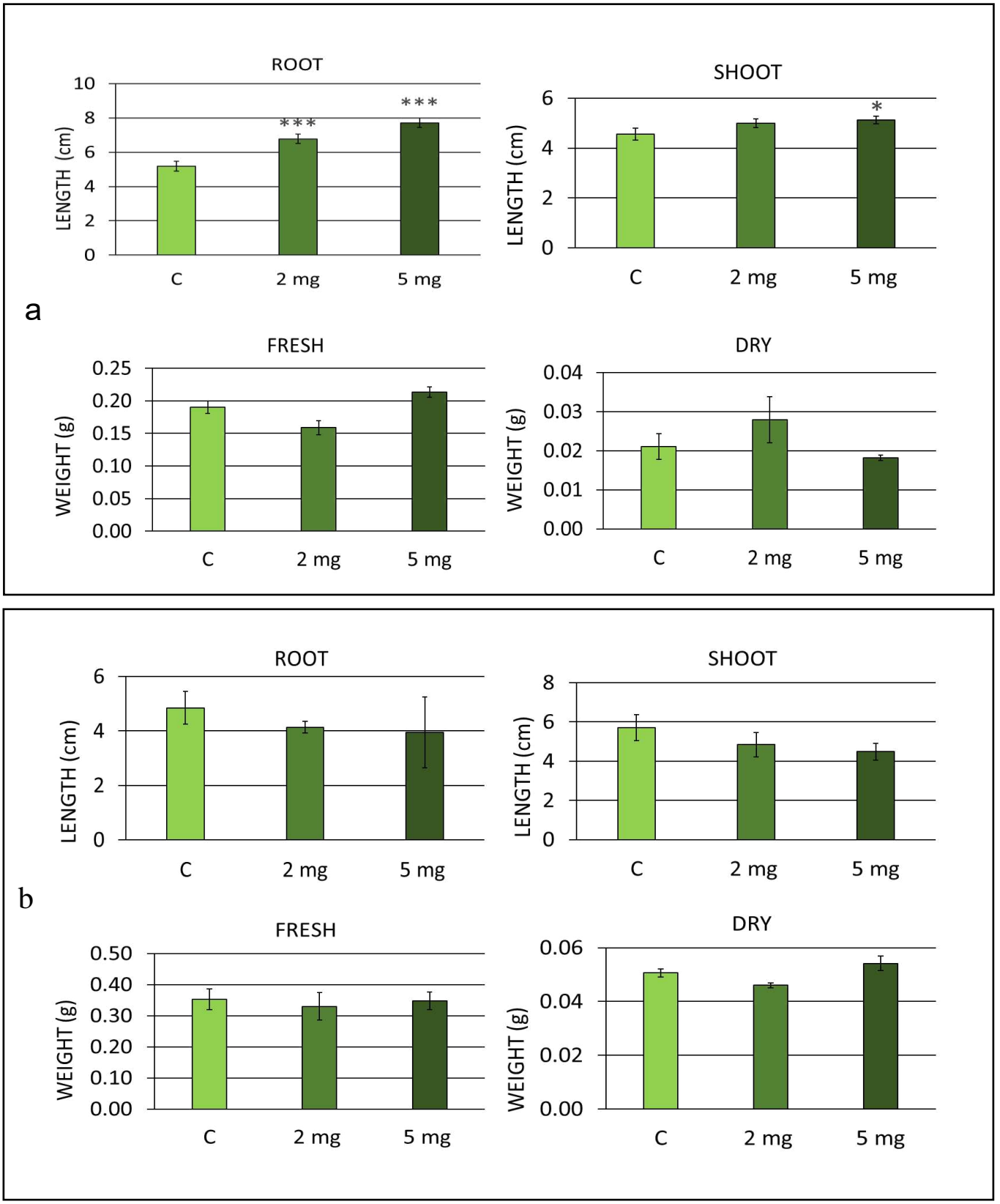

Figure 3. Biometric data of cucumber (a) and sunflower (b) seedlings grown in distilled water (control, C) and distilled water with 2 or 5 mg biochar. The vertical line on each bar represents the standard error (n = 3). The data were statistically analysed with ANOVA and the means of the treatments were compared to the control by the least significant differences test (LSD). *$P \leq 0.05$; *** $P \leq 0.001$.

Compared to the control (water only), cucumber seedlings grown in the presence of two different doses of biochar showed greater root elongation, while the height of the aerial part was significantly greater only at the highest dose of biochar (Figure 3a). No significant differences were observed in the fresh and dry weight of cucumber seedlings (Figure 3a). Differently, none of the biometric parameters of sunflower seedlings were significantly affected by any dose of biochar (Figure 3b).

Based on the measured parameters and the growth phase examined, it can be concluded that biochar did not exhibit inhibitory effects on the early growth of both plant species. The stimulatory action observed may be attributed to the nitrogen content of the biochar, including hydrolysable nitrogen, non-hydrolysable nitrogen, and water-soluble nitrogen (Hou et al. 2022). These findings are in line with those of Mumme et al. (2018) who reported no inhibitory effects of biochar on cress germination. Other studies documented positive effects of biochar on root and shoot elongation of various agricultural species (Olmo and Villar 2018; Öz 2018). A recent study by Parlavecchia et al. (2021) investigated the effects of different doses of biochar on lettuce and tomato seedlings. In that study, no toxicity was observed at any biochar dose, while stimulatory effects were reported for both plant species.

4.4 Conclusions

Biochar from the high-temperature gasification of a woody biomass showed alkaline pH, high C content, significant ash content and trace elements concentrations under the regulatory limits for safe application in agriculture. SEM analysis highlighted the presence of woody biomass structures typical of the original feedstock and the presence of abundant and widespread porosity. FTIR spectroscopy revealed the presence of functional groups typical of carbonaceous materials. BET analysis showed a large surface area and a mesoporous structure with pores of average width of a few nanometres. These properties, reasonably attributable to the high production temperature, contributed to the excellent adsorptive performance of biochar. Adsorption experiments demonstrated a remarkable capacity and rapidity of biochar to retain the fungicide BOS. Adsorption kinetics model data suggested that the interaction between biochar and BOS occurred through the formation of both chemical and physical bonds. The adsorption isotherm data were adequately described by the Freundlich model, indicating surface heterogeneity of the material and a multilayer adsorption of BOS. Desorption experiments demonstrated minimal release of the compound, indicating the ability of biochar to retain BOS for a long time. Furthermore, biochar showed high efficiency in immobilizing BOS and significantly reducing its leaching, thus mitigating the risk of groundwater contamination in vulnerable agricultural systems. In germination tests, biochar did not show inhibitory effects on young cucumber and sunflower plants, but rather a stimulating effect on

the growth of cucumber seedlings. Although this study is the first to consider multiple aspects of the behaviour of biochar in BOS-contaminated soil and on plants, it suffers from the limitations of examining a single pollutant. However, the overall results encourage the application of biochar to soil due to its contribution to controlling the bioavailability of hydrophobic pesticides, reducing their spread into the environment, particularly aquatic, and, in some cases, for its phytostimulant activity. Further evaluations of biochar performance at the field scale, in the rhizosphere compartment, and under conditions of multi-contamination of the soil are certainly needed.

References

Bhatt D, Srivastava A, Srivastava PC (2023). An insight into the sorption kinetics of boscalid onto soils: Effect of general soil properties. Chemosphere, 32, 138274. https://doi.org/10.1016/j.chemosphere.2023.138274

Brunauer S, Emmett PH, Teller E (1938). Adsorption of Gases in Multimolecular Layers. Journal of the American Chemical Society, 60, 309-319. http://dx.doi.org/10.1021/ja01269a023

Carnimeo C, Gelsomino A, Cirrottola G, Panuccio MR, Loffredo E (2022). Compost and vermicompost in cucumber rhizosphere promote plant growth and prevent the entry of anthropogenic organic pollutants. Scientia Horticulturae, 303, 111250. https://doi.org/10.1016/j.scienta.2022.111250

Colantoni A, Evic N, Lord R, Retschitzegger S, Proto AR, Gallucci F, Monarca D (2016). Characterization of biochars produced from pyrolysis of pelletized agricultural residues. In Renewable and Sustainable Energy Reviews, 64, 187–194 https://doi.org/10.1016/j.rser.2016.06.003

Colatorti N, Digregorio NV, Camposeo S, Loffredo E (2024). Solid fraction of digestate from olive pomace modulates abiotic and biotic processes in soil: Retention of agrochemicals and inhibition of fungal pathogens. Scientia Horticulturae, 337, 113545. https://doi.org/10.1016/j.scienta.2024.113545

Dugan ST, Muhammetoglu A, Uslu A (2023). A combined approach for the estimation of groundwater leaching potential and environmental impacts of pesticides for agricultural lands. Science of the Total Environment, 901, 165892. https://doi.org/10.1016/j.scitotenv.2023.165892

El-Naggar A, El-Naggar AH, Shaheen SM, Sarkar B, Chang SX, Tsang DCW et al. (2019). Biochar composition-dependent impacts on soil nutrient release, carbon mineralization, and potential

environmental risk: a review. J. Environ. Manag. 241, 458-467. https://doi.org/10.1016/j.jenvman.2019.02.044.

Gascó G, Cely P, Paz-Ferreiro J, Plaza C, Méndez A. (2016). Relation between biochar properties and effects on seed germination and plant development. Biological Agriculture & Horticulture, 32(4), 237–247. https://doi.org/10.1080/01448765.2016.1166348

Gautam RK, Goswami M, Mishra RK, Chaturvedi P, Awashthi MK, Singh RS, Giri, B.S., Pandey, A. (2021). Biochar for remediation of agrochemicals and synthetic organic dyes from environmental samples: A review. Chemosphere, 272, 129917. https://doi.org/10.1016/j.chemosphere.2021.129917

Ho YS (2006) Second-order kinetic model for the sorption of cadmium onto tree fern: a comparison of linear and non-linear methods. Water Research, 40, 119–125. https://doi.org/10.1016/j.watres.2005.10.040

Ho YS, McKay G (1999). Pseudo-second order model for sorption processes. Process Biochemistry, 34, 451-465. https://doi.org/10.1016/S0032-9592(98)00112-5

Hou J, Pugazhendhi A, Sindhu R, Vinayak V, Thanh NC, Brindhadevi K, Chi NTL, Yuan D. (2022). An assessment of biochar as a potential amendment to enhance plant nutrient uptake. Environmental Research, 214, Part 2, 113909. https://doi.org/10.1016/j.envres.2022.113909

Hung CY, Tsai WT, Chen JW, Lin YQ, Chang YM (2017). Characterization of biochar prepared from biogas digestate. Waste Management, 66, 53–60. https://doi.org/10.1016/j.wasman.2017.04.034

Jongbloed RH, Hulskotte, JHJ, Kempenaar C (2004). Contribution of agricultural and non-agricultural use of pesticides to the environmental impact on aquatic life in regional surface water systems. Water Science & Technology, 49 (3), 125-134. https://doi.org/10.2166/wst.2004.0178

Kumar A, Bhattacharya T, Shaikh WA, Chakraborty S, Owens G, Naushad M. (2022). Valorization of fruit waste-based biochar for arsenic removal in soils. Environmental Research, 213, 113710. https://doi.org/10.1016/j.envres. 2022.113710

Kumar KV (2006). Linear and non-linear regression analysis for the sorption kinetics of methylene blue onto activated carbon. Journal of Hazardous Materials, 137, 1538–1544. https://doi.org/10.1016/j.jhazmat.2006.04.036

Kumar KV, Sivanesan, S. (2006). Pseudo second order kinetic models for safranin onto rice husk: Comparison of linear and non-linear regression analysis. Process Biochemistry, 41, 1198-1202. https://doi.org/10.1016/j.procbio.2005.11.014

Lehmann J, Joseph S (2024) Biochar for environmental management: science, technology and implementation. 3rd edition, Earthscan, London. https://doi.org/10.4324/9781003297673

Leijenhorst EJ, Wolters W, van de Beld L, Prins W (2016). Inorganic element transfer from biomass to fast pyrolysis oil: Review and experiments. Fuel Processing Technology, 149, 96-111. https://doi.org/10.1016/j.fuproc.2016.03.026

Liu M, Lin Z, Ke X, Fan X, Joseph S, Taherymoosavi S, Liu X, Bian R, Solaiman ZM, Li L and Pan G (2021) Rice Seedling Growth Promotion by Biochar Varies With Genotypes and Application Dosages. Frontiers in Plant Science, 12, 580462. doi: 10.3389/fpls.2021.580462

Llovet A, Mattana S, Chin- Pampillo J, Gascò G, Sanchez S, Mondini C, Briones MJI, Marquez L, Alcaniz JM, Ribas A, Domene X (2021). Long-term effects of gasification biochar application on soil functions in a Mediterranean agroecosystem: Higher addition rates sequester more carbon but pose a risk to soil faunal communities. Science of The Total Environment, 801, 149580. https://doi.org/10.1016/j.scitotenv.2021.149580

Loffredo E, Carnimeo C, Silletti R, Summo C (2021a). Use of the Solid By-Product of Anaerobic Digestion of Biomass to Remove Anthropogenic Organic Pollutants with Endocrine Disruptive Activity. Environmental Processes, 9, 2018. https://doi.org/10.3390/pr9112018

Loffredo E, Picca G, Parlavecchia M (2021b). Single and combined use of Cannabis sativa L. and carbon-rich materials for the removal of pesticides and endocrine-disrupting chemicals from water and soil. Environmental Science and Pollution Research, 28, 3601-3616. https://doi.org/10.1007/s11356-020-10690-7

Loffredo E, Taskin E (2017). Adsorptive removal of ascertained and suspected endocrine disruptors from aqueous solution using plant-derived materials. Environmental Science and Pollution Research, 24, 19159–19166 https://doi.org/10.1007/s11356-017-9595-z

Lowell S, Shields JE, Thomas MA, Thommes M (2006). Characterization of Porous Solids and Powders: Surface Area, Pore Size and Density. Springer, Dordrecht, the Netherlands

Marsh H, Rodriguez-Reinoso F (2006). Activated Carbon. Elsevier Science & Technology Books, 536 p.

Mohan D, Sarswat A, Ok YS, Pittman Jr CU (2014). Organic and inorganic contaminants removal from water with biochar, a renewable, low cost and sustainable adsorbent e a critical review. Bioresource Technolology 160, 191-202. https://doi.org/10.1016/j.biortech.2014.01.120

Moreno JL, Bastida F, Díaz-López M, Li Y, Zhou Y, López-Mondéjar R, Benavente-Ferraces I, Rojas R, Rey A, Carlos García-Gil J, Plaza C (2022). Response of soil chemical properties, enzyme activities and microbial communities to biochar application and climate change in a Mediterranean agroecosystem. Geoderma, 407, 115536, https://doi.org/10.1016/j.geoderma.2021.115536

Mukome FND, Parikh SJ (2016). Chemical, physical, and surface characterization of biochar. In: Ok YK, Uchimiya SM, Chang SX, Bolan N (eds) Biochar: production, characterization, and applications. CRC Press, Boca Raton, pp 67–96. https://doi.org/10.1201/b18920

Mumme J, Getz J, Prasad M, Luder U, Kern J, Masek O, Buss W. (2018). Toxicity screening of biochar-mineral composites using germination tests. Chemosphere, 207, 91-100. https://doi.org/10.1016/j.chemosphere. 2018.05.042

Nandi R, Sarker A, Rana MM, Hasan AK (2025). Influence of Organic Matter and Growing Conditions on Dissipation Behavior and Mobility of Two Pesticides in Soils. Environments, 12, 123. https://doi.org/10.3390/environments12040123

Negi S, Srivastava A, Pachauri SP, Pathak A, Srivastava PC (2024). Modulating Leaching Behavior of Boscalid Fungicide in Soil Through Organic Amendments. Soil and Sediment Contamination: An International Journal, 34(1), 71–84. https://doi.org/10.1080/15320383.2024.2329965

Nkoh JN, Ajibade FO, Atakpa EO, Baquy MAA, Mia S, Odii EC, Xu R (2022). Reduction of heavy metal uptake from polluted soils and associated health risks through biochar amendment: A critical synthesis. Journal of Hazardous Materials Advances, 6, 100086. https://doi.org/10.1016/j.hazadv .2022.100086

Olmo M, Villar R (2018). Changes in root traits explain the variability of biochar effects on fruit production in eight agronomic species. Organic Agriculture, 9, 139-153. https://link.springer.com/article/10.1007/s13165-018-0217-y

Oz H (2018). A new approach to soil solarization: addition of biochar to the effect of soil temperature and quality and yield parameters of lettuce (Lactuca sativa L. Duna.). Scientia Horticulturae, 228, 153–161 https://doi.org/10.1016/ j.scienta.2017.10.021.

Parlavecchia M, Carnimeo C, Loffredo E (2020). Soil amendment with biochar, hydrochar and compost mitigates the accumulation of emerging pollutants in rocket salad plants. Water Air Soil Pollution, 231, 554. https://doi.org/10.1007/s11270-020-04915-1

Parlavecchia M, D'orazio V, Loffredo E (2019). Wood biochars and vermicomposts from digestate modulate the extent of adsorption-desorption of the fungicide metalaxyl-m in a silty soil.

Environmental Science and Pollution Research, 26, 35924–35934. https://doi.org10.1007/s11356-019-06729-z

Parlavecchia M, Gattullo R, Perri G, Loffredo E (2021). Modulatory effects of biochar, hydrochar and vermicompost on the growth of horticultural plants and phytopathogenic fungi. Acta Horticulturae, 1311, 541-548. https://doi.org/10.17660/ ActaHortic.2021.1311.69

Pérez-Lucas G, El Aatik A, Vela N, Fenoll J, Simón Navarro S (2020). Exogenous organic matter as strategy to reduce pesticide leaching through the soil. Archives of Agronomy and Soil Science, 67 (7),934-945 https://doi.org/10.1080/03650340.2020.1768531

PubChem (2025). Open chemistry database at the National Institutes of Health (NIH), U. S. National Library of Medicine. Available online: https://pubchem.ncbi.nlm.nih.gov/compound/Boscalid#section=Chemical-and-Physical-Properties. Accessed 03 June 2025

Qian K, Kumar A, Patil K, Bellmer D, Wang D, Yuan W, Huhnke RL (2013). Effects of biomass feedstocks and gasification conditions on the physiochemical properties of char. Energies, 6, 3972-3986. DOI: 10.3390/en6083972

Qian K, Kumar A, Zhang H, Bellmer D, Huhnke R. Recent advances in utilization of biochar (2015). Renewable and Sustainable Energy Reviews, 42, 1055-1064. https://doi.org/10.1016/j.rser.2014.10.074

Revellame ED, Fortela DL, Sharp W, Hernandez R, Zappi ME (2020). Adsorption kinetic modeling using pseudo-first order and pseudo-second order rate laws: A review. Cleaner Engineering and Technology, 1, 100032. https://doi.org/ 10.1016/j.clet.2020.100032

Rodriguez-Liebana JA, Mingorance MD, Pena A (2014). Pesticide mobility and leachate toxicity in two abandoned mine soils. Effect of organic amendments. Science of The Total Environment, 497-498, 561-569. https://doi.org/10.1016/j.scitotenv.2014.08.010

Rouquerol R, Rouquerol F, Llewellyn F, Maurin G, Sing K (2013). Adsorption by Powders and Porous Solids. Principles, Methodology and Applications 2nd Edition. Hardback ISBN: 9780080970356, eBook ISBN: 9780080970363

Shakya A, Vithanage M, Agarwal T (2022). Influence of pyrolysis temperature on biochar properties and Cr(VI) adsorption from water with groundnut shell biochars: Mechanistic approach. Environmental Research, 215, Part 1, 114243 https://doi.org/10.1016/j.envres.2022.114243

Stylianou M, Christou A, Micheal C, Agapiou A, Papanastasiou P, Fatta-Kassinos D (2021). Adsorption and removal of seven antibiotic compounds present in water with the use of biochar derived from the pyrolysis of organic waste feedstocks. Journal of Environmental Chemical Engineering, 9, 105868. https://doi.org/10.1016/j.jece.2021.105868

Taha SM, Amer ME, Elmarsafy AE, Elkady MY (2014). Adsorption of 15 different pesticides on untreated and phosphoric acid treated biochar and charcoal from water. Journal of Environmental Chemical Engineering, 2, 2013-2025 https://doi.org/10.1016/j.jece.2014.09.001

Tang J, Zhu W, Kookana R, Katayama A. (2013). Characteristics of biochar and its application in remediation of contaminated soil. Journal of Bioscience and Bioengineering, 116, 653-659. https://doi.org/10.1016/j.jbiosc.2013.05.035

Taskin E, Bueno CDC, Allegretta I, Terzano R, Rosa AH, Loffredo E (2019). Multianalytical characterization of biochar and hydrochar produced from waste biomasses for environmental and agricultural applications. Chemosphere, 233, 422–430. https://doi.org/10.1016/j.chemosphere.2019.05.204

Tsai WT, Fang YY, Cheng PH, Lin YQ (2018). Characterization of mesoporous biochar produced from biogas digestate implemented in an anaerobic process of large-scale hog farm. Biomass Conversion and Biorefinery, 8 (4), 945–951. https://doi.org/10.1007/s13399-018-0344-4

Wang J, Xiong G, Kuzyakov Y (2015). Biochar stability in soil: meta-analysis of decomposition and priming effects. Global Change Biology Bioenergy, 8, 512-523. https://doi.org/10.1111/gcbb.12266

Wang M, Cai H, Qiao Q, Zhang J (2022). Characterization techniques application on pesticide adsorption mechanism research of corn straw biochar based on KOH thermal activation. Hindawi, 2022, 3389112 https://doi.org/10.1155/2022/3389112

Yang W, Wang Z, Song S, Han J, Chen H, Wang X, Sun R, Cheng J (2019). Adsorption of copper(II) and lead(II) from seawater using hydrothermal biochar derived from Enteromorpha. Marine Pollution Bulletin, 149, 110586. https://doi.org/10.1016/j.marpolbul.2019.110586

Supplementary materials

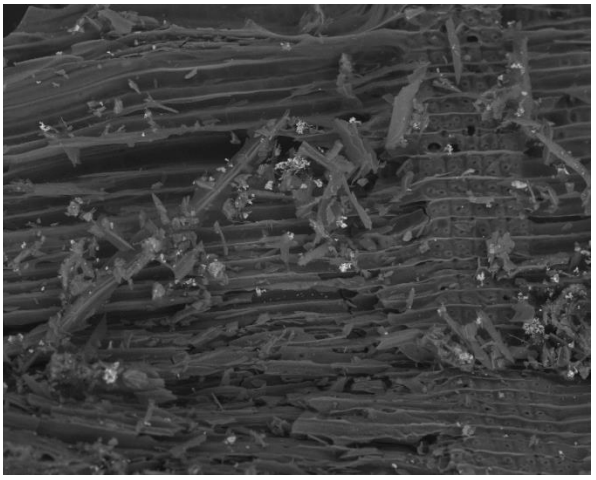

5k magnification

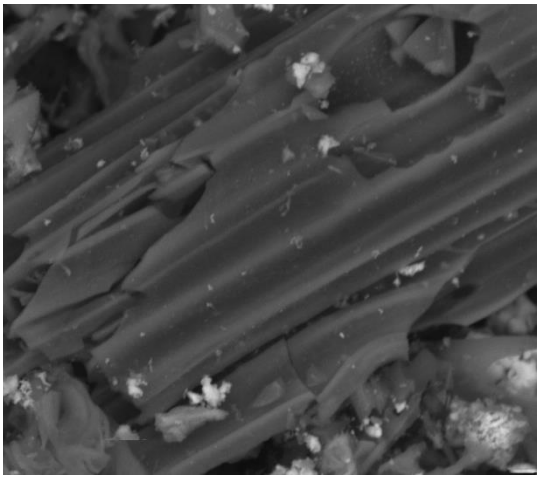

5k magnification

Figure S1. SEM images of biochar

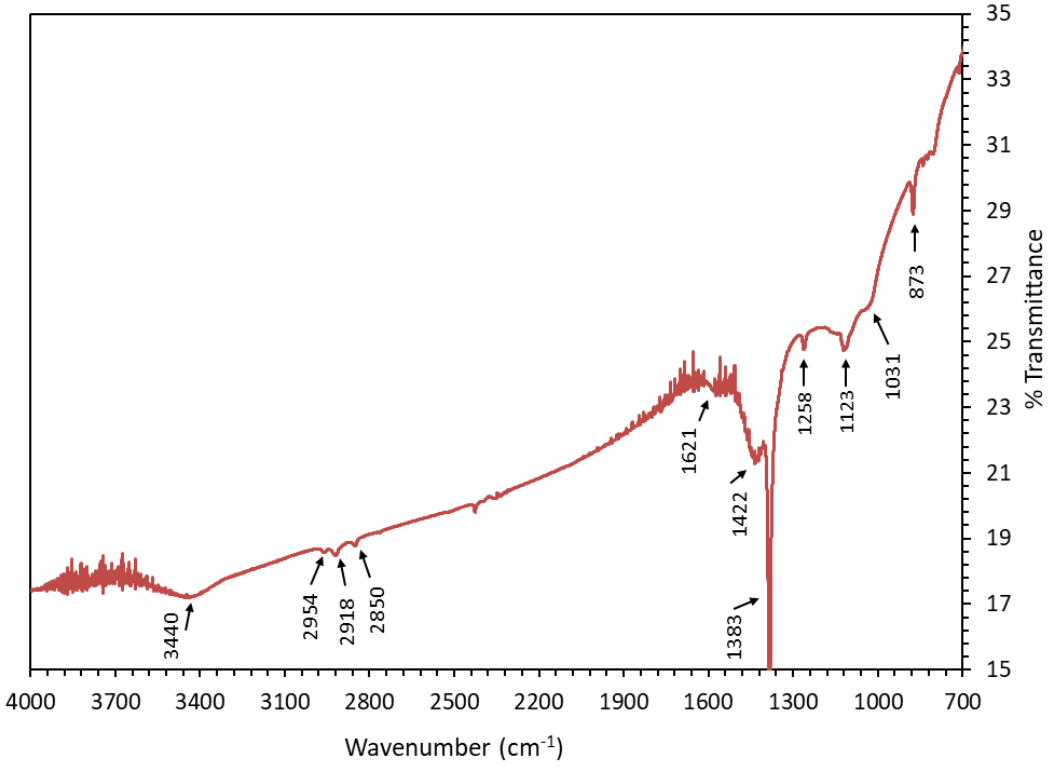

Figure S2. FTIR spectrum of biochar.

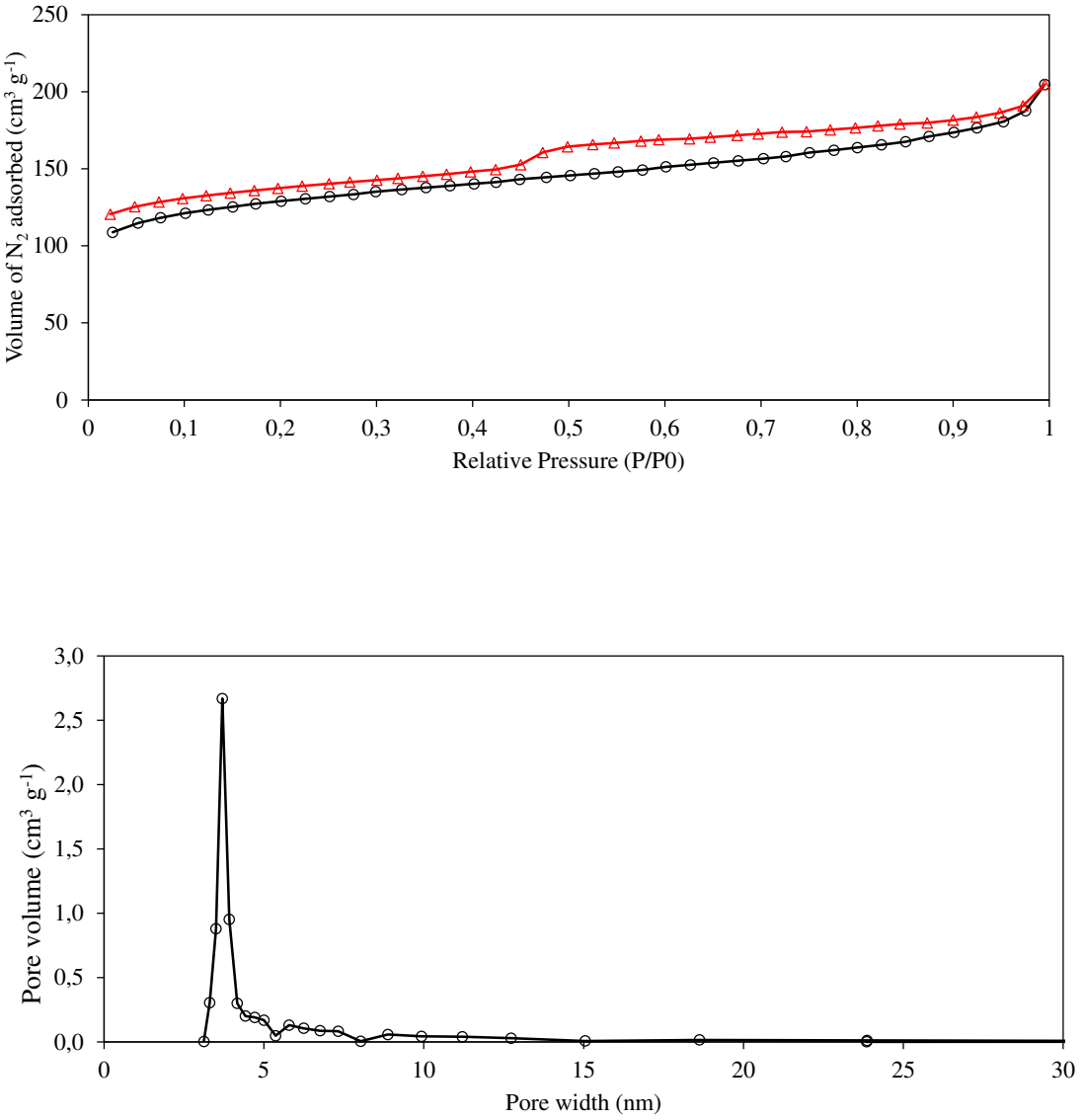

Figure S3. N_2 adsorption-desorption isotherms (a) and pore size distribution of biochar (b).

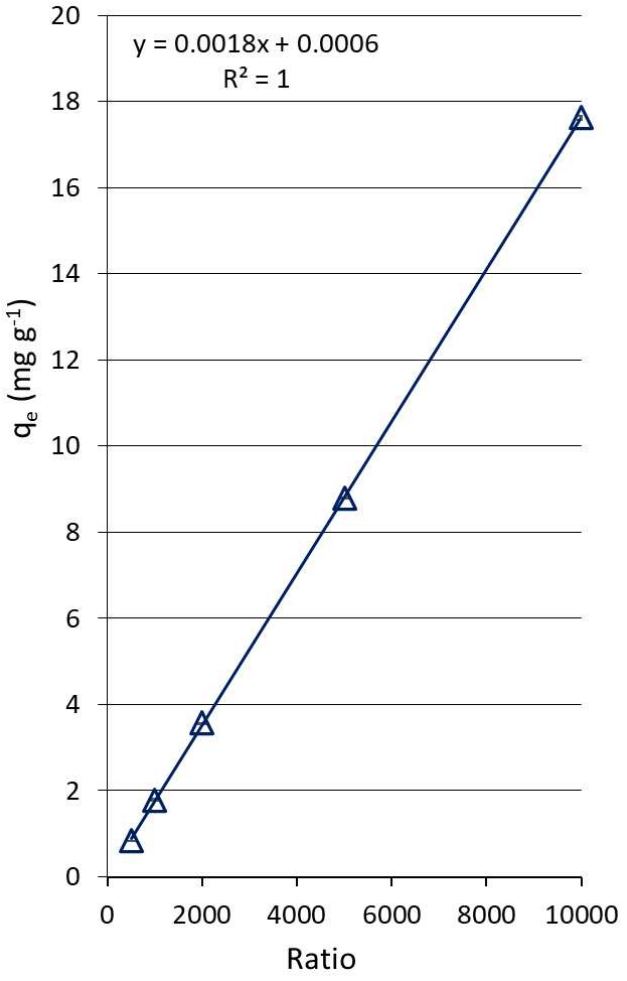

Figure S4. Relationship between solution:biochar ratio and the concentration of the adsorbed boscalid at equilibrium

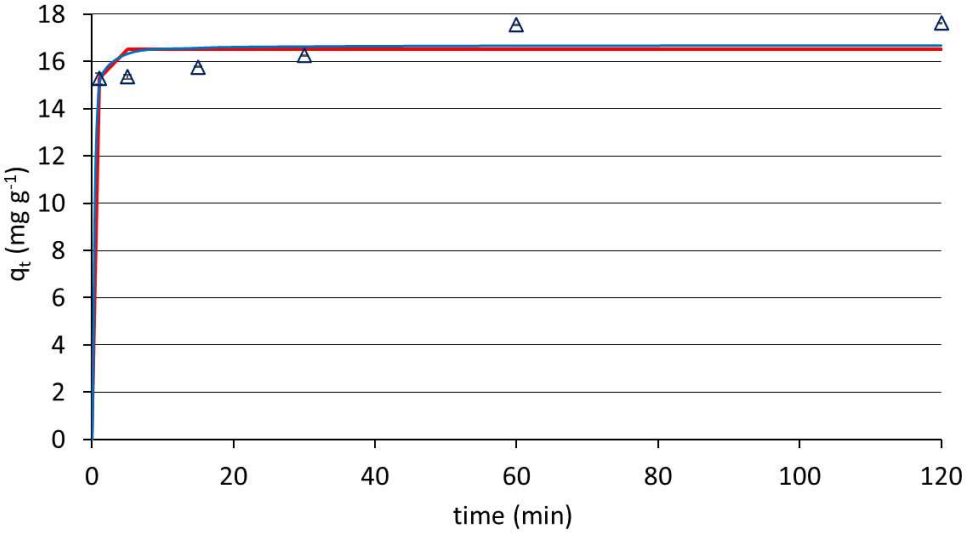

Figure S5. Adsorption kinetics data and plots of predicted PFO (red line) and PSO (blue line) kinetics of boscalid onto biochar. Standard error is reported as vertical bar on each point (n = 3)

Table S1. Some properties of boscalid

Compound	Chemical structure	Molecular formula	Molecular weight (g mol^{-1})	Water solubility (mg L^{-1}) at 20 °C	Log K_{ow}
Boscalid	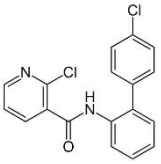	$C_{18}H_{12}Cl_2N_2O$	343.2	4.6	2.96

Data from Pubchem (2025)

CHAPTER - 5
EVALUATION OF SPENT FUNGAL SUBSTRATE AND WHEAT STRAW AS BIOSORBENTS OF AGROCHEMICALS

Abstract

The increasing use of agrochemicals in agriculture raises concern about their persistence and mobility in the environment, thus highlighting the need for sustainable and low-cost remediation strategies. This study evaluated the adsorption capacity of spent fungal growth substrate (SFGS) of the fungus *Pleurotus eryngii* and, comparatively, ground wheat straw (GWS) for the removal of two widely used agrochemicals, the fungicide metalaxyl-M (MET) and the herbicide cycloxydim (CYC), from aqueous solutions. Both materials were characterized for their physicochemical properties and tested through adsorption kinetics and equilibrium isotherm experiments.

The adsorption study conducted in batch showed that both SFGS and GWS were effective in removing both the compounds, with SFGS significantly exceeding the capacity of GWS. SFGS exhibited faster adsorption kinetics, the adsorption equilibrium is reached in 16 h compared with 24 h for GWS. Kinetic data were best described by the pseudo-second-order model, suggesting that chemisorption played a major role in agrochemical retention. SFGS also showed higher adsorption capacities for both MET and CYC, with respect to GWS. Adsorption isotherm data were best fitted by the Freundlich model, indicating heterogeneous surface of the material and multilayer adsorption.

The better performance of SFGS may be attributed to fungal-induced modification of the lignocellulosic matrix, resulting in increased porosity, surface heterogeneity, and functional groups. The overall results obtained demonstrated the potential of spent *P. eryngii* substrate to act as a promising, sustainable and low-cost biosorbent of agrochemical residues in water, supporting circular economy approaches for agricultural residues reuse

5.1 Introduction

In 2023, the global use of agrochemicals reached approximately 4 million tons of active ingredients (FAOSTAT 2023). This large use highlights the current importance of agrochemicals in conventional agriculture, in particular intensive and super intensive agriculture, especially under the pressure of climate variability and continuous world population growth (Fazli et al. 2025). Although agrochemicals play a key role in protecting crops against pests and pathogens, their widespread and

repeated application generates considerable concern among the population. These compounds can migrate into soil and water systems and affect non-target organisms, causing ecological imbalance and posing risks to human health (Wan et al. 2025). Agrochemical residues may accumulate in soil and in plants throughout the cultivation and storage phases of agricultural commodities (Gad et al. 2025).

Metalaxyl-M (MET) and cycloxydim (CYC) are two widely used agrochemicals in the mediterranean area. MET [*N*-(2,6-Dimethylphenyl)-*N*-(methoxyacetyl)-D-alanine methyl ester] is a systemic fungicide belonging to the phenylamide class. Placed on the market in 1977, MET is used to control *Oomycota* pathogens on tomato, potato, hop, tobacco, grape, and other crops. This fungicide acts as interferent of protein synthesis by inhibiting incorporation of ribonucleoside triphosphate into ribosomal RNA (Jing et al. 2016). CYC [(2-[1-(ethoxyimino)butyl]-3-hydroxy-5-(tetrahydro-2*H*-thiopyran-3-yl)-2-cyclohexen-1-one] is a systemic herbicide belonging to the cyclohexanedione oxime group. This herbicide, which is used for the control of grass weeds of many agricultural and horticultural broad-leaved crops, inhibits the acetylcoenzyme A carboxylase in chloroplasts of sensitive weeds (Monadjemi et al. 2012)

The use of residual biomasses as low-cost adsorbent materials has gained increasing attention in recent years as a promising strategy for the removal of organic contaminants from aqueous matrices and soil (Sharma et al. 2024). This approach aligns with the principles of circular economy and sustainable resource management, as it enables the valorisation of agricultural and agro-industrial waste that would otherwise require disposal or low-value uses. Converting such residues into functional materials for environmental remediation not only reduces waste streams but also provides cost-effective alternatives to conventional adsorbents, such as activated carbon, whose production and regeneration can be very demanding from an economic and energy perspective (Erdem & Oner 2025).

Among the wide range of currently studied lignocellulosic residues, SFGS derived from edible mushroom cultivation represents a particularly attractive candidate (Sahithya et al. 2022). These materials are typically available in large quantities, are renewable, biodegradable, and often require minimal pre-treatment before use. Their physicochemical characteristics, including high surface heterogeneity, porous structure, and the abundance of functional groups such as hydroxyl, carboxyl, phenolic, and amino moieties, make them suitable for interacting with a broad spectrum of organic and inorganic pollutants (Zhou et al. 2020).

Of particular interest is the SFGS originated from *Pleurotus eryngii* cultivation. This fungus, commonly named king oyster, is one of the most common and cultivated edible mushrooms in

southern Italy, being easy and inexpensive to produce (Melanuouri et al. 2019). The SFGS used for *P. eryngii* cultivation consists of wheat straw, remains of fungal mycelium, and small amounts of spent beet pulp. Chemically, this substrate is composed of lignin, cellulose and hemicellulose which are degraded by the fungus during its growth and used as carbon and energy sources. This fungus prefers woody, lignin-rich substrates and has low nitrogen requirements compared to other fungi such as *Agaricus bisporus*; therefore, its cultivation does not require the addition of substrates such as manure and pollen. Fungal degradation of this matrix results in the formation of extensive porosity which makes the substrate suitable for adsorption (Kulshreshtha et al. 2019). To study the contribution of *P. eryngii* mycelium to the SFGS adsorbent capacity, analytical data collected for this latter material were compared with those of GWS alone. Wheat straw, one of the most common agricultural residues worldwide, is also frequently studied as a reference lignocellulosic sorbent due to its known composition and widespread availability, making it an ideal benchmark material for comparative adsorption studies (Dang et al. 2008).

In light of the above, the main objective of this study was to evaluate the effectiveness of SFGS from *P.eryngii* cultivation and GWS to act as natural adsorbents of two agrochemicals, namely MET and CYC. from water. Quantitative data were obtained from adsorption kinetics and adsorption isotherms study. Furthermore, to relate the sorption capacity of these materials to their properties and structure, a preliminary extensive characterization was carried out.

5.2 Materials and methods

5.2.1 Chemicals and adsorbents

MET (Figure 1) with purity ≥ 98.0%, molecular mass of 279.33 g mol^{-1}, and water solubility of 8400 mg L^{-1}, (National Center for Biotechnology Information) and CYC (Figure 1) with purity ≥ 95.0%, molecular mass of 325.47 g mol^{-1}, and water solubility of 53 mg L^{-1} (Lewis et al. 2016) (were purchased from Merck KGaA, Darmstadt, Germany). The SFGS sample was supplied by Fungo Puglia s.c.a.r.l., Rutigliano, Italy, while GWS was collected from the agricultural company Denora s.s. located in Altamura, Italy. Before the experiments, the two samples were dried at a temperature of 40 °C for 48 h and finally ground to < 2 mm particles.

Figure 1. Chemical structure of metalaxyl-M (A) and cycloxidim (B).

The physico-chemical properties of these materials were determined using conventional methods and are reported in Table 1. Nutrients and trace elements of the two adsorbents were analyzed by inductively coupled plasma optical emission spectrometry (ICP-OES; Agilent 5800). The following emission wavelengths were used for element quantification (nm): B, 249.77; Na, 589.59; Mg, 280.27; P, 213.62; K, 766.49; Ca, 422.67; Mn, 257.61; Fe, 259.94; Cu, 324.75 and Zn, 213.85. A calibration curve was obtained using the blank solution as zero point and a multi-element calibration standard (Certipur® ICP Multi-element standard solution IV, Merck KGaA, Darmstadt, Germany) at the concentration of 2 mg L^{-1} and 10 mg L^{-1}. In addition to blank solution, P calibration was specifically performed using a specific standard solution for ICP-OES (Carlo Erba, Milano, Italy) at 2 and 10 mg L^{-1}. Macronutrients were measured after diluting the samples at 1:25 (v/v) with deionized water. The instrumental quality check was done by measuring the multi-element standard every ten samples (Allegretta et al. 2022). We determined the carbon and nitrogen mass percentage content of biomass samples by combustion elemental analysis. The elemental analyzer Vario PyroCUBE (Elementar Analysensysteme GmbH, Langenselbold, Germany) was used, with high purity He carrier gas (230 mL/min, 1.5 bar) and Thermal Conductivity Detector (TCD), and with Advanced Purge and Trap (APT) technology for combustion gas separation and focalization. The instrument settings were in CNS configuration, involving a combustion column based on WO_3 catalyst and a reduction tube column based on metal Cu catalyst. The analysis of each sample (2 replicates) consisted in the complete combustion of 5.0±0.5 mg of dried powder contained in a hand-closed tin capsule boat, thanks to a 90 s duration of high-purity oxygen gas injection, and lasted around 15 min. The verification of the instrument performances and of the analysis results reliability and accuracy was determined by analysing Sulfanilamide standard (Elementar Analysensysteme GmbH, Langenselbold, Germany) capsules (5.0±0.5 mg).

Table 1. Properties of SFGS and GWS

Parameter	SFGS	GWS
Moisture (%)	7.02 ± 0.03	4.91 ± 0.61
pH[a]	5.60 ± 0.03[b]	6.31 ± 0. 01
EC[a] (dS m^{-1})	5.46 ± 0.15	2.67 ± 0.09
TOC (%)	37.42 ± 0.00	45.52 ± 0.09
TN (%)	1.85 ± 0.05	0.86 ± 0.06
S (%)	0.40 ± 0.07	0.33 ± 0.05
Na (mg kg^{-1})	59.36 ± 3.25	21.14 ± 0.53
Mg (mg kg^{-1})	1846 ± 24.78	519 ± 1.94
P (mg kg^{-1})	1280 ± 17.82	118 ± 13.94
K (mg kg^{-1})	11672 ± 129	6053 ± 27.49
Ca (mg kg^{-1})	28585 ± 298	302 ± 16.25
B (mg kg^{-1})	0.65 ± 0.21	1.78 ± 0.74
Mn (mg kg^{-1})	198 ± 1.81	18.99 ± 0.47
Fe (mg kg^{-1})	17848 ± 329	734 ± 130
Cu (mg kg^{-1})	9.43 ± 0.72	3.93 ± 0.00
Zn (mg kg^{-1})	41.06 ± 14.39	43.93 ± 22.49

Data are given in mean ± standard deviation. Elemental concentration are expressed on dry weight.
[a] adsorbent/doble distilled H_2O, 1:10 (w/v); [b] SD (n = 3); TOC: total organic carbon; TN: total nitrogen

5.2.2 Adsorption experiments

The adsorption study was carried out performing adsorption kinetics and adsorption isotherms. The adsorption kinetics allows to evaluate the rate at which a solute is retained on a substrate over time and provides useful information on the nature of the interactions occurring between the adsorbent and the solute, also referred to as the adsorbate.

In the adsorption kinetic study, the rate of adsorption of two pesticides, namely MET and CYC, on SFGS and GWS was evaluated. To investigate the role of fungal biomass, the adsorption capacity of SFGS was compared with that of GWS. Then, a volume of 20 mL of aqueous mixed solution of MET and CYC at a concentration of 2 mg L^{-1} each was added to 40 mg of each biosorbents in corex glass centrifuge tubes and mechanically shaken in the dark at room temperature at 500 rpm for 0.17, 0.25, 0.5, 1, 2, 4, 16, 24, and 40 h. After each experimental time, the suspension was centrifuged at 10,000 *g* at 10 °C for 10 minutes. All experiments were performed in triplicate. Compound quantification was carried out by high performance liquid chromatography (HPLC) as described in section 5.2.3.

The amount of compound adsorbed on the substrate at time t, qt (mg kg^{-1}), was calculated using the equation $qt = (C_0 - C_t)\ V/m$, where C_0 (mg L^{-1}) is the initial concentration of the compound in solution, C_t (mg L^{-1}) is the concentration at time t, V (L) is the solution volume, and m (kg) is the mass of the substrate. The adsorption equilibrium time was determined using Student's t-test by statistically comparing ($P \leq 0.05$) the amounts adsorbed at each sampling time. Equilibrium time was established when no significant difference was observed between two consecutive samplings. To investigate the adsorption mechanism of the molecules on the adsorbents, the experimental kinetic data were interpreted using the pseudo-first-order (Kumar, 2006) and the pseudo-second-order (Ho, 2006) models.

Adsorption isotherms quantitatively describe the interaction between an adsorbent material and a sorbate at constant temperature. They allow the determination of key adsorption parameters, such as the adsorption constant and the maximum adsorption capacity, and provide insight into how the sorbate is distributed among the available adsorption sites.

To perform adsorption isotherms, 40 mg of substrate (spent fungal substrate and straw) was interacted with 20 mL of an aqueous mixture of MET and CYC at concentrations of 0.1, 0.2, 0.4, 0.5, 1, and 2 mg L^{-1} for 24 h. Subsequently, the samples were centrifuged and analyzed using the method described for the kinetics study. All experiments were performed in triplicate. To find the best suitable model to describe the sorption process of the two agrochemicals, adsorption isotherms data were fitted in the two non-linear equations of Freundlich and Langmuir and in the linear Henry model.

5.2.3 HPLC Analysis

Before HPLC analysis, samples were filtered through 0.45 µm Millipore™ cellulose acetate membrane filters. Chromatographic determinations were carried out using a Shimadzu Nexera series system (Kyoto, Japan) consisting of an LC-40D XR pump, a SIL-40C XR autosampler, and a CTO-40 °C thermostated column oven, and a Shimadzu Shim-pack GIST-HP C18 column (150 mm × 3 mm × 3 µm). The mobile phase was water/acetonitrile (40/60, v/v) which flowed at 0.6 mL min^{-1}. The retention times of MET and CYC were 2.35 and 3.40 min, respectively. The two compounds were detected using an SPD-M40 diode array detector at wavelengths of 210 and 249 nm, respectively.

5.3 Results and discussion

5.3.2 Adsorption experiments

According to the adsorption kinetic curves obtained (Figure 2), the *P. eryngii* SFGS showed a higher adsorption capacity than GWS for both molecules. In particular, the fungal substrate exhibited a faster adsorption of the compounds, which reached equilibrium after 16 h, compared with the 24 h required for GWS. The shorter time required for compounds retention suggests that fungal colonization and the resulting modification of the lignocellulosic matrix increased the number of accessible adsorption sites or enhanced the affinity of the molecules for the substrate. Fungal activity is also known to alter the surface chemistry of the material by introducing or exposing oxygen-containing functional groups, such as hydroxyl (–OH) and carboxyl (–COOH) groups. These changes can enhance the interaction with polar contaminants through hydrogen bonding and electrostatic interactions. At the same time, the partial degradation of lignin may modify the distribution of aromatic domains, potentially influencing interactions with organic compounds via hydrophobic and π–π mechanisms. Wu et al. (2019) demonstrated the rapid adsorption of three dyes on *P. eryngii* SFGS. The kinetic curves also highlighted how adsorption is a three-step process. The first step is the external diffusion, during which the adsorbate transfers through the liquid film around the adsorbent. The different concentrations occurring between the bulk solution and the adsorbent surface is the driving force of the external diffusion. The second step is the internal diffusion, that describes the diffusion of the adsorbate in the pores of the adsorbent. The third step is the adsorption of the adsorbate in the active sites of the adsorbent (Wang &Guo 2020).

At equilibrium, the amounts of MET and CYC retained by SFGS of *P. eryngii* were approximately 165 and 392 mg kg^{-1}, respectively, whereas values of 159 and 239 mg kg^{-1} were observed for GWS (Table 2). The curve fitting of the kinetics data for each compound adopted the PFO and PSO models with nonlinear regression. A better fit to the experimental data was attained with the PSO equation because it resulted in higher values of the correlation coefficients (r) and lower values of the sum of squares of the residuals (SSR) (Figure 2).

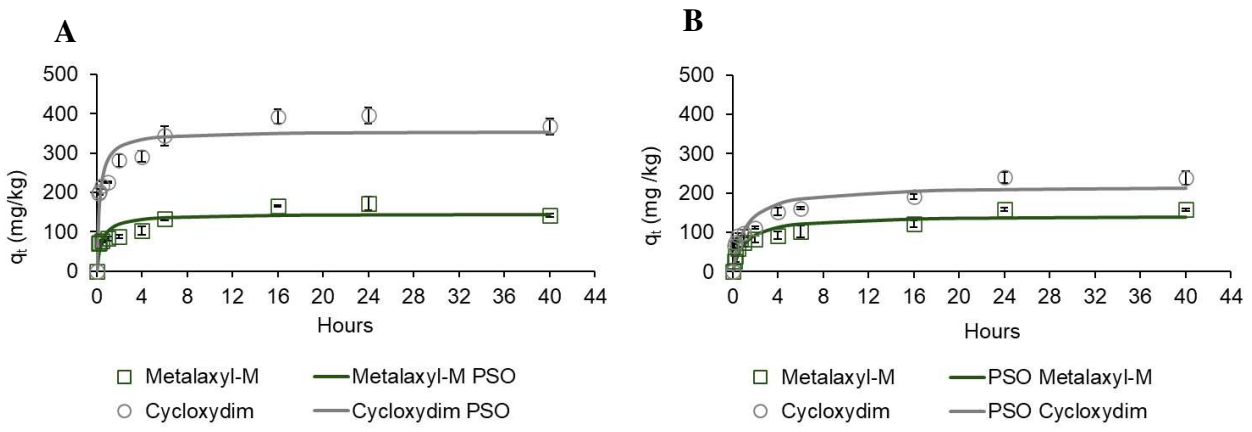

Figure 2. Adsorption kinetics of the two compounds on SFGS of *P. eryngii* (A) and GWS (B). Points represent experimental data, while the line is the PSO plot. The vertical line on each point indicates the standard errors (n=3).

Table 2. Parameters of adsorption kinetic models of MET and CYC on SFGS and GWS

	Theoretical models								
		Pseudo-First Order				**Pseudo-Second Order**			
Parameter	$q_{e,exp}$ (mg kg^{-1})	r	SSR	$q_{e,1}$ (mg g^{-1})	k_1 (h^{-1})	r	SSR	$q_{e,2}$ (mg kg^{-1})	k_2 (kg mg^{-1} h^{-1})
SFGS									
MET	172	0.779	7889	132	1.99	0.856	4804	145	0.016
CYC	396	0.797	27784	332	3.10	0.89	14260	356	0.011
GWS									
MET	159	0.903	4513	128	0.77	0.945	2333	143	0.007
CYC	239	0.908	11604	203	0.60	0.936	6435	218	0.004

The PFO model generally describes physisorption processes, where adsorption is governed by diffusion and weak interactions between sorbate and sorbent. In contrast, the PSO model assumes that chemisorption is the rate-limiting step, involving stronger interactions such as valence forces, electron sharing, or exchange between the adsorbent and the adsorbate.

In this study, as reported above, the PSO model provided a better fit to the experimental data. This suggests that the adsorption process is predominantly controlled by chemisorption mechanisms (Loffredo, 2022). In particular, the lignocellulosic fraction of the biosorbents likely interacted with

the target molecules through a combination of mechanisms, including hydrogen bonding, van der Waals forces, and stronger ionic or covalent interactions. Functional groups such as amino ($-NH_2$), carboxyl (-COOH), and hydroxyl (-OH) groups play a key role in these interactions, with their relative abundance influencing the overall sorption behavior.

These findings are consistent with previous studies, which have shown that the PSO model often provides the best fit for the adsorption kinetics of organic contaminants onto untreated biosorbents (Ofomaja, 2011; Papadaki et al., 2021).

The adsorption isotherm study confirmed the higher adsorption capacity of SFGS compared to GWS. The r and SSR values calculated for both molecules on the two materials indicated that experimental adsorption isotherm data were best described by the Freundlich equation (Figure 3). Marin-Benito et al. (2012) also found that MET adsorption on SFGS of *P. Eryngii* was better described by the Freundlich model. The Freundlich model describes a heterogeneous surface characterized by an exponential distribution of adsorption sites and their associated energies. The adsorption capacity of MET on SFGS observed in this study, quantified by the Freundlich constant (K_F) value, was of 123 mg kg^{-1}, while the K_F of this molecule on GWS was of 89 mg kg^{-1}. Using different fungal substrates to retain MET, Marin-Benito et al. (2012) reported K_F values lower than that found in this study. The K_F values of CYC was 210 and 139 mg kg^{-1} for SFGS and GWS, respectively (Table 3). As far as we know, no adsorption studies have been performed on this molecule. Alhujaily et al. (2018) studied the adsorption of several dyes on SFGS and reported adsorption constant values similar to those obtained in the present study.

Another Freundlich constant is “n” that indicates the intensity of adsorption. “1/n” indicates the degree of nonlinearity between the concentration in solution and the adsorbed quantity. Based on the parameter 1/n, adsorption of MET was C-type (1/n~1), whereas that of CYC was S-type (1/n >1). The Giles classification of adsorption isotherms relates to the shape of the sorption curve, in particular the slope of the initial portion of the curve, and is valid for both homogeneous and heterogeneous adsorption surfaces of the adsorbent (Giles et al. 1960). The S-type (sigmoidal shape) isotherm of Giles indicates the vertical orientation of the solute on the reactive sites of the adsorbent, and occurs when, as adsorption proceeds, it is increasingly easier for the solute molecules to find available sites on the absorbent; it is termed ‘cooperative adsorption’. The C-type isotherm can be represented as a straight line and indicates that a proportional distribution of solute molecules occurs between the adsorbent and the solution. In the C-curve, the availability of sorption sites remains constant at all solute concentration up to saturation. Hence, the parameter 1/n is related to the strength and feasibility of adsorption, while the reciprocal n is the heterogeneity factor. When

1/n < 1 the process is predominantly physical, it is mainly chemical when 1/n > 1, and linear when 1/n = 1. The 1/n value of CYC suggested the prevalent occurrence of chemisorption, the 1/n value of MET suggested the occurrence of physical and chemical interactions to a similar extent (Loffredo et al. 2024).

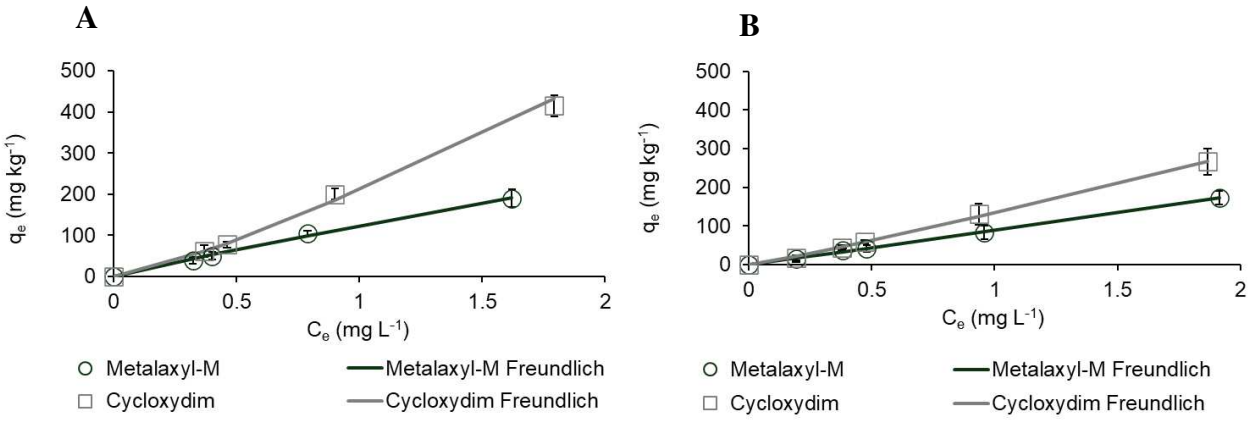

Figure 3. Adsorption isotherms of the two compounds on spent substrate of P. eryngii (A) and wheat straw (B). Points represent experimental data, while the line is the Freundlich equation plot. The vertical line on each point indicates the standard errors (n=3).

Table 3. Adsorption parameters of the compounds on SFGS and WGS

Compound	Theoretical models										
	HENRY			FREUNDLICH				LANGMUIR			
	SSR	r	Kd_{ads} mg kg^{-1}	SSR	r	K_{Fads}[a] mg kg^{-1}	1/n	SSR	r	b[a] mg kg^{-1}	K_L[b] L mg^{-1}
						SFGS					
MET	132	0.999	120	76	0.997	123	0.93	53	0.998	1394	0.098
CYC	1290	0.997	225	525	0.997	210	1.23	1321	0.990	98557	0.002
						WGS					
MET	23	0.999	90	20	0.999	89	1.02	42	0.999	3486	0.027
CYC	304	0.998	140	75	0.999	139	1.11	569	0.992	2864	0.053

5.4 Conclusions

This study demonstrated that both spent *P. eryngii* substrate and wheat straw can act as effective low-cost biosorbents for the removal of the agrochemicals MET and CYC from aqueous solutions. The SFGS sample showed a better adsorption performance compared with GWS. The presence of fungal mycelium and the associated transformation of the lignocellulosic matrix likely enhanced porosity and the availability of functional groups of the adsorbent, thereby improving sorption capacity. Sorption kinetics data of both biosorbents fitted preferentially a PSO kinetic equation, thus indicating the occurrence of chemical interactions between the agrochemicals and the surface sites of each adsorbent. Isotherms data were best fitted by the Freundlich model, indicating heterogeneous surface adsorption and multilayer sorption behaviour. Overall, the results highlight the potential of SFGS of *P. eryngii* to behave as a sustainable biosorbent for reducing the availability of the agrochemicals in the soil. SFGS reuse aligns with circular economy principles by converting an abundant agricultural by-product into a functional material for environmental remediation. Finally, we would like to point out that this study is still ongoing and will be completed by adsorption experiments of inorganic contaminants on the same adsorbents.

References

Alhujaily, A., Yu, H., Zhang, X., Ma, F. (2018). Highly Efficient and Sustainable Spent Mushroom Waste Adsorbent Based on Surfactant Modification for the Removal of Toxic Dyes. International Journal of Environmental Research and Public Health, 15(7), 1421. https://doi.org/10.3390/ijerph15071421

Allegretta, I., Squeo, G., Gattullo, C.E., Porfido C., Cicchetti A., Caponio, F., Cesco, S., Nicoletto, C., Terzano, R. (2022). TXRF spectral information enhanced by multivariate analysis: A new strategy for food fingerprint. Food Chemistry, 401, 134124. https://doi.org/10.1016/j.foodchem.2022.134124

Dang, V.B.H., Doan, H.D., Dang-Vu, T., Lohi, A. (2008). Equilibrium and kinetics of biosorption of cadmium(II) and copper(II) ions by wheat straw. Bioresource Technology, 100, 211-219. https://doi.org/10.1016/j.biortech.2008.05.031

Erdem, M., Oner, A. (2025). Preparation and Characterization of Low-Cost Bio-Sorbent and a Novel Activated Carbon from Agro-Wastes for Efficient Cr(VI) Removal. Water Air Soil Pollution, 236, 291. https://doi.org/10.1007/s11270-025-07910-6

FAOSTAT 2023. Pesticide use https://www.fao.org/faostat/en/#data/RP

Fazli, Q. S., Lorente, D. B., Hilal, I. S., Maulidar, P., & Idroes, G. M. (2025). Mapping global research on agrochemicals and sustainability: a bibliometric analysis of environmental and economic perspectives. Innovations in Environmental Economics, 1(2), 109-124. https://doi.org/10.48313/iee.v1i2.44

Gad, M. F., Todorova, T. I., & Mossa, A.-T. H. (2025). Eco-Friendly Adsorbents: Innovative Strategies for Pesticide Removal from Soil and Wastewater. Sustainability, 17(23), 10477. https://doi.org/10.3390/su172310477

Giles CH, MacEwan TH, Nakhwa SN, Smith D (1960) Studies in adsorption Part XI. A system of classification of solution adsorption isotherms, and its use in diagnosis of adsorption mechanisms and in measurement of specific surface areas of solids. Journal of the American Chemical Society,111, 3973–3993. https://doi.org/10.1016/S2095-3119(13)60429-3

Ho YS (2006) Second-order kinetic model for the sorption of cadmium onto tree fern: a comparison of linear and non-linear methods. Water Research, 40, 119–125. https://doi.org/10.1016/j.watres.2005.10.040

Jing, X., Yao, G., Wang, P., Liu, D., Qi, Y., Zhou, Z. (2016). Enantioselective Degradation and Chiral Stability of Metalaxyl-M in Tomato Fruits. Chirality, 28, 382-386 https://doi.org/10.1002/chir.22585

Kulshreshtha, S. (2019). Removal of pollutants using spent mushrooms substrates. Environmental Chemistry Letters, 17, 833–847 . https://doi.org/10.1007/s10311-018-00840-2

Kumar KV (2006).Linear and non-linear regression analysis for the sorption kinetics of methylene blue onto activated carbon. Journal of Hazardous Materials, 137, 1538–1544. https://doi.org/10.1016/j.jhazmat.2006.04.036

Lewis, K.A., Tzilivakis, J., Warner, D. and Green, A. (2016). An international database for pesticide risk assessments and management. Human and Ecological Risk Assessment: An International Journal, 22(4), 1050-1064. DOI: 10.1080/10807039.2015.1133242

Loffredo, E., Carnimeo, C., D'Orazio, V. *et al.* S (2024) Sorption and release of the pesticides oxyfluorfen and boscalid in digestate from olive pomace and in digestate-amended soil. Journal of Soils and Sediments 24, 1489–1506. https://doi.org/10.1007/s11368-024-03748-3

Loffredo, (2022). Recent Advances on Innovative Materials from Biowaste Recycling for the Removal of Environmental Estrogens from Water and Soil. *Materials*, *15*(5), 1894. https://doi.org/10.3390/ma15051894

Marin-Benito, J.M., Rodriguez-Cruz, S.M., Andrades, S., Sanchez-Martin M.J. (2012). Assessment of Spent Mushroom Substrate as Sorbent of Fungicides: Infl uence of Sorbent and Sorbate Properties. Journal of Environmental Quality, 41, 814-822 https://doi.org/10.2134/jeq2011.0437

Melanouri, E.M., Dedousi, M., Diamantopoulou, P. (2019). Cultivating *Pleurotus ostreatus* and *Pleurotus eryngii* mushroom strains on agro-industrial residues in solid-state fermentation. Part I: Screening for growth, endoglucanase, laccase and biomass production in the colonization phase. Carbon Resources Conversion, 5(1), 61-70 https://doi.org/10.1016/j.crcon.2021.12.004

Monadjemi, S., ter-Halle, A., Richard, C. (2012). Reactivity of cycloxydim toward singlet oxygen in solution and on wax film. Chemosphere, 89, 269-273 http://dx.doi.org/10.1016/j.chemosphere.2012.04.035

National Center for Biotechnology Information. (n.d.). *Metalaxyl* (CID 42586). PubChem. Retrieved February 24, 2026, from https://pubchem.ncbi.nlm.nih.gov/compound/Metalaxyl

Papadaki, M.I., Mendoza-Castillo, D.I., Reynel-Avila, H.E., Bonilla-Petriciolet, A., Georgopoulos, S. (2021). Nut Shells as Adsorbents of Pollutants: Research and Perspectives. Frontiers in Chemical Engineering, 3, 640983. doi: 10.3389/fceng.2021.640983

Sahithya, K., Mouli, T., Ankita B, Mercy S.T. (2022). Remediation potential of mushrooms and their spent substrate against environmental contaminants: An overview. Biocatalysis and Agricultural Biotechnology, 42, 102323. https://doi.org/10.1016/j.bcab.2022.102323

Sharma, N., Kumar, V., Sugumar V., Umesh, M., Sondhi, S., Chakraborty, P., Kaur, K., Thomas, J., Kamaraj, C., Maitra, S.S. (2024). A comprehensive review on the need for integrated strategies and process modifications for per- and polyfluoroalkyl substances (PFAS) removal: Current insights and future prospects. Case Studies in Chemical and Environmental Engineering, 9, 100623. https://doi.org/10.1016/j.cscee.2024.100623

Wan, N.F., Fu, L., Dainese, M., Kiaer, L.P., Hu, Y.Q., Xin, F., Goulson, D., Woodcock B.A., Vanbergen, A.J., Spurgeon, D.J., Shen, S., Sherber, C. (2025). Pesticides have negative effects

on non target organisms. Nature communications, 16, 1360 https://doi.org/10.1038/s41467-025-56732-x

Wang & Guo (2020). Adsorption kinetic models: Physical meanings, applications, and solving methods. Journal of Hazardous Materials, 390, 122156 https://doi.org/10.1016/j.jhazmat.2020.122156

Wu J, Xia A, Chen C, Feng L, Su X, Wang X. Adsorption Thermodynamics and Dynamics of Three Typical Dyes onto Bio-adsorbent Spent Substrate of *Pleurotus eryngii*. *International Journal of Environmental Research and Public Health*. 2019; 16(5):679. https://doi.org/10.3390/ijerph16050679

Zhou, J., Ge, W., Zhang, X., Wu, J., Chen, Q., Ma, D., Chai, C. (2020). Effects of spent mushroom substrate on the dissipation of polycyclic aromatic hydrocarbons in agricultural soil. Chemosphere, 259, 127462. https://doi.org/10.1016/j.chemosphere.2020.127462

CHAPTER – 6
BIOCHAR FOR WASTEWATER TREATMENT: REMOVAL OF ORGANIC CONTAMINANTS AND PHYTOTOXICITY ABATEMENT

Abstract

The occurrence of contaminants of emerging concern (CECs) in wastewater poses increasing environmental and reuse-related risks, requiring effective and sustainable treatment solutions. This study investigated the performance of biochar as a low-cost adsorbent for the removal of organic contaminants from different wastewater and the reduction of its phytotoxicity.

Adsorption experiments conducted on municipal and agro-industrial wastewater demonstrated that biochar can effectively remove a broad spectrum of organic contaminants, achieving total load reductions generally above 90%. Adsorption studies showed rapid retention of the contaminants and clear dose-dependent behaviour, with equilibrium generally reached within a few hours. Biochar was particularly effective toward aromatic and hydrophobic compounds, including several pharmaceuticals and fungicides. In contrast, PFAS removal was limited at low adsorbent doses and became significant only above a threshold biochar amount, highlighting matrix effects and the need for further optimization of both adsorption conditions and LC–MS quantification methods.

The detoxification potential of biochar was assessed on a dairy wastewater with high level of chemical oxygen demand (COD), through seed germination and seedling growth assays on lettuce, carosello melon, and tomato. Untreated effluent induced phytotoxic responses, whereas biochar-treatment significantly improved germination rates and biometric parameters. Batch adsorption treatments provided stronger toxicity reduction compared with continuous-flow configuration.

Overall, the results confirm that biochar is an effective and versatile material for wastewater remediation and phytotoxicity decrease in different liquid matrices, supporting its application within sustainable and circular approaches to water treatment and reuse.

6.1 Introduction

Water is a fundamental resource for life, ecosystems, and socio-economic development. Despite its importance, freshwater availability is limited and unevenly distributed across the globe (Feng et al. 2025). In recent decades, population growth, urbanization and the intensification of agricultural and industrial activities have contributed to a significant reduction in water availability (Qiu et al. 2022). Moreover, climate change and increasingly frequent and severe droughts have made the recovery of water resources more critical than ever. In this context, wastewater treatment and reuse systems play a key role in recovering water, particularly for use in the agricultural sector. Reusing wastewater in agriculture is especially advantageous due to its potential to recover essential plant nutrients, reduce fertilizer demand, and safely dispose of large volumes of effluents (Cristovao et al. 2026).

Depending on its origin, wastewater can be broadly categorized into municipal, industrial, agricultural, dairy and stormwater types (Wang et al. 2024). Among these, municipal wastewater is one of the most prevalent forms, generated from domestic, commercial, and institutional sources, as well as from surface runoff and stormwater that enter urban drainage systems. Agro-industrial wastewater, in contrast, arises from the processing of agricultural and livestock raw materials along the food production chain (Martinez et al. 2021). These processes often involve substantial water use for operations such as washing and pre-treating raw materials, handling of intermediate products, cleaning of equipment and facilities, among others. Dairy wastewater originates from milk spillage, and as a direct result of using phosphoric and nitric acid, or sodium hypochlorite solution for cleaning the systems and usually presents high level of COD. (Al Ananzeh 2021). COD represents the degree of contamination in water bodies due to organic matter and is an important parameter to monitor water quality (Aguilar-Torrejon et al. 2023). As a result, these different wastewater streams typically carry a mixture of suspended solids, pathogens, plant nutrients, inorganic contaminants and organic microcontaminants, which pose significant challenges for treatment and reuse (Mohammadi et al. 2022).

CECs have emerged as a major group of environmental contaminants and are now a central focus in wastewater treatment research in accordance with Directive (EU) 2024/3019 (European Parliament and Council, 2024). These trace-level compounds include pharmaceuticals, pesticides, endocrine-disrupting chemicals, and various industrial byproducts. Owing to their hazardous properties, such as toxicity, persistence, and potential carcinogenicity, some CECs pose considerable risks to human and animal health even at concentrations ranging from ng L^{-1} to µg L^{-1}. Their presence in

wastewater also hinders its direct and cost-effective reuse, particularly in agricultural applications (Hernandez-Zanoletty et al. 2025, Qiu et al. 2022; Cadena-Aponte et al., 2025).

Among industrial contaminants of emerging concern, per- and polyfluoroalkyl substances (PFAS), a broad class of synthetic organofluorine compounds widely used in manufacturing applications of consumer products, due to their high thermal stability and resistance to water and lipids (Criswell et al. 2025). PFAS are typically present in ng L^{-1} (parts-per-trillion) concentration in natural water, however, these molecules are toxic even at these low levels and do not degrade in the environment (Vitale et al. 2025). Moreover, certain PFAS undergo biotransformation within organisms, producing short-chain PFAS with potentially greater toxicity (Dai et al. 2025).

Conventional treatment trains in urban wastewater treatment plants, typically consisting of a multi-stage process designed to remove solids and organic matter are poorly effective to comprehensively remove CECs (Krzeminski et al., 2019), and advanced treatment steps must be implemented. Advanced wastewater treatment technologies, predominantly based on physicochemical processes such as ozonation, advanced oxidation, membrane filtration, and reverse osmosis, have been widely applied to CECs removal (Nasirabadi et al. 2016; Rizzo et al. 2019). Nonetheless, these methods often entail high operational complexity and capital investment, which limit their scalability and practical implementation, especially in resource-constrained contexts (Ambaye et al. 2020).

Adsorption has emerged as a simple, low-cost, and effective alternative for pollutant removal from wastewater. The process involves the accumulation of a solute at the interface between a solid adsorbent phase and a liquid solution (Loffredo 2022). Adsorption mechanisms are generally classified as either physical (physisorption) or chemical (chemisorption). Physisorption is governed by weak van der Waals forces and is typically reversible, while chemisorption involves the formation of stronger chemical bonds and tends to be irreversible. Conventional adsorbents, including activated carbon, alumina, silica, and zeolites, are widely used for contaminant removal from wastewater (Habila et al. 2023, Cui et al. 2020, Kumari et al. 2024, Gao et al. 2025). Activated carbon is widely recognized for its high efficiency in removing a broad range of contaminants (Heibati et al. 2014). However, its large-scale applications are often limited by high production and operational costs (Chen et al. 2011). Consequently, the development of alternative adsorbent materials is considered essential, with biochar emerging as one of the most extensively investigated alternatives in recent years.

Biochar is a carbonaceous solid material produced through thermochemical conversion (pyrolysis and gasification) of biomass of plant and animal origin, such as agricultural residues, forestry waste, sludge, and other organic waste. Biochar is characterized by a higher carbon content, diffuse

microporosity, and a great abundance of surface functional groups. Its large specific surface area, well-developed pore network, and the presence of functional moieties such as carboxyl, hydroxyl, and phenolic groups endow biochar with remarkable adsorption properties for contaminant removal (Pathak et al. 2023; Carnimeo et al. 2023). However, the physicochemical properties of biochar are strongly influenced by both the type of feedstock used and the pyrolysis parameters adopted in the production process (Loffredo et al. 2025). Variations in biomass composition, such as lignocellulosic content, ash, or mineral fractions, together with differences in thermal conditions, can significantly affect its surface area, porosity, functional groups, and overall adsorption performance. Thanks to these features, and due to its cost-effectiveness and environmentally sustainable nature, biochar derived from agricultural residues has emerged as a promising green adsorbent for water and wastewater treatment applications (Loffredo 2022).

In light of the above, the aim of this study was to assess the capacity of a wood-based biochar to (i) adsorb CECs from different wastewaters, (ii) remove PFAS from aqueous solution and (iii) reduce the phytotoxicity of a dairy wastewater.

6.2 Materials and methods

6.2.1 Biochar, Wastewater, Chemicals and Plants

Two biochar, hereafter referred to as BCA and BCB, supplied by Silpa S.r.l. (Crotone, Italy), were used in the decontamination experiments of different wastewaters. BCA was used in most of the experiments, while BCB was used only in experiments to reduce the phytotoxicity of a dairy wastewater. The two biochars were produced in different years and complied with the quality requirements established by the Italian Ministerial Decree of 10 October 2022 update of annexes 1, 6, 7, 8, 9, 13 and 14 to Legislative Decree No. 75 of 29 April 2010 for biochar application. Both materials were obtained through a gasification process conducted at 750 °C. However, in the case of BCA, the feedstock composition was different with respect to that used for the production of BCB. BCB was produced exclusively from virgin beech wood chips, whereas BCA was produced using selected chestnut wood chips as well. For BCB, the effect of particle size on adsorption performance was also investigated. To this end, one portion of the biochar was oven-dried and used as received (BCB), whereas another portion was ground and subsequently sieved using a 1 mm mesh sieve, yielding a finer particle-size fraction, hereafter referred to as BCBM.

Two filtered secondary municipal wastewaters were investigated. The effluents were collected from the wastewater treatment plants (WTPs) “EDAR El Toyo” and “Entrada 4 Vegas”, Almeria, Spain. In addition, an agro-industrial wastewater was studied, which was collected from the company

"Cítricos de l' Andarax"of Almeria, specialized in the production, processing, and commercialization of traditional citrus fruits. Dairy company "La Gioiella latticini", Gioia del Colle, provided the dairy wastewater. This wastewater showed a COD of 5610 mg L-1 exceeding the limit value required by Italian Legislative Decree 152/06. This parameter was determined using dedicated Hach test kits, after diluting each sample 1:5 with bidistilled water. The sample was prepared according to the kit instructions, and the vial was then placed in the Hach Lange DR 2800 photometer to measure the parameter. Preliminary ultra-high-performance liquid chromatography mass spectrometry (UHPLC-MS/MS) analysis of the two wastewaters showed the presence of 78 CECs, including pharmaceuticals from different therapeutic classes and selected metabolites, pesticides, and artificial sweeteners. The complete list of target contaminants is reported in Table 1.

Lettuce (*Lactuca sativa* L.), carosello melon (*Cucumis melo* L.), and tomato (*Solanum lycoperiscum* L.) seeds used in the phytotoxicity assays were purchased from the company 'Riccardo Larosa' of Andria (Italy).

Table 1. List and category of the CECs detected in the wastewaters.

Category	Sub-Category	Compound
Pharmaceuticals	Analgesics	Acetaminophen (Paracetamol)
		Ketoprofen
		Naproxen
		Niflumic acid
		Propyphenazone
		Antipyrine
		4-Aminoantipyrine (4-AA)
		4-Aminoantipyrine (4-AAA)
		4-Methylaminoantipyrine (4-MAA)
Pharmaceuticals	Cardiovascular	Atenolol
		Metoprolol
		Propranolol
		Sotalol
		Valsartan
		Irbesartan
		Eprosartan
		Flecainide
		Triamterene
		Pentoxifylline
Pharmaceuticals	Antibiotics	Azithromycin
		Ciprofloxacin
		Clarithromycin
		Clindamycin
		Doxycycline
		Levofloxacin
		Ofloxacin
		Sulfamethoxazole
		Sulfapyridine
		Tetracycline

Category	Sub-Category	Compound
Pharmaceuticals	Antiepileptics	Amitriptyline
		Amisulpride
		Citalopram
		Clomipramine
		Sertraline
		Venlafaxine
		O-desmethylvenlafaxine
		N-desmethylcitalopram
		Lamotrigine
		Primidone
		Gabapentin
		Oxcarbazepine
		Carbamazepine epoxide
		Methadone
		O-desmethyltramadol
		Trazodone
		Sulpiride
Pharmaceuticals	Other drugs	Cetirizine
		Dextromethorphan
		Famotidine
		Lidocaine
		Mepivacaine
		Nicotinamide
		Oxypurinol
		Salbutamol
		Theophylline
		Cyclophosphamide
		Fenofibric acid
		Diatrizoic acid
		Iomeprol
		Iopamidol
Agrochemicals	Fungicides	Myclobutanil
		Azoxystrobin
		Propiconazole
		Thiabendazole
Agrochemicals	Herbicides	Isoproturon
		Terbuthryn
Agrochemicals	Insecticides	Acetamiprid
		Chlorantraniliprole
		Cyantraniliprole
		Dimethoate
		Pirimicarb
		Chlorfenvinphos
Industrial / Urban markers	Corrosion inhibitors	Benzotriazole
Industrial compounds	Aromatic heterocycles	Acridone
		9-Acridinecarboxylic acid
Lifestyle markers	Stimulants	Caffeine
		Paraxanthine
		Trigonelline

6.2.2 Biochar Characterization

The physicochemical characteristics of BCA and BCB are reported in Table 2.

Table 2. Physicochemical properties of BCA and BCB.

	BCA		BCB	
Parameter	mean	Sd	mean	Sd
Moisture (%)	5.26	0.09	4.56	0.08
pH[a]	9.63	0.03	9.08	0.05
EC (ds m^{-1})[a]	0.90	0.01	0.89	0.01
Ash (%)	19.4	1.35	7.80	0.26
TC (%)	63	-	57	-
Ba	418	17	306	18.9
Fe	4476	491	1528	35.8
Sr	472	33	450	19.0
Cr	20.9	2.5	7.3	4.0
Cu	24.7	2.6	19.1	0.7
Mn	756	49	437	1.1
Ni	8.78	1.08	4.7	0.5
Rb	22.67	5.06	12.5	0.4
Ca	74512	3401	50327	2238
K	9723	686	7063	231
Ti	410	147	92.0	12.4
Zn	71.2	7.4	53.6	0.7
P	3179	313	2275	272
Cl	496	44	1572	27.2
Br	5.6	0.7	8.9	0.2

[a]biochar/H_2O, 1:10 w/v

Biochar properties were determined using conventional methods. The pH value and electrical conductivity (EC) were determined using a pH meter (CRISON 50+) and a conductivity meter (CRISON CM 35), respectively. Ash content was calculated after dry combustion in a furnace at 750 °C for 6 h. Total carbon were measured using a CNS analyzer (Elementar pyrocube).

Minor and trace elements in both biochars were determined by total reflection X-ray fluorescence (TXRF) spectroscopy using an S2 Picofox spectrometer (Bruker Nano GmbH, Berlin, Germany). The instrument was equipped with a Mo microfocus X-ray tube (30 W, 50 kV, 600 μA), a multilayer

monochromator, and an XFlash® silicon drift detector with an active area of 30 mm². The energy resolution of the detector, evaluated at the Mn Kα line, was <150 eV at 10 kcps.

Before analysis, dried samples were finely ground for 5 min using a vibratory ball mill (MM200, Retsch). For each sample, 10 mg of powdered material were dispersed in 3 mL of Triton X-100 solution (1:100, v/v in bidistilled water) in 10 mL plastic tubes and sonicated in an ultrasonic bath for 10 min. Subsequently, 10 µL of a 1000 mg L^{-1} yttrium standard solution (Sigma-Aldrich) were added as an internal standard.

After vortex mixing for 30 s, 10 µL of each suspension were deposited onto siliconized quartz reflectors and dried on a heating plate at 50 °C under a laminar flow hood. All samples were analyzed in triplicate with a counting time of 1000 s. Data acquisition and processing were performed using Spectra 7 software (Bruker GmbH, Germany).

6.2.3 Adsorption study on wastewater samples

Preliminary adsorption tests were first conducted on the filtered secondary municipal wastewater collected from the EDAR El Toyo WTP in order to identify the biochar exhibiting the highest adsorption capacity toward the contaminants present in the effluent. To this aim, 20 mg of each biochar (BCA, BCB and BCBM) was allowed to interact dynamically with 10 ml of wastewater for 24 hours.

Subsequently, the effect of biochar dosage was evaluated using BCA, which showed the best performance in the preliminary screening. Different amounts of BCA (1, 2.5, 5, 10, and 20 mg) were added to 10 mL of wastewater and allowed to interact for 24 h.

Adsorption kinetics were then investigated by adding 2.5, 10, and 20 mg of BCA to 10 mL of wastewater for different interaction times (5, 15, 30 min; 1, 2, 4, 6 h).

For the filtered secondary municipal wastewater collected from the Entrada 4 Vegas WTP, adsorption kinetic experiments were carried out by adding 20 mg of BCA to 10 mL of wastewater for interaction times of 1, 2, 4, 6, 10, and 24 h.

The adsorption capacity of biochar toward the contaminants of the agro-industrial wastewater from Cítricos del Andarax was evaluated by interacting 20 mg of BCA with 10 mL of wastewater for 24 h.

At the end of each experiment, the suspensions were filtered, and the supernatants were collected using 13 mm PTFE syringe filters (0.22 µm pore size; Scharlau, Barcelona, Spain) before chemical analysis.

6.2.4 UHPLC-MS/MS analysis

Analyses were performed using a UHPLC system (Exion LC AC, Sciex, Foster City, CA, USA) equipped with a Luna Omega Polar column (100 × 2.1 mm, 1.6 µm; Phenomenex, Torrance, CA, USA). The mobile phases consisted of (A) LC–MS-grade water containing 0.1% formic acid and (B) methanol. The elution gradient was programmed as follows: 0–1 min, 5% B; 1–12 min, 100% B; 12–17 min, 5% B, with a total run time of 17.5 min.

The flow rate was set at 0.30 mL min^{-1}, the injection volume was 10 µL, and the column temperature was maintained at 30 °C.

Detection and quantification of the target analytes were carried out using a hybrid quadrupole–linear ion trap mass spectrometer (5500 QTRAP System, Sciex Instruments, Foster City, CA, USA) equipped with an electrospray ionization source (Turbo IonSpray) operating in positive ion mode (ESI^+).

6.2.5 PFAS adsorption study

A mixture of PFAS was added to the EDAR El Toyo wastewater in an amount sufficient to obtain a final concentration of 10 ppt of each molecule. The analytical set included 20 PFAS selected and classified according to the nature of the terminal functional group (carboxylic acids and sulfonic acids) and the length of the perfluorinated chain (short chain and long chain) (Table 3). In the tests conducted, 1, 2.5, 5, 10 and 20 mg of BCA were interacted with 10 mL of wastewater for 24 hours.

PFAS residue analyses were performed by liquid chromatography coupled to triple quadrupole mass spectrometry (LC–MS/MS; 7500 QTRAP System, Sciex Instruments, Foster City, CA, USA), a technique that ensures high sensitivity and selectivity for the determination of PFAS in complex aqueous matrices. The adopted chromatographic separation method is currently being tested and optimized

Table 3. Molecular formula of PFAS

Compound	Molecular formula
Perfluorobutanoic acid (PFBA)	$C_4HF_7O_2$
Perfluoropentanoic acid (PFPeA)	$C_5HF_9O_2$
Perfluorotridecanoic acid (PFTriA)	$C_{14}HF_{27}O_2$
Perfluorohexanoic acid (PFHxA)	$C_6HF_{11}O_2$
Perfluorododecanoic acid (PFDoA)	$C_{12}HF_{23}O_2$
Perfluoroundecanoic acid (PFUnDA)	$C_{11}HF_{21}O_2$
Perfluoroheptanoic acid (PFHpA)	$C_7HF_{13}O_2$
Perfluorodecanoic acid (PFDA)	$C_{10}HF_{19}O_2$
Perfluorooctanoic acid (PFOA)	$C_8HF_{15}O_2$
Perfluorononanoic acid (PFNA)	$C_9HF_{17}O_2$
Perfluorooctanesulfonic acid (PFOS)	$C_8F_{17}SO_3H$
Perfluorononanesulfonic acid (PFNS)	$C_9F_{19}SO_3H$
Perfluoroethanesulfonic acid (PFHpS)	$C_7F_{15}SO_3H$
Perfluorodecanesulfonic acid (PFDS)	$C_{10}F_{21}SO_3H$
Perfluorohexanesulfonic acid (PFHxS)	$C_6F_{13}SO_3H$
Perfluoroundecanesulfonic acid (PFUnS)	$C_{11}F_{23}SO_3H$
Perfluoropentanesulfonic acid (PFPeS)	$C_5F_{11}SO_3H$
Perfluorododecanesulfonic acid (PFDoS)	$C_{12}F_{25}SO_3H$
Perfluorobutanesulfonic acid (PFBS)	$C_4HF_9O_3S$
Perfluorotridecanesulfonic acid (PFTriA)	$C_{13}HF_{27}O_3S$

6.2.6 Phytotoxicity studies on dairy wastewater

Germination assays were carried out on lettuce, carosello melon, and tomato to evaluate the potential phytotoxic effects of dairy wastewater, both untreated (UW) and after treatment with BCB using a continuous-flow method (CTW). In addition, in the tomato germination assays, the effects of wastewater treated with BCB through batch adsorption tests (BTW) were also evaluated. Tomato assays were also conducted using the aqueous extract of BCB obtained after the CTW test (CAE) and the BTW test (BAE) to understand the effect of biochar on plant growth.

6.2.6.1 Continuous-flow wastewater treatment

An aliquot of wastewater (100 mL), either undiluted (100% UW) or diluted 1:1 with bidistilled water (50%), was placed in a separatory funnel and allowed to flow at a rate of approximately 0.5 mL min^{-1}, through 100 mg of biochar placed on filter paper (Cordenons Perfecte 2 Extra Rapida) in a glass funnel (Figure 1).

Germination tests were performed by placing lettuce and carosello seeds in 90-mm Petri dishes on filter paper and adding 3 mL of the following treatments: 20% UW, 50% UW, 100% UW, 50% CTW, 100% CTW, and bidistilled water only (control). The Petri dishes were incubated in a growth

chamber (Phytotron model 60043/THTL, F.lli Della Marca s.r.l., Rome) at 22 ± 1 °C for 8 days. All germination tests were performed with five replicates.

At the end of the experiments, root length, shoot length, fresh weight, and dry weight (after drying at 70 °C for 2 hours) were measured for each seedling, and germination percentage was calculated. All biometric data were statistically analyzed using ANOVA and the least significant difference (LSD) test at $P \leq 0.05$, $P \leq 0.01$, and $P \leq 0.001$.

Figure 1. Continuous-flow method used for wastewater treatment with biochar.

6.2.6.2 Batch wastewater treatment

A volume of 100 mL of untreated wastewater (UW) was poured into a 250 mL beaker and allowed to interact for 3 hours with 100 mg of biochar enwrapped in a nonwoven fabric sheet (Figure 2). The wastewater was then filtered using filter paper (Cordenons Perfecte 2 Extra Rapida).

Subsequently, germination tests were performed by placing tomato seeds in 90-mm Petri dishes on filter paper and adding 3 mL of the following treatments: 100% UW (control), 100% CTW, 100% BTW, CAE, BAE, and H_2O. The Petri dishes were incubated in a growth chamber (Phytotron model 60043/THTL, F.lli Della Marca s.r.l., Rome) at 22 ± 1 °C for 7 days. All germination tests were carried out with five replicates.

The biometric data obtained from these tests were subjected to statistical analysis following the same procedures previously described for the germination assays conducted on lettuce and carosello melon.

Figure 2. Batch method used for wastewater treatment with biochar.

6.3 Results and discussion

6.3.1 Adsorption experiments with EDAR el Toyo wastewater

The experiments demonstrated the high efficiency of the three biochar samples in reducing the total load of organic contaminants in wastewater. Specifically, BCA, BCB, and BCBM achieved removal efficiencies of 96%, 97%, and 97%, respectively. Most of the analyzed compounds were almost completely removed, with the exception of 4-aminoantipyrine (4-AAA), acetaminophen, gabapentin, nicotinamide, oxypurinol, and myclobutanil.

Adsorption tests conducted at different BCA dosages showed a progressive increase in removal efficiency with increasing biochar dose. At 1 mg, approximately 66% removal was achieved. Increasing the dose to 2.5 and 5 mg resulted in removal efficiencies of 85% and 87%, respectively. At higher doses (10 and 20 mg), removal approached completion, reaching 97% and 99%, respectively (Figure 3).

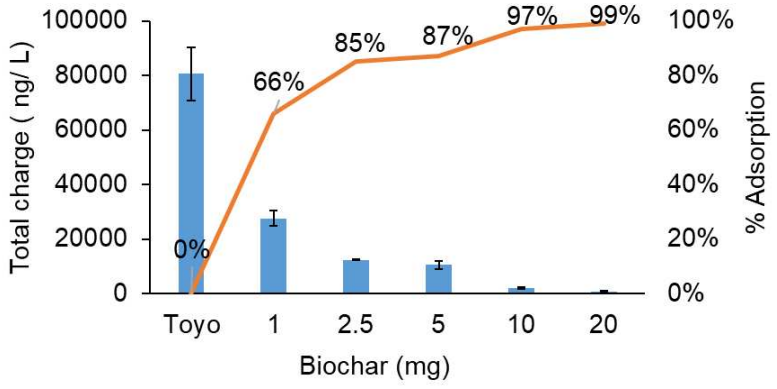

Figure 3. Adsorption of CECs present in the EDAR El Toyo effluent using different amounts of biochar. The vertical bar at each point represents the standard error (n=3).

The adsorption kinetics varied with biochar dosage (Figure 4). At 2.5 mg, adsorption increased gradually, reaching about 62% within the first hour and approximately 71% after 6 hours. At 10 mg, the process was faster, with more than 50% removal within 15 minutes and about 70% within 1 hour. Maximum removal (≈95%) was achieved after approximately 4 hours. The decrease in adsorption observed after 6 hours of interaction may be attributed to analytical error. At 20 mg, adsorption was rapid and efficient, with more than 70% removal within 5 minutes and approximately 97% reached after 1 hour, indicating near-equilibrium conditions.

The results indicate that biochar exhibits a strong affinity for a wide range of organic contaminants, enabling high removal efficiencies even at relatively low dosages. The progressive increase in adsorption with increasing biochar dose suggests a greater availability of active sites, although the diminishing improvement at intermediate doses (2.5–5 mg) indicates a gradual saturation of readily accessible sites.

The faster kinetics observed at higher dosages can be attributed to the increased surface area and number of available adsorption sites, which enhance the probability of contaminant–sorbent interactions. The rapid initial phase observed in all cases reflects the occupation of readily accessible active sites, followed by a slower stage likely controlled by diffusion processes and site saturation. The persistence of a few compounds in solution suggests lower affinity or higher solubility, highlighting the influence of molecular properties on adsorption behavior.

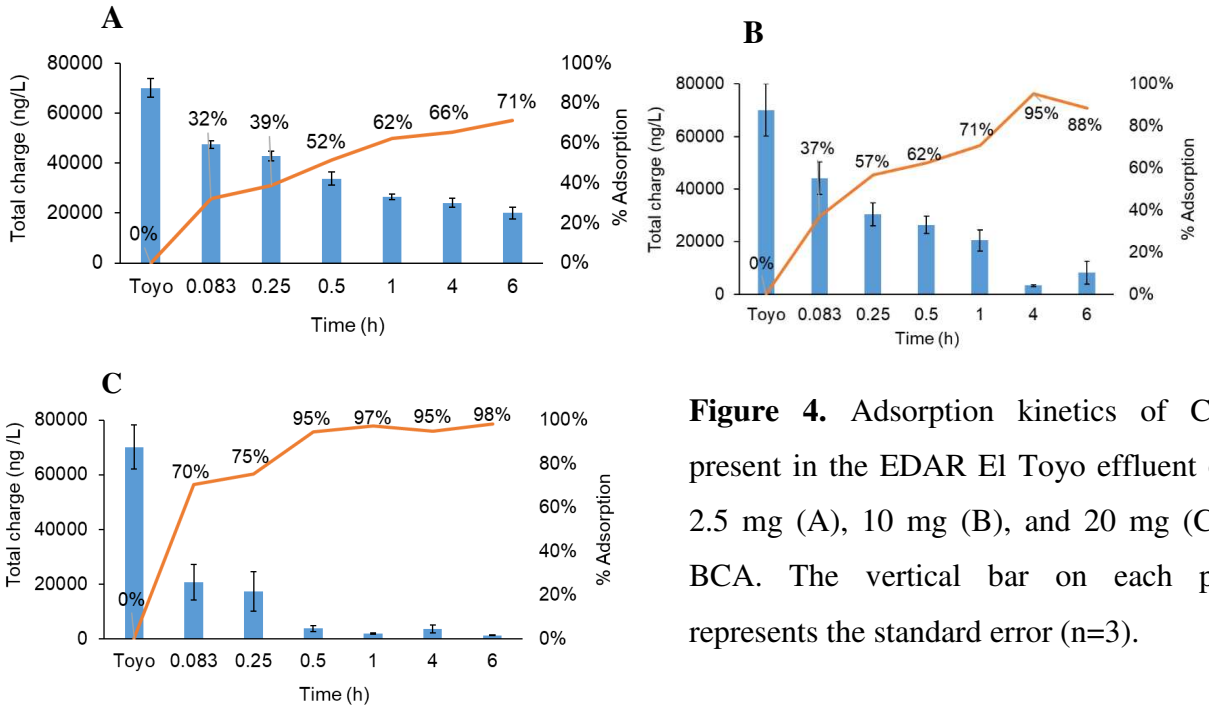

Figure 4. Adsorption kinetics of CECs present in the EDAR El Toyo effluent onto 2.5 mg (A), 10 mg (B), and 20 mg (C) of BCA. The vertical bar on each point represents the standard error (n=3).

6.3.2 Adsorption test with Entrada 4 Vegas wastewater

Based on the results obtained with the EDAR El Toyo wastewater (section 6.3.1), the adsorption kinetics of the pollutants on filtered secondary civil wastewater from Entrada 4 Vegas was investigated. This wastewater initially showed a higher total contaminant load compared to EDAR el Toyo effluent. The study demonstrated that, even with this more contaminated wastewater, biochar reached adsorption equilibrium within a relatively short time (≈ 2 hours), removing up to 97% of the total contaminant load (Figure 5).

Another finding was that, at equilibrium, 81% of the CECs were completely removed. Overall, the results suggested that relatively short contact times were sufficient to achieve substantial pollutant removal, while longer times allow maximization of the process, although with only marginal additional gains**.** The literature reports several studies where biochar is used to remove CECs from municipal wastewater. Srikhaow et al. (2023) showed that various agrochemicals reached the adsorption equilibrium on a pineapple residue-originated biochar in approximately 2 hours; however, in that study, a higher quantity of biochar was used (5 g of adsorbent per liter of solution) compared with those used in this study. Coimbra et al. (2025) showed that the adsorption of selected pharmaceuticals of secondary municipal effluent onto a pyrolyzed pulp mill sludge reached equilibrium within 200 min.

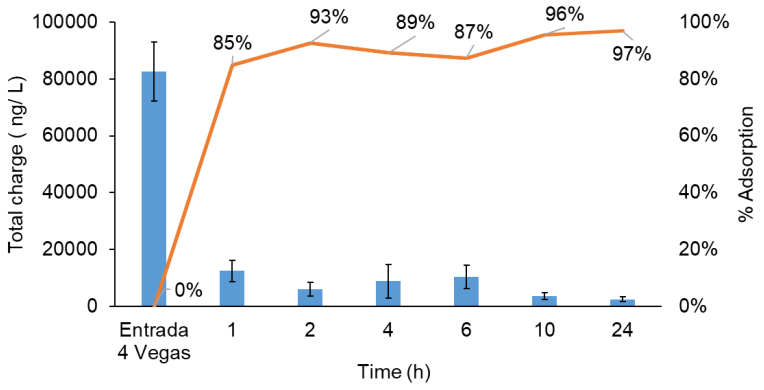

Figure 5. Adsorption kinetics of CECs present in the Entrada 4 Vegas wastewater onto BCA. Vertical bars at each point represent the standard error (n = 3).

6.3.3 Adsorption tests of contaminants from the Citricos del Andarax wastewater

The adsorption capacity of biochar was also tested on an agro-industrial wastewater collected from the Citricos del Andarax company. Compared with the two municipal wastewaters reported in

sections 6.3.1 and 6.3.2 (rich in pharmaceuticals), this effluent showed a higher concentration of agrochemicals, especially of the two fungicides carbendazim and propamocarb.

The study confirmed the effectiveness of BCA in adsorbing a wide range of organic compounds, with an overall contaminant removal of 94%. Moreover, after treatment, 71% of the total number of detected compounds were completely removed. The effectiveness of this biochar was particularly evident for aromatic and hydrophobic compounds, such as benzotriazole, carbendazim, fenhexamid, and several pharmaceutical metabolites, which showed very marked reductions. In any case, removal efficiency with biochar was always higher than 80% for all compounds present in the wastewater.

6.3.4 PFAS adsorption experiments

When 5 mg of BCA was applied to 10 mL of wastewater, no significant reduction in PFAS concentration was observed, with only a 2% decrease compared to the initial level. Increasing the adsorbent dose to 10 and 20 mg led to a more pronounced reduction, with removal efficiencies of 32% and 39%, respectively, indicating a clear dose-dependent trend. These results suggest that, in the condition of this study, 5 mg represents a threshold below which the interaction between PFAS and biochar is too limited to produce a measurable effect.

The removal of PFAS by biochar can be attributed to a combination of adsorption and partitioning mechanisms. Adsorption likely occurs through hydrophobic interactions, electrostatic forces, and, to a lesser extent, specific interactions with surface functional groups. At the same time, partitioning into the carbonaceous matrix may contribute to PFAS retention, particularly for compounds with higher hydrophobicity. At low biochar doses, both mechanisms are limited by the reduced availability of sorption domains, making the system more sensitive to matrix effects and analytical variability.

It is important to note that the experiments were conducted in real wastewater, where dissolved organic matter and co-existing contaminants may compete with PFAS for adsorption sites or block pore accessibility. These interactions can reduce both adsorption and partitioning efficiency compared to simplified systems. Although the observed trends are promising, further studies are needed to optimize analytical methods (e.g., LC–MS) and to better elucidate the relative contribution of adsorption and partitioning mechanisms under realistic conditions.

6.3.5 Phytotoxicity assays using CTW

Plant assays demonstrated that 100% UW as germination medium decreased the germination percentage of lettuce seeds by 18%, compared with the control, while that of carosello seeds

remained almost unchanged. Biometric data revealed a progressive reduction in lettuce root length with increasing UW dose. Differently, the addition of 20% UW produced a stimulatory effect on lettuce shoot growth (Figure 6).

In the experiments conducted with carosello melon, 100% UW caused significant reductions in root length, fresh weight, and dry weight, compared with the control (Figure 7).

When CTW was used as germination medium, a reduction in phytotoxicity was observed, particularly in lettuce, for which the germination percentage increased by 12%. Biometric data also showed that, compared with 100% UW and 50% UW, the treated wastewater produced an increase in all the examined parameters in both species (Figure 8 and 9). These results suggest that the observed reduction in phytotoxicity could be directly linked to the removal of organic contaminants during treatment. The adsorption of potentially toxic compounds by biochar likely reduced their bioavailability and toxicity to plants, thereby promoting seed germination and seedling development. This highlights the effectiveness of the treatment not only in contaminant removal but also in improving the agronomic quality of wastewater for potential reuse.

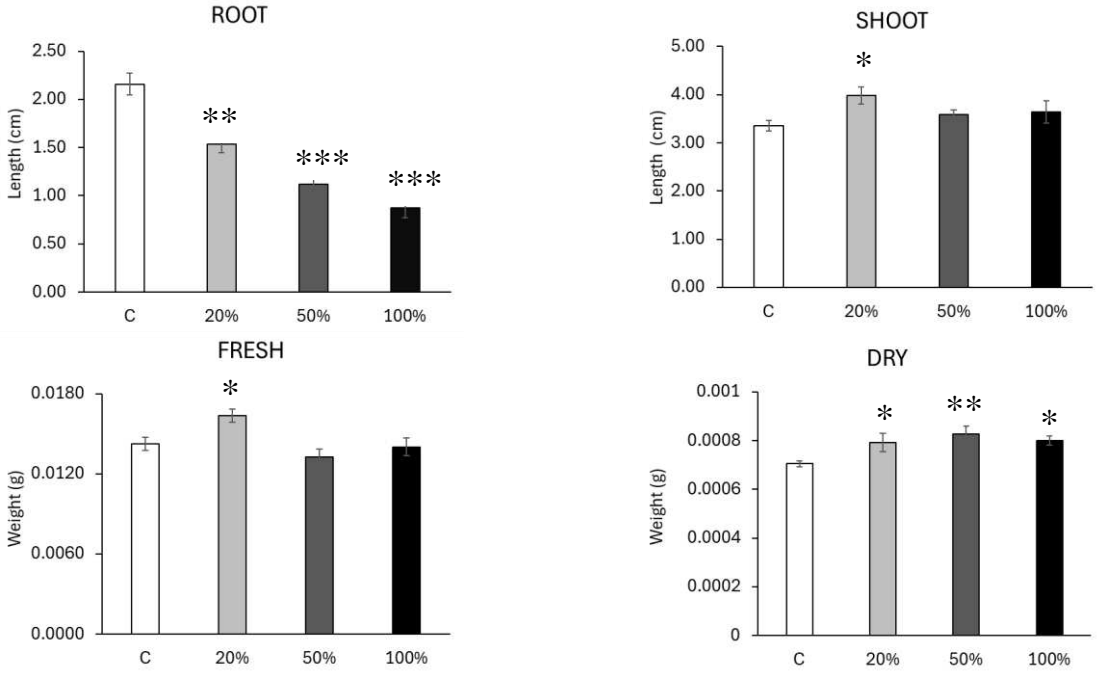

Figure 6. Effects of bidistilled water (C, control) and various UW doses on lettuce seedlings. Vertical lines on each bar indicate the standard error. Data were statistically analyzed by ANOVA, and treatment means were compared with the control using the least significant difference (LSD) test at * $P \leq 0.05$, ** $P \leq 0.01$, and *** $P \leq 0.001$.

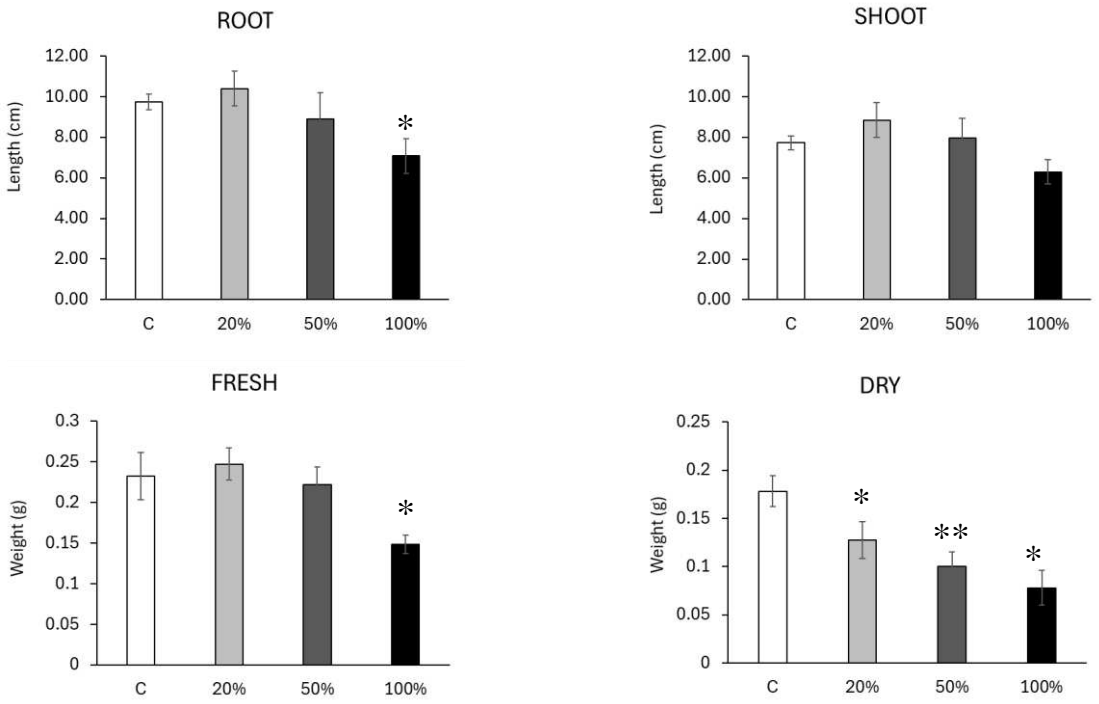

Figure 7. Effects of bidistilled water (C, control) and various UW doses on carosello seedlings. Vertical lines on each bar indicate the standard error. Data were statistically analyzed by ANOVA, and treatment means were compared with the control using the least significant difference (LSD) test at * $P \leq 0.05$, ** $P \leq 0.01$.

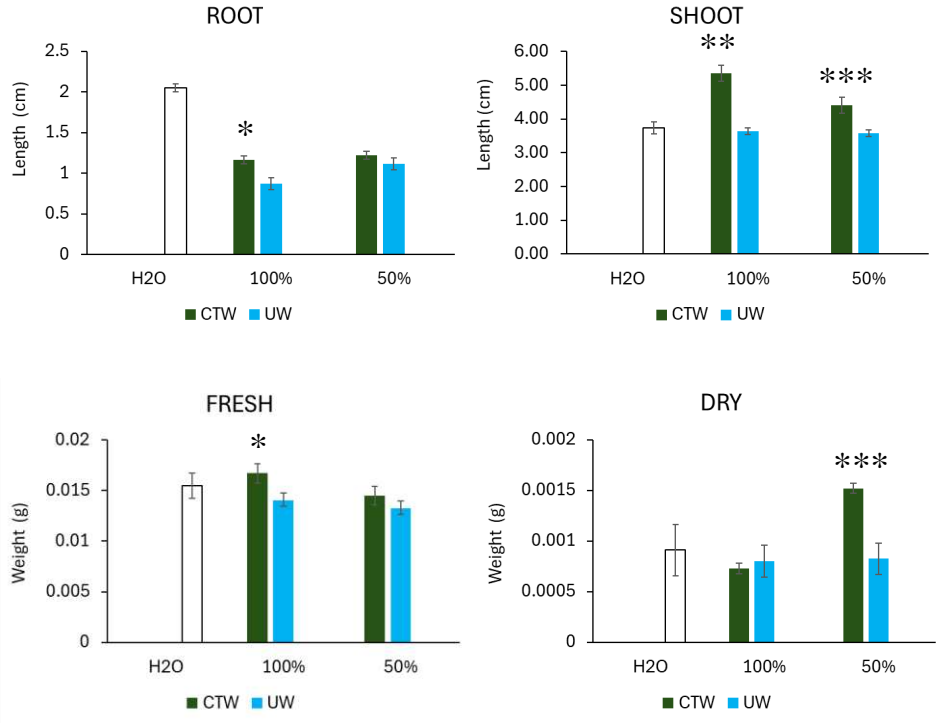

Figure 8. Effects of CTW on lettuce seedlings. Vertical lines on each bar indicate the standard error. Data were statistically analyzed by ANOVA, and the means of the treatments were compared with 100% UW using the least significant difference (LSD) test at * $P \leq 0.05$, and *** $P \leq 0.001$.

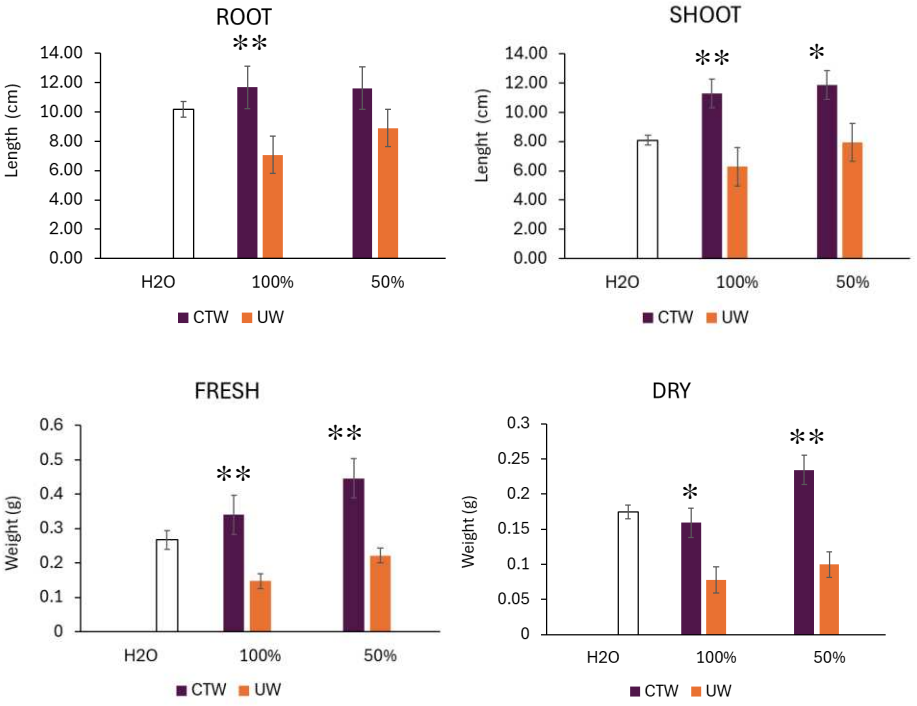

Figure 9. Effects of CTW on carosello seedlings. Vertical lines on each bar indicate the standard error. Data were statistically analyzed by ANOVA, and the means of the treatments were compared with 100% UW using the least significant difference (LSD) test at * $P \leq 0.05$, and *** $P \leq 0.001$.

6.3.6 Phytotoxicity assays using BTW, CTW, BAE and CAE

These assays were conducted on tomato seedlings comparing the effects of the different treatments, namely BTW, CTW, BAE and CAE, and water alone with the raw wastewater (100% UW).

Based on the values of the plant parameters measured, it can be stated that the BTW treatment produced the best results in terms of plant growth, increasing both root and shoot elongation (Figure 10). This result suggests that the treatment effectively reduced the phytotoxic compounds originally present in the wastewater, allowing a more favourable environment for seedling development. However, considering the biomass production, BTW and CTW exerted a significant stimulation on this plant whose biomass was more than doubled (Figure 10). This highlights the effectiveness of biochar in reducing phytotoxicity, likely through adsorption mechanisms that remove inhibitory compounds.

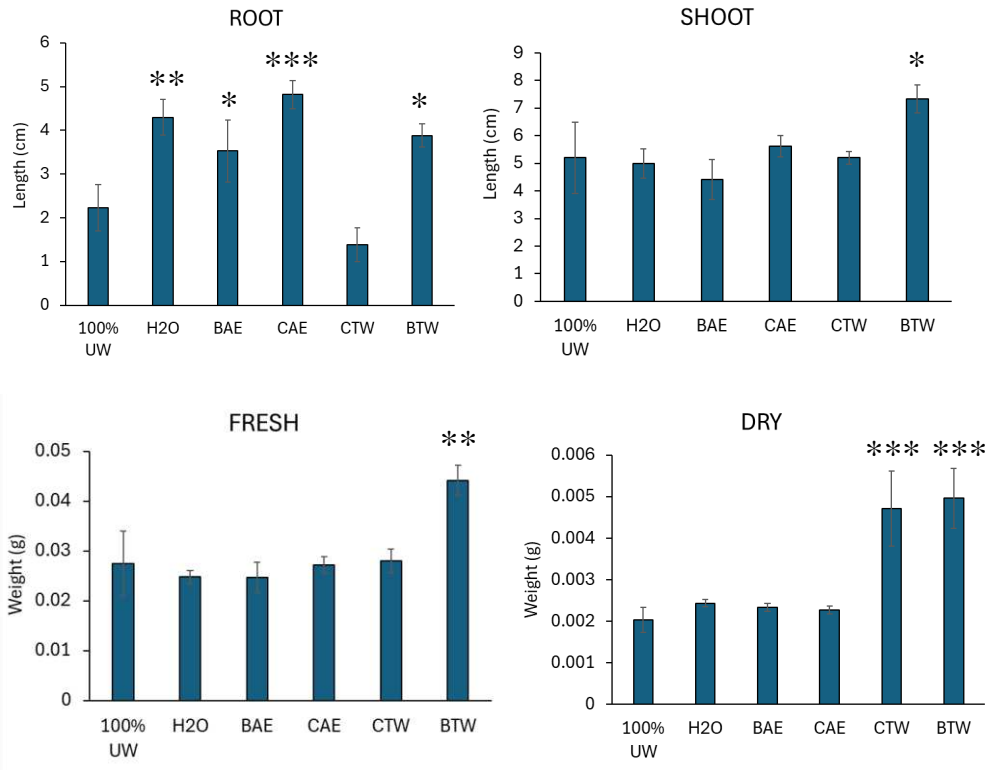

Figure 10. Effects of different treatments on carosello seedlings. Vertical lines on each bar indicate the standard error. Data were statistically analyzed by ANOVA, and the means of the treatments and bidistilled water were compared with 100% UW using the least significant difference (LSD) test at * $P \leq 0.05$, ** $P \leq 0.01$, and *** $P \leq 0.001$.

6.4 Conclusions

This study demonstrated that the investigated biochar is an effective, versatile, and low-cost adsorbent material for the removal of CECs from different wastewaters and for the reduction of phytotoxicity of dairy effluent. For all tested municipal and agro-industrial wastewaters, biochar showed very high adsorption performance, achieving contaminant load reductions generally above 90% and complete removal for a large fraction of the target compounds.

Adsorption experiments conducted on two different secondary municipal wastewaters confirmed both the high affinity of biochar toward a broad spectrum of pharmaceuticals and other CECs and the rapid retention of the pollutants, especially at higher adsorbent doses. A similar biochar efficacy was observed for citrus-processing wastewater, particularly for the removal of aromatic and hydrophobic compounds, including fungicides, confirming the robustness of biochar performance with pollutants with diverse physicochemical properties. Conversely, under the tested conditions, biochar efficiency in retaining highly persistent PFAS contaminants was lower and only became

appreciable above a threshold biochar dose. At low doses, removal was limited and strongly affected by matrix effects and analytical uncertainty. This last aspect requires further investigation to revise methodology and the optimize the LC–MS analytical protocol. Phytotoxicity assays performed on dairy wastewater demonstrated that the inhibitory effects of raw effluent on seed germination and seedling growth of horticultural species can be reduced by treating the effluent with biochar. Among the treatments tested, batch adsorption generally produced better detoxification effects than continuous-flow treatment, as confirmed by tomato germination and early growth tests. The overall results of this study encourage the use of biochar as an effective and sustainable bioadsorbent for wastewater remediation.

References

Aguillar-Torrejon J.A., Balderas-Hernandez P., Roa-Morales G., Barrera-Diaz C.E., Rodriguez-Torres I., Torres-Blancas T. (2023). Relationship, importance, and development of analytical techniques: COD, BOD, and, TOC in water—An overview through time. SN Applied Sciences, 5, 118 https://doi.org/10.1007/s42452-023-05318-7

Al-Ananzeh N.M. (2021). Treatment of wastewater from adairy plant byadsorption using synthesized copper oxide nanoparticles: kinetics and isotherms modeling optimization. Water Science & Technology, 83 (7), 1591–1604. https://doi.org/10.2166/wst.2021.089

Ambaye T.G., Vaccari M., van Hullebusch E.D. et al. (2020). Mechanisms and adsorption capacities of biochar for the removal of organic and inorganic pollutants from industrial wastewater. International Journal of Environmental Science and Technology 18, 3273–3294 https://doi.org/10.1007/s13762-020-03060-w

Cadena-Aponte F.X., Plaza-Bonalos P., Aguera A., Nahim-Granados S., Berruti I., Abeledo-Lameiro M.J., Polo-Lopez M.I. (2025). From the reclaimed water treatment plant to irrigation in intensive agriculture farms: assessment of the fate of antibiotics, antibiotic resistance bacteria and genes,and microbial pathogens at real scale. Environmental Science & Tecnology. 59, 19953-19965 https://doi.org/10.1021/acs.est.5c02823

Carnimeo C., Colatorti C., D'Orazio V., Trotti P., Loffredo E. (2023). Potential of Biochar from Wood Gasification to Retain Endocrine Disrupting Chemicals. Materials 16, 569. https://doi.org/10.3390/ ma16020569

Chen Y., Zhu Y., Wang Z. Li Y., Wang L., Ding L., Gao X., Ma Y., Guo Y. (2011). Application studies of activated carbon derived from rice husks produced by chemical-thermal process— A

review. Advances in Colloid and Interface Science 163, 39-52. https://doi.org/10.1016/j.cis.2011.01.006

Coimbra R.N., Calisto V., Ferreira C.I.A., Esteves V.I., Otero V. (2025). Removal of pharmaceuticals from municipal wastewater by adsorption onto pyrolyzed pulp mill sludge. Arabian Journal of Chemistry, 12 (8), 3611-3620 http://dx.doi.org/10.1016/j.arabjc.2015.12.001

Cristovao MB, Serio J, Marques AP, Bento-Silva A, Grossard M, Vergara-Diaz O, Silva AF, Nunes M, Bronze MR, de Oliveira PB, Crespo MTB, Crespo JG, Pereiro VJ (2026). Treatment of wastewater effluents using nanofiltration and low-pressure UV photolysis to produce high quality water for food production. Water research, 289, 124782. https://doi.org/10.1016/j.watres.2025.124782

Criswell R., Senechal K., Mullin A.M., Calafat A.M., Cook Botehlo J., Rokoff L.B. Abby F. Fleisch A.F. (2025). Concentrations of per- and polyfluoroalkyl substances (PFAS) in private well drinking water and serum of individuals exposed to PFAS through biosolids: The Maine Biosolids Study. Environmental Pollution 386, 127 https://doi.org/10.1016/j.envpol.2025.127259

Cui J., Wang G., Wang C., Ke P., Tian Q., Tian Y. (2020). Characterization, adsorption isotherm, and kinetic of mesoporous silica microspheres for dyeing wastewater. Desalination and Water Treatment 217, 358–366 doi: 10.5004/dwt.2021.26922

Dai Y., Ding D., Cui M., Duan P., Liu Y., Liu X., Yue T., Zhao J., Wang Z., Xing B. (2025). Biotransformation of per- and polyfluoroalkyl substances (PFAS) in organisms. Chemical Engineering Journal 524, 168618 https://doi.org/10.1016/j.cej.2025.168618

European Parliament and Council of the European Union. (2024). Directive (EU) 2024/3019. Official Journal of the European Union.

Feng C., Wu F., Zhang L., Yang X., Zhuang Y. (2025). Assessing provincial integrated wastewater treatment efficiency and influencing factors considering triple bottom line. Journal of Cleaner Production, 491, 144724. https://doi.org/10.1016/j.jclepro.2025.144724

Gao X., Ju Y., Hou G., Liu C. (2025). Efficient treatment of coking wastewater by coal-based activated carbon prepared through coal blending method. Colloids and Surfaces A: Physicochemical and Engineering Aspects 705, 135675 https://doi.org/10.1016/j.colsurfa.2024.135675

Habila M.A., AL Othman Z.A., Hakami H.M., Alanazi A.G. (2023). Influence of Synthesis-Heating Conditions on the Porosity and Performance of a Carbon Nanotube/SDS-Alumina

Nanocomposite for Effective Wastewater Treatment: Fabrication, Characterization, and Adsorption Modeling. Industrial & Engineering Chemistry Research 62 (32), 12571-12588. https://doi.org/10.1021/acs.iecr.3c01236

Heibati B., Rodriguez-Couto S., Amrane A., Rafatullah M., Hawari A., Al-Ghouti M.A. (2013). Uptake of Reactive Black 5 by pumice and walnut activated carbon: Chemistry and adsorption mechanisms. Journal of Industrial and Engineering Chemistry 20, 2939–2947 http://dx.doi.org/10.1016/j.jiec.2013.10.063

Hernandez-Zanoletty A., Polo-Lopez M.I., Berruti I., Jambrina-Hernandez E., Oller I., Plaza-Bolanos P., Agüera A (2025). Up-scaling solar photochemistry quaternary treatment of urban wastewaters to a demonstrative level. Journal of Environmental Chemical Engineering 13, 116766 https://doi.org/10.1016/j.jece.2025.116766

Krzeminski P, Tomei MC, Karaolia P, Langenhoff A, Almeida CMA, Felis E, Gritten F, Andersen HR, Fernandes T, Manaia CM, Rizzo L, Fatta-Kassinos D (2019). Performance of secondary wastewater treatment methods for the removal of contaminants of emerging concern implicated in crop uptake and antibiotic resistance spread: a review. Sci. Total Environ., 648, 1052-1081 https://doi.org/10.1016/j.scitotenv.2018.08.130

Kumari S., Chowdhry J., Kumar M., Garg M.C. (2024). Zeolites in wastewater treatment: A comprehensive review on scientometric analysis, adsorption mechanisms, and future prospects. Environmental Research 260, 119782 https://doi.org/10.1016/j.envres.2024.119782

Loffredo E. (2022). Recent advances on innovative materials from biowaste recycling for the removal of environmental estrogens from water and soil. Materials 15, 1894. https://doi.org/10.3390/ma15051894

Loffredo E., Denora N., Vona D., Gelsomino A., Porfido C., Colatorti N. (2025). Wood Gasification Biochar as an Effective Biosorbent for the Remediation of Organic Soil Pollutants. Soil systems 9, 18 https://doi.org/10.3390/ soilsystems9010018

Martinez-Burgos W.S., Sydney E.B., Medeiros A.B.P., Magalhães A.I, de Carvalho J.C., Karp S.G., de Souza Vandenberghe L.P., Junior Letti L.A., Soccol V.T., de Melo Pereira G.V., Rodrigues C., Woiciechowski A.L., Soccol C.R. (2021). Agro-industrial wastewater in a circular economy: Characteristics, impacts and applications for bioenergy and biochemicals. Bioresource Technology 341, 125795 https://doi.org/10.1016/j.biortech.2021.125795

Ministry of Agricultural, Food and Forestry Policies (Italy). (2022). Ministerial Decree of 10 October 2022: Update of Annexes 1, 6, 7, 8, 9, 13 and 14 to Legislative Decree No. 75 of 29 April 2010.

Mohammadi M., Ghasemi M., Sedighi M. (2022). Comparative study of energy production and treatment of municipal and dairy wastewater via microbial fuel cell technology: process evaluation towards optimization. Biomass Conversion and Biorefinery 14, 6285–6298 https://doi.org/10.1007/s13399-022-02979-z

Nasirabadi P.S., Saljoughi E., Mousavi S.M (2016). Membrane processes used for removal of pharmaceuticals, hormones, endocrine disruptors and their metabolites from wastewaters: a review. Desalination and Water Treatment 57, 24146-24175. https://doi.org/10.1080/19443994.2016.1140081

Pathak S., Pant K.K., Kaushal P. (2023). Analysis of naphthalene adsorption from wastewater using activated and non-activated biochar produced from bagasse. Biomass Conversion and Biorefinery 14, 19661–19674 https://doi.org/10.1007/s13399-023-04070-7

Qiu, M., Liu L., Ling Q., Cai Y., Yu S., Wang S., Fu D., Hu B., Wang, X. (2022). Biochar for the removal of contaminants from soil and water: a review. Biochar, 4, 19. https://doi.org/10.1007/s42773-022-00146-1

Rizzo L, Malato S, Antakyali D, Beretsou VG, Đolić MB, Gernjak W, Heath E, Ivancev-Tumbas I, Karaolia P, Lado Ribeiro AR, Mascolo G, McArdell CS, Schaar H, Silva AMT, Fatta-Kassinos D (2019). Consolidated vs new advanced treatment methods for the removal of contaminants of emerging concern from urban wastewater. Science of Total Environment, 655, 986-1008 https://doi.org/10.1016/j.scitotenv.2018.11.265

Srikhaow A., Win E.E., Amornsakchai T., Kiatsiriroat T., Kajitvichyanukul P., Smith S.M. (2023). Biochar Derived from Pineapple Leaf Non-Fibrous Materials and Its Adsorption Capability for Pesticides. ACS Omega 8 (29), 26147-26157 https://doi.org/10.1021/acsomega.3c02328

Vitale D.S, Reeves D.M., Coffin E.S., Cassidy D.P. (2025). Naturally occurring surface water foams as a PFAS sampling matrix. Journal of Hazardous Materials 496, 139456 https://doi.org/10.1016/j.jhazmat.2025.139456

Wang Y., Chen L., Zhu Y., Fang W., Tan Y., He Z., Liao H. (2024). Research status, trends, and mechanisms of biochar adsorption for wastewater treatment: a scientometric review. Environmental Sciences Europe 36, 25 https://doi.org/10.1186/s12302-024-00859-z

CHAPTER – 7
CONCLUSIONS

The research conducted within the three-years PhD program focused on various aspects of different adsorbent matrices obtained from raw and processed waste biomass, with the aim of employing them for soil and wastewater remediation of organic contaminants. All aspects investigated contribute to the implementation of innovative and sustainable solutions for soil management in marginal areas, which is the general focus of this PhD research.

Through a multidisciplinary approach combining physicochemical characterization, microstructural and spectroscopic analyses, adsorption studies, column experiments, and biological assays, this work demonstrated the remarkable potential of these plant-derived adsorbents as low-cost and eco-compatible tools for pollution control within agricultural and agro-industrial systems. By systematically comparing different feedstocks and transformation processes, the research provides a structured framework for understanding how biomass origin and processing influence environmental performance of these materials.

The results obtained highlight how the intrinsic properties of each biomass, such as lignocellulosic composition, porosity, surface functional groups (-NH_2, -COOH, -C=O), mineral fraction, and degree of biological or thermochemical transformation, play a decisive role in determining adsorption performance, interaction mechanisms with pollutants, and possible benefits for soil quality and plant growth. It has been demonstrated that the interplay between structural features and surface chemistry of the interacting agents governs not only adsorption but also the selectivity, reversibility, and long-term stability of pollutants on these substrates under environmentally relevant conditions.

A solid digestate (DG) derived exclusively from olive pomace showed a strong capacity to modulate the retention and release of agrochemicals in soil, significantly reducing their mobility and bioavailability. Incorporating solid DG into the soil altered the partitioning of contaminants between soil and water and slowed the leaching process, indicating significant potential for reducing the risk of groundwater contamination. Furthermore, DG interaction with a soil humic acid revealed complex synergistic and antagonistic effects on phytopathogenic fungi, suggesting that this material can influence soil biological processes in ways that go beyond simple nutrient supply. These findings indicate a multifunctional role of DG both as a soil remediator and a modulator of biotic interactions.

An investigation focused on untreated agricultural waste, such as orange peel, olive stones and pistachio shells (OP, OS, and PS) demonstrated that, even minimally treated, plant biomass can act as effective biosorbent, particularly for hydrophobic and aromatic contaminants. In fact, the richness of oxygenated functional groups enabled multilayer adsorption of various contaminants, including the herbicides oxyfluorfen and metribuzin, the insecticide imidacloprid (IMI), and the xenoestrogen bisphenol A. Similarly, the spent growth substrate used for *P. eryngii* cultivation showed highly promising biosorbent performance, likely due to the fungal-induced structural modifications in the wheat strow mixture, which improved important characteristics of the substrate, such as porosity and abundance of reactive functional groups. This finding highlighted the value of fungal biotransformation as a natural pretreatment capable of transforming agricultural residues into remediation materials, while requiring low energy input and low environmental impact.

A wood gasification biochar (BC) exhibited exceptional adsorption efficiency for the widely used fungicide boscalid, as well as a remarkable ability to reduce leaching in soil columns and stimulate plant growth. Its high surface area, well-developed porosity, aromatic carbon structure, and persistence in soil proved very effective for the long-term immobilization of pollutants and for improving early plant growth. In addition to its sorptive efficacy, BC demonstrated the capacity to mitigate phytotoxic effects in contaminated matrices, confirming its dual function as a soil remediation agent and a soil plant promoter.

The adsorption studies conducted using BC for real wastewater remediation further confirmed the versatility of BC in removing a broad spectrum of pharmaceuticals, agrochemicals, and industrial contaminants, achieving, under optimized conditions, removal efficiencies often exceeding 90%. These experiments demonstrated the robustness of BC performance in complex systems characterized by competing solutes and variable physicochemical parameters. Although PFAS proved more challenging to remove, especially at low adsorbent doses, the results indicate that BC can still contribute to their removal when appropriately dosed. Furthermore, phytotoxicity assays demonstrated that BC treatment can significantly reduce the inhibitory effects of dairy wastewater on seed germination and seedling growth of some horticultural plants, reinforcing BC role as a multifunctional material that can be used for improving both chemical and biological water quality. These biological validations complement the adsorption data, confirming that contaminant immobilization translates into measurable ecological benefits.

Overall, this PhD thesis demonstrated that the valorization of agricultural and agro-industrial waste as biosorbents represents a concrete and scalable strategy for adhering to the principles of circular economy, reducing waste flows and mitigating the environmental impact of agrochemicals and

emerging contaminants. The materials studied are abundant, renewable, and inexpensive, and their use requires minimal technological input, making them suitable for widespread adoption in both developed and resource-limited contexts. Furthermore, their multifunctionality, ranging from pollutant retention to soil fertility improvement, from modulation of microbial interaction to pathogen suppression, renders them valuable components of integrated environmental management strategies aimed at improving the sustainability of the agri-food sector, particularly in marginal areas.

In conclusion, the findings of this PhD thesis not only advance scientific knowledge on the adsorption mechanisms and environmental functions of natural biosorbents but also pave the way for innovative, sustainable, and circular strategies for soil and water protection. The investigated biosorbents show strong potential in up scaled systems because of their low cost and compatibility with circular economy approaches. Their scalability is supported by the widespread availability of biomass residues, although further efforts are needed to standardize materials and optimize performance under complex environmental conditions. By continuing to refine these materials, optimizing their production parameters, and integrating them into holistic environmental management frameworks, future research can significantly contribute to the development of resilient agricultural systems and the mitigation of emerging environmental challenges in a context of increasing ecological pressure and resource scarcity.